Soft Exosuit for Paretic Ankle Assistance in Post-Stroke Gait Rehabilitation

Soft Exosuit for Paretic Ankle Assistance in Post-Stroke Gait Rehabilitation

A dissertation presented
by
Jaehyun Bae

to

The John A. Paulson School of Engineering and Applied Sciences

in partial fulfillment of the requirements
for the degree of
Doctor of Philosophy
in the subject of
Engineering Sciences

Harvard University,
Cambridge, Massachusetts
July 2019

Dissertation Advisor:
Professor Conor J. Walsh

Author:
Jaehyun Bae

Soft Exosuit for Paretic Ankle Assistance in Post-Stroke Gait Rehabilitation

Abstract

In the last decade, wearable robotics technology has been growing rapidly for various applications. One of the main drivers of this growth is recent research studies demonstrating that wearable robots could generate positive impact on human locomotion in both healthy and clinical populations. This dissertation highlights my contributions to the first soft wearable robots, called soft exosuits, designed to assist with paretic ankle function in post-stroke walking, the main contributor to their slow, asymmetric, and energetically inefficient gait. Through multi-disciplinary research with a team with diverse backgrounds in robotics, biomechanics, physical therapy, and apparel design, we developed multiple iterations of exosuits ranging from a tethered exosuit prototype for treadmill-based feasibility studies to a portable exosuit for clinical studies in overground walking and beyond. In order to ensure the design was suitable for the heterogenous post-stroke population, our team actively integrated user feedback from both patients and clinicians as well as experimental data collected from biomechanical experiments (human-in-the-loop development process). The result of a multi-phase iterative development process is a compact and portable exosuit with a robust controller that can deliver well-timed, biomechanically-appropriate assistance to a wide range of post-stroke patients without manual tuning. Through extensive human subject experiments and biomechanical analysis, we demonstrated that exosuits could improve energetic economy, symmetry, and gait speed in post-stroke walking. Given this foundational finding, our research led to a licensing agreement to ReWalk Robotics for the translation of soft exosuit technology to clinics. The foundational work presented herein demonstrates the potential of exosuit technology to improve post-stroke gait training.

Acknowledgments

I would like to fist express my sincere gratitude to my PhD advisor Professor Conor J. Walsh for giving me the opportunity to work on such an exciting project with great collogues. My PhD project presented herein was truly exciting and motivating for me with its final outcome being translated to real-world clinics. I feel extremely fortunate to have this opportunity to do research in the field of clinical wearable robotics that I am passionate about and see how the technology nurtured from academia translates to the practice. Professor Walsh taught me the importance of setting a clear goal and making realistic plans towards the goal. He also taught me how to systematically approach engineering problems based on the integrative understanding on both scientific and practical challenges to advance technology. Further, working in such an interdisciplinary environment like Harvard BioDesign Lab taught me the importance of communication and team management to achieve common aims.

I would like to thank Professor Louis Awad for being a great mentor from the beginning of my project with his expertise in rehabilitation therapy and pathological gait biomechanics. I learned from him effective way of writing and hypothesis-drive approach. His broad interest stretching from physical therapy, gait biomechanics, motor learning to robotics gave me insights on how to integrate knowledges spread out across different fields to generate novel findings. I would also like to thank Dr. Scott Kuindersma for rounding out my PhD committee and giving valuable advices on my PhD research and future career. His detailed and clear advices and lectures enabled me to see my research from different angles with optimal control and machine learning theories. I would also like to thank Drs. Terry Ellis and Ken Holt from Boston University, for enabling my multidisciplinary research and leading it to become clinically meaningful. Without their advices, my research would have been just an engineering work which would never be implemented in real-world clinics.

I would like to thank my colleagues/friends in the Harvard BioDesign lab and Neuromotor Research Laboratory at Boston university who made my experience at Harvard unforgettable. There are far too many

amazing people to name and the list that follows is by no means exhaustive. First off, I would like to thank Dr. Josh Gafford for introducing me Harvard Design lab when we were at Stanford in 2012 and being a great colleague throughout our PhD. I would like to thank Kathleen O'Donnell and Dr. Stefano De Rossi who paved the way for my research from the beginning. I would like to thank Frey Tesfaye for supporting all the lab administrative matters. I would like to thank Nikolas Menard and Mike Rouleau for their work on software and hardware development of our project. I would like to thank Ignacio Galiana who has led exosuit project. I would like to thank Dr. Ye Ding for always bringing positive vibes and making the lab a happy place. I would like to thank all the exosuit team members, to name a few, including Sangjun Lee, Brendan Quinlivan, Jinsoo Kim, Chris Siviy, Evelyn Park, Krithika Swaminathan, Dabin Choe, Dr. Franchino Porciuncula, Dr. Lizeth Sloot, Dr. Nikos Karavas, Dr. Richard Nuckols, Dr Philippe Malcolm, David Perry, Asa Eckert Erdheim, Pat Murphy, Philipp Arens, Dheepak Arumukhom Revi, Lauren Baker, Dorothy Orzel, Taylor Greenberg Goldy, Lexine Schumm, and Dani Ryan. I would like to also thank all other lab members outside exosuit project including Ciaran O'Neill, Kate Zhou, Vanessa Sanchez, Jinwon Chung, and Yichu Jin.

I would also like to thank Katy Hendron, Regina Sloutsky, and Teresa Baker for their significant contribution on my project as onsite physicial therapists from Boston University. I would like to thank Saman Nasar and coworkers at Rewalk Robotics for their effort on the translation of my PhD work to real world. I would like to thank the American National Science Foundation (CNS-1446464), National Institutes of Health (1R01HD088619-01A1 and 1KL2TR001411), DARPA Warrior Web Program (W911NF-14-C-0051), Harvard University Star Family Challenge, Rolex Award for Enterprise, Wyss Institute for Biologically Inspired Engineering, and Harvard John A. Paulson School of Engineering and Applied Sciences for providing the funding to get this research off of the ground.

Finally, I would like to thank my family who unconditionally supported me throughout 6 years of my PhD training with love. I'd like to thank my parents for trusting and praying for me from abroad. I'd also like to thank my son, Sean Bae who was recently born and immediately became one of the most important people

in my life. Most importantly, I'd like to thank my wife, Yoon-young Cho for taking this journey with me, supporting me with the greatest love, and being my life-long partner. My achievements would not have happened without her, and I attribute all of my successes, this dissertation included, to her. I love you and will support my family unconditionally as she has done for my PhD. I look forward to our next chapters in our lives as a family of three.

Table of Contents

Chapter 1. Introduction....1

1.1. Background....1
1.1.1. Post-stroke locomotor impairment....1
1.1.2. Post-stroke locomotor rehabilitation....3
1.1.3. Robotic devices for post-stroke gait rehabilitation....4
1.1.4. Soft exosuit to reduce metabolic cost of transport in healthy walking and running....7
1.2. Specific aims....9
1.3. Research contributions....11

Chapter 2. Development of tethered soft exosuit prototype for paretic ankle assistance and its feasibility study....15

2.1. Introduction....15
2.2. Soft exosuit for post-stroke gait assistance....17
2.3. Textile and actuation implementation....18
2.3.1. Functional textiles....18
2.3.2. Mobile offboard-actuation unit....20
2.4. Sensor and controller implementation....21
2.5. Feasibility study with post-stroke individuals....27
2.5.1. Experimental protocol....27
2.5.2. Data analysis....28
2.6. Result and discussion....29
2.7. Conclusion....31

Chapter 3. Soft exosuits improve walking in patients after stroke....32

3.1. Introduction....32
3.2. Materials and methods....34
3.2.1. Experimental design....35
3.2.2. Participants and inclusion/exclusion criteria....36
3.2.3. Overview of soft exosuit controller....37
3.2.4. Clinical evaluations....39
3.2.5. Motion capture and metabolic data acquisition and analysis....40
3.2.6. Statistical analyses....41
3.3. Results....42
3.3.1. Participant baseline characteristics....42
3.3.2. Effective targeting of paretic limb ground clearance and forward propulsion deficits....43
3.3.3. Exosuit-generated assistive forces....44
3.3.4. Different PF assistance onset timing and their impact on biomechanical outcomes....45
3.4. Discussion....46
3.5. Supplementary studies....51
3.5.1. Impact of inactive exosuit on forward propulsion and metabolic expenditure....51
3.5.2. Proof of principle: overground walking with an portable exosuit prototype....52

Chapter 4. Reducing compensatory gait patterns with tethered soft exosuit....54

4.1. Introduction....54
4.2. Materials and Methods....55
4.2.1. Data collection and analysis....55
4.2.2. Statistical analysis....57

4.3. Results 57
4.3.1. Baseline characteristics 57
4.3.2. Changes in compensatory gait patterns spatiotemporal and kinematic variables 57
4.3.3. Kinematic Contributors to Reductions in Hip Hiking and Circumduction 59
4.4. Discussion 60
4.5. Limitation 63

Chapter 5. Biomechanical mechanism underlying exosuit-induced metabolic cost reduction 65

5.1. Introduction 65
5.2. Materials and Methods 68
5.2.1. Data collection 68
5.2.2. Data analysis 69
5.2.3. Normalization and statistical analysis 70
5.3. Results 71
5.3.1. Individual limb body center-of-mass (COM) power and its relationship with net metabolic power 71
5.3.2. Lower-limb joint power generated during trailing limb double support 73
5.3.3. Relationship of ankle power with total limb COM power and net metabolic power 76
5.4. Discussion 78
5.5. Conclusion 82
5.6. Supplementary materials 83

Chapter 6. A lightweight and efficient portable soft exosuit for paretic ankle assistance in walking after stroke 85

6.1. Introduction 85
6.2. Soft exosuit hardware 88
6.2.1. Functional apparel and insole anchors 89
6.2.2. Actuation system 90
6.2.3. Textile-integrated sensors 92
6.3. Exosuit modeling on the paretic ankle 92
6.4. Controller implementation 93
6.4.1. Gait event detection algorithm 94
6.4.2. PF cable position trajectory generator 96
6.4.3. DF cable position trajectory generator 97
6.5. System validation 98
6.5.1. Performance evaluation of gait event detection algorithm 100
6.5.2. Performance evaluation of PF cable position trajectory generation algorithm 100
6.5.3. Biomechanical evaluation 102
6.6. Conclusion 103

Chapter 7. Biomechanical and physiological benefits of wearing portable exosuit in overground walking post-stroke 104

7.1. Introduction 104
7.2. Methods 106
7.2.1. Participant recruitment 106
7.2.2. Ankle assistance generated by portable soft exosuit 108
7.2.3. Experimental protocol 108
7.2.4. Data measurement and analysis 110
7.3. Results 115
7.3.1. Increased walking speed and step length 115
7.3.2. Preserved metabolic cost of transport and stability 116

7.3.3. Increased paretic limb propulsion 117
7.3.4. Correlation between walking speed and forward propulsion power 118
7.3.5. Restored heel landing and ground clearance 119
7.3.6. Preserved paretic propulsive muscle activity 121
7.4. Discussion 123

Chapter 8. Controller performance of portable exosuit in post-stroke overground walking 132

8.1. Introduction 132
8.2. Control strategy of portable soft exosuit for paretic ankle assistance 133
8.3. Methods 136
8.3.1. Data collection 136
8.3.2. Data analysis 137
8.4. Results 140
8.4.1. Baseline gait event timing 141
8.4.2. Accuracy of gait event timings estimation by exosuit 141
8.4.3. Delay in segmentation points from exosuit-estimated toe-offs and baseline toe-offs 142
8.4.4. Consistency of exosuit-generated force 142
8.4.5. Biomechanical validity of exosuit-generated force timings 144
8.5. Discussion 145
8.5.1. Accuracy of gait event timings estimated by exosuit 145
8.5.2. Evaluation of PF assistance force 146
8.5.3. Evaluation of DF assistance force 148
8.6. Conclusion and future work 149
8.7. Supplementary materials 152

Chapter 9. Real-time gait metric estimation with portable exosuit 159

9.1. Introduction 159
9.2. State-of-the-art spatiotemporal gait metric estimation strategies with foot IMUs 161
9.2.1. Temporal gait metric estimation 161
9.2.2. Spatial gait metric estimation 162
9.3. Exosuit real-time spatial gait metric estimation algorithm 166
9.3.1. ZUPT detection method 167
9.3.2. Strap-down double integration with linear drift compensation 168
9.3.3. Implementation of real-time drift compensation 170
9.3.4. Gait Metric Computation 171
9.4. Validation 174
9.4.1. Validation 1: Healthy treadmill Walking (N=3) 174
9.4.2. Validation 2: Post-stroke overground walking (N=2) 176
9.4.3. Validation 3: Comparison of different ZUPT methods in post-stroke walking (N=1) 178
9.5. Discussion 186
9.6. Conclusion and future work 189

Chapter 10. Impact of exosuit intermittent assistance on assisted and unassisted gait patterns in post-stroke overground walking 191

10.1. Introduction 191
10.2. Methods 194
10.2.1. Intermittent assistance implementation 194
10.2.2. Experimental design 194
10.2.3. Data collection 196
10.2.4. Data analysis 197
10.3. Results and discussion 198

10.3.1. Changes in gait speed 198
10.3.2. Changes in paretic limb circumduction and temporal symmetry (P3) 200
10.4. Discussion 203
10.5. Conclusion and future work 207

Chapter 11. Proof-of-concept pilot study on gait training with portable exosuit 209

11.1. Introduction 209
11.2. Methods 211
11.2.1. Participant recruitment 211
11.2.2. Study design 212
11.2.3. Gait training interventions 212
11.2.4. Evaluation sessions 214
11.2.5. Motion analysis for evaluation sessions 215
11.2.6. Gait metric estimation during training days 215
11.2.7. Outcomes 216
11.2.8. Statistical analyses 216
11.3. Results 217
11.3.1. Exosuit intervention 217
11.3.2. Clinical outcomes from pre- and post-training evaluations 217
11.3.3. Biomechanical outcomes at pre- and post-training and retention evaluations 218
11.3.4. Gait changes across training sessions 220
11.4. Discussion 221

Chapter 12. Conclusion 227

12.1. Limitations and future work 228
12.1.1. Gait event detection and segmentation 228
12.1.2. Spatial gait metric estimation 229
12.1.3. Force tracking performance 230
12.1.4. Improving immediate assistive effect through assistance profile individualization 232
12.1.5. Intermittent/variable exosuit assistance to promote motor learning 234
12.1.6. Participant-centric approach for experimental study design 235
12.1.7. Longitudinal study on exosuit-assisted gait training 236

Reference 237

List of Tables

Table 2.1. Participant characteristics 28
Table 2.2. Changes in spatiotemporal gait symmetry in exosuit-assisted walking 30
Table 2.3. Changes in paretic propulsion and stride time in exosuit-assisted walking 30
Table 3.1. Participant baseline characteristics and gait performance 42
Table 3.2. Exosuit plantarflexion assistive force 45
Table 4.1. Spatiotemporal parameters 59
Table 4.2. Swing phase kinematic parameters 59
Table 5.1. Participant characteristics and onset timing of PF actuation 69
Table 5.2. Positive powers generated during trailing limb double support and their inter-limb symmetry 76
Table 6.1. Participant baseline characteristics and gait performance 100
Table 6.2. Peak PF force consistency (%BW) 101
Table 6.3. Average electrical power consumption of PF motor over single stride (W) 101
Table 7.1. Participant characteristics 107
Table 8.1. Gait events estimated by a portable exosuit and their definitions 134
Table 8.2. Exosuit gait segmentation points and their definitions 134
Table 8.3. Exosuit force parameters with which exosuit controller adapts assistance force profiles 135
Table 8.4. Baseline gait events and their calculations 137
Table 8.5. Group statistics on baseline gait event timings 141
Table 8.6. Group statistics of absolute error of different gait event timings estimated by exosuit 141
Table 8.7. Group statistics of delays in gait phase segmentation from baselines toe-offs ($Event_{base}$) and toe-offs estimated by exosuit ($Event_{exo}$) 142
Table 8.8. Group statistics in PF assistance timing and magnitude variables 143
Table 8.9. Group statistics in DF assistance timing and magnitude variables 143
Table 8.10. PF assistance timings in relation to gait event timings. 144
Table 8.11. DF force timings in relation to baseline gait event timings 145
Table 8.12. Individual baseline gait event timings represented in paretic gait cycle percentage (%GC). 152
Table 8.13. Individual data of absolute error in different gait event timings estimated by exosuit 153
Table 8.14. Individual data of toe-off event confirmation delays compared to gait event timings estimated by exosuit (GC_{exo}) and baselines(GC_{base}). 154
Table 8.15. Individual data of PF assistance magnitude and timing variables 155
Table 8.16. Individual data of PF force timings in relation to baseline gait event timings 156
Table 8.17. Individual data of DF assistance magnitude and timing variables 157

Table 8.18. Individual data of DF force timings in relation to baseline gait event timings.....158
Table 9.1. Temporal gait metrics estimated with exosuit 162
Table 9.2. Spatial gait metrics estimated with exosuit.....162
Table 9.3. IMU measurement errors and resulting integration drifts.....164
Table 9.4. Linear regression analysis outcomes from validation 1.....176
Table 9.5 Participant's stroke and gait characteristics.....176
Table 9.6. Linear regression analysis outcomes from validation 2.....177
Table 9.7. Number of error occurrence for different ZUPT methods during post-stroke treadmill walking 183
Table 9.8. Number of error occurrence for different ZUPT methods during post-stroke treadmill walking 184
Table 10.1. Participant stroke and gait characteristics.....195
Table 10.2. Gait metrics for the validation of intermittent assistance 196
Table 11.1. Peak paretic forward propulsions for different walking conditions in pre-training evaluation session.....217
Table 11.2. Biomechanical changes in paretic leg at pre, post, and retention from exosuit-assisted gait training.....219
Table 11.3. Biomechanical changes in paretic leg at pre, post, and retention from conventional gait training 219

List of Figures

Figure 1.1. Evolution of rehabilitation robots for post-stroke locomotor training and their examples 6
Figure 1.2. Soft exosuit to reduce metabolic cost of transport in healthy walking and running 9
Figure 1.3. Our vision towards continuum of gait rehabilitation care using soft exosuit 11
Figure 2.1. Soft exosuit prototype for paretic ankle assistance with a mobile off-board actuation unit 16
Figure 2.2. Stroke-specific exosuit textile modules 20
Figure 2.3. Gyroscope signals segmented by consecutive heel strikes (FS) from both legs for two different subjects 25
Figure 2.4. Illustration of PF cable-pull command trajectory and experimental data 27
Figure 2.5. Sample data in of spatiotemporal symmetry improvement 30
Figure 3.1. Illustration of soft exosuit assistance to augment paretic limb function during hemiparetic walking 34
Figure 3.2. Illustration of experimental setup 36
Figure 3.3. Overview of exosuit controller 39
Figure 3.4. Exosuit-induced changes in post-stroke gait mechanics and energetics 44
Figure 3.5. Exosuit controller performance during post-stroke treadmill walking 46
Figure 3.6. Effects of wearing a passive exosuit on post-stroke propulsion and energy expenditure 52
Figure 3.7. Overview of an untethered, unilateral, ankle-assisting exosuit prototype adapted for overground walking 53
Figure 4.1. Circumduction and hip hiking for a representative participant during walking with the exosuit unpowered and powered 56
Figure 4.2. Group statistics and individual data in paretic limb hip hiking and circumduction during exosuit unpowered and powered walking conditions 58
Figure 4.3. Correlation between changes in joint kinematics and hip hiking 60
Figure 5.1. Illustration of exosuit actuation and exosuit-generated force trajectory 66
Figure 5.2. Individual limb COM power across the gait cycle 72
Figure 5.3. Correlation between COM power during trailing limb double support and net metabolic power 73
Figure 5.4. Individual joint power across the gait cycle 75
Figure 5.5. Correlation between ankle and COM power during trailing limb double support 77
Figure 5.6. Correlation between ankle power during trailing limb double support and net metabolic power 78

Figure 5.7. Group average of sagittal plane joint kinematics segmented by % gait cycle for two different conditions on the paretic and nonparetic limbs 83
Figure 5.8. Group average of sagittal plane joint moments segmented by % gait cycle for two different conditions on the paretic and nonparetic limbs 84
Figure 6.1. Evolution of soft exosuits for paretic ankle assistance in walking after stroke 88
Figure 6.2. Exosuit hardware components and their masses 89
Figure 6.3. Diagram of actuation unit and pulley cartridge 91
Figure 6.4. Picture and diagram of a paretic ankle wearing the soft exosuit 93
Figure 6.5. Schematic block diagram of exosuit controller 94
Figure 6.6. Sagittal plane foot trajectories and foot IMU measurements during the paretic gait cycle, a time period between two consecutive paretic foot strikes (PFS) 95
Figure 6.7. Illustration of cable position and delivered force trajectories in two consecutive gait cycles (GCs) 98
Figure 6.8. Experimental setup for preliminary system evaluation with patients after stroke 100
Figure 6.9. Sample data to compare old and new PF cable position trajectory generators 101
Figure 6.10. Average biomechanical changes of individual subjects in paretic forward propulsion and ground clearance 102
Figure 7.1. Overview of experimental setup 110
Figure 7.2. Summary of the effect of exosuit assistance in post-stroke patients compared to baseline walking 116
Figure 7.3. Effect of exosuit assistance on body center-of-mass (COM) power in both limited and full community ambulatory groups 118
Figure 7.4. Correlations between changes in walking speed, paretic step length, and propulsive power generation 119
Figure 7.5. Effect of exosuit assistance on paretic limb sagittal plane ankle kinematics and kinetics in both limited and full community ambulatory groups 120
Figure 7.6. Effect of exosuit assistance on sagittal plane lower-limb kinematics in both limited and full community ambulatory groups 121
Figure 7.7. Effect of exosuit assistance on paretic limb ankle muscle activation 123
Figure 8.1. Illustration of exosuit controller and exosuit-generated force profile 133
Figure 8.2. Illustrations of exosuit gait event estimation and cable position command generation algorithms 136
Figure 8.3. Illustration of baseline gait events ($Event_{base}$) calculated using GRF data, gait events estimated by exosuit, and gait segmentation points (SP_{exo}) 138

Figure 8.4. Healthy sagittal plane biological ankle angle, moment, and power and exosuit-generated forces 140
Figure 9.1. Example of a threshold based ZUPT detection method using sagittal plane gyroscope signals 166
Figure 9.2. Zero-Velocity Update (ZUPT) algorithm based on exosuit gait event detection 168
Figure 9.3. Implementation of exosuit ZUPT method and double-Integration with linear drift compensation 169
Figure 9.4. Example of strapdown double integration with linear drift compensation in vertical axis 170
Figure 9.5. Adjusted drift correction in real time implementation 171
Figure 9.6. Illustration of stride length and circumduction defined by transverse plane foot trajectory 173
Figure 9.7. Illustration of ground clearance defined by sagittal plane foot trajectory 173
Figure 9.8. Experimental setup for treadmill walking in healthy individuals (validation 1) 175
Figure 9.9. Linear regression outcomes between exosuit-estimated gait speed and treadmill speed 176
Figure 9.10. Experimental setup for post-stroke overground walking (Validation 2) 177
Figure 9.11. Definition of neutral ZUPT/foot-flat moments 179
Figure 9.12. Comparison of different ZUP methods in post-stroke treadmill walking 180
Figure 9.13. Comparison of different ZUP methods in post-stroke overground walking 181
Figure 9.14. Detailed comparison showing how different ZUPT methods work and their challenges 183
Figure 9.15. Comparison of estimated foot velocity averaged over 15 strides based on treadmill walking study for our method and one of other methods (SHOE) 185
Figure 9.16. Sensitivity analysis on the impact of the order of drift function on stride length estimation error 188
Figure 10.1. Illustration of intermittent assistance and sample exosuit data collected from overground walking with exosuit intermittent assistance 193
Figure 10.2. Illustration of experimental conditions 196
Figure 10.3. Gait speed changes induced by exosuit intermittent assistance in a limited community ambulator 199
Figure 10.4. Gait speed changes induced by exosuit intermittent assistance in a household ambulator 200
Figure 10.5. Changes in paretic circumduction and foot clearance induced by intermittent assistance 201
Figure 10.6. Changes in step time symmetry index induced by intermittent assistance. 203
Figure 11.1. Schematic diagram of training study design 212
Figure 11.2. Clinical training progression strategy in exosuit-assisted gait training 214
Figure 11.3. PF assistance profiles tested during pre-training evaluation 215

Figure 11.4. Gait speeds and distance based on 10-meter walk test and 6-minute walk test at pre- and post-training evaluations for both exosuit-assisted and conventional training.....218
Figure 11.5. Percent change in biomechanical measures at post-training and retention compared to pre-training.....220
Figure 11.6. Percent changes in number of steps and average gait speed across training sessions from first training day for both exosuit-assisted and conventional gait training. 221
Figure 12.1. Force controller implementation for PF assistance with portable exosuit 232
Figure 12.2. Proposed multi-objective Human-in-the-loop (HIL) optimization to improve immediate benefit of wearing exosuits in post-stroke walking.....234

Chapter 1.

Introduction

1.1. Background

1.1.1. Post-stroke locomotor impairment

Bipedal locomotion is a defining trait of the human lineage, with a key evolutionary advantage being a low energetic cost of transport [1]. However, the low economy of bipedal gait may be lost because of neurological injury such as stroke, one of the leading causes of long-term disability [2]. Locomotor impairment after stroke is characterized by hemiparetic walking [3]–[8] which is a slow, asymmetric, and highly inefficient gait [9], [10]. Despite rehabilitation, the vast majority of stroke survivors retain neuromotor deficits that prevent walking at speeds suitable for normal, economical, and safe community ambulation [11]. Impaired motor coordination [12], muscle weakness and spasticity [13], and reduced ankle dorsiflexion (i.e. drop foot) and knee flexion during walking are examples of typical deficits after stroke that limit walking speed and contribute to gait compensations such as hip circumduction and hiking [14]–[18], increase the risk of falls, and reduce fitness reserve and endurance [4], [5], [10], [12], [19]–[21]. Even those able to achieve near-normal walking speeds present with gait deficits [22], [23] that hinder community

reintegration and limit participation to well below what is observed in even the most sedentary older adults [24], [25], ultimately contributing to reduced health and quality of life [2], [26], [27].

Walking independence is an important short-term goal for post-stroke survivors; however, independence can be achieved via compensatory mechanisms. The persistence of neuromotor deficits after rehabilitation often necessitates the prescription of passive assistive devices such as canes, walkers, and orthoses to enable walking at home and in the community [28]–[30]. Unfortunately, commonly prescribed devices compensate for post-stroke neuromotor impairments in a manner that prevents normal gait function. The stigma associated with the use of these devices is also important to consider, especially for the growing population of young adult survivors of stroke [31], [32]. The major personal and societal costs of stroke-induced walking difficulty and the limitations of the existing intervention paradigm motivate the development of rehabilitation interventions and technologies that enable the rapid attainment of more normal walking behavior.

A major contributor to post-stroke locomotion is impaired paretic ankle function, specifically during the push-off and swing phases of the gait cycle [33]–[37]. During push-off, diminished paretic ankle plantarflexion (PF) function inhibits the paretic limb's contribution to forward propulsion [34]–[36]. During swing, diminished paretic ankle dorsiflexion (DF) function leads to poor foot clearance [36], increasing the risk of tripping and falling [38]. Together, impaired paretic PF and DF contribute to slow walking speed [39], inter-limb gait asymmetry in spatiotemporal parameters [37], and increased metabolic cost of transport [3], [40]. Impaired paretic ankle often necessitates the use of an ankle foot orthosis (AFO). AFOs are passive assistive devices with a rigid mechanical structure that prevents foot drop during swing. Unfortunately, AFOs have been shown to inhibit normal push-off during walking [41] and reduce gait adaptability [42]. One alternative to the passive ankle support provided by an AFO is functional electrical stimulation (FES) [43], [44] which delivers mild electrical stimulus to ankle muscles and helps muscle activations for walking. Previous studies using such devices have shown improved paretic ankle function and reduced gait impairment [39], [45]. Although promising, the FES devices introduce high fatigability, weakness, and

reduced neuromuscular capacity of the paretic limb musculature [46]. New interventions to assist impaired ankle function post-stroke are therefore warranted.

1.1.2. Post-stroke locomotor rehabilitation

Current locomotor rehabilitation is largely based on physical therapy interventions with robotic approach still only marginally employed [47]. According to Cochrane review [48], physical therapy intervention for locomotor rehabilitation can be classified in two main categories: neurophysiology-based and motor learning-based approaches. In neurophysiology-based framework, therapists support to actively correct patient's movement patterns while the patient being a relatively passive recipient [49]. In contrast, motor learning-based approach which has gained more recent attention focuses on patients' active involvement [50]. The motor learning-based approach highlights the importance of specificity, dose, and intensity to facilitate plasticity of neuromuscular and cardiopulmonary systems and result in improved locomotor function [51]. Specifically, task-specific locomotor training is a well-accepted strategy in the motor learning-based framework, which suggests to train for specific goals that are relevant for the needs of patients [52]. Context-specific training is also widely discussed to give training in the patient's own environment, though its implementation is not common due to practical limitations [53]. Importantly, Task- or context- specific trainings could be effective when provided intensively at the acute stage of stroke recovery (less than 3-month post-stroke). Indeed, previous research found strong evidence that patients benefit from exercise in which functional tasks are directly and intensively trained [54], [55]. This evidence supports motor learning theory that large amounts of task-specific practice to learn a motor skill is a critical variable to enhance plastic changes in neural circuits serving the practiced behavior.

High-intensity gait training therapy is also widely thought to be beneficial [56]–[58], where intensity is defined as the amount of work done by patients in unit time (i.e. rate of work). Previous studies support this strategy by demonstrating that training at higher treadmill velocities could generate more therapeutic gain in walking speed and independence in post-stroke individuals [59], [60]. However, the majority of previous

studies did not successfully separate the effects of dose versus intensity in locomotor training, therefore more systematic validation is warranted. Moreover, high-intensity training could generate negative side effect such as development of compensatory gait patterns [61], therefore it should be carefully implemented in clinical practice.

Although our fundamental understanding on the recovery of locomotor function after stroke is limited, given the aforementioned considerations the latest Clinical Practice Guideline for post-stroke locomotor training [62] suggests that high-intensity task-specific practice may enhance walking competency in patients with stroke better than other methods. Specifically, the guideline suggests that overground gait training during the acute stage of stroke recovery, making it more common in modern physical therapy interventions for post-stroke rehabilitation. Other systematic reviews suggest the benefit of overground gait training when is combined with treadmill training or body weight support treadmill training (BWSTT) [63], [64] or with exercise protocols in acute and chronic stroke patients [65][86].

1.1.3. Robotic devices for post-stroke gait rehabilitation

Robotic devices, when engineered and utilized based on understanding of motor learning and brain plasticity, carry great potential in enabling recovery of post-stroke gait function [66]–[68]. Existing robotic technologies for post-stroke gait training can be broadly classified into treadmill-based exoskeletons and portable wearable exoskeletons (**Figure 1.1**) [69]. The former were firstly introduced to gait training in early 1990s with Lokomat (Hocoma Inc, Switzerland, **Figure 1.1**(b)), which combines body-weight supported treadmill-training (BWSTT) with the assistance of a robotic exoskeleton [70]. Lokomat was originally developed for patients with almost complete loss of mobility as a consequence of spinal cord injury (SCI). To support the significant mobility impairments of patients after SCI, it implemented high-impedance actuators and delivered high assistive torque. With the penetration of grounded exoskeleton technologies into post-stroke gait training, new control approaches [71] and hardware platforms with intrinsically low impedance [72] were developed to realize more natural (i.e. less robotic) and intuitive

interaction between the robot and post-stroke patients. Other such approaches for post-stroke gait training includes Robotic Gait Trainer [73], LOPES [72], and TPAD [74].

In the last 10 years, portable exoskeletons have gained significant momentum thanks to their ability to provide gait assistance both in the clinical and community environments [75], [76]. These devices have additional benefit over grounded exoskeletons because they can enable gait training in a real-world environment and provide higher levels of participant engagement and challenge [67]. They offer an incredible opportunity for mobility and independence in those needing full mobility assistance such as patients after complete SCI, thus first implemented for these patients. Recently, a number of these systems such as EksoGT (Ekso Bionics, USA, **Figure 1.1**(c)) and Indigo (Parker Hannifin, USA) have received FDA approval for the use in post-stroke gait training, with clinical validation ongoing.

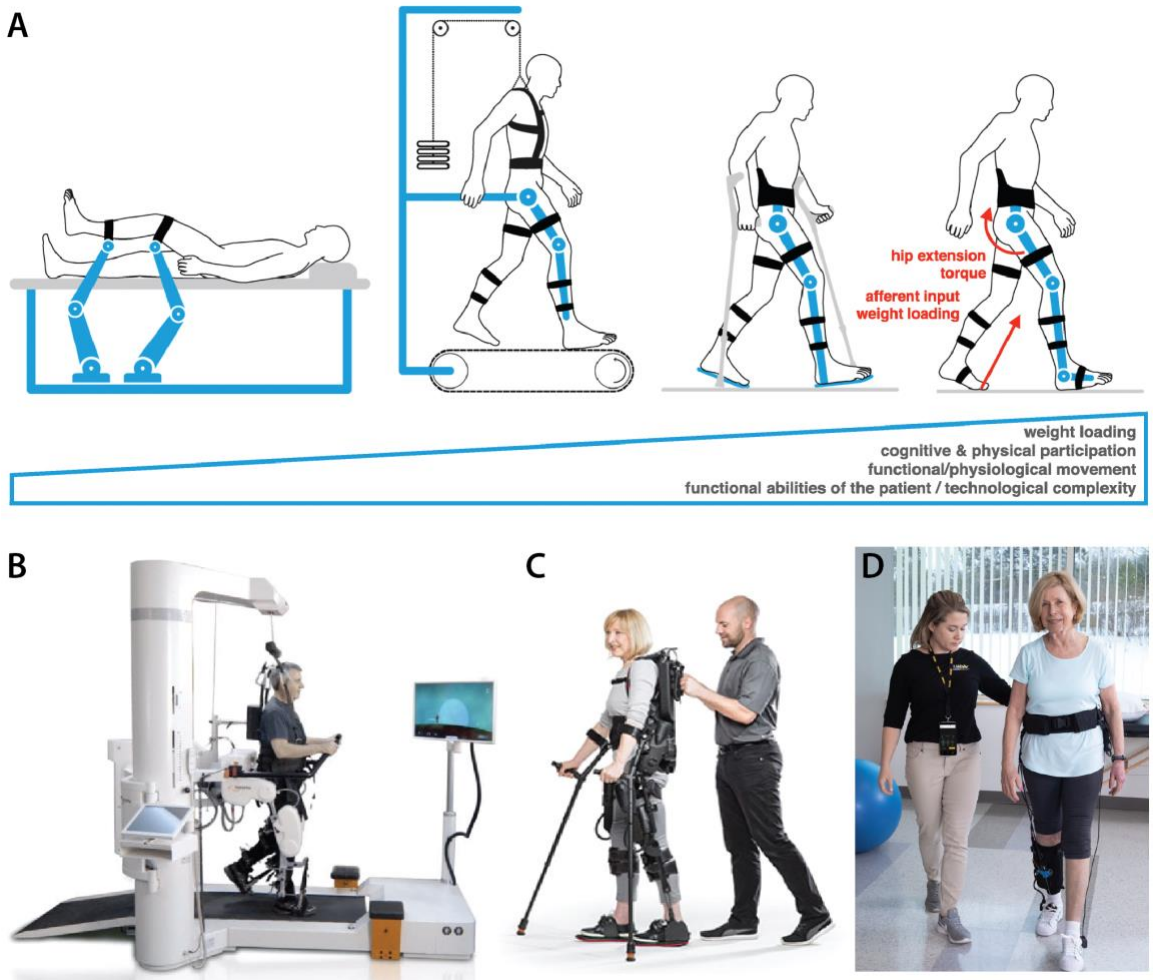

Figure 1.1. Evolution of rehabilitation robots for post-stroke locomotor training and their examples. (a) Rehabilitation robots for the lower extremity have evolved from stiff industrial robot arms to guide the limb passively to portable systems allowing for active engagement of patients through adapted support and body weight unloading. Wearable exoskeletons are recently being introduced into clinical practice, promoting even more active engagement of the patient. From left to right, patients require increasing functional abilities, while the robotic systems provide less support. (b)-(d) examples of rehabilitation robots for post-stroke locomotor training (b) treadmill-based gait training robot called Lokomat (Hocoma Inc,Switzerland), (c) EksoGT portable rigid exoskeleton for post-stroke gait training (Ekso Bionics, USA), (d) Portable soft robotic exosuit called Restore (ReWalk Inc, USA). This system was developed based on the work presented herein.
* Figure (a) was adapted from [69]

Although rehabilitation robotics technology for post-stroke locomotor training has rapidly evolved, it is still at an early stage and therefore more research effort on the development and validation is warranted. Indeed, the number of new developments of rehabilitation robots has been disproportionate to the penetration of these technologies into the clinical setting, likely due to the technology-driven approach of many engineering groups and the limited, albeit increasing, exchange of the field with therapists and clinicians [69]. While a few randomized-controlled trials were conducted to demonstrate efficacy of robot-assisted therapy [77], [78], the majority of published devices were never clinically evaluated, or such an evaluation was limited to pilot studies on a few patients. Even more, clinical studies on post-stroke locomotor training with treadmill-based exoskeletons (e.g. Lokomat and Gait trainer) could not yet demonstrate clear therapeutic benefits over conventional training [62], and therefore the latest Clinical Practice Guidelines [62] do not recommend the use of these robots to post-stroke gait rehabilitation. Potential reasons for the insufficient therapeutic benefit from these devices could be found from the aforementioned motor-learning based rehabilitation framework highlighting the importance of amount, intensity, and specificity (Section 1.1.2). These devices to enable greater time for interventions. However, because of the mechanical assistance and stability provided by these devices, patients may reduce their own metabolic and muscle exertion (i.e. reduce volitional work to produced motion; reduced intensity). Further, constrained walking on a treadmill may not provide sufficient specificity for the gait training to provide benefit in real-world ambulation scenarios.

As of now, portable exoskeletons are in the process of being evaluated for their efficacy in post-stroke gait training. It is likely that these devices will provide benefit for some individuals (e.g. for those with more

severe gait impairments); however, they may not be the most suitable for stroke survivors with partial gait impairments. Significant mass added by the exoskeletons to the wearer's limbs impose restrictions on their kinematics, ultimately leading to a slow and inefficient gait that may not be better than a patient's baseline gait. Moreover, the additional significant mass attached to the wearer may pose a safety concern should a fall occur. Furthermore, misalignments of the exoskeleton's rigid joints with the user's biological joints can cause significant stress on the bones and soft tissue. Lastly, rigid exoskeletons face several practical challenges that may limit their adoption in a community setting. For example, the power requirements for such devices are relatively high and they would become impossible to transport by patients should they lose power.

It is clear that further research is warranted to focus on acquiring a better fundamental understanding on the interaction between the rehabilitation robots and humans through extensive and rigorous biomechanical and physiological studies. Moreover, it would seem beneficial that future development of rehabilitation robotic systems and robot-assisted gait training strategy is developed based on motor-learning framework. Ideally approaches will encourage patients to maximize their exertion to walk (intensity), promote great walking distances (amount) with natural gait patterns similar to healthy walking (i.e. not developing compensatory gait patterns), and be conducted in the environment similar to patients' daily surroundings (specificity).

1.1.4. Soft exosuit to reduce metabolic cost of transport in healthy walking and running

Our laboratory has developed soft wearable robots, called soft exosuits that use soft textiles to provide conformal, unobtrusive, and compliant means to interface to the human body [79]–[100]. Exosuits deliver mechanical assistance to the lower-limb joints via the interaction of Bowden cables driven by off-board [81], [84], [85], [97]–[100] or body-worn [86]–[88] actuators and functional apparel components. Exosuits differ from the current state-of-the-art exoskeletons in that they do not use a rigid structure or provide full

gait assistance; rather, exosuits are lightweight and unobtrusive functional apparel designed to generate partial mechanical assistance to individual joints to supplement existing joint abilities.

The initial development of exosuits aimed to augment walking and running in healthy individuals [79], [80], [94]–[100], [81]–[87], [91] (**Figure 1.2**). Previous work has shown that exosuits for healthy individuals can securely and comfortably transmit mechanical assistance to the wearer via textiles, actuators, and cable-based transmissions and generate biologically appropriate moments during locomotion [79], [80], [91]. The textiles are structured in a manner that anchors the exosuit to key locations on the body (e.g. pelvis, thigh, calf, and foot) and provide load paths that generate tensile forces across joints when an actuated segment reduces the relative length between two points in the suit. Depending on the load path of the textile, mechanical assistance can be provided at a single joint, or simultaneously across multiple joints, in a way that mimics the mono-articular and multi-articular function of biological muscles. Biomechanical experiments with healthy individuals have shown that exosuit could reduce metabolic cost of transport in healthy walking through mechanical assistance to hip [85], [98], ankle [83], [96], [100], or both [87]–[89], [95], [99]. Furthermore, we recently demonstrated exosuit could reduce metabolic cost of transport in healthy running with hip extension assistance provided by either offboard [84] or portable actuators [86]. These encouraging results prompted study of the exosuit in the post-stroke population.

Figure 1.2. Soft exosuit to reduce metabolic cost of transport in healthy walking and running. (a) Tethered exosuit to assist with hip extension using an offboard actuation unit for treadmill-based study (b) Portable exosuit for multi-joint assistance (hip extension and flexion, and ankle plantarflexion) in healthy walking (c) Portable exosuit for hip extension assistance in healthy walking and running.

1.2. Specific aims

The ultimate goal of the work presented herein is to improve post-stroke gait training through the development of soft exosuit technology that is suitable for use across the continuum of rehabilitation (i.e. from a clinical setting to the community). See **Figure 1.3** for illustration. We hypothesize that exosuit technology could improve clinic-based post-stroke gait rehabilitation by promoting high-intensity overground gait training sessions to achieve specificity, amount, and intensity described in Section 1.1.3 and thereby overcoming the limitation of the current state-of-the-art rehabilitation robots. The concept is

that an exosuit would be a tool used by a therapist to provide targeted assistance to individual joints during overground walking in a manner similar to what is done in the clinic today, but in a more controlled and less labor-intensive way. Moreover, it is possible that exosuit assistance could increase the amount of walking by enabling the patient to walk farther with improved gait patterns within the same training session duration (amount), while still requiring patients' own effort (intensity). Finally, the overground walking training enabled with a portable exosuit has more contextual similarity with real-world ambulation than training with treadmill-based exoskeletons (specificity). Such a system would also not be restricted to only in-clinic use. Due to their simple, unobtrusive, low power, highly portable, and lightweight design, exosuits may offer a unique platform for continuous, targeted gait rehabilitation in the community. Specifically, through the provision of well timed, small to moderate assistive forces to individual joints (e.g. the ankle) during walking, exosuits could be utilized as personal gait training devices at home or in the community such that patients could continue to self-train and maintain improved gait patterns.

Towards this goal, this work aims to generate fundamental understanding on the biomechanical and physiological impact of exosuit assistance on post-stroke walking and to demonstrate the potential of this technology for improved post-stroke gait training. Three specific aims of this work are as follows:

- **Aim 1:** Gain a fundamental understanding on the biomechanical and physiological impact of paretic ankle assistance generated by an exosuit on post-stroke treadmill-walking using a tethered exosuit prototype.

- **Aim 2:** Understand the biomechanical and physiological impact of a portable exosuit on overground walking post-stroke.

- **Aim 3:** Demonstrate utility of real-time gait metric estimation in exosuit-assisted gait training and proof-of-concept of exosuit-assisted gait training through a clinical case study.

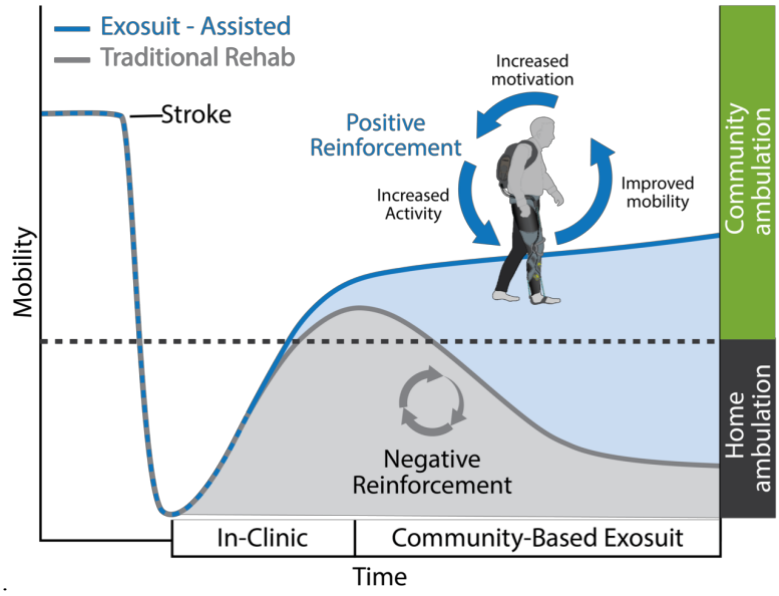

Figure 1.3. Our vision towards continuum of gait rehabilitation care using soft exosuit. Traditional clinic-based gait training often enables patients to achieve community ambulatory gait functions upon the end of the training program. However, after the training program, patients do not sufficiently utilize the improved gait functions in community, and therefore lose the functions, remaining sedentary at home. We envision that exosuits could improve gait function in the clinics more than the traditional gait training with high-intensity overground gait training session with targeted joint assistance. Furthermore, exosuits could serve as personal gait training devices outside the clinics to enable further improvement of gait function after discharged from clinics.

1.3. Research contributions

The work presented in this dissertation contributes to the field of rehabilitation and wearable robotics through the first demonstration of soft exosuits to assist post-stroke locomotion and gait training. Through multidisciplinary research across people from wide range of fields including robotics, biomechanics, textile design, and physical therapy, this work successfully validated the potential of a soft exosuit in post-stroke gait training. The specific contributions of this thesis are as follows:

- Developed a control strategy for a tethered exosuit prototype designed for treadmill-based study. The controller consists of (1) a gait segmentation algorithm robust to foot tremor during swing and pathological foot strike using foot-flat detection and (2) Force-based position trajectory generator and user interface for manual adjusting of assistance patterns (Chapter 2).

- Experimentally evaluated biomechanical and physiological performance of the tethered exosuit by comparing treadmill walking with powered exosuit to unpowered exosuit with 9 post-stroke

individuals. This study demonstrated that exosuit assistance could reduce metabolic cost of transport (-10%) and forward propulsion inter-limb asymmetry (-20%), while increasing ankle dorsiflexion angle during swing for improved ground clearance (+5.3°) (Chapter 3). This study also demonstrated that exosuit assistance could reduce compensatory gait patterns such as hip hiking (-27%) and circumduction (-20%) (Chapter 4). Finally, biomechanical analysis revealed that improved symmetry in body center-of-mass (COM) power generation for step-to-step transition (-22%) was a major contributor of the aforementioned metabolic cost reduction (Chapter 5).

- Contributed to the design of a portable exosuit by calculating electromechanical requirements and exploring different component options based on experimental data collected from the tethered exosuit. For the portable exosuit, developed a control strategy to deliver consistent assistance in heterogenous post-stroke overground walking with minimal manual tuning. This control strategy consists of (1) a gait segmentation algorithm specifically designed for highly variable post-stroke overground walking, and (2) event-based PF cable trajectory generator with within-stride and stride-to-stride adaptations that does not require inaccurate gait cycle percentage (%GC) calculation and reduces electrical power consumption (50%) (Chapter 6).

- Collaborated with other lab members to experimentally validate biomechanical and physiological performance of portable exosuit in post-stroke overground walking. By comparing overground walking with the portable exosuit to walking without the exosuit in 19 post-stroke individuals ranging from limited community ambulators to full community ambulators, the study demonstrated that the portable exosuit improved walking speed (5%), especially in the limited community ambulators (13%), while preserving metabolic cost of transport and stability of gait. The exosuit also increased paretic limb body COM power generation for push-off (14%), control of foot landing (400%) and ground clearance (4.3°). Correlation analysis suggests that the increased walking speed was correlated with increased step length induced by increased ankle and body COM push-off power (**Error! Reference source not found.**).

- Validated controller performance of portable exosuit in post-stroke overground walking. The validation showed that exosuit accurately estimated the timings of gait events with average error of 1.5%GC. Exosuit-generated force profile was consistent across gait cycles in both PF (RMSE=1.35 %BW) and DF (RMSE=1.58%BW) assistance. Further, the timing of PF and DF assistance were biomechanically sensible, with PF assistance coinciding with paretic forward propulsion and DF assistance with swing and foot landing. This analysis also revealed the limitation of current controller, suggesting future development direction (**Error! Reference source not found.**).

- Collaborated with other lab members to implement real-time spatiotemporal gait metric estimation with portable exosuit for online gait monitoring. Leveraging the robust gait event detection presented in Chapter 6, the gait metric estimation algorithm compensates for integration error in IMU-based position estimation to improve the accuracy. Experimental validation studies demonstrated that the algorithm was more robust in compensating integration error every stride than previously presented algorithms [101], [102] with similar estimation error range (**Error! Reference source not found.**).

- Conducted a case-series study with 3 post-stroke individuals to investigate the impact of intermittent assistance generated by portable exosuit on both assisted and unassisted overground gait patterns. The study demonstrated that similar to continuous assistance from exosuit, exosuit intermittent assistance could improve post-stroke overground gait speed and patterns. It also demonstrated that the improved gait induced by exosuit assistance could be carried over through post-assistance periods when assistance was turned off, suggesting a potential that intermittent assistance could promote gait training session with improved gait patterns (**Error! Reference source not found.**).

- Collaborated with other lab members to conduct a single-subject pilot study on exosuit-assisted gait training with intermittent assistance to compare gait training with an exosuit to conventional gait training without an exosuit. Results showed that gait training with exosuit (EXO) compared to conventional gait training (CONV) had significant differences in clinical measures such as 6-minute

walking distance (EXO: +86m, CONV: +37m) and 10-meter walking speed (EXO: +0.12m/s, CONV: +0.04m/s). Furthermore, exosuit assisted gait training improved paretic limb forward propulsion, while conventional training reduced forward propulsion (EXO: 59%, CONV: -9%), demonstrating more biomechanically sensible gait pattern induced by exosuit assisted training (**Error! Reference source not found.**). This pilot motivates more formal clinical evaluation.

- Contributed to develop the commercial version of soft exosuit for post-stroke gait training named Restore exosuit (Rewalk Robotics, USA). In collaboration with Research and Development team at Rewalk Robotics, my contribution included translation of exosuit control algorithm to a new exosuit hardware, validation of controller performance with the new hardware, and review documentation for FDA clearance. Restore exosuit has recently received CE mark for the commercialization in European countries, and also been cleared by the US Food and Drug Administration (FDA) for the use in post-stroke rehabilitation in the US.

Chapter 2.

Development of tethered soft exosuit prototype for paretic ankle assistance and its feasibility study

2.1. Introduction

This chapter presents our first prototype of soft exosuit to assist with paretic ankle function in post-stroke walking and its feasibility study with three individuals in chronic phase of post-stroke recovery. The exosuit consists of textile-based wearable components and mobile off-board actuation unit. By avoiding the use of rigid wearable structures, exosuit offers greater comfort, facilitate donning/doffing, and do not impose kinematic restrictions on the wearer – all while retaining the ability to generate significant moments at target joints during walking. This chapter describes stroke-specific design considerations, the design of the textile components, the development of a research-focused, mobile off-board actuation unit capable of testing the exosuit in a variety of walking conditions, a real-time gait detection and control algorithm, and proof-of-principle data validating the use of the exosuit in the chronic stroke population. At the end of the

chapter, we demonstrate appropriate timing of assistive forces and improvements in key gait metrics induced by the exosuit assistance. Specifically, in the subsequent sections of this chapter, we first describe the soft exosuit prototype for paretic ankle assistance in walking post-stroke (**Figure 2.1**) and its feasibility study in post-stroke treadmill walking. Specifically, Section 2.2 presents the design principles for the stroke-specific exosuit. Section 2.3 presents the exosuit hardware, including the soft exosuit textiles and a mobile off-board actuation unit developed to facilitate laboratory-based feasibility testing of the exosuit. Section 2.4 describes sensor implementation, a gait event detection algorithm, and a control strategy for assisting post-stroke gait that facilitates input from clinicians. Finally, Section 2.5 presents a preliminary experimental validation of the exosuit on three stroke patients.

Figure 2.1. Soft exosuit prototype for paretic ankle assistance with a mobile off-board actuation unit. The exosuit uses garment-like functional textile anchors worn around the waist and calf and Bowden cable-based mechanical power transmissions to generate assistive joint torques to the paretic ankle. One end of the Bowden cable is connected to the mobile off-board actuation unit, and the other end is connected to the exosuit textiles. The off-board actuation unit contracts the Bowden cables by changing the motor position, resulting in torque generated at the ankle.

2.2. Soft exosuit for post-stroke gait assistance

Soft exosuits offer three distinct advantages that increase their usability in the post-stroke population when compared to rigid exoskeletons. First, through the proximal-mounting of motors, electronics, and batteries (i.e. actuator packs) and flexible cable-based transmissions to the lower extremity, exosuits minimize the addition of mass on the extremities. This allows for the components on the legs to be very light and non-restrictive – an important consideration for stroke survivors as any added mass or constraints could negatively impact their residual mobility and create discomfort/safety risks. Through the use of unobtrusive and conformal materials, exosuits also have a very low profile and can thus be worn underneath regular clothing. Considering that a major goal for such wearable technology is use in the community, a non-visible wearable robot is advantageous for aesthetic and psychosocial reasons. Lastly, due to their garment-like design, exosuits can be easily donned/doffed – another important consideration for those post-stroke in whom upper extremity impairments are prevalent.

The stroke-specific exosuit presented in this chapter deviates from our previous designs for healthy gait augmentation [79], [80], [91], [94], [95], [103]–[105] by providing only unilateral assistance to the paretic ankle during push off, and additionally provides dorsiflexion assistance during the swing phase via a new textile module. Post-stroke gait impairments vary widely, and separate suit modules for different assistance targets provide the flexibility to address a wide variety of gait deficits. For example, a suit module for dorsiflexion assistance can prevent foot drop and facilitate better ground clearance while a module for plantarflexion assistance can improve the paretic limb's ability to generate forward propulsion. Moving to a unilateral design allows a substantial reduction in the weight of the total system while not sacrificing efficacy. Indeed, improving the function of the paretic limb – especially by targeting two key subtasks of walking (i.e. ground clearance and forward propulsion) known to be impaired after stroke [4], [10]– can yield bilateral improvements in gait such as improved kinematic and kinetic symmetry. It should be noted that although an exosuit provides a platform for targeted unilateral assistance of the paretic limb, it could also be used bilaterally.

For exosuits to be practical in a community setting, it will be important for them to have a low overall mass and in particular a low-profile body-worn actuation system. The requirements for a body-worn actuation system (e.g. how much assistance to provide) and the sensors and controls needed to achieve these requirements are currently not known. Thus, as a first step, we have designed a mobile off-board actuation unit that enables feasibility testing with an exosuit both on the treadmill and overground. This actuation unit mimics the function of a body-worn actuation system, enabling the experimental testing of different sensing and control strategies. Our goal is to leverage this basic science research to guide the future development.

2.3. Textile and actuation implementation

2.3.1. Functional textiles

As a first step toward the development of exosuits to assist walking after stroke, we implemented new unilateral 2 degrees of freedom (DoF) exosuit textiles. These textiles consist of two separate modules: a unilateral plantarflexion (PF) suit module and a dorsiflexion (DF) suit module (**Figure 2.2**).

The PF suit module was adapted from previous multi-articular exosuits for healthy individuals described in [79], [80], [91]. A waist belt anchors the suit to the pelvis and supports most of the downward forces. Unlike previous exosuits, the waist belt of the new PF suit module is fabricated from highly stable woven textiles (Safety Components, Greensboro, NC) instead of polyester webbing straps to improve suit comfort and fit around the waist. These were deemed important to improve exosuit fit across diverse body types and shapes in persons post-stroke. The connecting straps and thigh brace are routed to transmit the force from the waist to the leg in a manner that minimizes pressure on the skin and unwanted joint moments (e.g. the knee moment). The Bowden cable sheath attaches to the distal end of the suit near the calf, whereas its inner cable attaches at the heel of a semi-rigid insole with cable attachment straps. With this multi-articular suit architecture, the cable contraction generates ankle plantarflexion and hip flexion torques simultaneously.

We developed the DF suit module to assist with ankle dorsiflexion because improving paretic limb ground clearance during swing phase is a stroke-specific requirement. The DF suit module consists of a single vertical reinforced strap on the shin connected to three separate straps that route forces posteriorly around the calf to a common anchor point located anteriorly at the tibial tuberosity. Rotational pivots on each strap enable a customized fit across a wide range of calf shapes and overlapping hook and loop panels secure the straps in place to improve anchoring. Similar to the PF suit module, the Bowden cable sheath attaches at the lowest part of the DF suit module and its inner cable attaches on the front of the shoe over the metatarsophalangeal joint. Thus, with a contraction of the cable, dorsiflexion torque is generated. Furthermore, the cable can be aligned medial or lateral to the subtalar joint to additionally assist eversion or inversion of the foot when needed. The overall mass of the exosuit's functional textile anchors, cables, and sensors is about 0.90 kg (waist textile anchor, 0.15 to 0.20 kg; thigh connecting straps, 0.20 to 0.22 kg; calf textile anchor and integrated sensors, 0.30 to 0.35 kg; cables and sheath, 0.12 to 0.15 kg).

Throughout the textile design process, we actively integrated the feedbacks provided by individuals in the chronic phase of stroke recovery. Because the suit anchors to the body via functional textiles that distribute forces evenly, pressure points are minimized, and the suit is generally well tolerated by individuals. Participants have noted that the suit is snug, but still comfortable, around the paretic limb. Over time, participants generally report that this sensation of tightness is no longer perceivable. These reports of suit tolerance have been independently confirmed through skin checks performed by a physical therapist before and after prolonged suit wear.

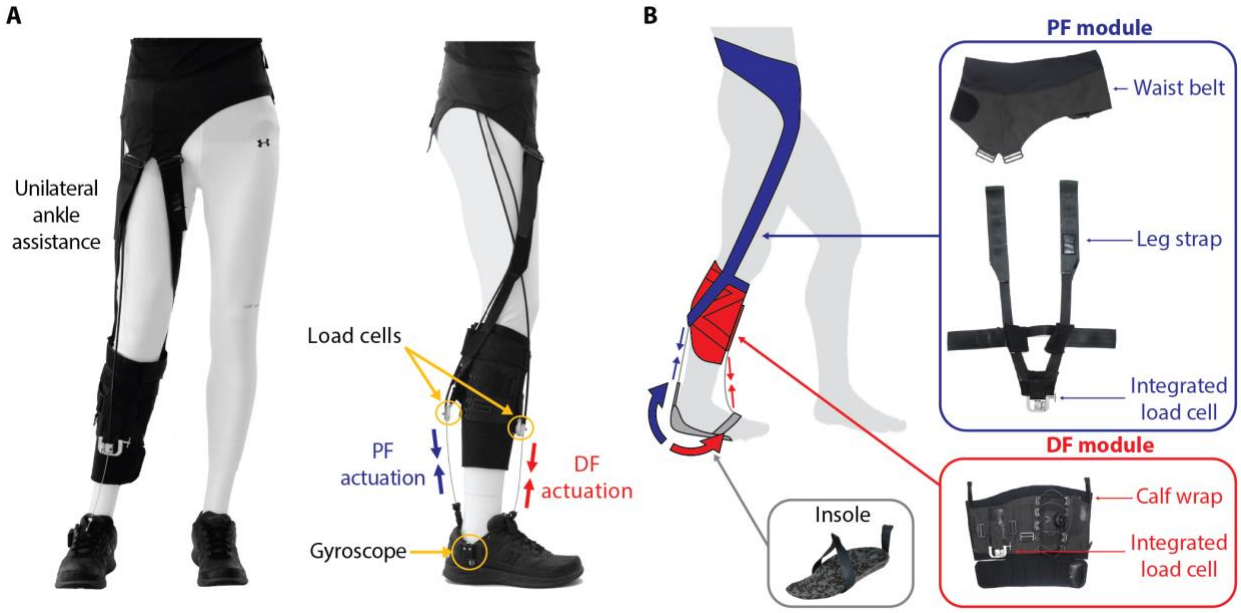

Figure 2.2. Stroke-specific exosuit textile modules. (a) Unilateral plantarflexion (PF) and dorsiflexion (DF) suit modules and semi-rigid insole are worn on a mannequin. The exosuit assists PF by contracting a Bowden cable between the calf and the heel, and assists DF by contracting a cable between the anterior shank and the dorsal surface of the foot. Mediolateral cable alignment can be modified to provide additional assistance for weakness in foot inverters and everters. Further, integrated sensors (load cells and gyroscopes) are used to detect gait events and in a cable position–based force controller that modulates force delivery (b) textile components of PF and DF module and semi-rigid insole.

2.3.2. Mobile offboard-actuation unit

A reconfigurable multi-joint actuation platform was previously presented to explore human-exosuit interaction in an efficient and controlled manner [95], [99]. The platform contained three modular actuation boxes, each with two actuated linear DoFs that connected to Bowden cables. The actuation box translated the rotational motion of a brushless motor (Maxon, Fall River, MA) into linear motion of an aluminum carriage that connected to the inner cable of the Bowden cable. All of the electrical components necessary for programming of the actuators (desktop PC, motor controllers, and power supply) were included in the platform. The platform was designed to meet requirements based on the biomechanical data of healthy people during walking. In particular, the linear actuators move at a speed of 1.5m/s, enabling the ankle to rotate at a speed of 2.8 rad/s – which is the average ankle speed during walking. Ultimately, the actuators can exert forces up to 250N during walking at 1.25m/s, with sufficient control bandwidth for applying assistance to healthy individuals [95]. We previously demonstrated that biologically realistic torques could

be provided either separately or simultaneously at the ankle and hip joints during walking. In this work, we extended the capability of this platform such that it was capable of simulating a body-worn exosuit actuation system during both treadmill and overground walking (see the mobile off-board actuation unit in **Figure 2.1**). The cart-like outer frame has four casters underneath and the handle at the back, therefore clinicians can follow the patient with the actuation unit to facilitate overground walking with exosuit assistance. It was designed to have a low height and a non-reflective surface so as not to disrupt motion capture data collection. The mobile off-board actuation unit provides all the necessary components to control the exosuit in its compact mobile frame. It contains two actuator boxes that are directly adapted from [99] and allow up to 4 DoF actuation, a mini fanless desktop (Advantech America, Milpitas, CA), motor controller (Copley controls, Canton, MA), power supplies with different voltages (5V, 15V, and 48V), and a monitor to display input and output data. To facilitate intermittent walking during overground experiments, a mode selector button was added to the handle to switch controller between walking and standby mode. An emergency stop button was also added to the handle in order to quickly and safely disable tension in the suit when required. Since the actuator box satisfies the biological requirements for a healthy subject's walking, and patients after stroke generally walk at a slower speed, we expect that the actuator unit is sufficient for this patient population.

To our knowledge, this is the first demonstration of an off-board actuation unit for use in overground walking study. Although the actuation unit is not suitable for use in a community setting, it can enable feasibility studies with post-stroke patients walking on the treadmill and overground. This will guide the development of stroke-specific actuator requirements that will be used for the development of a body-worn actuator.

2.4. Sensor and controller implementation

The stroke-specific exosuit we present here is equipped with a variety of sensors enabling a closed loop control system to deliver well-timed assistance to each DoF. The control system was designed to be robust

to the highly variable gait patterns found in stroke patients. In addition to control, sensor data can be used to calculate gait temporal variables (e.g. step time) in real-time to provide quantitative feedback for clinicians during walking experiments.

Sensor implementation

Two load cells (Futek, Irvine, CA) were integrated into the distal ends of the PF suit module and of the DF suit module, where Bowden cable outer sheaths attach to the textiles. This configuration allowed measurement of the interaction force between the exosuit and the wearer. A gyroscope (SparkFun, Niwot, CO) was attached on the lateral part of each shoe to measure foot rotational velocities in the sagittal plane. Each actuator box inside the actuation unit was equipped with an incremental encoder (Maxon, Fall River, MA), a linear potentiometer (P3 America, Inc, San Diego, CA) to measure the displacement of the actuation cable, and a load cell (Futek, Irvine, CA) to measure the force at the proximal end of the Bowden cable. A data acquisition card and two DAQ connector blocks (National Instruments, Austin, TX) in the actuation unit collected all the sensor signals. The system was designed to be reconfigurable and so the number and type of sensors can easily be modified for future development of exosuit embodiments and walking experiments.

Real-time gait event detection

Control algorithms for walking assistance often rely on gait event data such as toe off (TO) and foot strike (FS) to generate assistance profiles [106]. However, the significant step-to-step variability of post-stroke gait poses a challenge in implementing conventional gait event detection algorithms that heavily rely on gait periodicity [107]. To address these difficulties, we designed a gait event detection algorithm that uses gyroscope sensor signals from both feet and accounts for inconsistencies in the gait pattern and differences in sensor signals between the paretic and nonparetic limbs and from subject-to-subject. The algorithm can detect TO and FS from both sides independently and divide the gait cycle into four different phases (weight acceptance, paretic limb support, pre swing, and swing). Additionally, it enables evaluating temporal

variables such as temporal symmetry between the paretic and nonparetic legs. Previous study from other research group [108] showed that the profile of the foot velocity in the sagittal plane as measured by the gyroscopes has two negative peaks in each gait cycle, which correspond to TO and FS. **Figure 2.3** shows an example of measured foot velocity on both the paretic and the nonparetic feet for two different subjects. It can be seen that there is significant variability both in the paretic velocity profiles across different subjects, and between the paretic and nonparetic profiles. The algorithm is adaptive, thus can be applied to both the paretic and the nonparetic sides without changing parameter settings. The algorithm divides each gait cycle into four regions (R1-R4) in real time, and searches the peaks only in specific regions (R2 and R4) as described:

- R1: Foot flat during stance, with the foot velocity signal being close to zero. Mean (μ_{100ms}) and variance (σ_{100ms2}) of the signal are computed over a sliding window of 100ms. This region starts when μ_{100ms} and σ_{100ms2} satisfies conditions (2.1) and (2.2), and terminates when either of the conditions does not hold. No event is detected during R1.

$$|\mu_{100ms}| < 10 \tag{2.1}$$

$$|{\sigma_{100ms}}^2| < 100 \tag{2.2}$$

- R2: Pre-swing, beginning with the termination of R1 and ending with the detection of a negative peak that corresponds to TO. The peak is detected within this region in real-time based on an adaptive threshold method in the following paragraph). The time when the peak is detected is recorded (t_{TO}) and used in (2.4).

- R3: Early and mid-swing, beginning with the termination of R2. No event is detected during this region as experimental data showed significant variation in sensor signals across subjects due to foot instability during swing phase. R3 terminates after the calculated duration based on an average of the last three swing time measurements as described in (2.3). N in (2.3) is an index of gait cycle (i.e. $T_{swing}(N)$ is the swing time of Nth gait cycle). The same notation is used in the following equations.

$$T_{s3}(N+1) = 0.8 \cdot \frac{1}{3} \cdot \sum_{i=N-2}^{N} T_{swing}(i) \tag{2.3}$$

$$T_{swing}(i) = t_{FS}(i) - t_{TO}(i) \tag{2.4}$$

- R4: Late swing and early stance, beginning with the termination of R3. The negative peak corresponding to FS is detected in this region similarly to R2. The time when the peak is detected is recorded (t_{FS}) for use in (2.4),(2.6), and (2.7). R4 ends when the next R1 starts.

An adaptive threshold-based detection algorithm similar to [109] was implemented to allow the robust detection of the TO and FS negative peaks. The algorithm detects the TO (or FS) peak when the sensor signal passes the threshold twice (from above to below, and back to above). Two different thresholds were defined for each the paretic and nonparetic limbs, one for detecting TO ($thres_{TO}$) and one for FS ($thres_{HS}$). Each threshold is computed based on the magnitude of the last three velocity peaks as described in (2.5). The adaptive thresholds allow the algorithm to be robust to the high variability of the impaired gait as well as to the differences between the paretic and nonparetic foot velocity patterns.

$$\left|thres_{TO/HS}(N+1)\right| = 0.8 \cdot \frac{1}{3} \cdot \sum_{i=N-2}^{N} \left|V_{peak_{TO/FS}}(i)\right| \tag{2.5}$$

As described in Section 2.6, we demonstrated that the algorithm can accurately estimate the timing of the TO and FS events. In particular, the paretic stride time (the time period between consecutive HSs from the paretic side) calculated based on this algorithm was very close to that calculated based on motion capture data with an average error of less than 20ms, and the nonparetic stride time was also accurate with an average error of less than 10ms. Throughout the complete human subject testing sessions described, the algorithm detected 100% of FS and TO events from both lower limbs when the exosuit was active. However, the event timing errors slightly increased at faster speeds (i.e. the error calculated from the data of a subject walking at 0.5m/s is larger than that with the same subject walking at 0.3m/s).

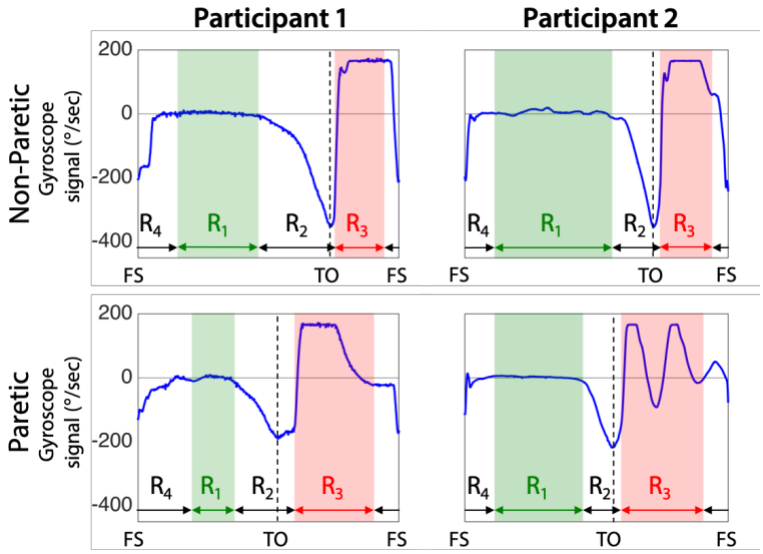

Figure 2.3. Gyroscope signals segmented by consecutive heel strikes (FS) from both legs for two different subjects. A comparison of the gyroscope signals to gait events segmented by kinematics data validated that the two negative peaks corresponded to FS and TO respectively. In addition, the green region of the gyroscope signal (R1), corresponding to foot flat during stance, was consistently at a value of zero for legs across subjects, while the illustrated red regions (R3), corresponding to early and mid-swing, were not consistent. The gait event detection algorithm used identifies R1 based on definitive conditions in equations (1) and (2). The algorithm searches for TO and FS during R2 and R4 respectively. It deliberately does not rely on the sensor signals in R3 since the sensor signals during the swing phase were inconsistent as shown. In addition, since the absolute magnitudes of peak signals were different in the nonparetic side and the paretic side, adaptive peak detection threshold is implemented in the algorithm in order to address the difference.

Feedback controller and adjustable trajectory generator

Previous exosuits from our group generate assistive forces by contracting Bowden cables with a change in the position of a linear actuator as commanded by a position controller [79], [80], [91]. The position command results in an assistive force to the wearer due to the inherent human-suit series stiffness. Given the variability in post-stroke gait, it is desirable to have the capability of delivering an individualized assistive profile to each patient. In response to this need, we developed a control strategy that enables the timing, magnitude and profile of the actuator position command trajectory (i.e. cable-pull command trajectory) to be adjustable for each patient, as well as within each session among different walking experiments. The resulting control system was implemented with a Matlab-based user interface (Matlab, Mathworks, MA) that enabled the cable-pull command trajectory to be adjusted manually in real-time. The patient-specific command trajectory is defined as a function of the gait cycle f(GC) (**Figure 2.4** (a)). In real time, clinicians can adjust key parameters of the command trajectory, such as the start timing of cable pull

and release, pull and release speed, and maximum cable pull. The command trajectory is then scaled by estimated stride time and applied to the controller at the paretic HS of each gait cycle. (2.6)-(2.9) give the details on the calculation of the estimated stride time (T_{stride_est}), the current percentage of the gait cycle (GC_{curr}), and the cable-pull command (P_{des}) at each time. To be specific, T_{stride_est} is calculated as an average of the last three stride time measurements (2.6)(2.7), and GC_{curr} is estimated by dividing the time elapsed after the last HS by T_{stride_est}. (2.8). Finally, the cable-pull command at current time (P_{des} (t_{curr})) is calculated by substituting the current gait cycle percentage to the command trajectory (f(GC_{curr})) adjusted by a clinician (2.9).

$$T_{stride\_est}(N+1) = \frac{1}{3} \cdot \sum_{i=N-2}^{N} T_{stride}(i) \tag{2.6}$$

$$T_{stride}(i) = t_{FS}(i) - t_{FS}(i-1) \tag{2.7}$$

$$GC_{curr} = \frac{t_{curr} - t_{FS}(N)}{T_{stride_{est}}(N+1)} \cdot 100\ (\%) \tag{2.8}$$

$$P_{des}(t_{curr}) = f(GC_{curr}) \tag{2.9}$$

A closed loop PID feedback controller was programmed in the xPC Target environment (Matlab, Mathworks, MA) with a closed-loop frequency of 1kHz so that the actuator could accurately follow the prescribed command trajectory. The feedback controller and adjustable trajectory generator described here were successfully used in the preliminary testing in Section 2.5. The comparison between assistance force timing and gait phase segmented with motion capture data validated that we could deliberately control the timing of the provision of assistive force (**Figure 2.4**).

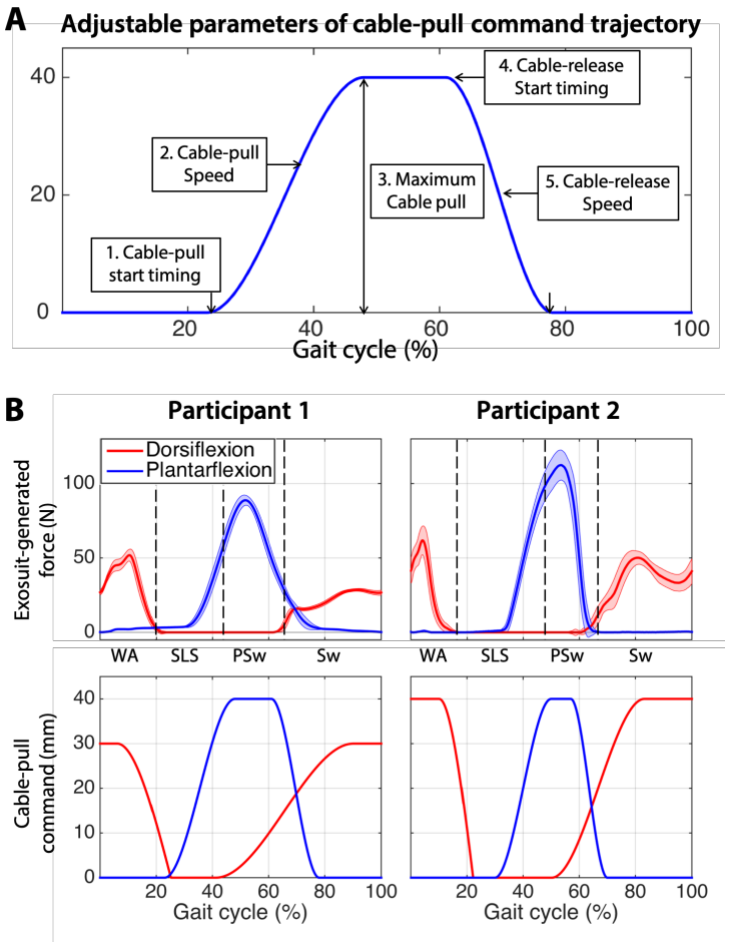

Figure 2.4. Illustration of PF cable-pull command trajectory and experimental data (a) PF cable-pull command trajectory and manually adjustable parameters (1-5). Clinician can change the start timing of cable pull and release, the pull and release speed, and the maximum cable pull. (b) PF and DF Cable-pull command trajectories (bottom) and corresponding applied forces for two different subjects (top). The gait sub-phases shown on force plots (dotted lines in (b)) are identified using motion capture data. The four sub-phase indices under the applied force plots indicate weight acceptance (WA), single limb support (SLS), pre-swing (PSw), and swing (Sw). Based on the force plots, it is clear that different cable-pull commands correspond to well-timed assistive forces that DF assistance is effective during swing and weight acceptance and PF assistance is effective during mid and late stance.

2.5. Feasibility study with post-stroke individuals

2.5.1. Experimental protocol

Three participants with chronic stroke with broad age and different post-stroke profiles, all of whom were community ambulators with the use of their regular assistive devices, were recruited for this preliminary study (**Table 2.1**). The study was approved by the Harvard Medical School Institutional Review Board. Participant inclusion criteria included being between 25 and 75 years old, at least 6 months post-stroke, ability to walk independently for at least 6 minutes continuously, and sufficient passive range of motion at

the paretic ankle joint to reach the neutral position with the knee extended. Participants were excluded if they were unable to communicate with research team members, if they had serious musculoskeletal, cardiovascular, or neurological comorbidities, if they had fallen more than twice within the previous month, or if they were currently participating in a physical rehabilitation program. Consent was obtained from the participants and a licensed physical therapist participated in every session. Data were collected at a baseline session (Baseline) and at a session where the suit provided assistance (Active). During Baseline testing, subjects walked on an instrumented treadmill (FIT Bertec, Columbus, OH) at their self-selected treadmill speed, and full body motion capture data were collected through a 9-camera Vicon optical motion analysis system (Oxford Metrics, Oxford, UK) with 70 body markers. Between three and five acclimatization sessions with the exosuit followed the baseline session so that the patient could become familiar with the exosuit and the physical therapist could tune the actuator command trajectories. This was done through visual inspection by at least one expert in observational gait analysis of how the patient's gait changed in response to different types of assistance and through the interpretation of a select number of temporal gait variables that were exported from the exosuit and displayed on the interface. After the training sessions, the assistive trajectories were held constant for the remaining sessions.

Table 2.1. Participant characteristics

Participant	Age (years)	Time post-stroke (years)	Gender	Height (m)	Weight (Kg)	Self-selected speed (m/s)
P1	29	6	Female	1.62	49.9	0.3
P2	63	2	Male	1.83	98.4	0.5
P3	60	12	Male	1.83	95.3	0.45

* Self-selected speed is measured on the treadmill without gait assistive devices.

2.5.2. Data analysis

Motion capture and ground reaction force (GRF) data were analyzed using Vicon Nexus and Visual 3D (C-motion Inc., Rockville, MD, USA) software. Raw data were filtered (fourth order low-pass Butterworth filter, 12Hz cut-off frequency) prior to processing, and spatial gait variables such as step length and foot trajectories were calculated based on motion capture data. The spatial gait variables were segmented and

normalized to 0-100% of the gait cycle, as defined by consecutive HSs. Gait events (HS and TO) were identified from GRFs and marker data. Spatiotemporal gait data were analyzed only for steady-state walking in the final minute of each condition, and the average across all measured strides in each final minute was used for analysis. Gait symmetry and paretic propulsion were calculated based on motion capture and GRF data given their importance in post-stroke gait rehabilitation [110]. Specifically, spatiotemporal gait symmetry was evaluate using symmetry index (SI) using (2.10) [111].

$$SI = \frac{(X_{np} - X_p)}{0.5 \cdot (X_{np} + X_p)} \cdot 100\ (\%) \tag{2.10}$$

X_{np} and X_p were gait parameters from the nonparetic and paretic sides, respectively. Further, propulsive impulse was calculated as the integral of positive anterior-posterior GRF (AP GRF) during stance [112], and paretic propulsion was also calculated based on the proportion of the total propulsive impulse produced by paretic side [113].

2.6. Result and discussion

We observed an improvement in step time symmetry by 6.26% (**Table 2.2**) and in stance time symmetry by 3.52%. Moreover, stride time decreased by 11.43% (**Table 2.3**, see **Figure 2.5** (b) for an example of stance and stride times). In terms of spatial gait symmetry, two subjects had less significant improvement in their step length symmetry (**Table 2.2**). However, the abnormal lateral movement of the foot during swing phase was significantly reduced when a subject with circumduction gait (P1) was assisted by the exosuit (**Figure 2.5** (a)). In terms of propulsion, the activation of the suit facilitated all subjects to have more propulsion symmetry. We observed an average 7.15% increase in propulsion symmetry. These initial preliminary results show a promising positive effect of the exosuit on temporal (step time and stance time) symmetry and paretic limb propulsion. In addition, because spatial symmetry (step length symmetry) also improved - albeit to a lesser extent - and excess lateral motion of the foot resulting from circumduction was reduced, these results imply an effect of the exosuit on compensatory gait patterns. These results suggest that the exosuit could promote a more efficient walking pattern in individuals post-stroke. The decrease in

stride length for all subjects may imply that subjects were unable to take long strides due to a restrictive nature of the suit. On the other hand, it could suggest that subjects increased their cadence with a desire to walk faster over a treadmill-constrained speed.

Table 2.2. Changes in spatiotemporal gait symmetry in exosuit-assisted walking

	Step time symmetry (%)			Step length symmetry (%)		
	Baseline	**Active**	**Change**	**Baseline**	**Active**	**Change**
P1	24.91	15.71	9.20	-50.43	-48.81	1.62
P2	9.68	3.26	6.42	21.36	25.60	-4.24
P3	19.09	15.94	3.15	-13.90	-10.26	3.64

* 0% SI is perfect symmetry;

Table 2.3. Changes in paretic propulsion and stride time in exosuit-assisted walking

	Paretic propulsion (%)			Stride time (sec)		
	Baseline	**Active**	**Change**	**Baseline**	**Active**	**Change**
P1	10.27	10.54	0.27	1.55	1.47	-0.08
P2	37.04	42.77	5.73	1.78	1.43	-0.35
P3	5.77	21.23	15.46	1.90	1.72	-0.18

* 50% paretic propulsion is perfect symmetry

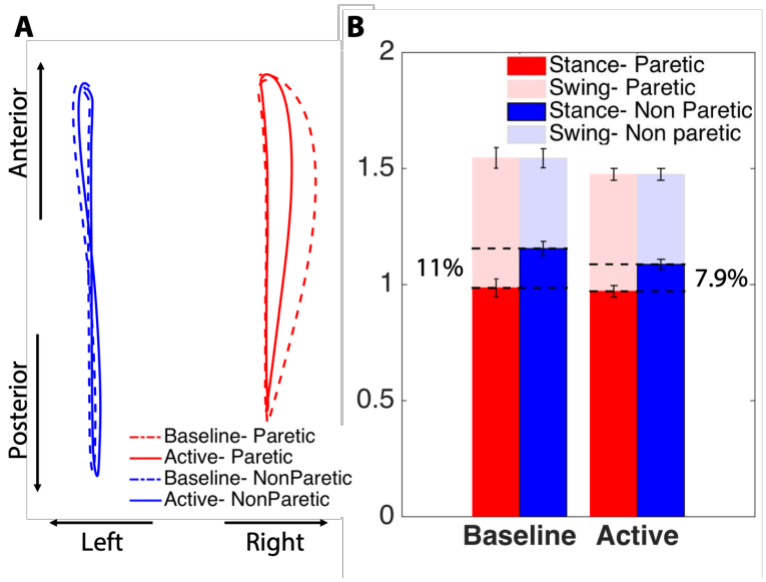

Figure 2.5. Sample data in of spatiotemporal symmetry improvement. (a) Foot trajectory of a subject with circumduction gait pattern (S1). The subject significantly reduced excess lateral foot motion when suit was active. (b) Stance time symmetry also increased while stride time decreased.

2.7. Conclusion

This chapter presents our early-stage development of a soft exosuit prototype for post-stroke paretic ankle assistance. Newly developed exosuit textile modules, a mobile off-board actuation unit, and control algorithms were described that enable human subjects testing in patients with stroke both on the treadmill and overground. Preliminary experiments were conducted on three patients with chronic stroke to validate the system robustness and evaluate the effect on walking biomechanics. Initial results demonstrated that a soft exosuit could improve patients' gait symmetry and paretic limb progression. This work thus presents proof-of-concept and motivates further effort in this area. Future work will be directed towards optimizing the design of the soft exosuit. In particular, we plan to optimize the design of the textile components to enable the application of higher forces and improve the controller to provide greater tuning of the assistance to the wearer. We will also focus on using the data from these initial studies to guide the development of a body-worn actuation system and a graphical user interface to facilitate clinicians' use of the exosuit. Finally, we plan more extensive human subject testing of the exosuit to demonstrate its potential across a larger number of patients with stroke.

Chapter 3.

Soft exosuits improve walking in patients after stroke

3.1. Introduction

Recent years have seen the development of powered exoskeletal devices designed to enable walking in individuals who are unable to walk [68], [114]. Central to this remarkable engineering achievement is a rigid structure that can support its own weight and provide high amounts of assistance; however, these powerful machines may not always be necessary to restore more normal gait function in individuals who retain the ability to walk after neurological injury, such as the majority of those after stroke. To address this opportunity, we developed a soft exosuit that interfaces to the paretic limb of persons after stroke via garment-like, functional textile anchors and presented its first prototype in Chapter 2.

Several factors, such as the compliance of the exosuit-human system [79], [91], prevent exosuits from providing the assistance necessary to enable non-ambulatory individuals to walk again [115]; however, for ambulatory individuals, the lightweight and nonrestrictive nature of this technology has the potential to

facilitate a more natural interaction with the wearer and minimize disruption of the natural dynamics of walking [116]. Our first efforts developing exosuits for healthy individuals led to the creation of systems that could comfortably deliver assistive forces to healthy users during walking [79], [80], [91], [95], [96], [100], [117]. Recently, we demonstrated that assistive forces delivered through the exosuit interface produce marked reductions in the energy cost of healthy walking [87], [100]. Thus, although exosuits can only augment, not replace, a wearer's existing gait functions, we posit that they have the potential to work synergistically with the residual abilities of individuals with impaired gait to improve walking function.

The primary objective of this foundational study was to evaluate the potential of using the exosuit technology to restore healthy walking behavior in individuals after stroke. Toward this end, we evaluated the effects on hemiparetic gait of actively assisting the paretic limb during treadmill walking using a tethered, unilateral exosuit designed to supplement the wearer's generation of paretic ankle plantarflexion (PF) during stance phase and dorsiflexion (DF) during swing phase (see **Figure 3.1**). We posited that this targeted assistance of the paretic ankle's gait functions would facilitate more symmetrical propulsive force generation by the paretic and nonparetic limbs and reduce the energetic burden associated with post-stroke walking, which previous work has shown can be more than 60% more costly [118]. Previous work on wearable assistive robots for persons after stroke has suggested that the timing of PF force delivery during walking could be an important contributor to positive outcomes in this heterogeneous population [119]. Hence, we also evaluated different onset timings of PF force delivery for each individual, hypothesizing that this timing would need to be individualized to optimize outcomes.

Designed to be unobtrusive to the wearer when not powered, the mass of exosuit textile-based wearable components (~0.9 kg) is distributed along the length of the paretic limb similar to a pair of pants. Nonetheless, to understand the net effect of walking with an exosuit powered and assisting the paretic limb, it is necessary to evaluate whether there are effects because of simply wearing the exosuit passively (worn but unpowered). A secondary objective was thus to evaluate the effects of walking with the passive exosuit relative to walking with the exosuit not worn (see Section 3.5.1). Moreover, because one of the compelling

aspects of soft wearable robots, such as exosuits, is their potential to provide gait assistance and, potentially, rehabilitation benefit during community-based walking activities, in addition to treadmill-based biomechanical investigation into the effects of a tethered exosuit, our final objective was to evaluate the effects of exosuit assistance delivered from a first-generation, body-worn (untethered) exosuit prototype during overground walking (see Section 3.5.2). Ultimately, by investigating how individuals with post-stroke hemiparesis respond to exosuit-generated active assistance of ankle PF and DF during treadmill and overground walking, this study serves to define the technology's potential for improving mobility and enabling more effective neurorehabilitation after stroke.

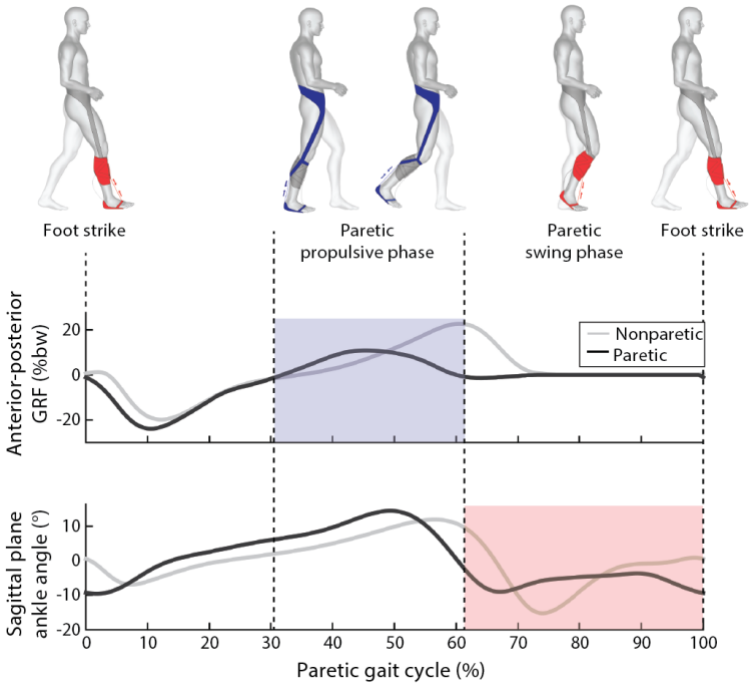

Figure 3.1. Illustration of soft exosuit assistance to augment paretic limb function during hemiparetic walking. Exosuit-generated ankle plantarfexion (PF) and dorsiflexion (DF) forces are designed to restore the paretic limb's contribution to forward propulsion (GRF) and ground clearance (ankle DF angle during swing phase)—subtasks of walking that are impaired after stroke. Post-stroke deficits in these variables are demonstrated through a comparison of paretic (black) and nonparetic (gray) limbs. Means across participants are presented (n=7).

3.2. Materials and methods

In brief, individuals in the chronic phase of stroke recovery participated in evaluating the feasibility of using the tethered exosuit prototype presented in Chapter 2 (see **Figure 2.2**). We expected exosuits to have an immediate effect on key biomechanical subtasks that are impaired after stroke, specifically ground

clearance by assisting ankle DF during swing phase and propulsive force generation by assisting ankle push-off during stance phase (**Figure 3.1**). We focused on the immediate improvements in post-stroke walking observed during exosuit assistance, not on long- term therapeutic changes that may arise from sustained use.

3.2.1. Experimental design

The feasibility of influencing post-stroke walking using a unilateral soft exosuit was evaluated through three experiments. The primary experiment focused on evaluating the effects of a tethered exosuit on post-stroke gait mechanics and energetics during treadmill walking (**Figure 3.2**). This investigation is detailed in this section and focuses on nine individuals in the chronic phase of stroke recovery. In addition, we performed two secondary studies to better define the promise of the exosuit technology. The secondary studies are detailed in Section 3.5.

Given the exosuit design to support the paretic limb's generation of forward propulsion and ground clearance by augmenting the paretic ankle's PF during stance phase and DF during swing phase (**Figure 3.1**), we hypothesized that symmetry of the propulsive force output from the lower extremities would be increased, and the energy cost of walking reduced during exosuit-assisted walking compared to walking with the tethered exosuit unpowered. To validate our hypotheses, we used a 2-day testing protocol to evaluate the effects of two different onset timings of exosuit-generated PF force delivery on participants' forward propulsion, with the peak amplitude of PF force delivered constrained across testing days to 25% of each participant's body weight (**Table 3.2**). This allowed us to determine whether the effects of exosuit on post-stroke walking depend on the timing of ankle PF assistance [119]. Each day tested the effects of a different onset timing (randomized order) to minimize the influence of participant fatigue and after-effects on this evaluation. To minimize the influence of participant day-to-day variability, each testing day measured the effects of the exosuit relative to a daily baseline, with within-session changes from each day compared for each individual.

The two PF force delivery onset timings evaluated occurred during the paretic midstance (early-onset) or terminal stance (late-onset). The same DF assistance profile was used on both testing days. Each testing day included two 8-min testing bouts on a treadmill set to a speed comparable to each participant's usual overground walking speed (**Table 3.1**), with as much rest as needed provided between bouts. The first trial consisted of walking with the exosuit unpowered, and the other trial with the exosuit powered. Participants were allowed to hold a side-mounted handrail during treadmill testing if it was necessary for safety (**Table 3.1**). All participants who used a handrail used one during both bouts of testing and were instructed to use the smallest amount of handrail support needed. Data from the 8th minute of walking from each condition were used for all analyses.

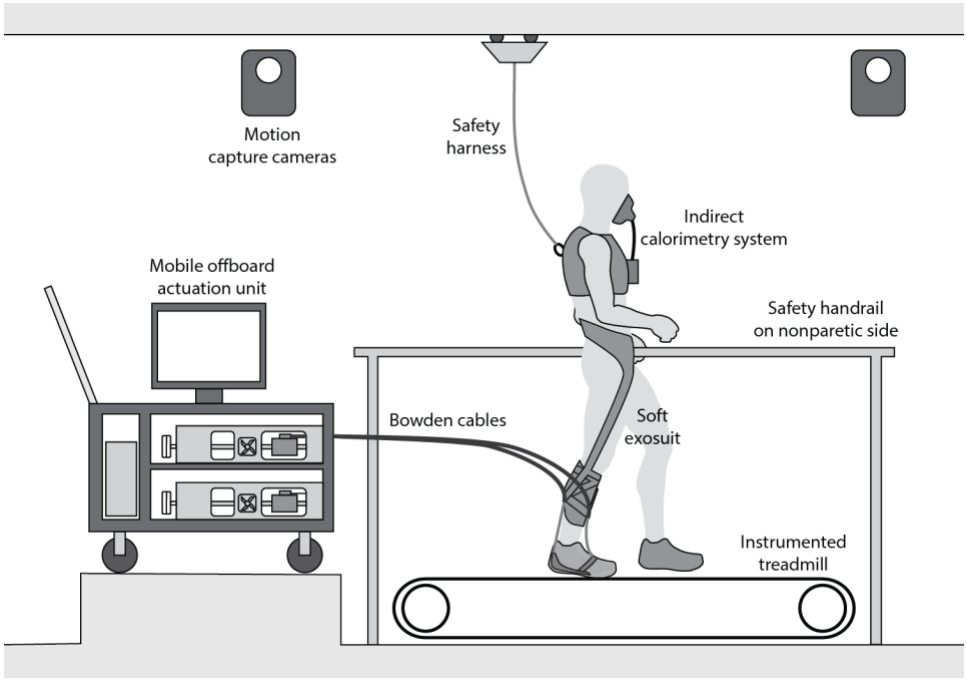

Figure 3.2. Illustration of experimental setup. Ground reaction force and kinematic data were collected concurrently with metabolic data as participants walked on an instrumented treadmill with the exosuit worn either powered (delivering forces generated by an off-board actuation unit) or unpowered. Participants were harnessed, but no body weight was supported. Participants were allowed to hold a side-mounted handrail if necessary for safety.

3.2.2. Participants and inclusion/exclusion criteria

Participants (age, 49±4 years; time since stroke, 4.38±1.37 years; female, 44%; left hemiparetic, 56%; see **Table 3.1** for more details) were recruited from rehabilitation clinics in the greater Boston area. Participant inclusion criteria included the following: age between 25 and 75 years, at least 6 months after stroke, able

to walk independently for 6 min with- out stopping, sufficient passive ankle range of motion with the knee extended to reach a neutral position, and pass cognitive screening. Cognitive screening differed for those with versus without aphasia. Those without aphasia had to score ≥23 on the Mini Mental State Examination (MMSE). Those with aphasia had to score ≥19 on the MMSE, as well as ≥35 on the Auditory Verbal Comprehension section of the Western Aphasia Battery (WAB) and ≥10 on the Sequential Commands section of the WAB. Exclusion criteria included Botox injections within the past 6 months, substantial knee recurvatum during walking, serious comorbidities (including musculoskeletal, cardiac, and neuromuscular, skin, and vascular conditions), inability to communicate and/or be understood by investigators, a resting heart rate outside the range of 50 to 100 beats per minute or blood pressure outside the range of 90/60 to 200/110 mmHg, pain in the extremities or spine that limits walking, and experiencing more than two falls in the past month. Medical clearance and signed informed consent forms approved by the Harvard University Human Subjects Review Board were obtained for all participants.

3.2.3. Overview of soft exosuit controller

The tethered soft exosuit prototype described in Chapter 2 was used for this study, and an iterative, force-based, position controller was developed and implemented to control the exosuit (**Figure 3.3**). Because exosuit-generated force is a composite outcome of the Bowden cable position, the wearer's joint kinematics, and the exosuit-human series stiffness—a parameter that accounts for the mechanical properties of the textile anchors, Bowden cables, and the compliance of the human tissue that supports the textile anchors (**Figure 3.3** (a)) [91], a simple closed loop position controller was not able to deliver consistent assistance force profiles. To overcome this limitation, the exosuit controller iteratively adapted the cable position trajectories. Specifically, the exosuit controller utilized measurements from shoe-mounted gyroscopes to detect key gait events (foot strike and toe off) for each limb (Gait detection algorithm). Exosuit-generated forces were then delivered to the wearer based on the paretic gait cycle calculation (%GC) determined by these gait events. Our preliminary study in Chapter 2 showed that the exosuit gait segmentation algorithm

can robustly detect these key events during both the paretic and nonparetic gait cycles and effectively scale the duration of force delivery on a stride-to-stride basis using the information.

PF force was generated by the exosuit during the paretic stance phase, with the timing of force delivery defined as a percentage of the paretic gait cycle (%GC) and the amplitude of force delivery defined as a percentage of participants' body weight (%BW). The PF controller adapted the baseline cable position and the cable position before and after cable retraction in a manner that tensile force began to be generated at the commanded onset timing. Moreover, it adapted the maximum cable pull position relative to the baseline position such that the peak force magnitude was consistently 25% of the wearers' body weight for each stride. Similarly, the DF controller adapted the baseline DF cable position such that the cable tensile force started to build at a commanded onset timing (paretic foot off and thus the start of swing phase) and diminishes after initial foot contact. The onset timing of PF force delivery and peak amplitude of PF force delivered (constrained to 25%BW) were selected by the research team before testing and controller on a step-to-step basis through adjustments in the commanded cable position based on measurements of delivered force made by a load cell integrated into the exosuit's textiles. The timings of peak PF force and PF force cessation were not directly controlled and varied with the wearer's kinematics (**Figure 3.5** (a)).

A DF cable position command profile was generated as a function of the paretic gait cycle with the onset and off timings of force delivery linked by the controller to the paretic swing phase. More specifically, the amplitude of the DF cable position command was selected by the research team before testing and was set to match the position of a neutral ankle angle, or the smallest ankle PF angle if neutral was not achievable, as identified through visual observation. Unlike the PF controller, as described previously, the maximum DF pull position is fixed to the position of a neutral ankle. With this approach, the amplitude of DF force that was delivered to the wearer during swing phase within and across steps varied with the wearer's gait in a manner that maintained the commanded cable position and thus ankle angle.

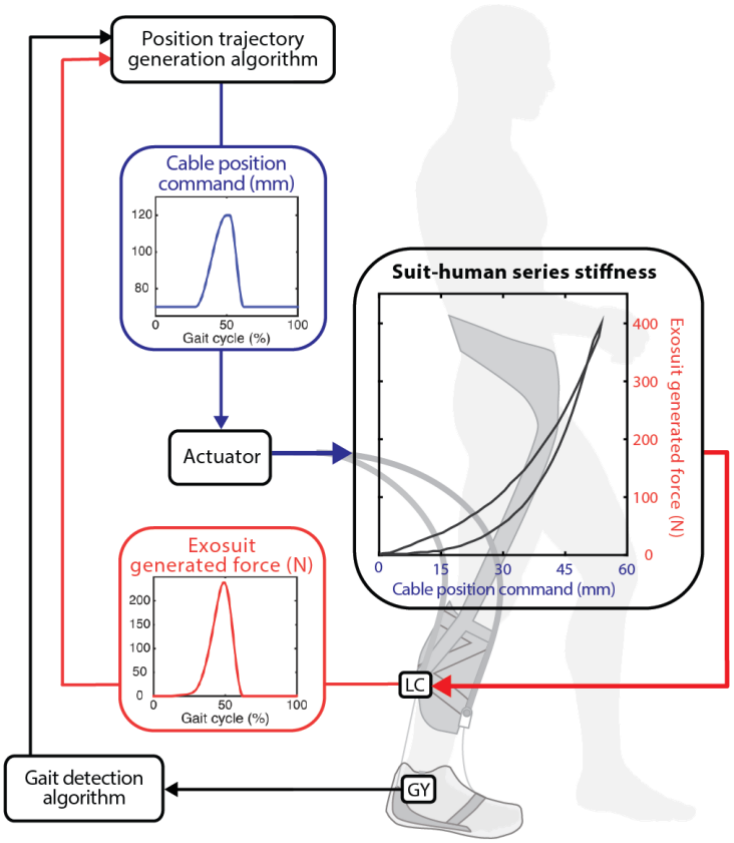

Figure 3.3. Overview of exosuit controller. Commanded position trajectories (blue) translate to exosuit-generated forces (red) based on the exosuit- human series stiffness. This parameter reflects the interaction of the cable position command with the compliance inherent to the textiles, cables, and human tissue. On a step-by-step basis, the timing of exosuit-generated force delivery is controlled as a function of gait subphases identified using shoe-mounted gyroscope sensors (GY). The amplitude of force produced by the exosuit is measured by load cells (LC) that measure the force delivered at the ankle—one for each PF and DF (only PF is shown). The delivered force is continuously monitored, and adjustments are made by the controller to maintain specific features of the delivered force profile.

3.2.4. Clinical evaluations

Treadmill speed was set based on participants' usual overground walking speed. This speed was measured using the 10-m walk test (10MWT). The 10MWT was also used to quantify participants' walking disability [120] and evaluate their ability to safely walk without their regular orthoses, which could not be used with the exosuit because of their restriction of ankle PF. Participants who required the frontal plane ankle support provided by an ankle orthosis for safe ambulation were provided an optional exosuit module that passively controlled ankle in- version. This passive module was used by two participants (**Table 3.1**) during all testing. Participants were allowed to use their regular assistive device (cane) during the 10MWT if they

typically used one for safety. A handrail was provided during treadmill testing for participants requiring one to safely walk on the treadmill (**Table 3.1**).

3.2.5. Motion capture and metabolic data acquisition and analysis

Participants walked on an instrumented split-belt treadmill (Bertec, Ohio, USA) to measure GRFs independently from each limb. There was no barrier between the two treadmill belts, the small gap between the belts was not perceivable during walking, and participants were instructed to walk naturally. GRFs were used to compute paretic limb forward propulsion (PP) and nonparetic limb propulsion (non-PP) and this study's primary kinetic outcome: interlimb propulsion symmetry. PP was defined as the anterior GRF measured during the paretic limb's stance phase, normalized by body weight (%BW) [39], [113], [121]–[124]. Interlimb propulsion symmetry was calculated as follows:

$$Propulsion\ Symmetry = PP/NP \tag{3.1}$$

where non-PP represents the nonparetic limb's propulsive force during its stance phase. For this metric, 1 represents perfect symmetry. Using this metric, the magnitude of propulsion asymmetry was calculated as follows:

$$Propulsion\ Asymmetry = 1 - Propulsion\ Symmetry \tag{3.2}$$

Three-dimensional motion capture (VICON, Oxford Metrics) was used to measure participants' ankle motion during walking, with the peak DF angle during the paretic swing phase serving as this study's primary kinematic outcome. All marker and force data were filtered using a zero-lag, fourth-order, low-pass, Butterworth filter with a 9-Hz optimal cutoff frequency that was selected using a residual analysis algorithm (MATLAB, MathWorks Inc., MA, USA) [125]. Kinetic and kinematic analyses were performed using Visual 3D (C-Motion, MD, USA). The last 15 good strides from each testing condition were extracted for data analysis, with good strides defined as the absence of crossed force plate strikes. Indirect calorimetry (K4b2, Cosmed, Rome, Italy) was concurrently used to measure participants' energy consumption (ml

O2/min) at rest (quiet standing) and during walking, with resting energy consumption subtracted from energy consumption during walking to yield participants' net energy consumption during walking. Participants' net energy cost of walking (EC_{net}) was computed by normalizing net energy consumption by body weight (kg) and walking speed (m/min). Similar to [126], participants' deviation from the normal energy cost of walking was computed as EC_{net}-N where N represents the normal energy cost of walking (0.151 ml O2/kg/m)

3.2.6. Statistical analyses

Interparticipant means and SEs are reported unless otherwise indicated. Peak PP, interlimb propulsion symmetry, peak paretic limb swing phase ankle DF angle, and mass- and speed-normalized energy consumption served as dependent variables because of their popularity and importance in the post-stroke gait rehabilitation literature [3], [22], [25], [34], [113], [118], [119], [121], [127]–[129]. All analyses were directed toward evaluating the exosuit's influence on post-stroke gait. Given previous work positing that the optimal timing of PF force delivery may vary across participants because of post-stroke heterogeneity, paired t tests on individual participant data were used to determine each participant's more effective PF force delivery onset timing in terms of the exosuit's influence on propulsion symmetry. Paired two-tailed t tests subsequently evaluated group-level effects, with PF assistance onset timings individualized. For these analyses, a=0.05 and a Holm-Šídák correction was applied to adjust for multiple comparisons. To evaluate our hypothesis that improvements in propulsion symmetry would contribute to reductions in the energy cost of walking, linear regression measured the relationship between exosuit-induced changes in these two variables. To inform clinical translation, linear regression was also used to determine whether participants' baseline function (walking speed) influenced the effects of the exosuit. To evaluate differences in delivered PF force on the days testing an early-onset and late-onset of PF force delivery, we compared the magnitude of delivered force at each point in the gait cycle using paired t tests. As has previously been done [130], to minimize type 1 error, significance was concluded only if 40 consecutive pairs (4% of the gait cycle) indicated significance at p=0.05.

3.3. Results

3.3.1. Participant baseline characteristics

Participants, on average, were not able to produce sufficient ankle DF to reach a neutral paretic ankle position during swing phase when walking with the exosuit unpowered, with the average peak ankle DF angle during swing phase measured at −1.85±1.98° (1.85° of PF) for the nine participants recruited for this study. Forward propulsion data were not measurable for two participants who walked with a gait pattern that prevented independent measurement of GRFs for each limb by the independent treadmill force plates. The remaining seven participants presented with, on average, 46% less peak paretic propulsion (PP) (11.39±2.31%BW) compared to peak non-PP (20.08±2.03%BW), 52% less PP impulse (1.98±0.38%BW.s) compared to non-PP impulse (4.23±0.21%BW.s), and an energy cost of walking (0.22±0.03 ml O2/kg/m) 46% higher than what has been reported to be normal (0.151 ml O2/kg/m) (54) (See **Table 3.1** for more details).

Table 3.1. Participant baseline characteristics and gait performance

Participant	Side of Paresis	Sex	Age *(y)*	Chronicity *(y)*	Regular AD	Handrail	Walking Speed *(m/s)*	Peak P Ankle Angle *(degrees)*	Peak P AGRF *(%BW)*	Peak NP AGRF *(%BW)*	Cost of Transport *(mL O_2/kg/m)*
01	R	F	30	7.08	AFO	Y	1.05*	-0.02	12.80%	24.57%	0.28
02	L	M	56	3.58	None	N	1.05	4.20	7.09%	20.32%	0.20
03	L	F	52	0.75	Cane	Y	0.53	0.30	3.89%	11.05%	0.28
04	L	M	51	2.83	AFO†	Y	0.93	-14.73	9.48%	17.60%	0.15
05	L	F	37	1.08	AFO†& Cane	N	0.67	0.39	7.64%	17.43%	0.33
06	R	M	44	2.33	None	N	1.29	-2.34	18.77%	22.27%	0.14
07	R	F	46	4.25	None	N	1.3*	-0.80	19.82%	27.34%	0.18
08‡	R	M	61	14.17	AFO	Y	0.92	-7.52			
09‡	L	M	67	3.33	Cane	Y	0.81	3.85			

* The participant's actual 10-m overground walk test speed was higher than the speed tested on the treadmill. Participant #01's actual overground speed was 1.16 m/s, but this participant was not safe walking at this speed on the treadmill. Participant #07's speed was 1.72 m/s, but this speed was beyond the capabilities of the electromechanical actuator used for this study.

† Participant #04 typically used a foot-up brace. Participant #05 used a custom brace that supported frontal plane motion. ‡GRF data unavailable.

Abbreviation: AD, assistive device; P, paretic; NP, nonparetic; AGRF, anterior GRF; F, female; M, male; Y, yes; N, no.

3.3.2. Effective targeting of paretic limb ground clearance and forward propulsion deficits

On average, participants walked with 5.33±0.91° more peak ankle DF angle during swing phase (p<0.001, effect size (ES)=1.96) with the tethered exosuit powered (3.49±1.52°) versus unpowered (−1.85±1.98°) (**Figure 3.4** (a)). This increase was six times larger than the 0.90° minimal detectable change (MDC) score reported for this key metric of swing phase gait function (55). For all subsequent analyses, which are focused on the exosuit's effects on propulsion and walking economy, only data from when the onset timing of PF force delivery was tuned for each participant to their more effective timing were used (see the following "PF assistance timing" section). Participants' peak PP increased by 11±3% (p=0.009, ES=1.44) when walking with the exosuit powered (12.66±2.35%BW) versus unpowered (11.39±2.31%BW)—a change 1.6 times larger than the 0.80%BW MDC reported for this variable [128]. Concurrently, participants' energy cost of walking was reduced by 10±3% (p=0.009, ES=1.42) when walking with the exosuit powered (0.1979±0.0218 ml O2/kg/m) versus unpowered (0.2204±0.0275 ml O2/kg/m). These improvements ultimately contributed to a 20±4% reduction in interlimb peak propulsion asymmetry (p=0.002, ES=1.93; **Figure 3.4** (b)), a similar 19±8% reduction in propulsion impulse asymmetry (p=0.021, ES=1.19), and a walking economy 32±9% closer to the normal walking economy of 0.151 ml O2/kg/m (p=0.009, ES=1.81; **Figure 3.4** (c)). A subgroup analysis of exosuit-induced changes in propulsion asymmetry for individuals who used (n=3) and individuals who did not use (n=4) a handrail during testing revealed that both groups reduced propulsion asymmetry by a similar magnitude (handrail group %Δ, −22.8±4.3%; no handrail group %Δ: −17.4±5.5%; p=0.45).

Across participants, relative improvements in walking economy were highly related to relative improvements in propulsion symmetry (R_2=0.89, F(1,5)=41.09, p=0.001; **Figure 3.4** (d)). Although all participants presented with an improvement in propulsion symmetry, slower participants presented with the largest relative gains (R_2=0.63, F(1,5)=8.50, p=0.03; **Figure 3.4** (e)).

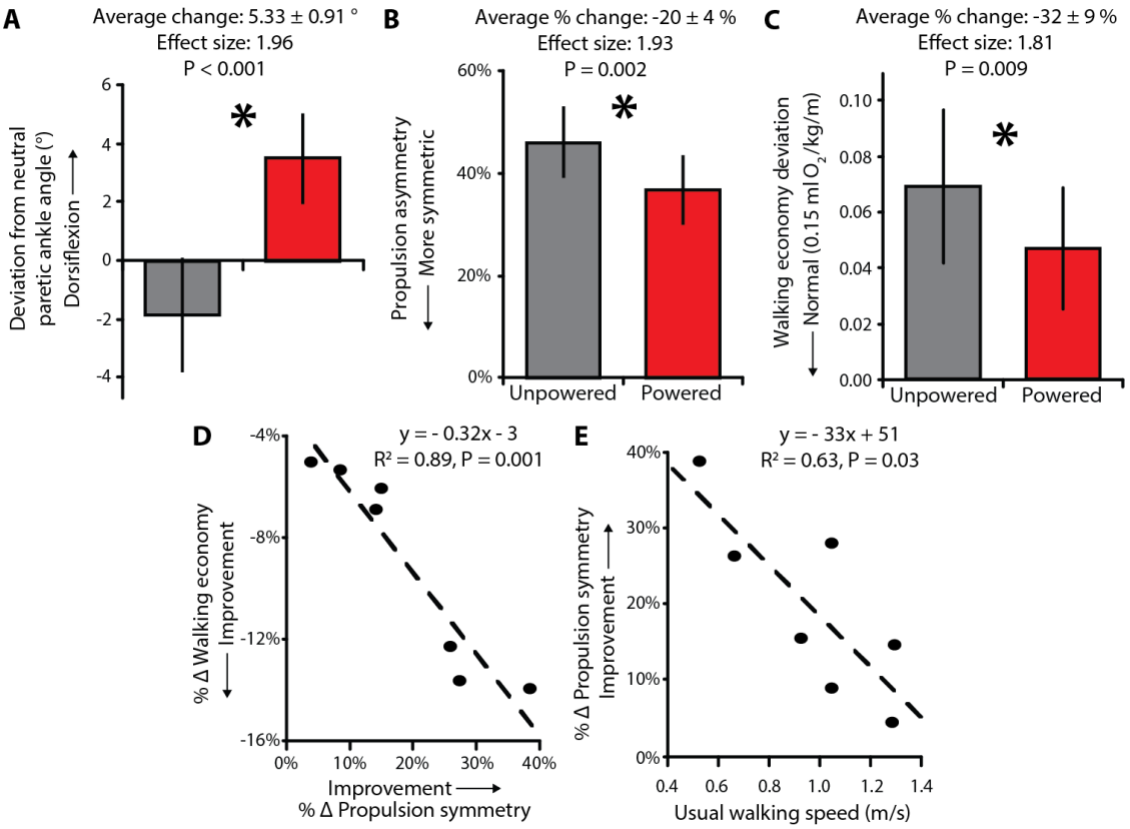

Figure 3.4. Exosuit-induced changes in post-stroke gait mechanics and energetics. Changes in (a) peak paretic ankle DF angle during swing phase (n=9; p<0.001, paired t test), (b) interlimb propulsion asymmetry (perfect symmetry=0%; n=7; p=0.002, paired t test), and (c) walking economy (normal walking economy=0%; n=7; p=0.009, paired t test) during walking with the exosuit powered versus unpowered. Relationship between (d) relative changes in propulsion symmetry and walking economy (correlation: n=7, p=0.001) and (d) participants' usual walking speed and relative change in propulsion symmetry (correlation: n=7, p=0.03). Means and SE are presented in (a) to (c). *: p<0.05.

3.3.3. Exosuit-generated assistive forces

The reliable delivery of exosuit-generated forces was evidenced in low variability of the prescribed exosuit parameters within and across the 2-day testing protocol conducted to evaluate the differential effects of an early-onset versus late-onset timing of ankle PF force. Across the 2 days of testing, the average±SE of the SD observed for PF onset, DF onset, and DF off timings were 1.51±0.26%GC, 2.71±0.16%GC, and 0.91±0.20%GC, respectively. Similarly, the average±SE of the SD in peak PF force was 1.15±0.08%BW (**Figure 3.5** (b)). Further, as prescribed, exosuit-generated peak PF forces averaged 25.02±0.92%BW, with an SE across days of 0.13%BW (**Figure 3.5** (b)). The peak PF assistive torque delivered to participants thus approximated 0.15 Nm/kg (**Table 3.2**), which is 12% of the average peak paretic ankle moment that

was observed across participants (1.26±0.13 Nm/kg) and 9% of the average peak nonparetic ankle moment (1.68±0.12 Nm/kg).

Table 3.2. Exosuit plantarflexion assistive force

Participant	Participant parameters		Exosuit PF force parameters		
	Weight (kg)	Peak paretic PF ankle moment (Nm/kg)	Commanded peak PF force (N)	PF assistance moment arm (m)	Delivered peak PF torque (% of peak paretic PF ankle moment)
1	49	1.01	120	0.066	16%
2	73	1.47	180	0.059	10%
3	90	1.09	220	0.055	12%
4	79	1.21	195	0.075	15%
5	73	0.78	180	0.073	23%
6	80	1.88	200	0.062	8%
7	60	1.41	150	0.065^	12%

^ Moment arm data for this participant were not available. Given the low variability in moment arm values across the other 6 participants, the average across participants (0.065 m) was used for this participant.
Ŧ Exosuit peak PF torque values are computed as (Commanded Peak PF Force x PF Moment Arm)/ Weight)

3.3.4. Different PF assistance onset timing and their impact on biomechanical outcomes

The only parameter manipulated across the 2 days of testing was the onset timing of PF force delivery. Across participants, a difference in baseline gait performance (walking with the exosuit unpowered) across these 2 days of testing was not observed for either primary variable of interest (p>0.05). For each participant, the effect of an onset timing during terminal stance (late-onset) was compared to the effect of an onset timing about 10% earlier in the gait cycle, during midstance (early-onset). The exact timing varied across participants depending on the duration of each participant's paretic stance phase, with the actual commanded PF onset timings tested across participants averaging 36.9±0.76%GC and 27.5±1.94%GC for late- and early- onset timings, respectively (**Figure 3.5** (a)). The order that these onset timings were tested was randomized across participants.

An early-onset timing of PF force delivery generated higher PF forces between 19% and 47% of the paretic gait cycle as compared to a late-onset timing (p<0.05; **Figure 3.5** (a)), demonstrating our ability to control the delivery of exosuit-generated forces. As previously described, exosuit-generated peak PF forces did not

differ between days (p>0.05; **Figure 3.5** (a)). As hypothesized, the effect of exosuit-generated PF forces on participants' interlimb propulsion symmetry depended on whether participants received an early- or late-onset timing of PF force delivery (**Figure 3.5** (c)). More specifically, four participants benefited more from a late-onset timing of PF force delivery and two benefited more from an early-onset timing. One participant benefited equally from both onset timings. Three of four who benefited more from a late onset of PF force delivery experienced greater propulsion asymmetry with an early-onset timing of PF force, whereas no participants experienced negative effects from a late-onset timing of PF force.

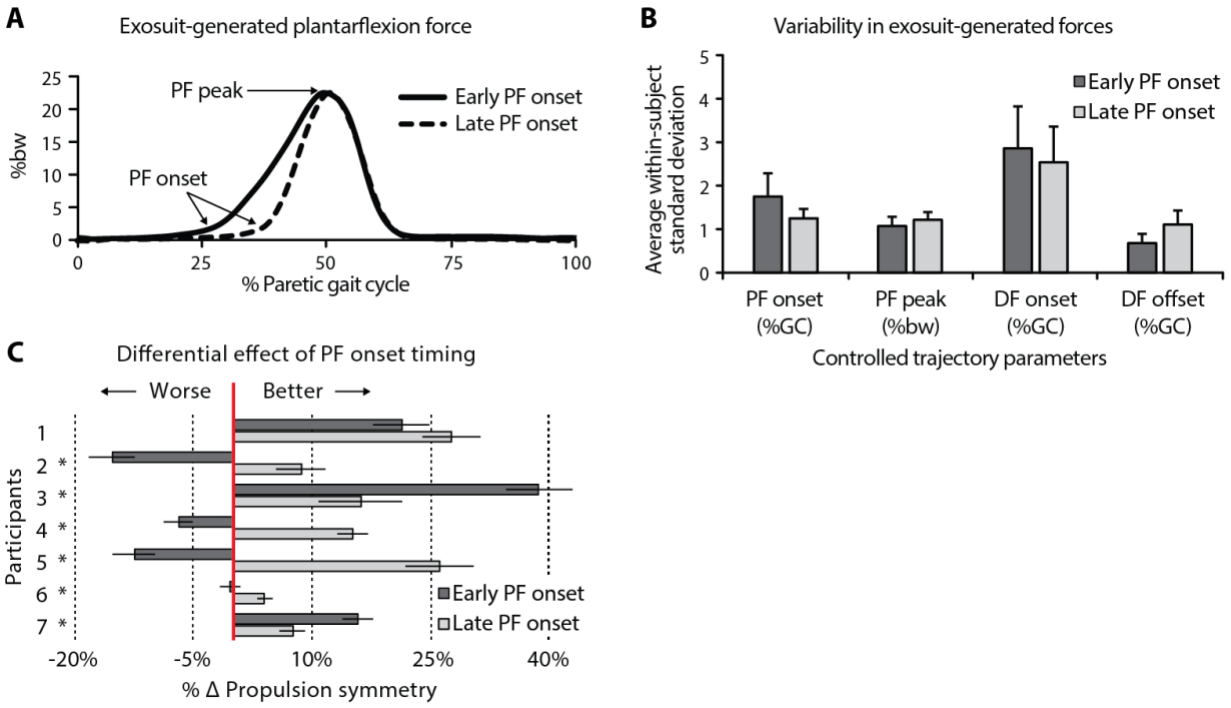

Figure 3.5. Exosuit controller performance during post-stroke treadmill walking. (a) Average exosuit-generated PF forces as a function of the paretic gait cycle (x axis). Two ankle PF force delivery onset timings were evaluated. PF forces were delivered during terminal stance or about 10% earlier in the paretic gait cycle, during midstance. (b) Variability in commanded force parameters (x axis). The force features prescribed by the controller on a step-by-step basis included the onset timing of PF force (PF onset), the peak amplitude of PF force (PF peak)—constrained to 25%BW, the onset timing of DF force (DF onset), and the off time of DF force (DF offset). (c) Relative changes in participants' interlimb propulsion symmetry based on the onset timing of exosuit-generated PF forces. Four participants benefited more from a late onset of PF force timing, two participants benefited more from an early onset, and one participant (#1) benefited equally from both timings. Means and SE are presented in (b) and (c). *p<0.05.

3.4. Discussion

Exosuits function in synchrony with the paretic limb of persons after stroke to overcome deficits in forward propulsion and ground clearance during hemiparetic walking, ultimately facilitating more economical

locomotion. Using a tethered exosuit research platform, this study demonstrates the feasibility of unilateral assistance of paretic ankle function through a soft human-machine interface and the efficacy of minimal assistance (~12% of biological PF torques) delivered through this interface. Moreover, using a first-generation, untethered exosuit, this study demonstrates the potential for exosuits to provide gait assistance and training during overground walking. These findings support future research and development of gait-restorative exosuits, with studies using optimized body-worn actuators and evaluating clinic- and community-based outcomes especially warranted.

Impaired forward propulsion is posited to be a major contributor to walking dysfunction after stroke [14], [23], [34]–[36], [112], [131]–[133], with the magnitude of interlimb propulsion asymmetry differentiating individuals as limited community versus community ambulators [134]. Recent work has also linked gains in propulsion to improvements in the long- distance walking ability of persons after stroke [121], a factor identified by individuals in the chronic phase of recovery as limiting engagement at home and in the community [9]. Commonly prescribed AFOs have been shown to restrict ankle range of motion and impair the generation of forward propulsion during walking [41], effects shown to increase the energetic demands of walking [135]. A high energy cost of walking has been posited to be a primary contributor to physical inactivity in older adults [136] and persons with neurologically based walking deficits [137]–[139], as well as a predictor of impending declines in walking speed [140]—a powerful marker of reduced health and mobility [120], [141] and mortality [142]. Because it targets deficits in propulsion and improves walking economy, the exosuit technology is a promising alternative to the passive assistive devices typically used by ambulatory individuals with walking-related disabilities [143].

An existing alternative to AFOs is functional electrical stimulation (FES). Like exosuits, FES systems provide gait assistance through a lightweight and unobtrusive human-device interface; however, exosuits apply assistive joint torques in parallel with the underlying impaired musculature, whereas FES directly activates the impaired musculature. One limitation of FES that is directly addressed by exosuits is the high fatigability, weakness, and reduced neuromuscular capacity of the paretic limb musculature. By functioning

in parallel with the paretic limb, exosuits provide supplemental assistive forces and may thus be better suited for use by individuals with larger impairments or during activities requiring longer walking durations such as community walking or gait training. Future study of how exosuits and FES may be optimally used to assist hemiparetic gait is needed. The results of this study suggest that successful translation of the exosuit technology may require refinement of selection criteria to identify appropriate candidates. For example, the findings of this study suggest that lower-functioning individuals may benefit more from exosuit intervention than higher-functioning individuals (**Figure 3.4** (e)). Although this requires validation, it supports the potential use of the exosuit in more disabled cohorts after stroke. It is also not clear if higher-functioning participants could have seen added benefit with a higher amount of assistance, assistance at joints other than the ankle, or with directed training. Further investigation will be necessary.

A detailed analysis of the biomechanical mechanisms underlying exosuit-induced improvements in post-stroke walking will be necessary to inform the development of future systems. Given the heterogeneity of post-stroke motor impairment, customizable solutions to the particular biomechanical needs of wearers and the goals of rehabilitation are needed to enable widespread use [144]. For example, the exosuit's effects appeared dependent, in part, on the onset timing of exosuit-generated PF force, with the optimal timing varying across participants (**Figure 3.5**). Although this finding requires validation, it is consistent with the heterogeneous nature of post-stroke motor impairment and highlights the importance of understanding the interaction between human and machine when designing and implementing controllers for gait-restorative wearable devices [114]. On the basis of a biomechanical understanding of the role of the plantarflexors during walking, an earlier-onset timing of plantarflexor force generation would be beneficial to participants requiring assistance to control the anterior translation of the tibia over the foot, whereas a later-onset timing would be beneficial in those requiring assistance with push-off. It is likely that individuals after stroke will require some degree of assistance with both of these important functions of the plantarflexors; however, our finding that mistimed assistance of PF force delivery could negatively affect propulsive force generation highlights the need for individualization of timing. The personalization of wearable active assistive devices

will require substantial investigation into biomechanical markers that can accurately predict optimal assistive strategies. On the basis of the aforementioned biomechanical framework, variables such as stance phase control of the tibia and ankle PF velocity may be promising indicators of effective PF assistance onset timing using our ankle exosuit. Further study and detailed biomechanical analyses are required.

Exosuit-induced improvements in post-stroke gait were observed within minutes of powering the device and were comparable to, if not greater than, therapeutic gains observed after single-session [145], [146] and multisession [21], [39], [121], [147] clinical gait training programs. Although this study does not demonstrate a therapeutic effect, several benefits can be derived from such an immediate and substantial in- crease in post-stroke walking performance. For example, an immediate improvement in walking capacity may increase the opportunity for walking practice of higher intensity and variability—key ingredients for effective neurorehabilitation [51], [139], [148]. Improved walking capacity may improve self-efficacy and reduce barriers to community engagement [9], [149], [150]. Together, these factors may facilitate better leveraging of key plasticity mechanisms such as salience, intensity, and repetition during gait training [148], [151], [152]. Moreover, as observed with rehabilitation approaches centered on targeting ankle deficits during post-stroke gait training [113], [118], [153], the exosuit technology's ability to facilitate walking practice of more normal gait mechanics also has the potential to promote locomotor restoration rather than compensation. For this proof-of-principle investigation, participants received no instruction on how to walk with the exosuit. Further study on how training may enhance exosuit-assisted walking is warranted.

Although this investigation's primary finding is an improvement in post-stroke gait mechanics and energetics during exosuit-assisted walking versus walking with an exosuit unpowered, our secondary study demonstrating that wearing a passive exosuit did not significantly influence participants' walking (See Section 3.5.1) is equally important for a complete appreciation of the exosuit technology. Together, these findings demonstrate that exosuits are capable of providing targeted gait assistance through a human-machine interface that imposes minimal biomechanical and metabolic penalties when worn unpowered.

The tethered exosuit research platform used for this study provided a suitable test bed for demonstrating proof of principle of the exosuit concept; however, recognizing that there are differences between treadmill and overground walking after stroke, it was also necessary for us to evaluate the effects of exosuit assistance during overground walking with an untethered exosuit. Despite using a non-optimized actuator pack, we observed improvements in PP and ground clearance that were com- parable to what was observed during treadmill walking. The actuator data collected from this study will enable optimization of this body-worn system to make it suitable for both clinic and free-living settings. We estimate that the total mass of these systems will be <4 kg, including batteries, with the majority worn discretely around the waist to minimize its impact on natural walking behavior [154].

This study revealed the potential importance of individualizing the timing of exosuit-generated PF assistance. Because of logistical constraints, we could only evaluate two PF assistance onset timings. Although the two onset timings that were tested may not have been optimal for individual patients, they allowed us to evaluate the effects of PF assistance during two distinct phases of the gait cycle. In addition, we did not evaluate the effects of manipulating other exosuit parameters, such as the amplitude of assistance. Although future work elucidating optimal parameter tuning will be necessary to inform translation, the present study demonstrates the potential of tuning the exosuit technology to meet the needs of different gait presentations.

Considering the day-to-day variability inherent in the outcomes used in this study, a 2-day testing protocol to evaluate the differential effects of PF assistance timing is a potential limitation of this study. Nonetheless, this experimental approach was deemed necessary to minimize the burden on participants and the fatigue inherent to longer testing sessions. It is important to note that we made efforts to minimize the influence of participant day-to-day variability on this evaluation. For example, our between-day analyses compared the effects of the exosuit relative to each day's baseline performance, which we demonstrated did not significantly vary across participants across the 2 days of testing.

For safety, three participants required use of a handrail during treadmill testing. Although it is possible that these participants may have modulated the amount of body weight supported by the handrail between testing conditions, our demonstration that the exosuit-induced change in propulsion symmetry did not differ between individuals who did and did not use a handrail reduces this concern, as does our finding of improvements in PP during overground walking without a handrail. These findings are consistent with previous work that has shown that in individuals after stroke, changes in handrail forces are unrelated to the mechanisms used to increase forward propulsion (89). Nonetheless, future work quantifying changes in handrail support during exosuit-assisted walking may be revealing. In addition, studies that evaluate the long-term changes in post-stroke gait because of extended use for gait training, on don/doff times, and on the robustness of the exosuit's effects to variability in exosuit placement are warranted before the utility of exosuits as assistive and rehabilitation robots is fully realized.

3.5. Supplementary studies

3.5.1. Impact of inactive exosuit on forward propulsion and metabolic expenditure

To evaluate if an exosuit worn unpowered would influence walking after stroke, five individuals in the chronic phase of stroke recovery participated in evaluating the effects of wearing an exosuit unpowered compared to not wearing the exosuit. Two primary outcomes were evaluated: (1) the propulsive force generated from each limb and (2) the energy cost of walking. Participants were 53±6 y old, 5.1±0.8y since stroke, 40% female, and 60% left hemiparetic. Testing for this secondary study consisted of two 8-min walking bouts on an instrumented treadmill at participants' overground self-selected walking speed, one bout per condition. The treadmill recorded ground reaction force data and indirect calorimetry was used to measure energy consumption. Paired t-tests were used to evaluate differences between conditions. This study revelated that walking with the passive exosuit did not significantly modify participants' generation of propulsion from their paretic and nonparetic limbs, nor energy cost of walking (**Figure 3.6**).

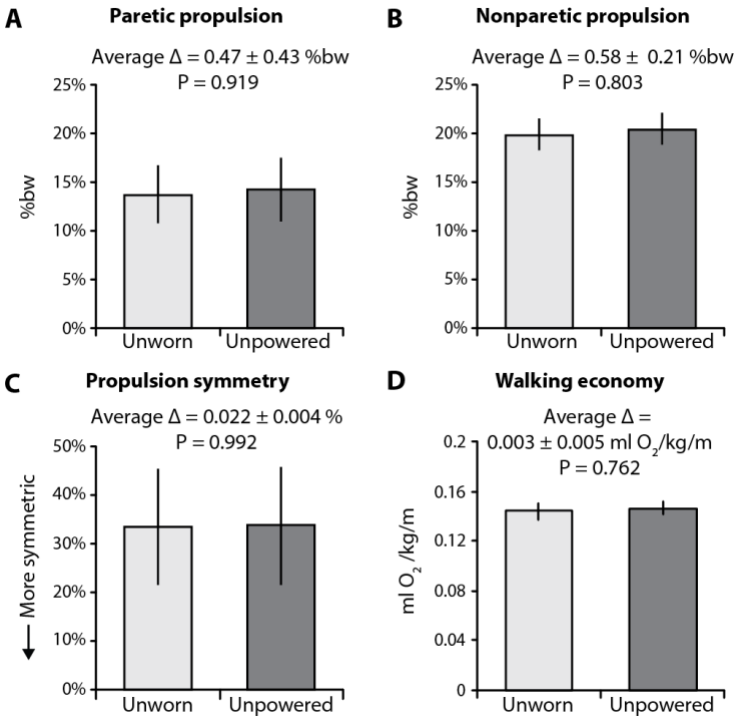

Figure 3.6. Effects of wearing a passive exosuit on post-stroke propulsion and energy expenditure. (a) Paretic propulsion, (b) nonparetic propulsion, (c) propulsion asymmetry, and (d) walking economy (energy expenditure per meter ambulated) for unworn and unpowered exosuit conditions. Means and standard error are presented. N=5.

3.5.2. Proof of principle: overground walking with an portable exosuit prototype

To evaluate if overground gait assistance delivered from a portable exosuit would improve paretic limb ground clearance during swing phase and propulsion during stance phase, nine individuals in the chronic phase of stroke recovery participated in evaluating the effects of wearing an portable exosuit prototype powered compared to unpowered. The portable exosuits prototype used for this study were developed based on the actuation module generated for healthy individuals [87]. These were comparable to the tethered exosuits used for treadmill walking, except that a 3.2 kg actuator and battery pack was mounted to the waist belt and the proximal attachment of the PF module was moved from the waist belt to the calf wrap (**Figure 3.7**). Two primary outcomes were evaluated: (1) peak paretic ankle dorsiflexion angle during swing phase and (2) interlimb propulsion asymmetry. This testing was conducted overground. Participants were 49±13 y old, 4.7±1.7 y since stroke, 44% female, and 56% left hemiparetic. Testing for this study consisted of participants walking at a self-selected, comfortable walking speed over two ground-level force-plates that collected ground reaction force data (AMTI OR-6 force plates) until at least five usable strides were

captured per condition. Concurrently, 3D ankle joint kinematics were measured by a motion-capture system. Paired t-tests were used to evaluate differences between conditions.

Consistent with our findings on the treadmill, walking overground with an untethered exosuit (**Figure 3.7** (a)) powered versus unpowered resulted in 4.9° more peak ankle DF angle during swing phase (p<0.002; **Figure 3.7** (b)), an increase from −4.13±1.82° (4° of PF) to 0.74±1.51° (0.74° of DF); 13% more peak PP, an increase from 10.3±0.60%BW to 11.6±0.60%BW (p=0.053); and 14% more PP impulse, an increase from 2.0±0.10%BW.s to 2.2±0.10%BW.s (p=0.029). Ultimately, a 16.3±6.8% reduction in propulsion asymmetry was observed during overground walking with versus without exosuit assistance (p=0.045; **Figure 3.7** (c)).

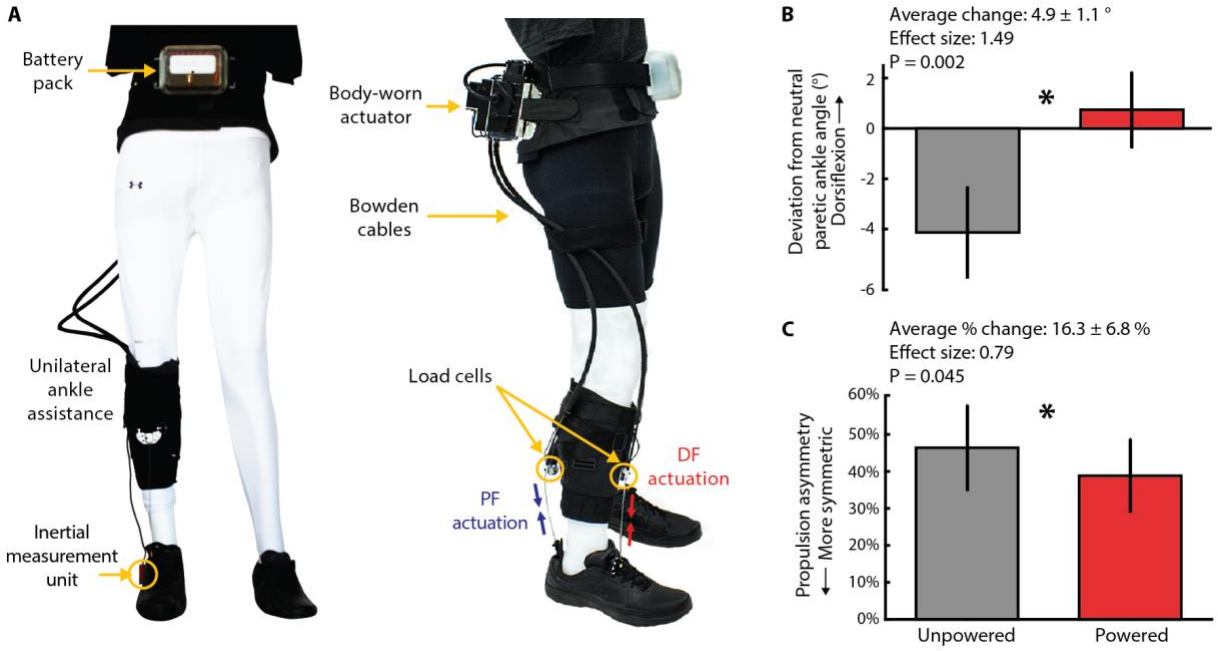

Figure 3.7. Overview of an untethered, unilateral, ankle-assisting exosuit prototype adapted for overground walking. (a) Mechanical power generated by a 2.63-kg actuator mounted posteriorly on the waist belt is transmitted to the wearer via cable-based transmissions. A 0.56-kg battery is attached anteriorly on the waist belt. The contractile elements of the exosuit are located anterior and posterior to the ankle joint and assist ankle DF and PF, respectively. Improvements in (b) peak paretic ankle DF during swing phase (n=9; p=0.002, paired t test) and (c) interlimb propulsion asymmetry (n=9; p=0.045, paired t test) during overground walking are presented. Means and SE are presented. *p<0.05.

Chapter 4.

Reducing compensatory gait patterns with tethered soft exosuit

4.1. Introduction

In the previous chapters, we presented the initial prototype of soft exsouit that transmits mechanical power generated by an off-board actuation unit to the paretic ankle using Bowden cables (Chapter 2), and demonstrated the exosuits can overcome deficits in paretic limb forward propulsion and ground clearance, ultimately reducing the metabolic cost of hemiparetic walking (Chapter 3). These results demonstrated that exosuit could improve impaired ankle mechanics and inefficient gait energetics post-stroke. The other emblematic characteristics of post-stroke gait are compensatory gait patterns such as hip hiking and circumduction [14], [16], [17] causing a slow, metabolically inefficient gait and an increased risk of falls [3], [12], [22], [133], [155]–[157]. Therefore, there is a need to investigate strategies for helping patients reduce their impairments and compensations.

The goal of this chapter was therefore to investigate the effects of exosuit assistance on common post-stroke gait impairments and compensations such as hip hiking and circumduction. We hypothesized reduced hip hiking and circumduction and more symmetrical spatiotemporal gait parameters in persons in the chronic phase of stroke recovery walking with versus without exosuit assistance. Furthermore, previous investigators have postulated that hip hiking and circumduction are secondary gait deviations used to achieve ground clearance during the paretic swing phase [14], [16], [158]. Thus, we also tested the hypothesis that reduced gait compensations would result from the effects that exosuit assistance would have on swing phase ankle dorsiflexion and knee flexion. To this end, we analyzed the dataset collected from the experiment in Chapter 3 for spatiotemporal gait metrics, joint kinematics, and ultimately gait compensations such as hip hiking and circumduction.

4.2. Materials and Methods

4.2.1. Data collection and analysis

This study builds on our previous experiment in Chapter 3 by evaluating the effects of exosuit assistance on compensatory gait patterns such as hip hiking and circumduction and other kinematic and spatiotemporal variables (See Section 3.2 for experimental design). For a focused analysis on hip hiking and circumduction, one participant from the nine individuals participated in the experiment (participant 8 in **Table 2.1**) were excluded from analysis because of one's crouch gait with flexed knee joints throughout entire gait cycle, another compensatory gait pattern outside hip hiking and circumduction. See **Table 2.1** for other participants' demographics. Furthermore, since Chapter 3 demonstrated that the more effective onset timing varied across participants, and presented the changes in the metabolic cost of walking from individualized onset timings selected based on the timing that produced the largest improvement in forward propulsion symmetry [117], the present study used the same individualized timings.

To calculate circumduction, the center of gravity (CoG) of the foot taken from the link-segment model generated based on motion capture data through Visual3D (C-Motion, Rockville, MD) was used. The

difference between the position of the foot's CoG during stance phase and its maximum lateral displacement during swing phase defined the severity of circumduction (**Figure 4.1**(a)) [14], [159]. To calculate hip hiking, the vertical position of the ASIS marker calculated during quiet standing was compared with the maximum vertical position during swing phase (**Figure 4.1**(b)). Similar to previous work [159] the difference in vertical position of the ASIS marker at these two points defined the severity of hip hiking. These variables were measured bilaterally. Due to obstructed markers during data collection for some individuals, although the circumduction analyses included all 8 individuals studied, the paretic hip hiking analyses included only 7 and the nonparetic hip hiking analyses included only 6.

Spatiotemporal gait metrics were calculated using kinematic gait events. The temporal metrics calculated were the following: stance time, swing time, step time, and stride time. Temporal measurements were normalized by stride time and expressed as a percentage of the stride cycle. The spatial measurements calculated were the following: step length, step width, and stride length. Sagittal plane kinematics were used to quantify peak knee flexion and peak ankle dorsiflexion angles during swing phase for both the exosuit unpowered and powered conditions. For consistency across participants, data from the final 30 strides recorded during each condition were used for generating all variables of interest.

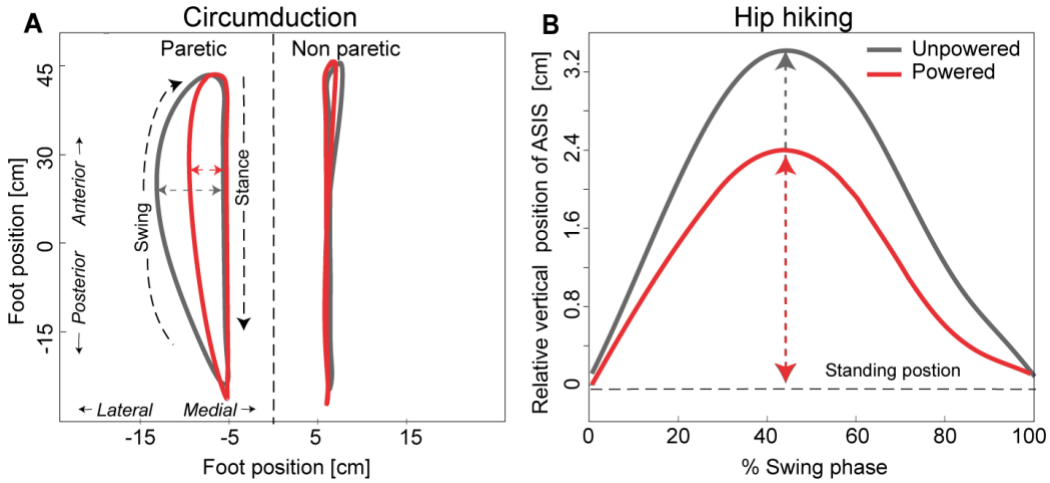

Figure 4.1. Circumduction and hip hiking for a representative participant during walking with the exosuit unpowered and powered. (a) The medial/lateral (x-axis) and posterior/anterior (y-axis) motion of the CoG of the paretic and nonparetic foot during their respective gait cycles. Stance and swing phase are denoted. Circumduction is defined as the maximum lateral difference of the CoG during stance and swing phase. (b) Hip hiking was measured during the paretic limb's swing phase (x-axis) as the difference between the vertical position of the paretic anterior superior illiac

spine (ASIS) during walking and its position during quiet standing (y-axis). A y-axis value of "0" indicates that the ASIS position during walking was the same as the position during quiet standing. The maximum vertical position of the ASIS during the swing phase was used in the analyses.

4.2.2. Statistical analysis

Statistical analyses were conducted in SPSS version 23. Unless otherwise indicated, inter-participant means and standard errors are reported. Paired t-tests were used to compare the exosuit unpowered and exosuit powered conditions at both the group and individual levels. Pearson correlation analyses measured the relationships between hip hiking, circumduction, swing phase peak knee flexion, and swing phase peak ankle dorsiflexion. Linear regression was subsequently used to determine the independent contribution of exosuit-induced changes in each ankle dorsiflexion and knee flexion to changes in each hip hiking and circumduction. Statistical significance level was set at p=0.05.

4.3. Results

4.3.1. Baseline characteristics

Walking with the exosuit unpowered, participants showed, on average, paretic limb hip hiking of 3.65± 0.77cm and circumduction of 4.83±0.71cm. On the nonparetic side, 0.69±0.17cm of hip hiking and 3.15± 0.69cm of circumduction were observed. Participants walked with a mean stride length of 1.16±0.07m and stride time of 1.22±0.06secs. Paretic step length was 56±5cm and step width was 16±1cm. On the nonparetic side, step length and width were, respectively, 58±4cm and 16±1cm. Of the paretic gait cycle, participants spent 35±2% in swing phase and 65±2% in stance phase. Of the nonparetic gait cycle, 29±2% was in swing phase and 71±2% was in stance phase. During paretic swing phase, the peak flexion angle of the knee was 43.4±3.4 degrees and the peak ankle dorsiflexion angle was -0.5±2.1 degrees (i.e., the ankle was plantarflexed). During nonparetic swing phase, these values were, respectively, 60.9±2.6 degrees and 1.7±1.9 degrees for the knee and ankle.

4.3.2. Changes in compensatory gait patterns spatiotemporal and kinematic variables

Compared with walking with the exosuit unpowered, walking with the exosuit powered reduced hip hiking by an average 27±6% (p=0.004) on the paretic side (**Figure 4.2**(a)). On the nonparetic side, changes in hip hiking between the powered and unpowered conditions were not observed (p=0.935). Compared with walking with the exosuit unpowered, walking with the exosuit powered reduced circumduction by an average 20±5% (p=0.004) on the paretic side (**Figure 4.2**(c)). On the nonparetic side, changes in circumduction were not observed (p=0.337). At the individual level, each participant presented with a significant decrease in paretic hip hiking (**Figure 4.2**(b)), circumduction (**Figure 4.2**(d)), or a reduction in both hip hiking and circumduction.

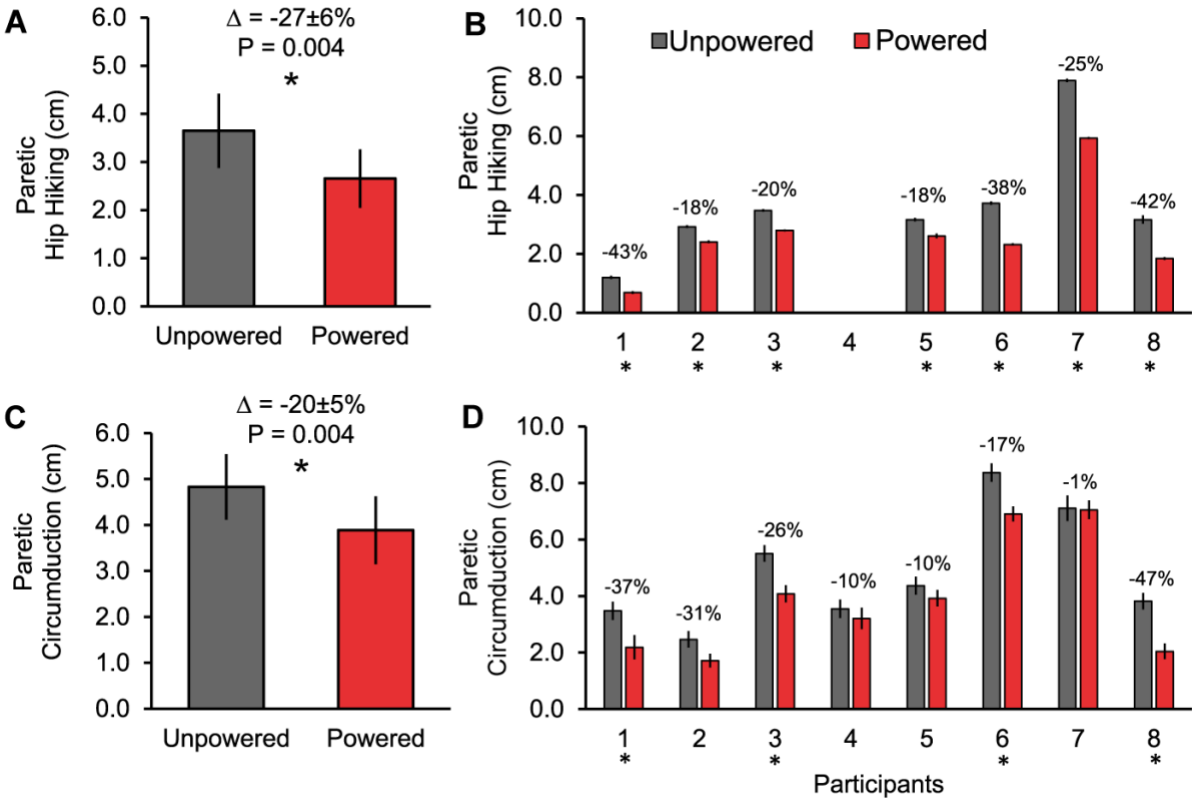

Figure 4.2. Group statistics and individual data in paretic limb hip hiking and circumduction during exosuit unpowered and powered walking conditions(a) Group statistics in paretic limb hip hiking, (b) individual data in paretic hip hiking, (c) group statistics in paretic circumduction, (c) individual data in paretic circumduction. Paired t tests were conducted at the group and individual levels. For panels (a) and (c), a significant difference between the exosuit powered and unpowered conditions is indicated by an asterisk. For panels (b) and (d), an asterisk located under the participant's number indicates a significant between-condition difference for that individual.

Examination of changes in spatiotemporal variables resulting from exosuit assistance revealed a significant increase (p=0.002) in the nonparetic step length during the exosuit powered versus unpowered conditions (**Table 4.1**). Examination of ankle and knee kinematics revealed that only the peak ankle dorsiflexion angle during swing phase increased (p=0.002) during the exosuit powered versus unpowered conditions (**Table 4.2**).

Table 4.1. Spatiotemporal parameters

	Unpowered	**Powered**	***p***		**Unpowered**	**Powered**	***p***
Swing time (%GC)				**Step length (m)**			
Paretic	35.1±2.1	35.2±1.9	0.975	Paretic	0.56±0.05	0.57±0.05	0.612
Nonparetic	29.3±1.5	29.5±1.4	0.376	Nonparetic	0.58±0.04	0.60±0.04	0.002
Stance time (%GC)				**Step width (m)**			
Paretic	64.9±2.1	65.0±1.9	0.878	Paretic	0.16±0.01	0.15±0.01	0.092
Nonparetic	70.8±1.5	70.6±1.4	0.433	Nonparetic	0.16±0.01	0.14±0.01	0.136
Step time (%GC)				**Stride length (m)**	1.16±0.07	1.14±0.08	0.148
Paretic	53.9±1.7	53.4±1.7	0.137	**Stride time (s)**	1.22±0.06	1.25±0.07	0.193
Nonparetic	46.1±1.7	46.6±1.7	0.137				

Table 4.2. Swing phase kinematic parameters

	Unpowered	**Powered**	***p***
Peak knee flexion (°)			
Paretic	43.36±3.42	44.98±3.58	0.323
Nonparetic	60.86±2.64	60.85±1.97	0.994
Peak dorsiflexion (°)			
Paretic	-0.52±2.06	4.26±1.84	0.002*
Nonparetic	1.73±1.88	2.04±1.88	0.512

4.3.3. Kinematic Contributors to Reductions in Hip Hiking and Circumduction

Bivariate correlation analyses of the relationships between changes in ankle dorsiflexion angle, knee flexion angle, circumduction, and hip hiking during swing phase revealed a relationship between only changes in knee flexion and changes in hip hiking (Pearson's r=-0.913, p<0.001) (**Figure 4.3**). Similarly, a multivariate regression model evaluating the independent contribution of changes in each knee flexion and ankle

dorsiflexion to changes in hip hiking revealed that changes in knee flexion (β=-0.912, p=0.007), but not ankle dorsiflexion (β=-0.194, p=0.341), independently predicted changes in hip hiking (R^2=0.87, F(2,4)=13.48, p=0.017). Exosuit-induced increases in swing phase knee flexion contributed to reductions in hip hiking during exosuit-assisted walking (**Figure 4.3**(a)).

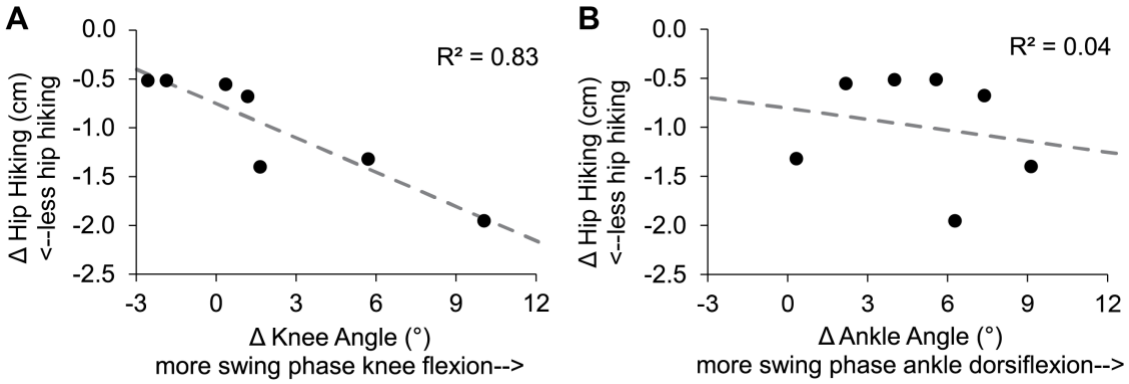

Figure 4.3. Correlation between changes in joint kinematics and hip hiking. (a) Relationship between exosuit-induced changes in peak paretic knee flexion angle and changes in hip hiking during swing phase. (b) Relationship between changes in peak paretic ankle dorsiflexion angle and changes in hip hiking during swing phase.

4.4. Discussion

Exosuits actively assist the paretic limb of individuals post-stroke in a manner that reduces hip hiking and circumduction-abnormal kinematic strategies commonly observed during hemiparetic walking [14]. These findings extend our previous evaluation of the exosuit technology in Chapter 3 and provide additional evidence that exosuits are a promising alternative to passive assistive devices (e.g., AFOs). The development of exosuits that can support ambulation by individuals after stroke in the clinic and the community is warranted.

For individuals post-stroke, hip hiking and circumduction are believed to be kinematic compensations-versus the product of intrinsic neuromotor changes-for impaired ankle dorsiflexion and knee flexion during swing phase [14]–[17]. Our findings of immediate reductions in both hip hiking and circumduction during exosuit-assisted walking support this hypothesis. That is, the rapid and substantial changes in the kinematic strategy used to advance the paretic limb during exosuit powered (vs. unpowered) walking support the notion that paretic hip hiking and circumduction are, at least partially, secondary deviations compensating

for deficits in paretic ankle plantarflexion and dorsiflexion-the targets of the exosuit's assistance-not primary impairments that need to be the direct targets of intervention. Further developments in the exosuit technology that allow direct assistance of knee and hip function may contribute to even greater reductions in frontal plane compensatory strategies, warranting investigation. That an exosuit acting to assist paretic limb propulsion and ankle dorsiflexion can have a substantial influence on a wearer's overall walking pattern also speaks to the potential use of exosuits during gait retraining, especially during the early phases of stroke recovery before individuals adopt compensatory walking strategies.

Previous work studying the relationship between hip hiking and lower limb joint impairments has demonstrated a strong link between hip hiking and deficits in ankle dorsiflexion, but not knee flexion [12]. Interestingly, we did not observe a relationship between exosuit-induced changes in ankle dorsiflexion and hip hiking; rather, changes in knee flexion strongly determined changes in hip hiking. Differences in experimental approach may explain these divergent findings. For example, the present study evaluates during treadmill walking the effects of an exosuit that provides active assistance of both ankle plantarflexion during stance phase and dorsiflexion during swing phase, whereas Cruz et al. [12] evaluated the effects of a passive AFO during overground walking. Unlike an AFO, an exosuit's assistance of ankle plantarflexion during late stance has the potential to increase paretic propulsion [90] and accelerate the knee into flexion during swing phase [45], [160], [161]. Although our testing was conducted on a treadmill, it is important to note that treadmill biomechanical assessments have several advantages over overground assessments, including the ability to compute averages of a large number of consecutive strides and the ability to monitor and control walking speed. Although future work is needed to directly evaluate differences in the effects produced by an AFO versus the exosuit technology, our finding that exosuit assistance reduces compensatory kinematic behaviors during treadmill walking is important. Indeed, this finding speaks to the modifiability of undesirable kinematic behaviors when deficits in key paretic limb biomechanical functions are targeted with a soft wearable robot. Given that treadmill walking is a popular gait training approach,

reducing compensatory behaviors during treadmill walking using a robotic exosuit may be desirable for gait rehabilitation.

Importantly, although exosuit assistance may be responsible for the reductions in hip hiking and circumduction observed, identifying the particular mechanisms responsible for these reductions is beyond the scope of this study. For example, given the multiarticular nature of the exosuit's plantarflexion assistance module (**Figure 2.2**), there is potential that the exosuit may generate forces about the knee (e.g., if the thigh connecting straps shift anterior or posterior to the knee joint, the exosuit would, respectively, generate a knee extension or flexion torque) concurrently with ankle plantarflexion. Further study is warranted to inform the design of future exosuit systems.

Post-stroke gait impairment is heterogeneous, and previous work has demonstrated that different compensatory strategies may be observed as a function of individuals' level of walking disability [158]. Indeed, Stanhope et al. [158] showed that among individuals in the chronic phase after stroke, slow walkers are more likely to employ hip hiking to achieve ground clearance, whereas fast walkers use circumduction. Despite our participants' average walking speed being relatively fast (0.95 m/sec), a broad range of speeds were recorded (0.53-1.30 m/sec). Moreover, all participants had observable gait deficits and five of the eight participants required regular use of an AFO or cane for community ambulation (**Table 3.1**). Consistent with the findings of Stanhope et al. [158], the fastest walker in our cohort (participant 7 in **Table 3.1**) had the smallest magnitude of hip hiking when walking with the exosuit unpowered. Interestingly, though, this participant reduced both hip hiking (-43%) and circumduction (-37%) when walking with the exosuit powered. In contrast to the findings of Stanhope et al.,24 the slowest walker in our cohort (participant 3 in **Table 3.1**) presented with the largest magnitude of circumduction when walking with the exosuit unpowered; however, with the exosuit powered, he reduced hip hiking (-38%) by a greater magnitude than circumduction (-17%). Ultimately, the exosuit's ability to reduce hip hiking, circumduction, and, in the case of four participants, both hip hiking and circumduction, is noteworthy and supports trialing the exosuit across the spectrum of disability among ambulatory individuals post-stroke.

A recent study of high-intensity stepping training versus conventional gait interventions in individuals with subacute stroke reported substantial functional improvements in those receiving experimental training, but also increased compensatory strategies [162]. Although further study is needed to understand the negative consequences of these increased compensatory behaviors, they represent a deviation from the typical walking behavior that is the ultimate goal of gait rehabilitation. A fruitful line of future research would be evaluating the potentially potent combination of high-intensity stepping training with gait-restorative wearable technology, such as the exosuit. This combination may maximize functional improvements while reducing gait compensations and facilitating the restoration of critical walking subtasks.

4.5. Limitation

The exploratory nature of the correlation and regression analyses employed with this small sample size is a potential limitation of this study and may explain why we were unable to identify a relationship between changes in ankle and knee function versus circumduction. Another limitation is that we did not randomize the order of testing, always testing the powered condition after the unpowered condition. This testing order was selected because of our previously reported finding that walking with an exosuit unpowered is comparable with walking without an exosuit worn [90], as well as the potential for carryover effects after exosuit-assisted walking. Given the potential for carryover effects after exosuit-assisted walking, a random order of testing would require including a washout bout between conditions to minimize carryover to the unpowered condition. The addition of an additional bout of walking could have contributed to fatigue and an increase in compensatory behaviors during the unpowered condition, which could have inflated the positive effects observed.

Another potential limitation is that the exosuit unpowered condition may not be a true reflection of baseline performance; however, it is important to note that the worn elements of the exosuit are compliant, unobtrusive, and weigh less than a pair of pants. Indeed, our previous work demonstrates that wearing the exosuit unpowered does not influence post-stroke propulsion or metabolic effort, which suggests that the

unpowered condition is comparable with walking with the exosuit unworn. Finally, although all participants studied presented with gait deficits and a majority required use of an AFO or assistive device for safe community ambulation, it should be noted that these participants had a higher than average walking speed for individuals post-stroke (0.95 m/sec). Future work is necessary to evaluate the effects of the exosuit on slower individuals, as well as to compare the effects of exosuit assistance to traditionally used braces.

Chapter 5.

Biomechanical mechanism underlying exosuit-induced metabolic cost reduction

5.1. Introduction

Chapter 3 demonstrated that paretic ankle assistance delivered from tethered exosuit prototype (**Figure 5.1**) could facilitate more symmetric forward propulsive force generation by the paretic and nonparetic limbs, and reduce the metabolic cost of walking [90]. Although this previous work demonstrates the substantial impact that exosuits can have on walking after stroke, propulsion symmetry and the metabolic cost of walking are composite variables that can be altered through a variety of biomechanical mechanisms. The objective of this chapter was thus to identify the specific biomechanical mechanisms underlying exosuit-induced improvements in metabolic power during hemiparetic walking.

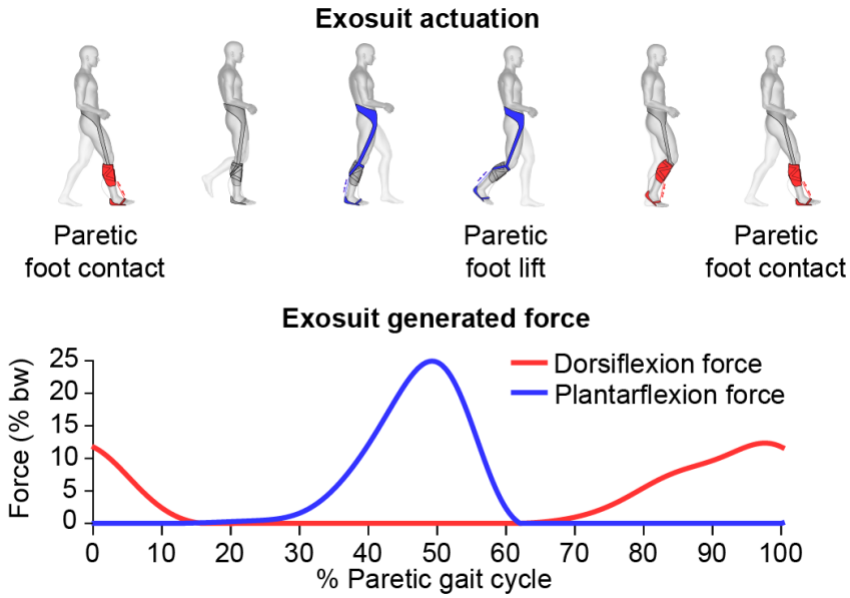

Figure 5.1. Illustration of exosuit actuation and exosuit-generated force trajectory presented with respect to the percentage of the paretic gait cycle. The exosuit delivers to the wearer's ankle PF force during late stance and pre-swing and ankle DF force during swing and initial contact.

Previous studies have demonstrated that the body center of mass (COM) power generated during the step-to-step transition plays a critical role in determining the metabolic cost of walking. Indeed, during this phase of walking when the mass of the body is transferred between limbs, the trailing limb generates COM power to redirect COM velocity while, simultaneously, the leading limb absorbs COM power [163]–[165]. Simulation and experimental studies have both shown that the COM power generated by the trailing limb during the step-to-step transition is correlated with metabolic power [164]–[167]. When the COM power generated by the individual trailing limbs is asymmetric, metabolic power requirements have been shown to increase in both healthy [167], [168] and neurologically impaired populations [3], [169]–[172]. Individuals with post-stroke hemiparesis generate less COM power from the paretic trailing limb during the step-to-step transition than healthy individuals and compensate for this by generating more COM power from the nonparetic trailing limb [34], [173], [174] during the subsequent step-to-step transition. This increased reliance on nonparetic limb COM power generation is correlated with an increased metabolic cost of walking [40]. Two of these studies, in particular, suggested that increased gait asymmetry in people post-stroke is correlated with the increased metabolic cost of walking [3], [175]. There is thus great interest

in the development of post-stroke gait interventions that can reduce the metabolic cost of walking by inducing more symmetrical walking [176].

Recent work has increased our understanding of the COM power generation during walking. More specifically, through a series of studies, Zelik and colleagues have demonstrated that changes in body COM power result from changes not only in hip, knee and ankle joint power but also in peripheral power (i.e. rate of kinetic power change of the lower limb segments relative to the body COM) and foot power. Specifically, Zelik and Kuo compared individual limb COM power to the sum of the 3 degrees-of-freedom (3DoF) ankle, knee and hip joint rotational power generated during healthy walking [177]. Although the limb's positive COM power matched well with the sum of the positive ankle, knee and hip joint power during push-off, during the collision phase of the gait cycle there was a substantial mismatch between the sum of the individual joint powers and the COM power generated. Furthermore, the sum of individual joint powers throughout the gait cycle presented with substantially more positive work than negative work – a paradoxical finding given that positive and negative work should be of equal magnitude during steady-state walking at constant speed. Taken together, these findings demonstrate that the sum of joint powers may not be an accurate reflection of body COM work. Expanding on this work, Zelik et al. [178] subsequently demonstrated that the relationship between the joint and COM power domains is more complete when accounting for peripheral power, foot power and 3DoF joint translational power (in addition to 3DoF rotational power).

Although COM power may be changed through various biomechanical mechanisms, it has been demonstrated that during the step-to-step transition, the ankle generates the largest power across all the lower extremity joints of the trailing limb in both healthy [161] and post-stroke [3] populations. Motivated by this biomechanical understanding of COM power generation and its previously defined relationship to metabolic power demands during walking, this investigation focused on evaluating the effects of exosuit assistance of paretic ankle function on the COM power and individual joint power generated by the paretic and nonparetic trailing limbs. Moreover, we focused our analyses on the double support phase of the gait

cycle, which is when the majority of the COM power generated during the step-to-step transition occurs [163]. A better understanding of how individuals after stroke use the mechanical power provided by exosuits to reduce the metabolic power requirements of walking would advance the field and facilitate the development of more effective wearable assistive devices. We hypothesized that the COM power generated by the paretic and nonparetic trailing limbs during the step-to-step transition would be more symmetric during exosuit-assisted walking than during walking without exosuit assistance and that more symmetric COM power generation would contribute to a reduction in metabolic power. We also hypothesized that more symmetric COM power generation would result from more symmetric ankle power generation.

5.2. Materials and Methods

5.2.1. Data collection

An experiment to evaluate the influence of the initial exosuit prototype designed to improve post-stroke gait mechanics and energetics was conducted on nine individuals in the chronic phase of stroke recovery, and described in Chapter 3 with details [90]. Our analysis in this chapter was conducted based on the data collected from this previous experiment. Two of the nine individuals who participated in the study were excluded from this analysis, because the way that they walked on the treadmill prevented independent collection of ground reaction forces from the individual limbs, which was required for the study's analyses. Demographics of the remaining seven subjects (age: 49±4 years; time since stroke: 4.38±1.37 years; 44% female; 56% left hemiparetic) are shown in **Table 5.1**. Moreover, our previous study in Chapter 3 demonstrated that the more effective onset timing varied across participants, and ultimately presented the changes in the metabolic cost of walking from individualized onset timings selected based on the timing that produced the largest improvement in forward propulsion symmetry [90]. The present study therefore used the same individualized timings (presented in **Table 5.1**).

The metabolic cost of walking was assessed by indirect calorimetry based on carbon dioxide and oxygen rates using a portable gas analysis system (Cosmed, Rome, Italy). Reflective markers were placed on

anatomical bony landmarks and on the Bowden cable anchor connection points for use in gait analysis. Three-dimensional (3D) motion capture was performed at 120Hz using a Vicon motion capture system (Vicon, Oxford Metrics, Yarnton, UK). An instrumented split-belt treadmill collected 3D ground reaction forces for individual limbs at 960Hz. Marker positions and ground reaction forces were filtered using a zero-lag low-pass 4th-order Butterworth filter with a cut-off frequency selected from residual analysis (5–9Hz) [125]. Data were also collected from the load cells and gyroscopes integrated into the exosuit at 1kHz. All data were time synchronized through Matlab and the Vicon Nexus motion capture software. The last 20 strides from each 8 min walking trial with ground reaction forces not contaminated by cross-over steps were used for data analysis.

Table 5.1. Participant characteristics and onset timing of PF actuation

Participant	Paretic Side	Sex	Age (y)	Chronicity (y)	Weight (kg)	Height (m)	Regular Assistive Device	Treadmill Walking Speed (m/s)	PF onset timing (%GC)
1	Right	F	30	7.08	49.4	1.62	AFO	1.05^	40.08±1.19
2	Left	M	56	3.58	73.0	1.77	None	1.05	38.15±2.32
3	Left	F	52	0.75	89.7	1.58	Cane	0.53	25.95±0.95
4	Left	M	51	2.83	79.0	1.84	AFO# & Cane	0.93	33.71±1.09
5	Left	F	37	1.08	79.6	1.72	AFO# & Cane	0.67	36.82±0.55
6	Right	M	44	2.33	79.7	1.86	None	1.29	35.54±1.55
7	Right	F	46	4.25	60.3	1.67	None	1.3^	33.35±1.57

^ Actual 10-meter overground walk test speeds were higher than used on treadmill. Participant 1's speed was 1.16 m/s, but this speed was not safe on the treadmill. Participant 7's actual overground speed was 1.72 m/s, but this speed was beyond the capabilities of the exosuit actuator used for this study.
# Participant 4 typically used a foot-up brace. Participant 5 used a custom brace that supported frontal plane motion.

5.2.2. Data analysis

Metabolic power was calculated using the modified Brockway equation [179] for the standing and walking trials and was averaged over the last 2 min of walking for each condition. Net metabolic power was obtained by subtracting the average metabolic power measured during the standing trial from the average metabolic power measured during each walking condition. Net metabolic power was normalized by body mass.

The individual limb body COM power was calculated using the individual limb method [164]. In brief, this method integrates the sum of the two ground reaction forces divided by the body mass to obtain a body

COM velocity with boundary conditions over a given stride such that (1) the average velocity in the anterior–posterior direction is equal to the treadmill speed and (2) there is no net velocity change in other directions. The individual limb COM power is then computed as the integral of the dot product of the COM velocity vector with the individual ground reaction force vector. Joint kinematics were calculated using the inverse kinematics method (Visual3D, C-Motion, Rockville, MD, USA). 3DoF joint rotational power (called joint power from here for simplicity) were calculated using the inverse dynamics method based on joint kinematics and ground reaction force data.

The markers located on the Bowden cable attachment points on the textiles and the insole were used to calculate the moment arms of the Bowden cable with respect to the ankle joint. The exosuit-generated ankle moment was calculated by multiplying the moment arm and the measured Bowden cable force. The exosuit-generated joint power was then calculated by multiplying the exosuit-generated joint moment and the joint velocity calculated through inverse kinematics.

5.2.3. Normalization and statistical analysis

Metabolic and biomechanical power variables were normalized to body mass to produce units of W/kg for statistical comparison. Individual limb/joint power data from each stride were then divided into four different phases: paretic limb single support, paretic limb double support (defined as nonparetic heel strike to paretic toe-off), nonparetic limb single support, and nonparetic limb double support (defined as paretic heel strike to nonparetic toe-off). The primary biomechanical variables analyzed were positive individual limb COM power and ankle, knee and hip joint power averaged during each limb's respective trailing limb double support (TDS). This was based on an understanding that the trailing limb generates the majority of body COM power for the step-to-step transition during double support [163], [164].

A symmetry index (SI) was used to evaluate inter-limb asymmetry of the biomechanical variables. The symmetry index was defined as:

$$SI = \left| \frac{(X_{np} - X_p)}{0.5 \cdot (X_{np} + X_p)} \right| \cdot 100\ (\%) \quad (5.1)$$

where X_{np} and X_p are, respectively, the biomechanical variables from the nonparetic and paretic limb [111]. This index is always positive or zero, and 0% means perfect symmetry. Statistical analysis was conducted in Matlab (MathWorks, Natick, MA, USA). One-sample paired t-tests compared the two conditions (exosuit unpowered and powered) to evaluate the effects of exosuit assistance. For variables studied across the gait cycle, statistically significant differences were confirmed only with consecutive rejection of the null hypothesis for more than 4% of the gait cycle. Linear regression was performed to investigate the correlation between the different biomechanical variables, and an F-test was performed on the regression model to assess the strength of the correlation. The statistical significance level was set at $p<0.05$ for all analyses.

5.3. Results

5.3.1. Individual limb body center-of-mass (COM) power and its relationship with net metabolic power

During walking with the exosuit unpowered, participants' nonparetic limbs generated 0.46±0.06W/kg of positive COM power and −0.29±0.04W/kg of negative COM power across the gait cycle (**Figure 5.2**(a)). In contrast, their paretic limbs generated 0.18±0.04W/kg of positive COM power and −0.29±0.04W/kg of negative COM power (**Figure 5.2**(a)). With the exosuit powered, participants reduced the positive COM power generated from their nonparetic limbs by 11.3±4.2% to 0.40±0.05W/kg (p=0.0407) and reduced the negative COM power generated from their paretic limbs by 9.0±3.7% to −0.26±0.05W/kg (p=0.0174). It should be noted that the average paretic limb's positive COM power increased to 0.20±0.04W/kg, but this change did not reach our a priori threshold for significance (p=0.0521).

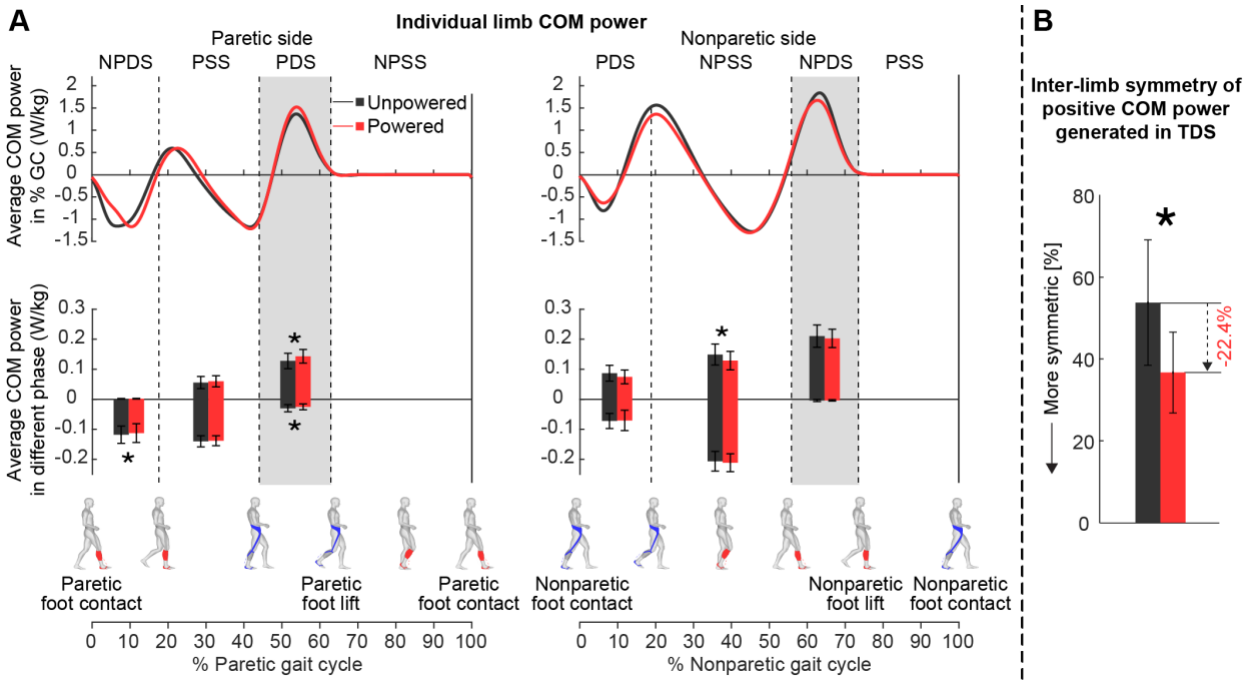

Figure 5.2. Individual limb COM power across the gait cycle. (a) Group average center of mass (COM) power segmented into percentage gait cycle (top) and sub-phases (bottom) for two different conditions (exosuit unpowered and powered) on the paretic and nonparetic limbs. The gait cycle was divided into four different sub-phases representing paretic and nonparetic limb double support (PDS and NPDS) and single support (PSS and NPSS). Trailing limb double support for each limb is indicated with gray shading. (b) Symmetry indices of average positive COM power generation during the trailing limb double support. These indices represent interlimb symmetry of positive COM power generated during the trailing limb double support (gray shading in A). *Statistically significant change from exosuit unpowered to powered condition.

Focusing the analysis on the positive power generated by the paretic and nonparetic trailing limbs during double support (gray shading in **Figure 5.2**(a), see **Table 5.2**), we observed that participants generated 0.21±0.04W/kg of positive COM power from their nonparetic limbs and 0.12±0.02W/kg from their paretic limbs (i.e. 56.48±15.21% SI; **Figure 5.2**(b)) during walking with the exosuit unpowered. With the exosuit powered, participants increased the positive COM power generated from their paretic limbs by 22.9±9.42% to 0.14±0.02W/kg (p=0.016), contributing to 39.06±7.78% more symmetric positive COM power generation between limbs during trailing limb double support (i.e. new SI of 34.07±10.27%, p=0.0112) (**Figure 5.2**(b)).

Linear correlations were observed between net metabolic power – computed as metabolic power during walking less the metabolic power at rest – and the positive COM power generated during trailing limb double support by the nonparetic limb, but not the paretic limb, in both the exosuit unpowered (R^2=0.77,

p=0.009) and powered (R_2=0.58, p=0.047) conditions (**Figure 5.3**(a)). Similarly, a reduction in nonparetic limb positive COM power during trailing limb double support was associated (R_2=0.80, I=0.007) with a 10.43±1.48% reduction in net metabolic power that was observed between testing conditions (suit unpowered: 4.18±0.43W/kg, powered: 3.72±0.34W/kg, p=0.005) (**Figure 5.3**(b)).

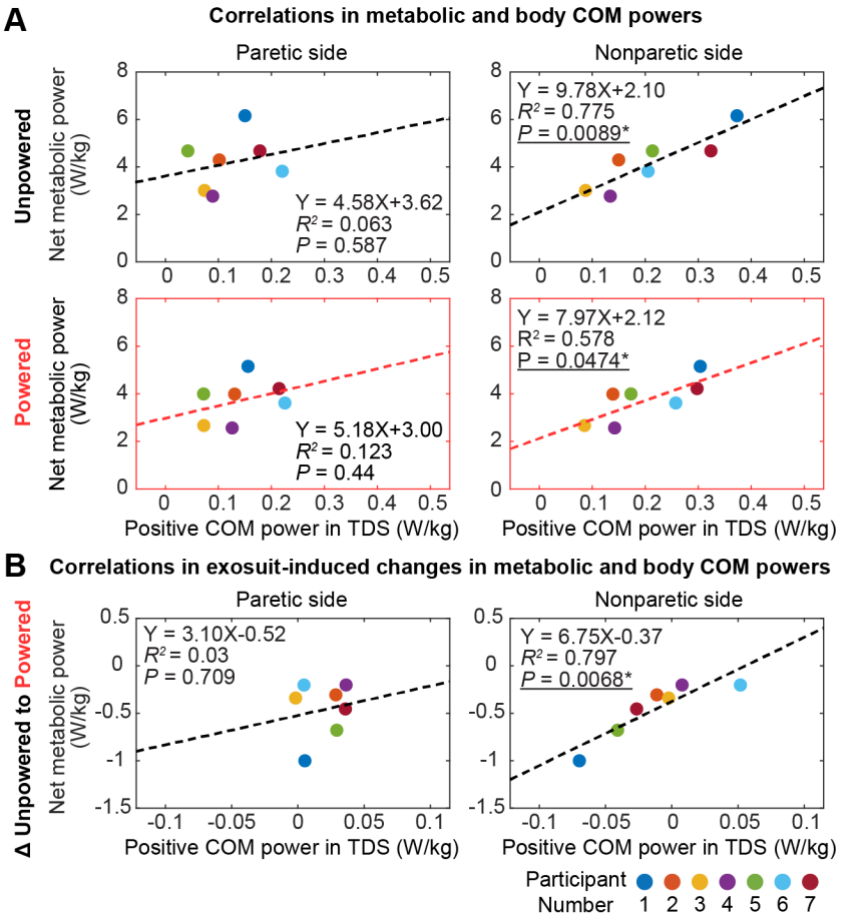

Figure 5.3. Correlation between COM power during trailing limb double support and net metabolic power. (a) Correlation of average positive COM power generated in trailing limb double support (TDS; x-axis) and average net metabolic power (y-axis) for the exosuit unpowered (top) and exosuit powered (bottom) conditions. Nonparetic COM power was linearly correlated to net metabolic power (P<0.05) in both conditions, while the correlation between paretic COM power and metabolic power was not statistically significant in either condition. (b) Correlation of the change in average positive COM power during trailing limb double support and the change in net metabolic power resulting from exosuit assistance. Exosuit-induced net metabolic power reduction was linearly correlated with the exosuit-induced change of nonparetic positive COM power during trailing limb double support, whereas a statistically significant correlation with paretic positive COM power was not observed. TDS, trailing limb double support.

5.3.2. Lower-limb joint power generated during trailing limb double support

A deeper investigation into the exosuit's effects on power generation during trailing limb double support was subsequently conducted by summing the joint power generated across the individual joints of the lower

extremities, with and without the exosuit powered (**Figure 5.4** and **Table 5.2**). When walking with the exosuit unpowered, the nonparetic lower limb joints (i.e. ankle, knee and hip) as a whole generated 0.25±0.03W/kg of positive power with minimal negative power absorption (−0.005±0.003W/kg). The paretic lower limb joints generated 0.13±0.03W/kg of positive power, significantly less than the nonparetic limb joints (p=0.0198, SI=72.04±18.53%), and absorbed a non-negligible amount of negative power (−0.04±0.01W/kg) (**Figure 5.4**(a)). When powered, the exosuit delivered 0.017±0.003W/kg of positive power to the paretic ankle with minimal negative power absorption (−0.0032±0.0015W/kg) (**Figure 5.4**(b)). Because of the multi-articular structure of the PF module, the exosuit concurrently delivered 0.0099±0.0024W/ kg of positive power and absorbed −0.0052±0.0017W/kg of negative power at the paretic hip. Despite the observed changes in individual limb COM power (described above), changes in the positive joint power generated across the lower limb joints were not observed in either the paretic or nonparetic limbs, or in their symmetry (ps>0.05; see **Table 5.2**).

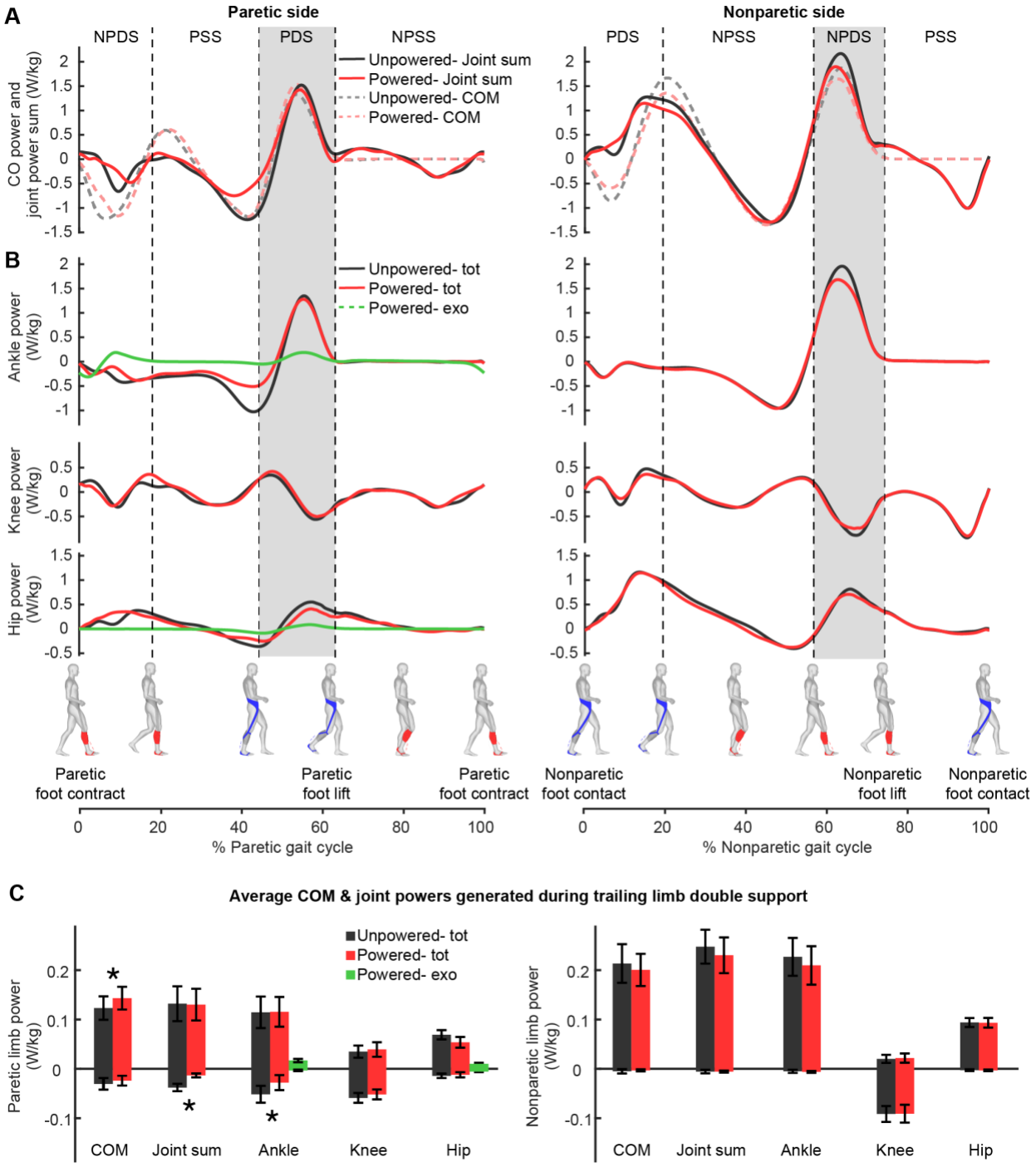

Figure 5.4. Individual joint power across the gait cycle. (a) Group average of body COM power and sum of lower-limb joint power segmented into percentage gait cycle. (b) Group average of ankle, knee and hip joint power segmented into percentage gait cycle. The trailing limb double support phase of each limb is indicated with gray shading. total: total power generated by human and exosuit; exo: ankle and hip power generated by exosuit when powered. (c) Average of positive and negative power variables generated during the trailing limb double support (gray shading in a,b). *Statistically significant difference between the exosuit powered and unpowered conditions. Note that ankle and hip power generated by the exosuit is zero in the unpowered condition.

Table 5.2. Positive powers generated during trailing limb double support and their inter-limb symmetry

	Nonparetic power (W/kg)		Paretic power (W/kg)		Inter-limb symmetry (%)	
	Unpowered	**Powered**	**Unpowered**	**Powered**	**Unpowered**	**Powered**
Body COM	0.213±0.039	0.201±0.033	**0.123±0.024**	**0.143±0.023***	**56.487±15.212**	**34.069±10.272***
Sum of joints	0.247±0.034	0.230±0.036	0.132±0.035	0.130±0.032	72.041±18.534	60.310±15.277
Ankle	0.227±0.038	0.210±0.039	0.115±0.032	0.116±0.030	**70.871±19.087**	**60.665±19.057***
Knee	0.020±0.008	0.022±0.009	0.035±0.012	0.039±0.015	116.658±25.364	118.865±21.667
Hip	0.094±0.009	0.093±0.010	0.069±0.009	0.054±0.011	**43.346±9.621**	**58.781±11.604***

Statistically significant changes from exosuit unpowered to powered condition are denoted as * (p<0.05).

Focusing our analysis on individual joint power generation during the trailing limb double support, we observed that positive ankle power generation was significantly asymmetric when walking with the exosuit unpowered; the nonparetic ankle generated significantly more positive power than the paretic ankle (nonparetic ankle: 0.23±0.04W/kg, paretic ankle: 0.11±0.03W/kg, SI=70.87±19.08%). With the exosuit powered, positive ankle power asymmetry reduced to 60.66±19.05% (p=0.049); however, changes in individual joint positive ankle power generation were not observed (**Table 5.2**). Individuals' hip joints produced substantially lower positive power during the trailing limb double support than the ankle joints when walking with the exosuit unpowered (nonparetic hip: 0.094±0.009W/kg, paretic hip: 0.069±0.009W/kg), but were also asymmetric (SI=43.346±9.621%). Unlike the ankle joint power, hip joint power generation became more asymmetric with the exosuit powered (SI=58.781±11.604%, p=0.0256), despite the absence of statistically significant changes in either the paretic or nonparetic hip joints (ps>0.05). The paretic and nonparetic knee joints generated relatively low positive power during the trailing limb double support, and changes in knee power with the exosuit powered were not observed (p>0.05, see **Table 5.2**).

5.3.3. Relationship of ankle power with total limb COM power and net metabolic power

Given the concurrently observed exosuit-induced changes in the interlimb symmetry of the ankle and COM positive power generated during the trailing limb double support (**Table 5.2**), the correlation between these variables was evaluated. Linear correlations were observed between the positive ankle power and positive

COM power generated during trailing limb double support for both the paretic and nonparetic limbs during both the exosuit unpowered and powered conditions (R_2>0.77, p<0.009) (**Figure 5.5**(a)). Similarly, for both conditions, the change in COM power generated by each limb during trailing limb double support correlated with the change in ankle power generated by each limb (R_2>0.73, p<0.014) (**Figure 5.5**(b)).

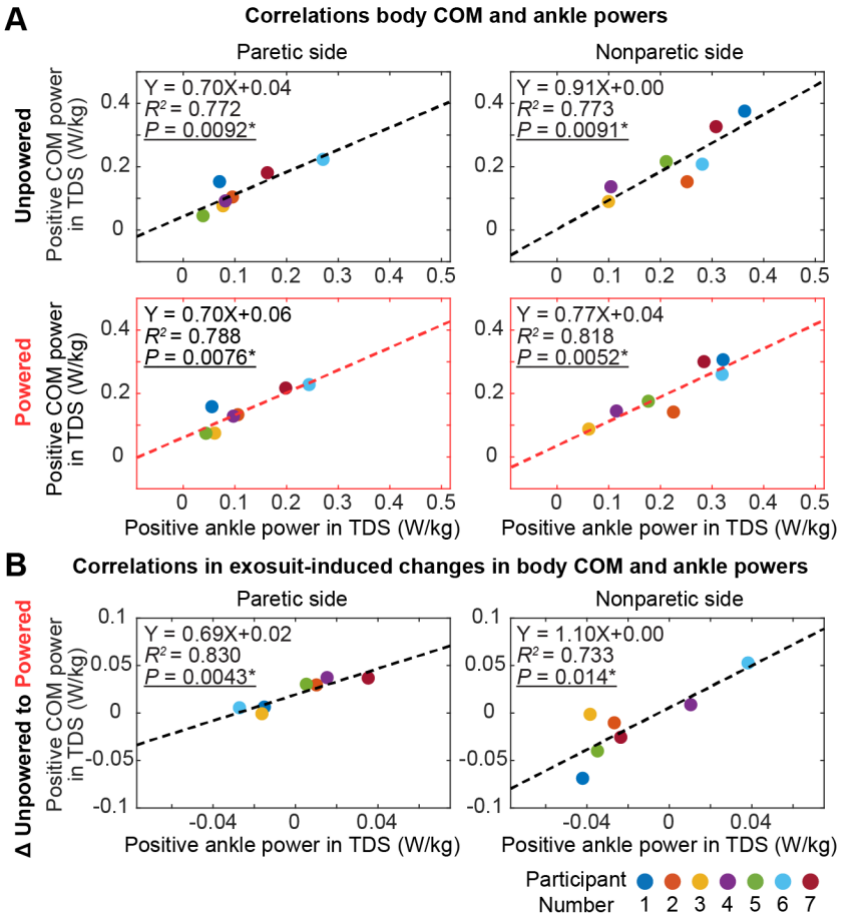

Figure 5.5. Correlation between ankle and COM power during trailing limb double support. (a) Correlation of average positive ankle power (x-axis) produced during trailing limb double support and average positive COM power over the same time period (y-axis) for the exosuit unpowered and powered condition. Positive ankle power was linearly correlated with positive COM power on both limbs in both conditions (p<0.05). (b) Correlation of the change of average positive ankle power and the change of COM power in exosuit-assisted walking. Exosuit-induced ankle power change was linearly correlated to the exosuit-induced change of positive COM power during trailing limb double support on both limbs (p<0.05). TDS, trailing limb double support.

Similar to the relationship between metabolic power and the positive COM power generated by the individual limbs during trailing limb double support (**Figure 5.3**(a)), we observed linear correlations between metabolic power and nonparetic (but not paretic) ankle positive power during both the exosuit unpowered (R_2=0.77, p=0.009) and powered (R_2=0.65, p=0.028) conditions (**Figure 5.6**(a)). However,

interestingly, changes in neither nonparetic (R_2=0.44, p=0.105) nor paretic (R_2=0.01, p=0.834) ankle power were correlated with changes in metabolic power (**Figure 5.6**(b)).

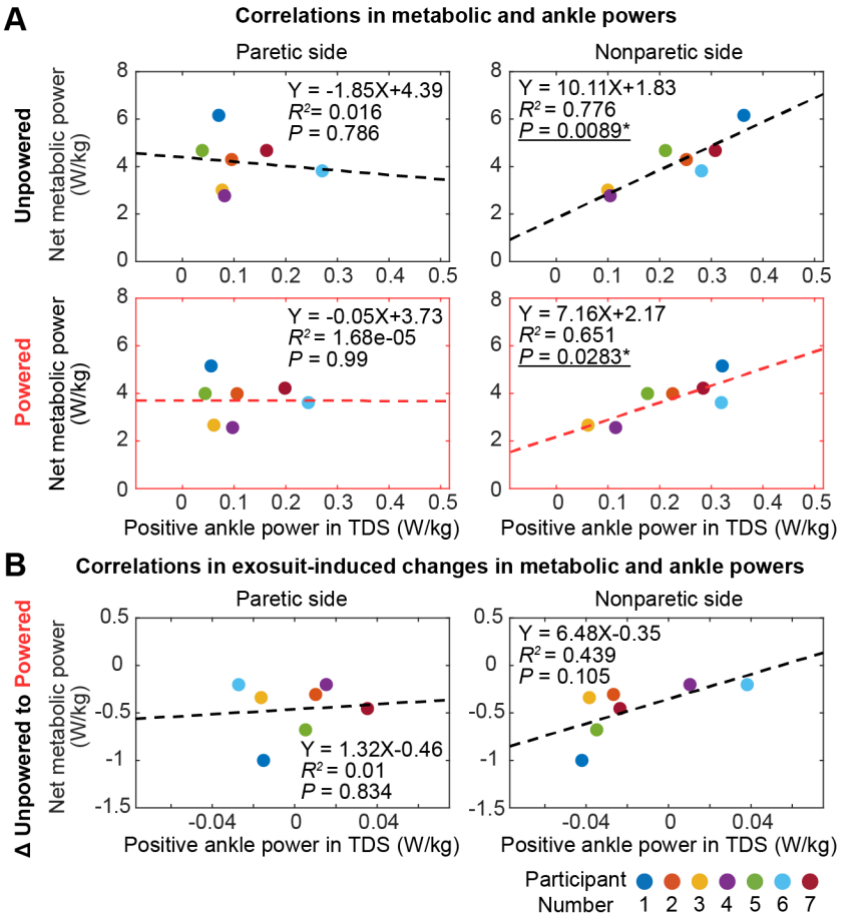

Figure 5.6. Correlation between ankle power during trailing limb double support and net metabolic power. (a) Correlation of average positive ankle power (x-axis) generated during trailing limb double support and net metabolic power (y-axis) for the exosuit unpowered and powered conditions. Nonparetic ankle power was linearly correlated to net metabolic power (p<0.05) in both conditions. The correlation between paretic ankle power and metabolic power was not statistically significant for either condition. (b) Correlation of the changes in average positive ankle power and net metabolic power in exosuit-assisted walking. No statistically significant correlation was found between exosuit-induced ankle power changes and changes in metabolic power (p>0.1). TDS, trailing limb double support.

5.4. Discussion

This chapter presents a systematic investigation into the biomechanical mechanisms underlying the reduced metabolic cost of walking observed during exosuit-assisted walking after stroke. Specifically, we evaluated the effects of walking with an exosuit assisting the paretic ankle on individual limb COM power and joint power, and investigated the relationship between changes in these biomechanical variables and changes in metabolic power. As hypothesized, exosuit assistance contributed to more symmetric COM power

generation by each limb during the step-to-step transition and a reduction in metabolic power. Interestingly, it was a reduction in the body COM power generated by the nonparetic limb during the step-to-step transition that strongly correlated with the reduction in metabolic power, with changes in nonparetic ankle power generation strongly contributing to this reduction. Collectively, these findings demonstrate that soft robotic exosuits can assist the paretic ankle during walking in a manner that positively influences whole-body gait mechanics and energetics.

Consistent with previous studies showing that post-stroke walking is energetically inefficient and mechanically asymmetric [169]–[171], [180], our participants expended 45% more metabolic power than healthy individuals to walk [181] and generated substantially less COM power from the paretic limb compared with the nonparetic limb during walking with the unpowered exosuit (**Figure 5.2**). Our observation that the COM power generated by the nonparetic limb during trailing limb double support was positively correlated with metabolic power during walking with an unpowered exosuit (**Figure 5.3**) also concurs with previous work [40]. Building on this previous understanding of post-stroke gait mechanics and energetics, our findings demonstrate that exosuit-induced reductions in nonparetic limb COM power generation during the step-to-step transition contribute to reductions in metabolic power (**Figure 5.3**(b)). This was surprising given that exosuits provide direct assistance to only the paretic limb. These findings suggest that individuals after a stroke are able to leverage the mechanical assistance provided to the paretic ankle to reduce a reliance on the nonparetic limb for walking. Indeed, other work has shown that individuals after stroke have a compensatory reliance on the nonparetic limb that can be altered with gait retraining [39]. Our finding that exosuits produced a similar change in inter-limb dynamics without any gait training provides compelling evidence for the promising use of exosuits to deliver targeted gait assistance during hemiparetic walking.

It is interesting to note that despite observing changes in the positive COM power produced by the paretic limbs when walking with the powered exosuit, we did not observe changes in the sum of the positive power produced by the hip, knee and ankle joints. This finding may be explained by prior work by Zelik and

colleagues that demonstrated the importance of accounting for peripheral power, foot power and 3DoF joint translation power in addition to the traditionally evaluated 3DoF joint rotational power [177], [178]. Although validation of this hypothesis is beyond the scope of this study, in our prior work, we observed exosuit-induced reductions in limb circumduction and hip hiking [182]. Such changes in foot and pelvis trajectories relative to the COM suggest a substantial reduction in peripheral power. A reduction in peripheral power without concurrent changes in joint power may explain the observed mismatch between changes in COM and joint power. Moreover, our previous report of the effects of exosuit-assisted walking on the anterior ground reaction force generated by the limb during walking [90] suggests changes in foot power [183]. Further study is required to reveal the exact source of COM power changes during exosuit-assisted walking.

Our findings that positive ankle joint power and COM power during trailing limb double support concurrently became more symmetric when walking with the exosuit powered (**Table 5.2**), and that exosuit-induced changes in these variables were highly correlated (**Figure 5.5**), suggest that targeted assistance of the paretic ankle is an effective strategy to improve gait mechanics after stroke at both the individual joint and whole-body levels. Future research into how targeted assistance of the biomechanical deficits of the paretic limb influences nonparetic limb biomechanics and overall walking ability after stroke would advance the field of wearable assistive robotics.

Our evaluation of the relationship between the ankle power generated during trailing limb double support and metabolic power (**Figure 5.6**) revealed that the positive power generated by the paretic and nonparetic ankles during their respective step-to-step transitions highly correlated with net metabolic power. It was surprising, however, that exosuit-induced changes in these variables were not related, especially given that changes in ankle power contributed strongly to changes in the body COM power generated by each limb (**Figure 5.5**(b)), which, as previously discussed, did contribute to changes in metabolic power (**Figure 5.3**(b)). This finding highlights the complex relationship between the mechanics and energetics of walking after stroke and suggests that, in response to the exosuit's targeted assistance of paretic ankle deficits, users

with hemiparesis achieve a metabolic benefit through heterogeneous biomechanical responses (see **Figure 5.7** and **Figure 5.8** for other biomechanical changes) in combination with ankle power generation strategies. Indeed, our team has recently shown exosuit-induced reductions in whole-limb compensatory gait motions that are known to increase metabolic power [156], such as circumduction and hip hiking [182]. Further study into the potential mediating role that exosuit-induced reductions in compensatory walking strategies plays in the relationship between changes in ankle power and metabolic power would enhance our understanding of how active assistance delivered through a wearable robot can improve walking after stroke.

Although this study presents a comprehensive analysis of exosuit-induced changes in post-stroke gait mechanics and energetics, it is limited by a small sample size. However, comparable sample sizes have been used successfully to evaluate other wearable assistive devices [119], [181], [184], [185] and we believe that the findings of this study provide a meaningful step toward understanding how individuals after stroke utilize robotic ankle assistance to achieve a more economical gait. Another limitation is that this investigation focused on the effects of walking with an exosuit worn unpowered versus powered. Although the exosuit is compliant and lightweight with its mass (~0.9kg) distributed along the length of the paretic limb, to evaluate the net effect of exosuit assistance on participants' walking behavior, it is important to know whether there are effects due to simply wearing the unpowered exosuit. In Chapter 3.5.1, we found that wearing the unpowered exosuit did not influence participants' ability to generate propulsion or their energy cost of walking compared with not wearing the exosuit. This result is consistent with a prior investigation of the effects on hemiparetic walking of additional load worn unilaterally above the paretic ankle [186]. These previous studies suggest that an exosuit worn unpowered does not substantially alter the biomechanics of post-stroke walking. Finally, this study used the trailing limb double support phase as a surrogate for the step-to-step transition. The step-to-step transition is often defined based on the change in sagittal plane COM velocity [163]; however, substantial variability in these data prohibited identification of the step-to-step transition using this approach. The trailing limb double support phase has been widely

used to represent the step-to-step transition, and the COM power generated during this phase of the gait cycle has successfully captured the broad trends in positive COM power observed during the step-to-step transition [163], [180].

5.5. Conclusion

In conclusion, this chapter demonstrates that a soft robotic exosuit can target deficits in paretic ankle function in a manner that induces more-symmetrical COM power generation and reduced metabolic effort during walking. These findings contribute to a fundamental understanding of how individuals after stroke interact with exosuit-generated paretic ankle assistive forces to reduce the metabolic cost of walking and support the use of exosuits for post-stroke gait assistance and rehabilitation. This work provides insight to guide future research and development of ankle-centered, active, gait assistive devices and their control strategies for individuals with neurologically based gait impairment.

5.6. Supplementary materials

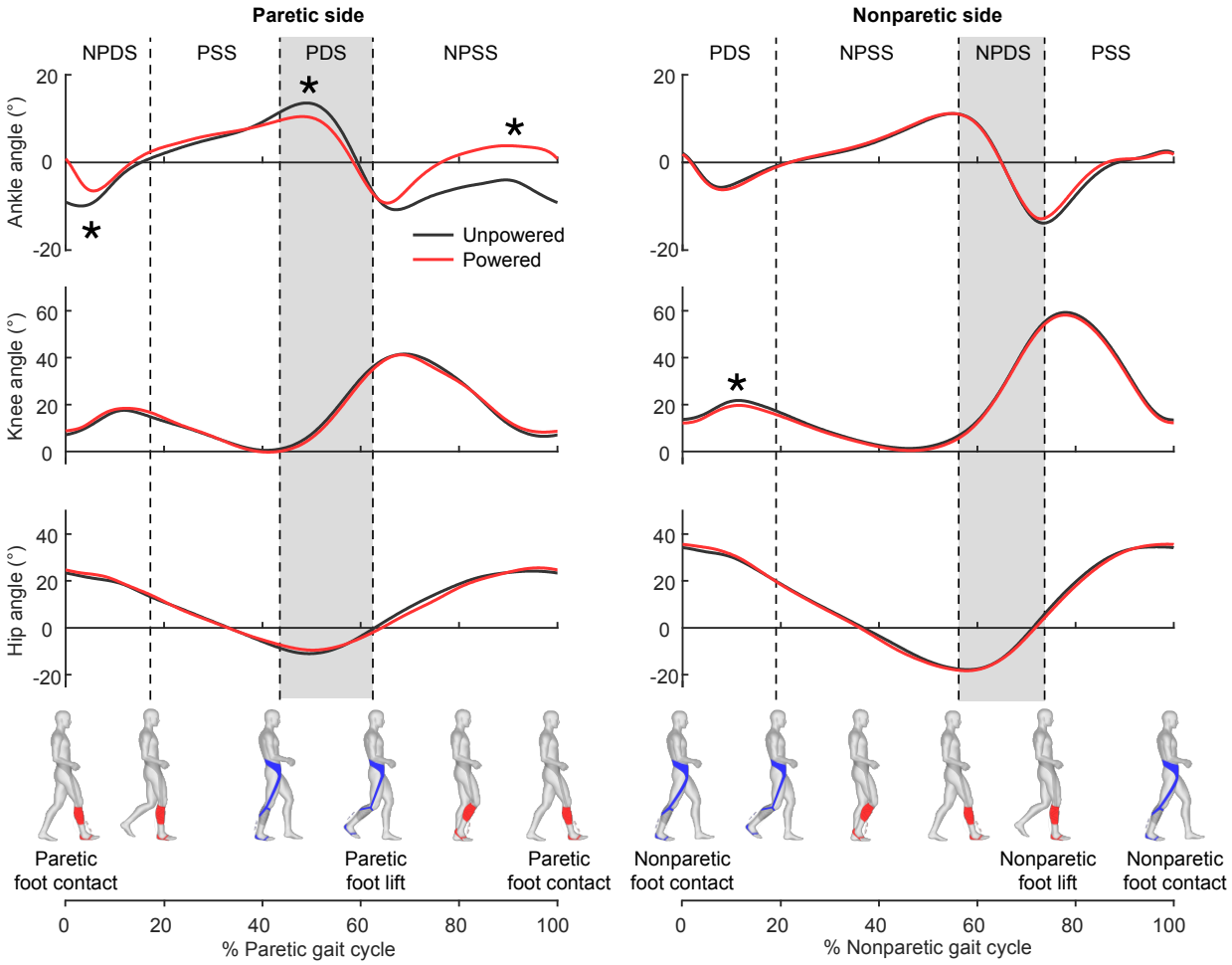

Figure 5.7. Group average of sagittal plane joint kinematics segmented by % gait cycle for two different conditions on the paretic and nonparetic limbs. The gait cycle was divided into four different sub-phases representing paretic and nonparetic limb double support (PDS and NPDS) and single support (PSS and NPSS). Trailing limb double support for each limb is highlighted with grey shading.
** Statistically significant change in exosuit-assisted walking was denoted as *. For simplicity in presentation, statistical significance was presented only at the local peak of the trajectory.

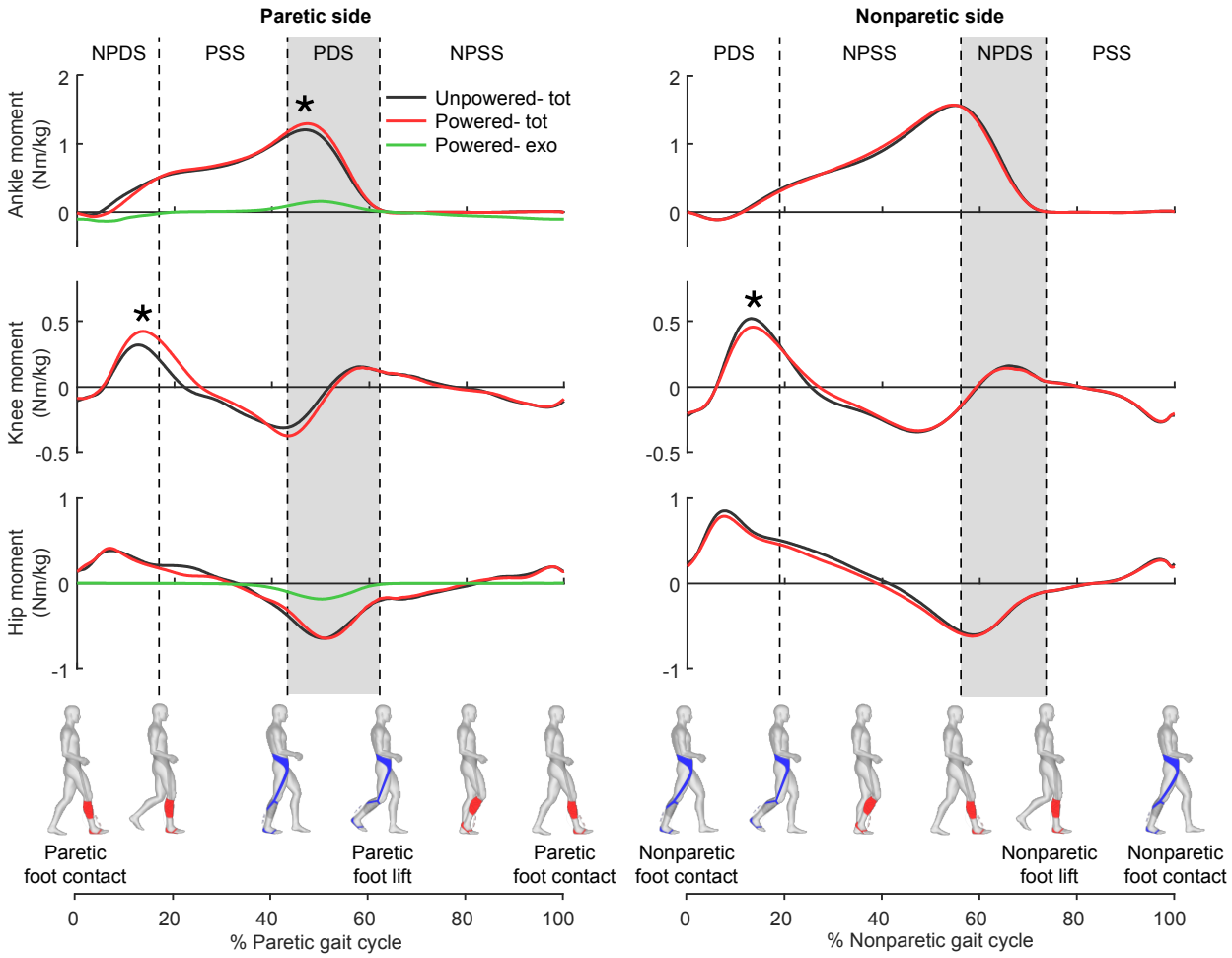

Figure 5.8. Group average of sagittal plane joint moments segmented by % gait cycle for two different conditions on the paretic and nonparetic limbs. The gait cycle was divided into four different sub-phases representing paretic and nonparetic limb double support (PDS and NPDS) and single support (PSS and NPSS). Trailing limb double support for each limb is highlighted with grey shading.

** Statistically significant change in exosuit-assisted walking was denoted as *. For simplicity in presentation, statistical significance was presented only at the local peak of the trajectory.

** Abbreviations: tot- Total power generated by human and exosuit. exo- Ankle and hip power generated by exosuit when suit powered.

Chapter 6.

A lightweight and efficient portable soft exosuit for paretic ankle assistance in walking after stroke

6.1. Introduction

In the previous chapters from Chapter 2 to Chapter 5, we presented our tethered exosuit prototype to assist with paretic ankle PF and DF developed for treadmill-based feasibility studies ((**Figure 6.1**(a) left) [187]) and demonstrated that exosuits could improve post-stroke walking efficiency and biomechanics. This prototype implemented a gait event detection algorithm for pathological gait and a force-based position controller that generated and adapted cable position trajectories based on force measurements (see Chapter 2 for further details). With this tethered prototype, we showed that when comparing walking with the exosuit powered to unpowered, patients improved forward propulsion symmetry and ground clearance (Chapter 3) [90], reduced compensatory gait patterns (Chapter 4)[182], and eventually reduced the metabolic cost of walking (Chapter 5) [90], [92]. A first autonomous body-worn exosuit prototype (**Figure**

6.1(a) right) was then developed to test the exosuit in overground walking (Section 3.5.2)[90]. This prototype employed similar control algorithms used in the tethered prototype and produced similar outcomes to the treadmill-based tests in overground walking; specifically, patients improved forward propulsion symmetry and ground clearance when comparing walking with exosuit powered versus unpowered suit.

Although promising, those exosuit prototypes were limited to the use in controlled laboratory environments and not applicable for clinical studies with multiple patients in real-world environment. Specifically, the tethered exosuit prototype was not applicable for the use outside laboratory environments, and the portable exosuit prototype was too bulky with significant electrical power consumption, limiting long duration of testing specifically with patients with limited endurance. Moreover, due to fixed Bowden cable connections to the actuation system, cable length and routing were not reconfigurable for diverse patients with different body shapes and different affected sides. Additionally, the wearable components took a long time to don and doff and adjust to the wearer and were non-washable.

In terms of software, the gait detection algorithm [187] was not robust enough in overground walking, as it relied on detecting heel strikes and the foot-flat phase of the gait cycle. However, individuals post-stroke may not walk with a heel strike, particularly in slow walking where many land with the mid-foot. Patients post-stroke often employ "vaulting" compensations to alleviate foot drop [188], eliminating the foot-flat phase altogether. We also observed that the aforementioned force-based position controller [90] would not deliver consistent forces during overground walking due to increased gait variability compared to treadmill walking. A switching admittance-position controller [81] has been implemented with other exosuits for use in healthy populations, which has shown improved force consistency. However, this technique requires accurate human and exosuit models, which may not be available in post-stroke populations due to the wide range of body types and heterogeneous gait patterns. Further, previous exosuit controllers were not optimized for electrical power consumption, important factors for in-clinic use.

To address these challenges that limited the suitability of the soft exosuit in overground gait training in a reliable and efficient manner, we developed an optimized portable exosuit and controller to assist paretic ankle PF and DF after stroke (**Figure 6.1**(b)). System data (e.g. motor and sensor data) collected with previous prototypes informed the development of an improved actuation system that was greatly reduced in both mass and volume, while still maintaining capacity to deliver significant ankle assistance to a wearer. Functional apparel elements and integrated sensors were simplified for quick donning and doffing. The gait detection algorithm was improved in its robustness to gait patterns, no longer relying on foot flat and heel strike events. The force-based position controller was also improved to enable better force profile tracking while reducing electrical power consumption. We evaluated this optimized exosuit system in overground walking with three patients in chronic phase of stroke recovery.

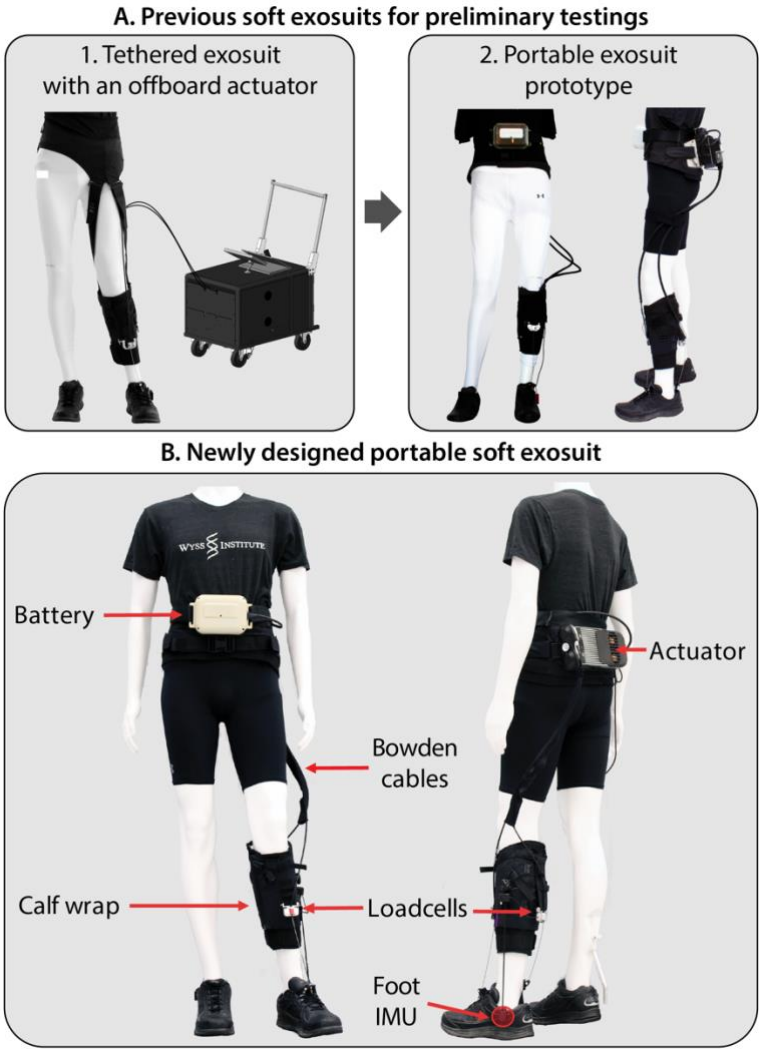

Figure 6.1. Evolution of soft exosuits for paretic ankle assistance in walking after stroke. (a) Two different exosuits were previously developed for preliminary tests. The first exosuit was a tethered system with an offboard actuator that allowed treadmill walking tests without adding extra mass from actuator and battery on wearer. The second system was a portable exosuit prototype for overground walking test. (b) A lightweight portable soft exosuit was newly developed for large-scale clinical research and practical use in clinics.

6.2. Soft exosuit hardware

The new protable soft exosuit to assist paretic ankle DF and PF comprises a waist belt that anchors an actuation system and a battery on the torso, two Bowden cables that connect the actuation system to the paretic ankle, a calf wrap that anchors the Bowden cable housings to the paretic shank, and an insole that anchors inner Bowden cables at the paretic foot (**Figure 6.2**). The total mass of the exosuit system is 3.8 kg, where its two heaviest components (actuator and battery) are worn close to body center of mass (COM), and only lightweight components such as a functional apparel and an insole are worn distally (See **Figure**

6.2 for component masses). As such, the system lessens its metabolic penalty to the wearer and adds minimal restrictions to the wearer's natural motion [154]. Additional modifications were made to the system components to reduce complexity and facilitate system setup in laboratories or clinics.

Figure 6.2. Exosuit hardware components and their masses

6.2.1. Functional apparel and insole anchors

New waist belt and calf wrap functional apparel components were designed for the exosuit system (**Figure 6.2**). The waist belt includes a plastic plate with built-in sliding connectors, with which an actuator can be easily secured to the back. The calf wrap has two textile loops on its anterior and posterior sides to connect DF and PF Bowden cable housings. A quick lacing mechanism (Boa Technology Inc, CO, USA) integrated into the calf wrap facilitates adjustability on a variety of calf shapes and sizes. Strain resistant textiles (Sailcloth, Dimension Polyant, USA) are integrated in the fabrication of the calf wrap to minimize deformation of the textile structure under load, and inner layers which directly make contact with wearer's skin are designed to be removable and washable to maintain hygiene between multiple users. Further, to fit a wide range of body shapes, multiple sizes of the waist belt and the calf wrap were built (three sizes for waist belt, seven for the calf wrap).

An insole with textile straps located anterior and posterior to the ankle joint is placed in the shoe of the wearer's paretic foot. Connectors at the distal ends of inner Bowden cables attach to these textile straps. With inner cables connected to the insole and the cable housings connected to the calf wrap, the inner cable retraction driven by the actuator generates a joint torque at the ankle, delivering mechanical power to the ankle.

6.2.2. Actuation system

The design of a two degree-of-freedom actuation unit and a pulley cartridge was informed by data collected from the previous exosuit actuation systems (**Figure 6.1**(a)) [90], [187]. Design efforts focused on minimizing mass and volume while covering different body shapes and sizes and right and left paretic legs (**Figure 6.3**). The assembly of actuation unit and pulley cartridge is 248 mm long, 135 mm tall, and 63 mm wide. With its narrow and compact design, the actuation system significantly reduced its effective inertia applied to the body COM. The actuation unit contains two motors (EC-4pole 22 90W, Maxon Inc, USA), gear boxes (GP 32 HP 123:1, Maxon Inc, USA), encoders (16 EASY, Maxon Inc, USA), and a custom-made electronics board using an Atmel processor (SAME70N21, Atmel Co, USA) and motor drivers (Gold Twitter, Elmo Motion Control Ltd, Israel). We chose 300 N as the maximum cable force requirement and 1.4 m/s as the maximum walking speed requirement and collected actuation data at these operating conditions for multiple healthy individuals and patients post-stroke with previous exosuit systems. The collected data was then used in combination with an analytical model of the actuation system, similar to that in [81], to predict the actuation and thermal performance of various potential motor and gear combinations. Based on simulation results and considering system mass and form factor, the motors and gear boxes listed above were selected.

The aforementioned actuation model was also used to derive the voltage, current, and power requirements of the power electronics. Motor drivers were therefore selected to be capable of 50 V and 60 A peak current, and the battery were selected to supply 48 V with 1450 mAh capacity, which makes the actuation system

capable of assisting for more than 90 minutes of continuous active walking, sufficient for running a maximum-duration rehabilitation session without recharging or replacing the battery.

The actuation unit can be connected to different pulley cartridges with Bowden cables of different lengths. Based on the size of the subject, the correct cartridge with Bowden cables of the most appropriate length can quickly and easily be attached to the system. The correct sizing of Bowden cables is important to allow free motion of a wearer and minimize excessive cable slack. The use of reversible cartridges also enables the system to be easily configured for either left or right hemiparesis patients as shown in **Figure 6.3** (a).

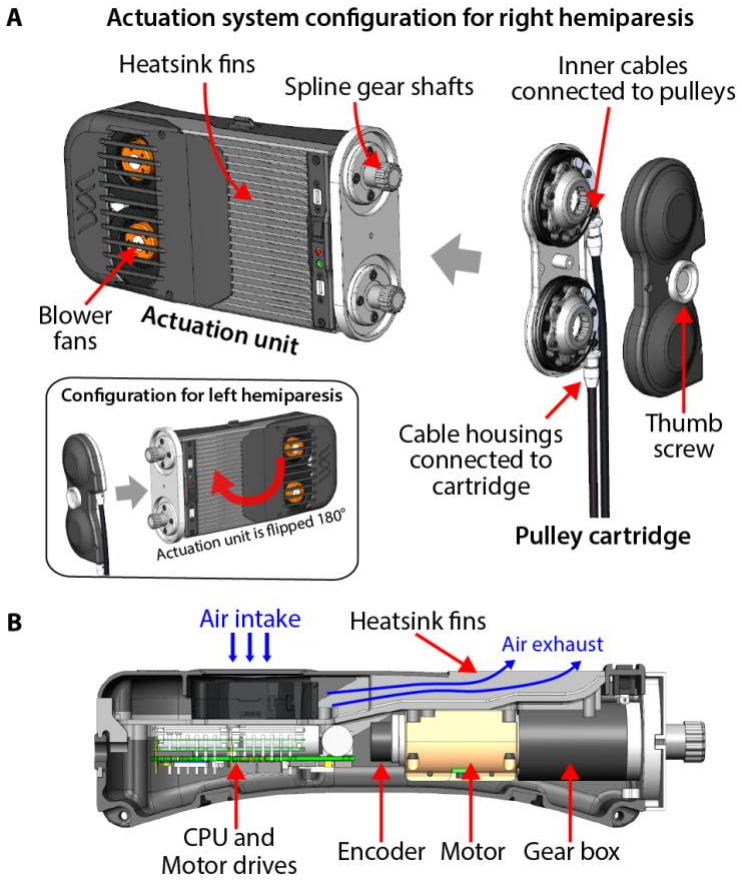

Figure 6.3. Diagram of actuation unit and pulley cartridge. (a) The actuation unit and pulley cartridge are easily assembled with a thumb screw and can be configured for patients with right hemiparesis (main figure), or ones with left hemiparesis (small window). The motors are coupled to the pulleys through the use of spline gear shafts. (b) A section view of the actuation unit shows the internal system hardware. The motors and motor drives are thermally grounded to the aluminum chassis which supplies rigidity to the system and transfers the generated heat to the integrated heatsink fins.

6.2.3. Textile-integrated sensors

Load cells and inertial measurement units (IMUs) are integrated in the exosuit functional apparel components to enable a hierarchical closed-loop controller described in section 6.4. Specifically, two load cells (LSB200, Futek, USA) were integrated in the textile loops of the calf wrap to measure DF and PF forces generated by Bowden cable retractions. The force measurements are used in the cable position trajectory generator of the high-level controller (See section 6.4.2 and 6.4.3). Additionally, IMUs (MTi-3, XSens, Netherlands) are mounted laterally on each shoe to measure foot angle and angular velocity. The IMU measurements are used in the gait detection algorithm (See Section Gait event detection algorithm6.4.1).

6.3. Exosuit modeling on the paretic ankle

To demonstrate how the functional apparel components and Bowden cables interact with the human body to deliver mechanical power to the paretic ankle, a simple model of the calf wrap worn on the shank was created (**Figure 6.4**). In this model, the relationship of the suit-generated force (f_{suit}) and the deformation of suit textiles and human soft tissues (d_{suit}), called exosuit-human series stiffness (F_{stiff}), is described by a nonlinear spring with hysteresis that presents different mechanical behaviors in loading and unloading [91], [189]. Specifically, two different posit dive monotonic functions describe loading and unloading behavior separately. Suit deformation occurs (i.e. d_{suit} becomes positive) when the inner cable length (d_{cable}) is shorter than the distance between two points fixed on the shank and foot (d_{ankle}, see **Figure 6.4**). The fixed points are located where Bowden cable anchor points on the foot and the shank are in an undeformed exosuit. The distance d_{ankle} captures the ankle movement when force is not applied by the suit. When d_{cable} is longer than d_{ankle}, the cable is slack, and the suit remains unchanged. Altogether, the ankle torque generated by the suit (τ_{suit}) can be described as follows:

$$d_{ankle} = d_0 - r_{ankle} \cdot \Delta\theta_{ankle} \tag{6.1}$$

$$d_{suit} = \begin{cases} d_{ankle} - d_{cable}, & d_{ankle} \geq d_{cable} \\ 0, & otherwise \end{cases} \tag{6.2}$$

$$f_{suit} = F_{stiff}\left(d_{suit}, \mathrm{sgn}\left(\dot{d_{suit}}\right)\right) \tag{6.3}$$

$$\tau_{suit} = r_{ankle} \cdot f_{suit} \tag{6.4}$$

where d_0 is the distance between the cable anchor points when the ankle is in a neutral position, $\Delta\theta_{ankle}$ is the ankle angle change from the neutral position, and r_{ankle} is the cable moment arm with respect to the ankle (see **Figure 6.4**). The stiffness model F_{stiff} depends on the direction of the change in d_{suit} due to hysteresis. Further details on F_{stiff} can be found in [91]. F_{stiff} may vary across wearers because of variation in body properties, such as the thickness of soft tissues and size of calf muscles. Note that this approach can be used to describe both PF and DF actuation.

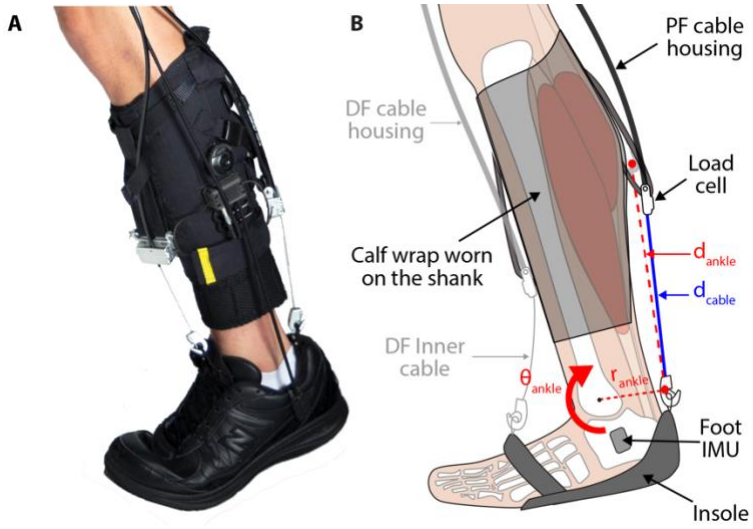

Figure 6.4. Picture and diagram of a paretic ankle wearing the soft exosuit. Two red points in the diagram illustrate Bowden cable anchor points when the suit is not stretched, which define dankle. The diagram highlights only PF cable actuation for simplicity.

6.4. Controller implementation

A hierarchical controller that consists of two nested control loops was implemented to generate consistent DF and PF force profiles at the appropriate timing during the gait cycle (**Figure 6.5**). The outer layer, a high-level controller, detects key events in the gait cycle based on foot IMU measurements (gait event

detection algorithm), and generates desired cable position trajectories based on the gait events and cable force measurements from load cells (cable position trajectory generator). The inner layer, a low-level controller, runs closed loop control on motor position for the actuation system to track the desired cable position trajectories generated by the high-level controller. The low-level position controller comprises two cascading loops in which outer position loop generates desired velocity (v_{des}) based on position error (p_{err}), and inner velocity loop regulates control effort (u_{com}) to actuation system based on velocity error (v_{err}). This section focuses on describing the high-level controller. Further details about the low-level controller can be found in [81].

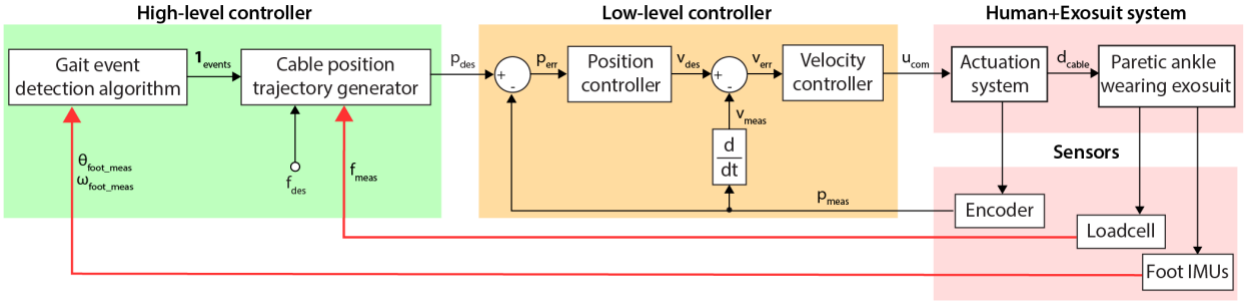

Figure 6.5. Schematic block diagram of exosuit controller. The diagram presents exosuit hardware (red), low-level controller (orange), and high-level controller (green). The high-level controller consists of a gait event detection algorithm that detects gait events based on foot IMU measurements (θfoot_meas, ωfoot_meas), and a cable position trajectory generator that generates desired cable position (Pdes) based on the gait events and force measurements (Fmeas). The low-level controller regulates control effort (ucom) for actuator system to track the desired position generated by high-level controller.

6.4.1. Gait event detection algorithm

A new gait event detection algorithm that detects paretic and nonparetic toe-offs (PTO and NTO) and nonparetic mid-swings (NMS) based on the sagittal plane foot IMU measurements was implemented (**Figure 6.6**). This algorithm differs from previous gait event detection algorithms [187] in that it does not detect heel strikes and foot flat phases, instead detecting NTO, PTO, and NMS. With this approach, the new algorithm can be used not only for post-stroke patients with mild gait deficits, presenting clear and consistent trends in IMU measurements, but also for patients with severe gait deficits who present diminished heel strike and foot flat phase.

To develop this new algorithm, we first sought consistent features in foot IMU measurement across various post-stroke walking patterns. By examining data from our previous studies [90], we identified that sagittal plane foot angular velocities consistently presented negative peaks, then changed direction at toe-off, a feature appearing in both the paretic and nonparetic side, as shown in **Figure 6.6**. Similar observations can be found in [108]. Also, sagittal plane nonparetic foot angles presented a consistent and monotonic increase during swing. Based on these observations, we designed a new gait event detection algorithm focused on detecting the negative peak in the sagittal plane foot angular velocity at toe-off and the mid-point of monotonic increase of the sagittal plane nonparetic foot angle during swing. Using the gait events detected with this algorithm, the gait cycle can be segmented into three distinct phases (P1-P3 in **Figure 6.6**): P1 is a paretic mid-stance phase (from NTO to NMS); P2 comprises a paretic terminal stance and pre-swing (from NMS to PTO); Last, P3 comprises a paretic swing and paretic weight acceptance (from PTO to NTO).

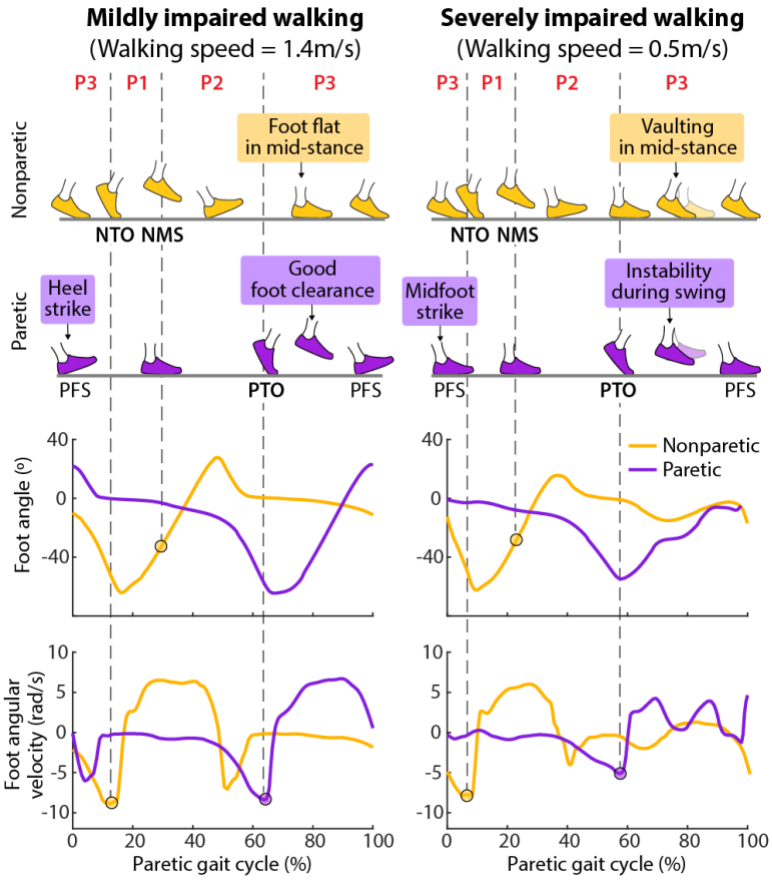

Figure 6.6. Sagittal plane foot trajectories and foot IMU measurements during the paretic gait cycle, a time period between two consecutive paretic foot strikes (PFS). The new gait detection algorithm detects paretic and nonparetic

toe-offs (PTO and NTO) and nonparetic mid-swing (NMS) based on the sagittal plane foot angle and angular velocity measured by foot IMUs. The algorithm can robustly detect PTO, NTO, and NMS in post-stroke patients with mild gait deficit (left) and severe gait deficit (right), and segment the gait cycle into three phases (P1- P3).

6.4.2. PF cable position trajectory generator

A force-based PF cable position trajectory generation algorithm was implemented to consistently deliver PF force to the paretic ankle at appropriate timings (**Figure 6.7**). The main goal was to generate PF cable force that has an onset at the end of paretic mid-stance, reaches a desired peak force (f_{des}) and diminishes before the beginning of the paretic swing phase. Our previous studies have validated that this form of PF force profile can improve forward propulsion symmetry and gait mechanics for patients after stroke [90], [92]. The second goal was to reduce motor power consumption by designing the position trajectory to reduce motor velocity and range of motion. To this end, the position trajectory generation algorithm adapts multiple cable position and velocity variables once per each walking stride (~1 Hz), and also adapts cable velocity iteratively per each control loop (1 kHz) when the cable retracts to give rise to the PF force.

Specifically, this algorithm adapts a position variable called baseline cable position (p_{base}) and three velocity variables consisting of pretension velocity (v_{pret}), initial pull velocity (v_{pull_i}), and pushout velocity (v_{push}) once per each walking stride identified by the gait detection algorithm. p_{base} is a cable position when force does not generate in the Bowden cable. v_{pret} is an average cable velocity in P1 when the cable starts to retract to onset PF force. v_{pull_i} is a cable velocity at NMS, a desired force onset timing since NMS coincides with the end of paretic mid-stance. v_{push} is a cable release velocity when the force ramps down. The velocity variables adapt in a same manner as follows:

$$v(n) = v(n-1) + k \cdot f_{err}(n-1) \tag{6.5}$$

where v(i) is a velocity variable in ith gait cycle, f_{err} (i) is a force error between desired and measured values in the ith gait cycle (i.e. f_{des}-f_{meas} (i)), and k is a force-velocity adaptation gain. For instance, v_{pret} (n-1) is adjusted based on the difference between desired onset force (7 N) and PF force measured at NMS in (n-1)th cycle to generate v_{pret} (n). v_{pull_i} adapts based on the difference of desired peak force and measured peak

force. Last, v_{push} is adapted based on the difference of desired offset force (7 N) and force measured at PTO (See **Figure 6.7** for further details). The adaptation of v_{push} therefore reduces push-out velocity as long as the exosuit does not deliver PF force in paretic swing.

The parameter p_{base} adapts to minimize slack in the cable when PF force is not generated in P3. The adaptation occurs as follows:

$$p_{base}(n) = \begin{cases} p_{base}(n-1) + \Delta p, & f_{max}^{p3}(n-1) > f_{thres} \\ p_{base}(n-1) - \Delta p, & otherwise \end{cases} \quad (6.6)$$

where f_{thres} is a force threshold where the algorithm determines if cable force is generated, f_{maxp3} is a maximum force measured during P3, and Δp is a position increment. Through this adaptation, p_{base} decreases up to the position boundary where cable force starts to generate in P3.

Further, the cable velocity (v_{pull}) adapts while PF cable retracts iteratively per each control loop as follows:

$$v_{pull}(t) = v_{pull\_i} \cdot \left(\frac{f_{des} - f_{meas}(t)}{f_{des} - f_{meas\_NMS}}\right) \quad (6.7)$$

where f_{des} is desired peak force, $f_{meas}(t)$ is a force measurement at each time stamp of control loop, and f_{meas_NMS} is force measurement at NMS, where cable velocity is v_{pull_i}. This with-in stride velocity adaptation increases peak force tracking by decreasing cable velocity as force reaches to f_{des}.

6.4.3. DF cable position trajectory generator

A similar algorithm to PF position trajectory generator was implemented to deliver DF force during paretic swing and weight acceptance (**Figure 6.7**). The algorithm adapts baseline cable position (p_{base_DF}) once per a stride to consistently onset DF force at PTO as follows:

$$p_{base\_DF}(n) = p_{base\_DF}(n-1) + k \cdot f_{err}(n-1) \quad (6.8)$$

where $f_{err}(n-1)$ is the difference between desired onset force (7 N) and force measurement at PTO in (n-1)th gait cycle. A cable travel from p_{base_DF} during swing (p_{travel_DF} in **Figure 6.7**) is manually selected by system operators based on their observation on patients ground clearance and foot landing.

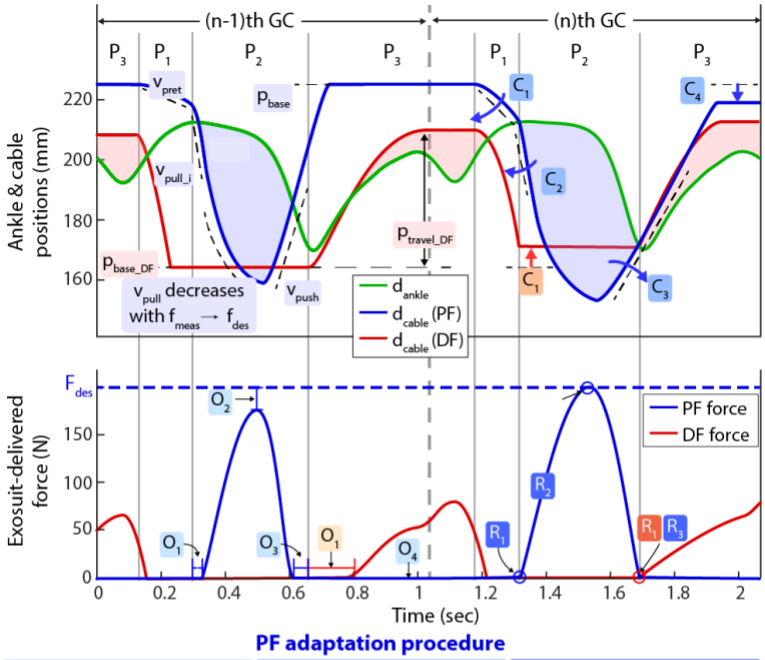

PF adaptation procedure

Observation in (n-1)th GC	Change made in (n)th GC	Outcome in (n)th GC
O_1: Force onset is later than NMS	C_1: Increase pretension set-up velocity (V_{pret})	R_1: Force onset happens at NMS
O_2: Peak force is lower than desired force (F_{des})	C_2: Increase initial pull velocity after NMS (V_{pull_i})	R_2: Peak force reaches F_{des}
O_3: Force offset is earlier than PTO	C_3: Reduce pushout velocity (V_{push})	R_3: Force offset happens at PTO
O_4: Force is 0 throughout P_3	C_4: Reduce baseline cable position (P_{base})	R_4: Reduce cable slack

DF adaptation procedure

O_1: Force onset is later than PTO	C_1: Increase baseline position (P_{base_DF})	R_1: Force onset happens at PTO

Figure 6.7. Illustration of cable position and delivered force trajectories in two consecutive gait cycles (GCs). PF cable position trajectory generator adjusts cable velocities (v_{pret}, v_{pull_i}, and v_{push}) and baseline cable position (p_{base}) for the next GC based on their previous values and force measurements from previous GC. Additionally, cable pull velocity (v_{pull}) is adapted when PF force ramps up to achieve desired peak force (f_{des}). DF trajectory generator also adjust baseline cable position (p_{base_DF}) to onset DF force at appropriate timings. This illustration demonstrates how the position trajectory generator recovers desired force profile when it observes undesired force profile in the previous GC.

6.5. System validation

To evaluate the exosuit's performance in assisting walking after stroke, we conducted a preliminary testing with three patients in the chronic phase of stroke recovery (see **Table 6.1**). Patients were asked to walk

along an overground track equipped with motion capture cameras (Oqus, Qualisys, Sweden) (**Figure 6.8**) for five minutes in three different conditions: first walking without wearing the exosuit (NOEXO), second walking with exosuit using the optimized control algorithm described in this chapter (EXO_ON1), and third walking with exosuit using a control algorithm similar to that presented in [90] (EXO_ON2). All the walking trials were supervised by a licensed physical therapist (PT). In walking trials with exosuit, the desired PF peak force (f_{des}) was set at 25% the wearer's body weight (%BW), and p_{travel_DF} was fixed for both conditions. Kinematic data were recorded with the motion capture cameras, and ground reaction force (GRF) data were also recorded with a set of nine instrumented force plates (Bertec CO, USA; sampling frequency 1500 Hz) over a portion on the track. Medical clearance and written informed consent forms approved by the Harvard University Human Subjects Review Board were received from all participants.

Joint kinematics were calculated with the inverse kinematics using Visual 3D software (C-Motion Inc, USA). Paretic forward propulsion for each stride was measured as peak anterior GRF (AP GRF) generated by the paretic limb. Of particular interest for performance evaluation were reliability of gait event detection and consistency of peak PF forces, a stated goal of our improved control algorithm. Electrical power consumption of the motor was another performance metric, calculated as

$$p_{motor} = i^2 \cdot R_{motor} + K_i \cdot i \cdot \omega \tag{6.9}$$

where i is a motor active current, R_{motor} is an effective motor resistance, K_i is a motor constant, and ω is motor angular velocity. Paired-sample t-tests were conducted to compare different walking conditions. The statistical significance level was set at p=0.05. We hypothesized that during overground walking the exosuit would increase paretic forward propulsion and improve paretic dorsiflexion during mid-swing, an important indicator of ground clearance. We also hypothesized that our improved controller would achieve these biomechanical goals with more consistent force profile and reduced motor electric power consumption.

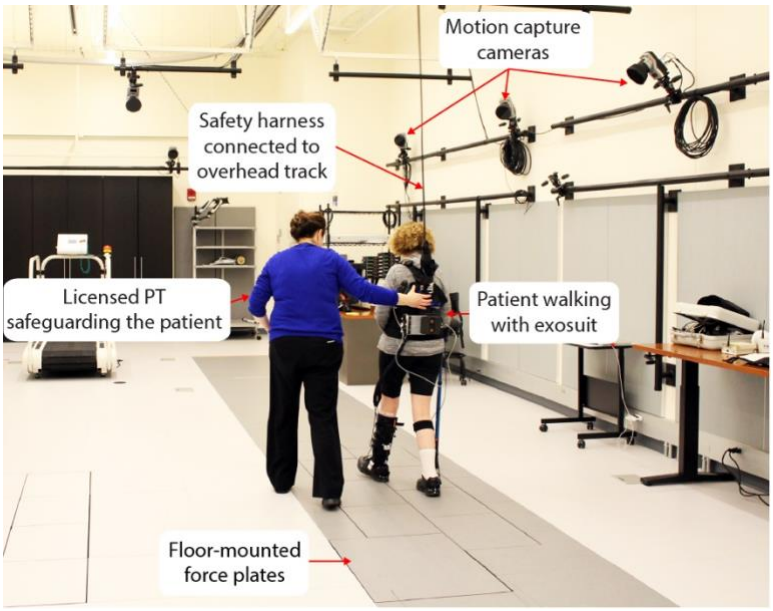

Figure 6.8. Experimental setup for preliminary system evaluation with patients after stroke

Table 6.1. Participant baseline characteristics and gait performance

Participant	Sex	Age (y)	Years after stroke (y)	Paretic side	Weight (kg)	Height (m)	Regular assistive device	Comfortable walking speed (m/s)
P1	Male	53	5.0	Left	77.5	184	Foot-up brace & Cane	0.9
P2	Female	64	6.2	Left	78	166	None	1.2
P3	Male	75	5.6	Left	97.5	179	FES	0.8

*FES: Functional Electrical Stimulation device

6.5.1. Performance evaluation of gait event detection algorithm

Gait events were also determined via motion capture using an automatic gait event detection algorithm based on ground reaction forces and measured kinematics using Visual 3D software. Synchronizing these events with exosuit data allowed calculation of the error between IMU-detected and actual gait events. For all the subject, average errors were under 90 ms. Specifically, the errors in each participant were: P1: -88.76±6.05 ms; P2: -49.70±8.41 ms; and P3: -49.52±11.96 ms. Negative numbers imply that real time events trailed those determined by motion capture.

6.5.2. Performance evaluation of PF cable position trajectory generation algorithm

The averages of peak PF forces achieved using different algorithms were both close to target PF peak force (25%BW) (**Figure 6.9**); However, standard deviations of the peak forces were 70% lower with the new

algorithm compared to the previous algorithm (see **Table 6.2** for individual data). Further, electrical power consumed by the PF motor significantly reduced with the new algorithm compared to the old algorithm (New: 7.93±3.06 W, Old: 15.63±3.35 W. See **Table 6.3**).

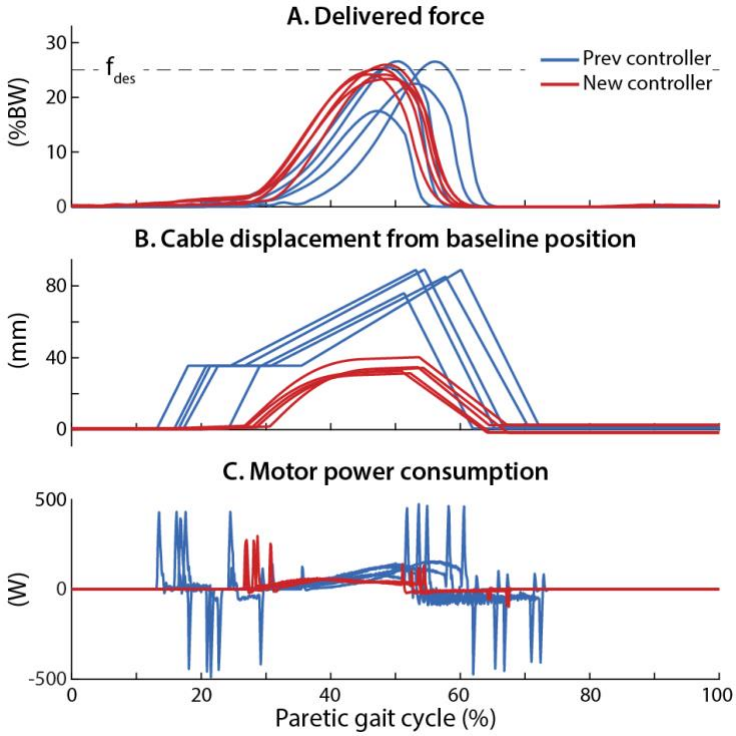

Figure 6.9. Sample data to compare old and new PF cable position trajectory generators. (a) delivered force, (b) cable displacement (retraction) from initial baseline position (p_{base}), and (c) motor power consumption. Data from 5 continuous strides in overground walking of a patient after stroke are presented for simplicity.

Table 6.2. Peak PF force consistency (%BW)

Participant No.	Old PF algorithm	New PF algorithm
P1	25.18±2.82	24.97±0.86
P2	25.18±2.54	24.92±1.27
P3	25.19±3.62	24.97±1.08

Table 6.3. Average electrical power consumption of PF motor over single stride (W)

Participant No.	Old PF algorithm	New PF algorithm
P1	16.97±2.53	8.29±0.38
P2	11.81±1.29	4.70±0.37
P3	18.10±3.24	10.79±0.76

6.5.3. Biomechanical evaluation

Figure 6.10 illustrates the biomechanical responses from individual subjects when walking with the exosuit. Compared to the NOEXO condition, all three participants increased paretic forward propulsion in the EXO_ON1 condition. Only two participants (P1 and P2) increased paretic forward propulsion in the EXO_ON2 condition. Regarding ground clearance, two participants (P1 and p3) increased their paretic peak dorsiflexion during mid-swing in both EXO_ON1 and EXO_ON2 conditions compared to NOEXO. It should be noted that S2 had the mildest gait impairment in our subject group, presenting good ground clearance in NOEXO condition, therefore did not require increased DF during swing (see **Table 6.1** and **Figure 6.10**). To summarize, with the new control algorithm, the exosuit improved paretic forward propulsion and ground clearance during swing phase, an improvement matching, or even slightly exeeding, the previous algorithm. Further, the exosuit could deliver better biomechanical outcomes to a patient with a more pronounced gait impairment compared to a mild one. Similar results can be found in [90]. Still, this preliminary validation study is limited by a small sample size, therefore further study including more patients is warranted.

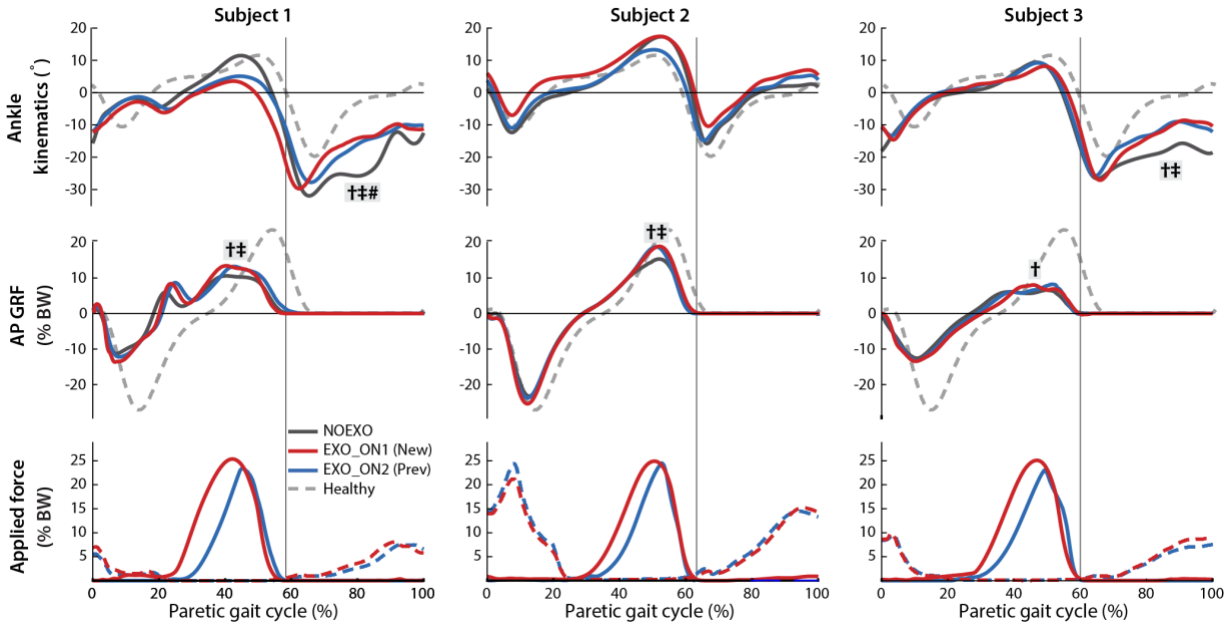

Figure 6.10. Average biomechanical changes of individual subjects in paretic forward propulsion and ground clearance. (Top) sagittal plane ankle kinematics. (middle) anterior-posterior ground reaction force (AP GRF). (bottom)

PF and DF force applied by exosuit. Solid lines are PF forces and dotted lines are DF forces. The vertical lines around 60% GC present paretic toe-off.
* † denotes statistically significant difference between NOEXO and EXO_ON1 condition; ‡ denotes the difference between NOEXO and EXO_ON2 condition: # denotes the difference between EXO_ON1 and EXO_ON2.
** Data collected from healthy individuals walking in 1.5 m/s were presented as a reference.

6.6. Conclusion

This chapter presents an optimized soft exosuit for paretic ankle assistance in walking after stroke. The exosuit was designed to improve suitability for translation to clinics by reducing complexity, mass, and volume based on data collected from previous studies with tethered and portable systems [90], [92], [118]. A new control algorithm was implemented to improve gait event detection reliability, PF peak force consistency, and efficiency of motor power consumption, all of which are critical for the use of exosuit in clinical gait training. The exosuit and controller were evaluated through a preliminary experiment with patients post-stroke during overground walking, with and without the exosuit. In this experiment, the control algorithm robustly detected PTO, NTO, and NMS and delivered more consistent force profiles, while using 50% lower motor electrical power consumption compared to the prior control algorithm [90]. Similar to what was found in previous studies [90], the patients generated more forward propulsion with the paretic limb and achieved increased ground clearance with improved paretic ankle kinematics during the swing phase. These preliminary results highlight the potential of the exosuit to improve post-stroke gait and begin evaluation in larger patient studies.

Chapter 7.

Biomechanical and physiological benefits of wearing portable exosuit in overground walking post-stroke

7.1. Introduction

Our previous biomechanical studies described in Chapter 3 demonstrated that a tethered exosuit could improve paretic limb forward propulsion and ground clearance during treadmill walking in post-stroke individuals. It also showed reduction in metabolic cost of transport and compensatory gait patterns with exosuit assistance. Although promising, the study was limited in treadmill walking and recruited only individuals with relatively mild gait impairments (See **Table 3.1** for participant gait characteristics in the study). Furthermore, it did not evaluate the effect of exosuit assistance on walking stability or muscle activities. Given that impaired muscle controls and gait stability are major contributors to the heterogenous presentation of functional gait impairments post-stroke [3,17,56,57], evaluation of the effect of exosuit

assistance on muscle activity and gait stability across a range of functional gait impairment levels is important for broad implementation of this technology.

One of the compelling aspects of exosuit technology is its capability to assist with overground walking, a favored gait training method because of its similarity to real-world community ambulation [47]. Evaluation of the exosuit during overground walking specifically is therefore important given the differences in gait mechanics and variability between overground and treadmill walking [190]–[196]. Our preliminary study in Section 3.5.2 presented the proof-of-concept portable exosuit prototype which demonstrated improvements in paretic propulsion and swing ankle dorsiflexion when comparing walking with active exosuit to walking with unpowered exosuit on a straight hallway [42]. Extending the preliminary work, an efficient and lightweight portable exosuit for paretic ankle assistance in post-stroke individuals was developed and presented in Chapter 6 [93]. A pilot study with three chronic post-stroke individuals wearing the new portable exosuit was conducted to demonstrate that the exosuit could deliver consistent mechanical assistance to the participants' paretic ankle and improve paretic forward propulsion and ground clearance during overground walking post-stroke. Although promising, the pilot study was limited in a small sample size, therefore more validation of the system with larger number of post-stroke patients was warranted.

Fundamental aspects of post-stroke gait training are the amount of dose, specificity and intensity of training [51]. While ankle-foot-orthosis limit specificity of training and the treadmill-based exoskeleton robots for rehabilitation may reduce the intensity [62], we believe portable exosuit could all of the aforementioned aspects. First, by actively supporting ground clearance and paretic push-off, the exosuit could facilitate walking faster and farther, thus increasing the amount of training. Second, the targeted ankle assistance could allow patients to focus on specific aspects of their gait without constraining movement or inducing compensatory strategies, thereby increasing the specificity of training. Third, the relatively low exosuit-applied torque could encourage active patient engagement, and thus complement high-intensity training without causing muscle slacking. Even though patient's voluntary muscle recruitment is important in effective gait training, only few studies evaluated the effect of wearable robotics on muscle activity and

show reductions in push-off ankle activity in healthy and 3 stroke participants [119], [197]–[203]. Our group also found reduced muscle activation in able-bodied subjects wearing a similar soft exosuit [87], [99]. Still, it remains unknown how the exosuit specifically designed for post-stroke gait affects paretic muscle effort.

To establish the potential of the portable exosuit for overground gait training in post-stroke patients, this chapter aims to first acquire fundamental understanding on the immediate impact of the new portable exosuit on overground walking in post-stroke individuals. To this end, we assessed the in-session response of wearing the portable exosuit compared to not wearing it during continuous overground walking at comfortable speeds; without cues or gait training. We conducted a comprehensive analysis including evaluation of the exosuit assistance on walking speed, gait energetics, stability, propulsion, voluntary leg muscle activity and biomechanics of ankle impairments. Moreover, to understand how different baseline functional gait performance levels influence participants' ability to leverage exosuit assistance, post-stroke participants across a range of baseline walking speeds were recruited, from limited (<0.93 m/s) to full (>0.93 m/s) community ambulatory groups [204]. We hypothesize that the exosuit assistance could improve impaired ankle function, thereby fostering voluntary muscle activation and improving walking speed, energetics and propulsion without affecting gait stability across all participants. We also hypothesize that the limited ambulatory group could benefit more from exosuit assistance than the full ambulatory group based on the similar observation found in Chapter 3.

7.2. Methods

7.2.1. Participant recruitment

19 individuals (Sex: 9 females 10 males; age: 53 ±11y; chronicity: 8±6y, see **Table 7.1**) in the chronic phase of recovery participated in the study. Inclusion criteria comprised of being between the ages of 18 and 80 years; diagnosis of stroke with gait deficiencies; and able to walk independently with or without assistive devices continuously for at least 4 minutes. Exclusion criteria comprised of severe aphasia and/or

speech/language disorder, limiting ability to express needs and comprehend instructions (based on the Mini Mental State Exam (MMSE score of 18 or lower) or Western Aphasia Battery (MMSE score of 20-22: score of 34 or lower on the Auditory Verbal Comprehension and Sequential Commands sections), serious co-morbidities; and more than two falls in the previous month. The protocol was approved by the Harvard Medical School Human Subjects Review Board, and medical clearance and signed informed consent were obtained for all participants.

Table 7.1. Participant characteristics

	No	Paretic side	Sex	Age (y)	Chronicity (y)	Type of stroke	Weight (kg)	Height (m)	Assistance in session	FAC (0-5)	MAS (0-4)	Walking speed (m/s)
Full ambulators	1	R	M	33	4.0	Hemorrhagic	86	1.81	None	5	0	0.97
	2	L	M	53	5.4	Ischemic	79	1.84	Arm sling	5	0	1.07
	3	R	F	32	10.3	Hemorrhagic	56	1.61	Lateral support	5	1+	1.03
	4	L	F	62	6.5	Ischemic	69	1.70	None	5	0	1.28
	5	R	F	48	6.5	Hemorrhagic	60	1.63	None	5	0	1.51
	6	R	F	56	8.8	Hemorrhagic	54	1.63	None	5	0	0.96
	7	L	M	59	9.0	Hemorrhagic	74	1.78	None	5	1	1.02
	8	L	M	46	12.7	Ischemic	81	1.75	None	5	0	0.96
	9	L	M	35	13.4	Ischemic	71	1.78	None	5	0	1.00
Limited ambulators	10	R	M	54	2.4	Hemorrhagic	81	1.76	Arm sling	4	0	0.53
	11	L	F	57	9.3	Ischemic	53	1.63	Cane & lateral support	4	0	0.45
	12	L	M	76	6.2	Hemorrhagic	99	1.82	None	5	0	0.88
	13	L	M	44	9.0	Ischemic	99	1.81	Cane & lateral support	4	1	0.70
	14	R	F	55	9.0	Hemorrhagic	114	1.65	Cane & lateral support	4	2	0.43
	15	L	F	49	4.3	Ischemic	43	1.60	None	5	1+	0.73
	16	L	M	62	4.3	Ischemic	65	1.75	Cane	5	1+	0.56
	17	L	M	57	3.5	Ischemic	111	1.69	Cane	5	0	0.69
	18	L	F	60	28.1	Ischemic	76	1.69	Cane & lateral support	4	1	0.67
	19	R	F	64	5	Ischemic	89	1.63	Cane & lateral support	4	2	0.34

FAC: Functional Ambulation Category (score 0-5) rating overall gait function independence; MAS: Modified Ashworth Scale (score 0-4) describing muscle tone in the main plantar flexor muscles on the paretic ankle; Walking speed: the baseline walking speed without wearing exosuit; Lateral support: an extra textile component integrated to exosuit to prevent ankle inversion.

7.2.2. Ankle assistance generated by portable soft exosuit

The design of portable, paretic ankle-assisting exosuit used in this study was presented in Chapter 6 with details. In brief, the exosuit consists of a body-worn actuation unit and a battery to generate mechanical power and deliver it to the paretic ankle by retracting Bowden cables, a waist belt to mount the actuation unit on the back, a calf wrap to anchor the Bowden cable housings on the shank, a semi-rigid insole in the paretic shoe to anchor the inner cables, and two inertial sensors mounted laterally on the shoes (**Figure 6.2**). The exosuit generates assistive plantarflexion (PF) and dorsiflexion (DF) forces through interaction between the calf wrap and insole and Bowden cable retraction (**Figure 6.4**). A new gait event estimation is implemented to robustly detect key gait events in highly variable pathological gait during overground walking. In addition, an upgraded force-based cable position trajectory algorithm is implemented to consistently provide PF and DF assistance during appropriate phases of a gait cycle of post-stroke overground walking. The Bowden cable for PF assistance connects the heel of the insole to the posterior side of the shank textile and generates force during push-off. PF assistance was generated from 30.5±3.2 to 62.6±2.9% of the gait cycle (%GC) with a peak magnitude at 23.8±1.6% body weight (%BW) during the experiments. The Bowden cable for DF assistance connects the anterior side of the shank textile with the forefoot of the insole and generates force during swing and initial contact. DF assistance was generated from 67.2±3.8% to 25.2±5.2%GC and the magnitude is adjusted based on visual observations by an experienced physical therapist to ensure sufficient ground clearance during swing, resulting in an average force of up to 16.0±6.1%BW.

7.2.3. Experimental protocol

Prior to an experimental session, each participant completed a prior session where fit and comfort of the components were evaluated, and the required level of dorsiflexion assistance to achieve normal ground clearance and heel landing were determined. For the actual experimental session, participants first walked for one or two laps with the exosuit active to verify comfort of the suit components and assistance, followed

by a break. Then, participants walked on a 36.9 m indoor walking track at comfortable walking speed with their paretic side to the inside of the track in two different conditions for 5 minutes each: One of the conditions was walking without wearing the exosuit (Baseline), and the other was walking wearing the active exosuit (Active). Three lower level participants walked for 4 minutes in both conditions because of limited baseline activity. (**Figure 1.1**). Participants were instructed to walk at their comfortable pace at the start of both conditions and to examine the natural response to the exosuit, no specific instructions on strategies in relation to exosuit-assisted walking were given. The order of walking conditions was randomized, with at least 10 minutes of seated break between conditions to reduce fatigue. Participants were secured with an overhead safety harness, and their vital signs were closely monitored. Some of participants used additional assistive devices during the testing if necessary (see **Table 7.1**), and when they used additional devices in one of walking conditions, they used them in both conditions.

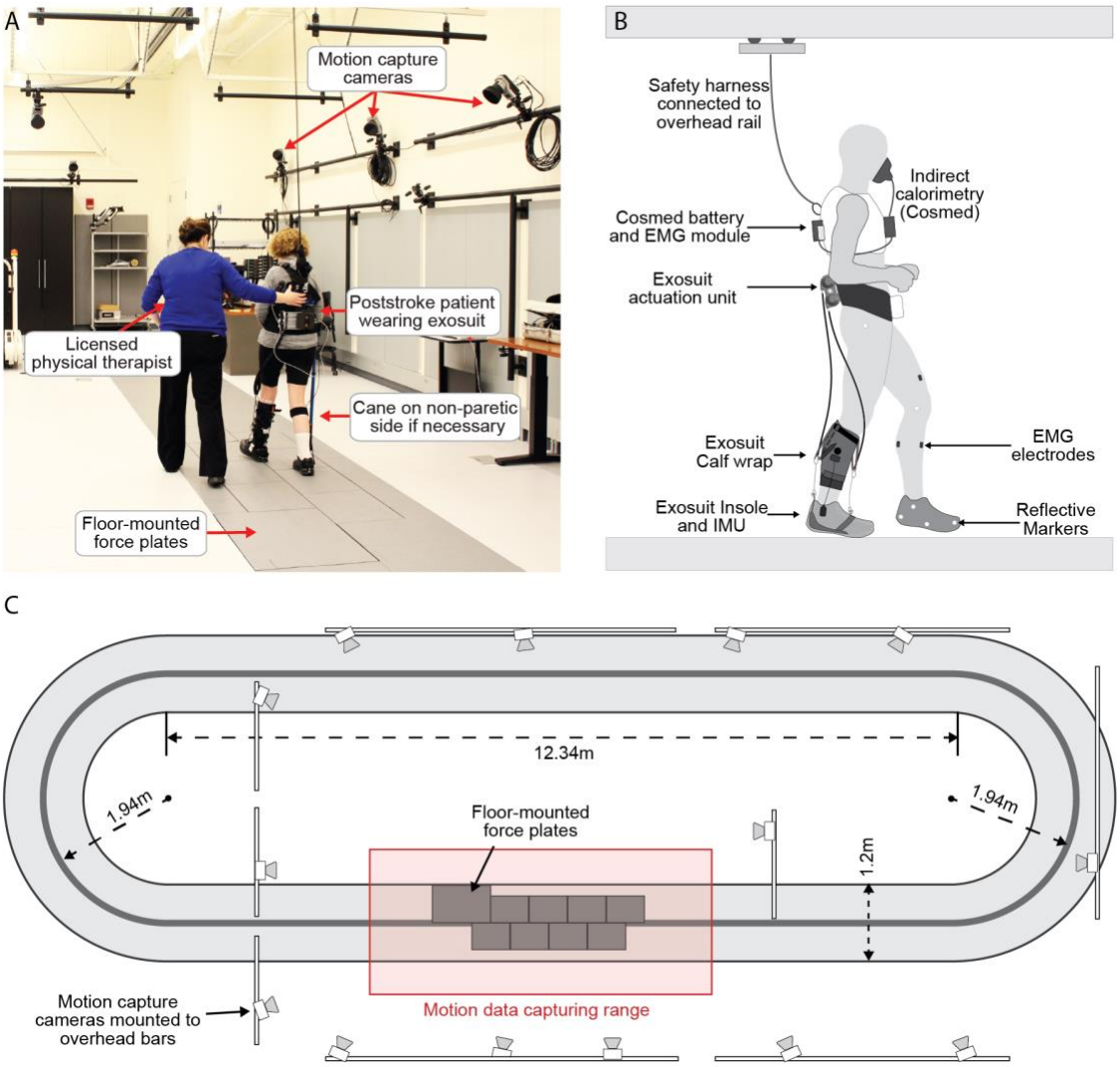

Figure 7.1. Overview of experimental setup. (a) Study participant walking with the portable soft exosuit, while motion capture cameras and floor-mounted force plates capture the movement. (b) In addition to the exosuit, participants wore an indirect calorimetry system, EMG electrodes and reflective markers. Safety measures included guarding by a licensed therapist, a safety harness connected to an overhead rail and the use of a cane on the nonparetic side if needed. (c) Study participants walked continuously for five minutes on an overground track of 36.9m in length.

7.2.4. Data measurement and analysis

Gait kinematics and kinetics

Lower-extremity joint kinematics were measured by a motion-capture system (Oqus, Qualisys Inc, Sweden), in which reflective markers were placed on anatomical landmarks and segments. To track the cables' orientation necessary for determining exosuit-exerted torques, markers were also placed on the Bowden cable connection points. Ground reaction forces were collected by nine ground-embedded force

plates (FP4060-10-2000, Bertec, USA). Load cell data measuring exosuit-exerted force was sampled at 100 Hz. Marker and ground reaction force data were low-pass filtered using a Butterworth filter with a 10 Hz cut-off frequency. Lower-body joint angles were calculated through inverse kinematics and total joint kinetics through inverse dynamics using motion analysis software (Visual3D, C-Motion, USA). Gait events were detected using the relative distance between foot markers and the ground and kinematic and kinetic data were time-normalized to 0-100% of the gait cycle. Kinetic variables were normalized to body weight. Strides with full, single foot landing on the force plates were selected for analysis.

Functional gait metrics

Primary gait function metrics included walking speed, metabolic cost of walking and stability. To allow for steady-state assessment of walking speed and metabolic cost, the last two minutes were used for calculation. Average walking speed was derived from sternum marker data. Metabolic cost of walking was assessed by indirect calorimetry using a portable gas analysis system (K4b2, Cosmed, Italy). Metabolic power was calculated using a modified Brockway equation [179]. Net metabolic power was obtained by subtracting the metabolic power during the standing trial from the walking trials and was subsequently normalized by body weight and walking speed to yield net metabolic cost of walking. Metabolic cost data from one full community ambulator participant was excluded due to malfunctions in the portable pulmonary gas exchange measurement device during testing. Stability of walking was assessed by step width (medio-lateral distance between the center of gravity of the feet) and coefficient of variance in step length, both have been shown to be related to different aspects of stability [205]. Secondary spatiotemporal parameters included paretic and non-paretic step length, step time and stance phase.

Paretic limb forward propulsion

Forward Propulsion was evaluated as the average body center-of-mass (COM) power generated during the step-to-step transition (i.e. when the positive COM power crosses zero during second double stance until toe-off), similarly to Chapter 5 [92]. Specifically, COM power was calculated as the dot product of the

COM velocity vector estimated by the average velocity of the iliac crest markers and the individual limb ground reaction force vector [206]. The effect of the plantar flexion exosuit assistance on the ankle propulsion was calculated as the positive total ankle power impulse (from zero crossing in the propulsive phase to toe-off). Secondary variables included the COM power during collision (first negative peak), rebound (first positive peak) and pre-loading (negative peak towards the second half of single limb support) phases [164] as well as the integral over the anterior ground reaction force during the propulsive phase. Additionally, we calculated the peak total ankle moment during stance, and the biological peak ankle moment and positive ankle power impulse by subtracting the exosuit delivered moment and power from the total moment and power. To understand any potential kinematic restrictions of the propulsive assistance, we evaluated peak ankle dorsiflexion, peak ankle plantarflexion, maximum trailing limb angle (TLA) during push-off, calculated as the maximum sagittal plane angle between the vertical axis of the lab and the vector joining the paretic limb's ankle joint center (taken from the link-segment model in Visual3D) and the greater trochanter [207].

Foot landing and ground clearance

To assess changes in foot landing in weight acceptance phase, the anterior-posterior location of the point of floor contact (center of pressure) was defined relative to the foot, with a center of pressure behind the ankles indicating a heel landing. In addition, the ankle dorsiflexion angle and knee flexion angle at initial contact were measured. To assess the control of rotating the foot to the ground (the level of foot slapping), the smoothness of the first peak of the vertical ground reaction force was evaluated, with a negative peak in the derivative indicating foot slap. Secondary variables included ankle at initial contact.

To assess the effect of exosuit assistance on ground clearance during swing, minimal toe clearance was calculated as the difference in vertical distance of the marker placed on the fifth metatarsal head (lateral toe marker) between the minimum during swing (approximately mid-swing) and the average during mid-stance [208], [209]. Secondary variables included the ankle dorsiflexion angle during mid-swing (when distance to the ground is minimal and ankle dorsiflexion is most critical); compensatory hip hiking, defined as the

maximum lateral difference in position of the center of gravity of the foot (from the model in Visual3D) during swing versus the vector from position at toe-off and at initial contact; and compensatory hip circumduction, defined as the maximum lateral difference in position of the center of gravity of the foot (from the model in Visual3D) during swing versus the vector from position at toe-off and at initial contact [182]. Secondary variables included peak knee flexion during swing.

Muscle activity

EMG data were collected for the gastrocnemius lateralis (GS), soleus (SO), tibialis anterior (TA), rectus femoris (RF) and bicep femoris (BF) on both legs, using a wireless system for the lower leg of the non-paretic side (Trigno, Delsys, USA) and a wired system for the other muscles (Bagnoli, Delsys, USA). EMG electrodes remained attached for the duration of the testing session. EMG signals were firstly band-pass filtered with 4th order Butterworth filter (cut-off frequency=20 and 450 Hz), rectified, and then low-pass enveloped with 4th order Butterworth filter, cut-off frequency=10 Hz). The same strides selected for kinematic and kinetic analysis were used for EMG analysis. Each muscle's EMG was normalized to its maximum average muscle activity over the gait cycle during baseline walking. To evaluate changes in muscle activation between the two conditions, the area under the curve was calculated during the loading phase (from paretic initial contact to non-paretic toe-off), the push-off phase (from non-paretic toe-off to paretic toe-off, to include plantarflexion muscle activation during mid-stance), and the swing phase, for all muscles on the paretic and the non-paretic side. EMG data of SO on the paretic side from one participant as well as GS data on the non-paretic side for another subject, both full community ambulators, were excluded from analysis as they were of bad quality. To evaluate if voluntary ankle muscle activity was affected, primary variables were dorsiflexion activity of the TA during loading and swing phases and plantarflexion activity of GS and SO during push-off.

Statistical analysis

Statistical analysis was conducted to evaluate the effect of walking with exosuit assistance compared to walking without exosuit assistance across all participants. First, as baseline walking speed is a major determinant of functional gait status [14], [158], a Spearman correlation analysis was performed between participants' baseline and exosuit-induced change in walking speed. This analysis elucidated the importance of baseline walking speed, therefore participants were divided into two functional ambulatory groups identified with their comfortable walking speed (CWS) based on the cut-off threshold value suggested in [204] i.e. lower-level limited community ambulators (n=10, CWS less than 0.93 m/s) and higher-level full community ambulators (n=9, CWS above 0.93 m/s;). For statistical comparison tests, we evaluated normality of distribution with Shaprio-Wilk tests. For normally distributed variables, we performed a two-factor repeated measures ANOVA using walking condition (effect of exosuit) as within-subject factor and ambulatory group (limited vs full ambulators) as between-subject factor. Significance level was set at $p<0.05$. When an interaction effect was found, post-hoc analysis of exosuit-induced differences within each ambulatory group was conducted using paired t-tests. For variables that were not normally distributed we tested similar effects: (1) the effect of exosuit across all participants (Wilcoxon signed-rank test), (2) "interaction effect" by comparing the exosuit-induced percentage change between the two ambulatory groups (unpaired rank-sum tests), and if the latter effect was present, (3) post-hoc analysis of exosuit-induced differences within each ambulatory group (Wilcoxon signed-rank test).

Moreover, if the aforementioned statistical comparison test did not signify statistically meaningful changes (i.e. $p > 0.05$), two one-sided tests (TOST) were performed to check the equivalence of paired sample data. Specifically, non-superiority testings were performed for metabolic cost and the stability metrics (i.e. lower bound set to infinity) and non-inferiority testing for paretic muscle activity (i.e. upper bound set to infinity), both using 90% confidence interval and $p<0.05$ significance level [210]–[212]. As standard equivalence boundaries values are not available for most of the variables used in this study, Cohen's standard effect sizes d_z were calculated, with boundaries set at Cohen's d of 0.2 – which is generally considered a small effect – and adjusted for paired samples by a factor of $\sqrt{2}$ [212]. Finally, to understand the potential

relation between changes in different functional parameters and exosuit-assisted ankle power during push-off, Spearman correlations were performed between change in walking speed, stride length, COM propulsion and ankle power. Statistical analysis was conducted in SPSS (v25, IBM Corp., USA) and correlation analysis in MATLAB (MathWorks, USA).

7.3. Results

7.3.1. Increased walking speed and step length

Walking speed increased by 5% (0.04 m/s, p=0.048) across all participants when wearing exosuit compared to not wearing it (**Figure 7.2**). Correlation analysis demonstrated that exosuit-induced changes in walking speed depended on participants' baseline walking speed (r_s=-0.51, p=0.03). Moreover, an interaction effect was observed between exosuit assistance and functional group (p=0.03), with limited ambulators increasing walking speed by 13% (0.08 m/s; p=0.008) while the group of full ambulators did not change their walking speed (0%, p=0.82). Paretic step length was increased by 4% across all participants (p=0.03), without a significant interaction effect (p=0.06). We did not observe differences in step length symmetry, paretic step time, or paretic stance time between conditions or interaction effects across subgroups of participants.

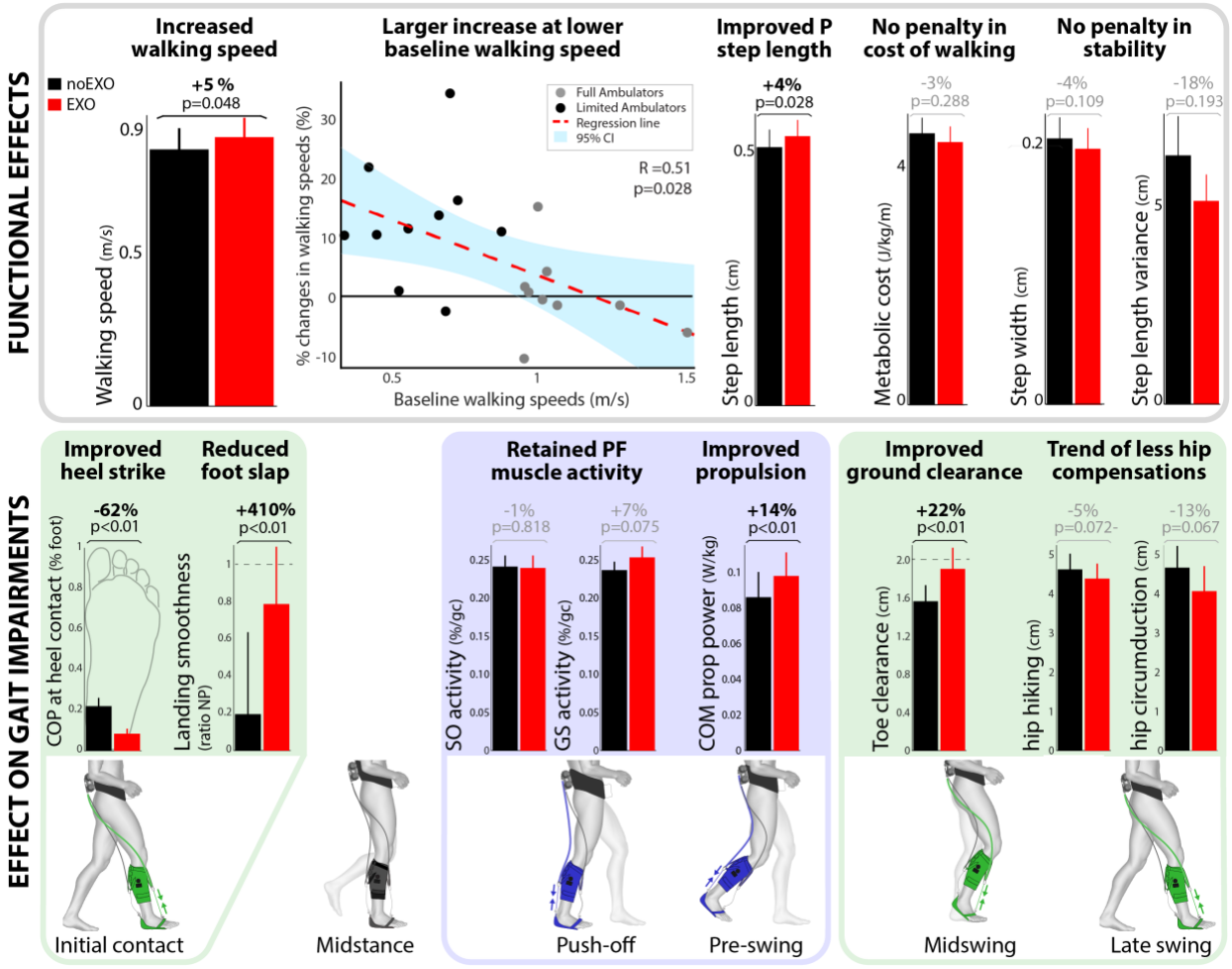

Figure 7.2. Summary of the effect of exosuit assistance in post-stroke patients compared to baseline walking. Exosuit improved walking speed and paretic step length, while not increasing the metabolic cost or gait instability (top). Interestingly, baseline walking speeds were negatively correlated with changes in walking speeds. The dorsiflexion support during the loading phase normalized flat foot landing to heel strike landing and decreased the occurrence of foot slap, while the assistance improved ground clearance and tended to reduce hip compensations during the swing phase (lower section). The plantarflexion assistance during push-off increased the center of mass propulsive power (COM prop power), without reducing voluntary muscle activity in the plantar flexor muscles during normal push-off. Bar graphs represent mean and standard error for walking with exosuit (red) and baseline walking without exosuit (black) based on all participants (n=19), except for metabolic cost of walking (n=17) and soleus muscle activity (n=18). For some metrics the non-paretic side is shown in a black dashed bar for reference. Overall exosuit effect across all participants from the repeated-measures ANOVA are indicated in black (p<0.05), the rest in gray.

7.3.2. Preserved metabolic cost of transport and stability

We did not find any statistically significant change in metabolic cost of transport (p=0.29), nor an interaction effect (p=0.89; **Figure 7.2**). Further, we did not find a difference in our metrics for walking stability, step width (p=0.11) or step length variability (p=0.19) between conditions or an interaction effect across subgroups of participants. Additionally, statistical equivalence analysis showed that metabolic cost

(p=0.01), step width (p<0.001) and step length variance (p=0.02) did not significantly change when walking with exosuit.

7.3.3. Increased paretic limb propulsion

Body COM propulsion power generated by the paretic limb during the push-off phase increased by 14% (p=0.003) across all participants when walking with the exosuit (**Figure 7.2**and **Figure 7.3**). At the paretic ankle, peak total PF moment during push-off increased by 14% (p<0.001), while peak biological moment reduced by 4% (p=0.005). There was no significant increase in paretic ankle power impulse during push-off (7%, p=0.13). Examining individual group responses, we found that COM propulsion power mainly increased in limited compared to full ambulators (32% vs. 5%; p=0.008). Paretic peak ankle moment also increased more in the limited ambulators (27% vs. 6%, p=0.002). Interestingly, biological peak moment was maintained in the limited but reduced in the full ambulators (2% vs. -9%, p=0.01). Similarly, paretic ankle propulsion power mainly increased in limited compared with full ambulators (28% vs. -1%, p=0.002), and biological ankle power decreased more in full ambulators (-22% vs. -6%, p=0.03). Regarding ankle kinematics, we did not observe changes in maximum ankle plantarflexion angle during push-off across all participants (p=0.26) or between sub-groups (interaction p=0.40). Maximum ankle dorsiflexion angle before push-off, however, was reduced by -2.2° across participants (p<0.001), with a more prominent reduction in full ambulators (-4.3° vs. -0.4°, interaction p<0.001).

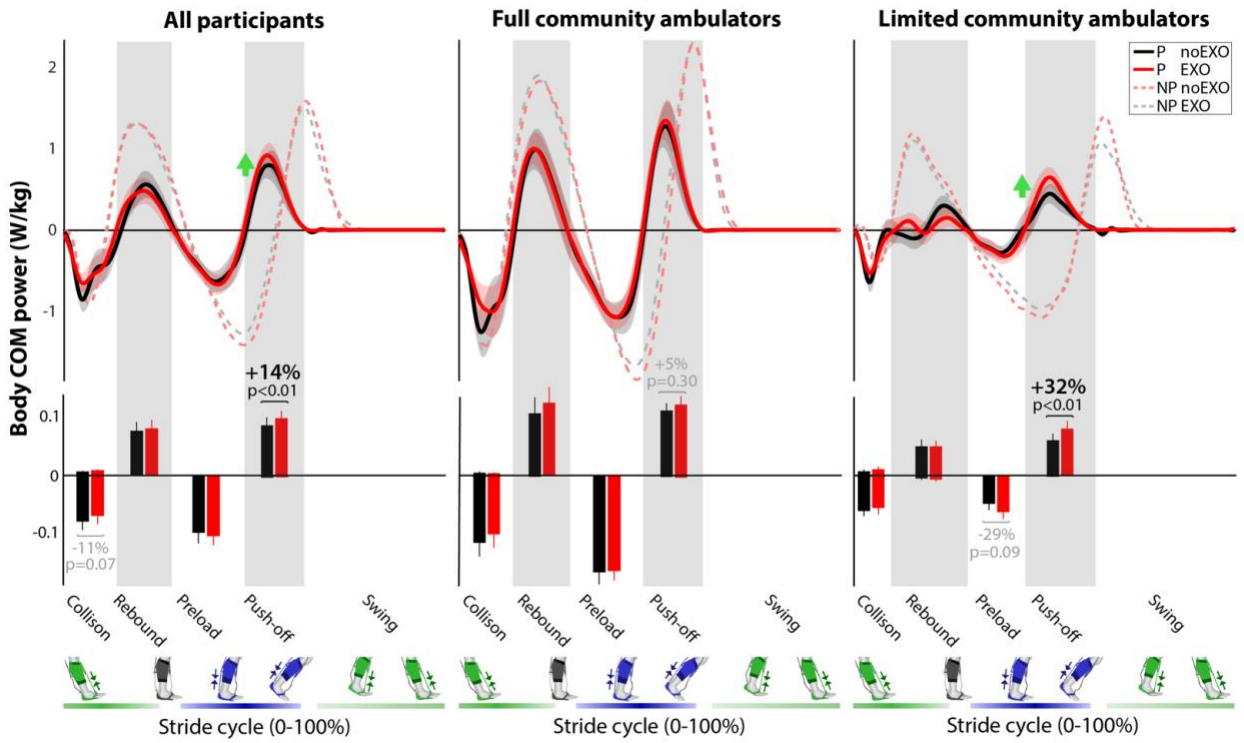

Figure 7.3. Effect of exosuit assistance on body center-of-mass (COM) power in both limited and full community ambulatory groups. Exosuit assistance improved positive body COM propulsion power for all participants (n=19), with greater improvement in the limited ambulators compared to full ambulators. The paretic side data is represented by a solid line and the non-paretic side by a dashed line. The bar graphs represent the average COM power of four different phases on the paretic side. From the repeated-measures ANOVA the within-in subject exosuit effect p-values are indicated in the left column and post-hoc t-test exosuit effect p-values per ambulatory group in the other two columns in black ($p<0.05$).

7.3.4. Correlation between walking speed and forward propulsion power

To understand the mechanisms underlying increases in walking speed, correlation analyses were performed between change in walking speed, paretic step length, COM propulsion power and total paretic ankle propulsion power (**Figure 7.4**). Increased walking speed was correlated with increased paretic step length (r_s=0.63, p=0.005). In turn, increased step length was related to increased COM propulsion power (r_s=0.66, p=0.003), and likewise increased COM propulsion power was related to increased ankle power (r_s=0.76, p<0.001).

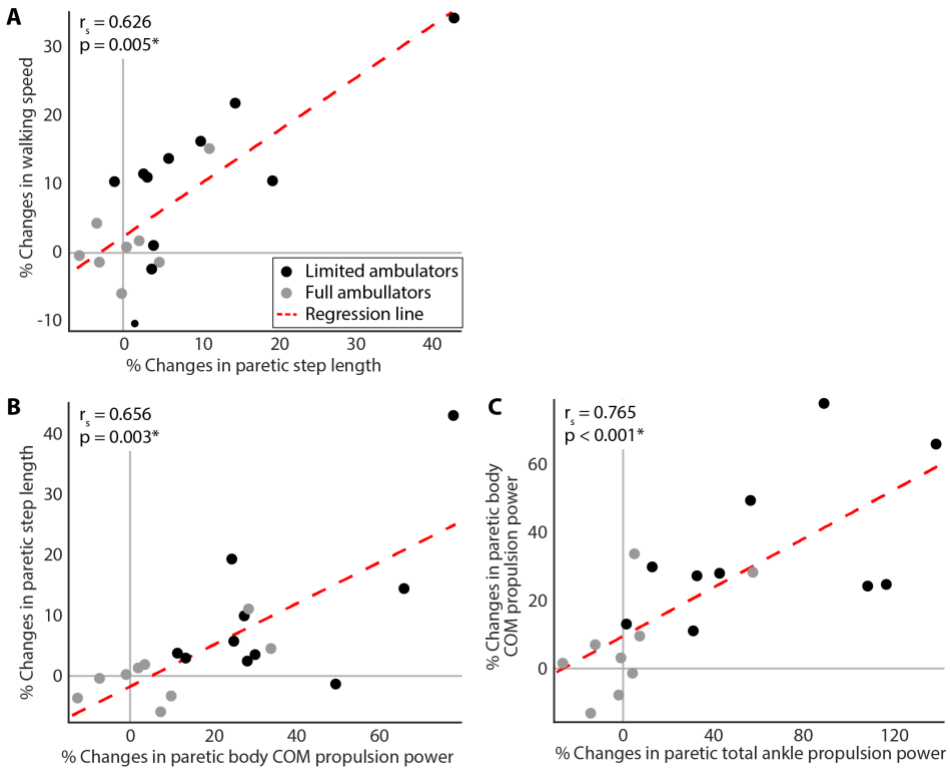

Figure 7.4. Correlations between changes in walking speed, paretic step length, and propulsive power generation. (a) Improved speed was related to increased paretic step length. (b) the increased paretic step length was related to the changes in paretic center-of-mass (COM) propulsive power. (c) Ultimately, the changes in COM propulsive power was related to the changes in the paretic total propulsive ankle power. Regression lines based on all participant data were presented in red dotted lines, with limited ambulators in black dots and full community ambulators in gray dots. Spearman correlation coefficient r_s and corresponding p-value were presented in the upper left corner.

7.3.5. Restored heel landing and ground clearance

During the loading phase (i.e. weight acceptance), heel landing on the paretic side improved when walking with exosuit assistance across all participants (p<0.003), with the point of contact at initial contact located 14% more towards the heel (**Figure 7.2**). Participants increased paretic ankle dorsiflexion angle by 7.1° (p<0.001; **Figure 7.5**). Control of foot landing became more than four times as smooth compared to baseline walking (p<0.001; **Figure 7.2**), with the number of participants exhibiting foot slap reducing from 14 during baseline walking to zero with exosuit assistance. There was no interaction effect in any of these variables.

During swing, toe clearance was increased by 22% (p=0.003) across all participants when walking with the exosuit assistance (**Figure 7.2**) Paretic dorsiflexion angle at mid swing was increased by 4.3° (p<0.001; **Figure 7.5**). Concurrently, there was a trend of reduced hip circumduction (-13%, p=0.07) and hip hiking

(-5%, *p*=0.07) on the paretic side across all participants. There was no interaction effect for any of these variables nor effect on knee flexion velocity during swing (p=0.12; **Figure 7.6**).

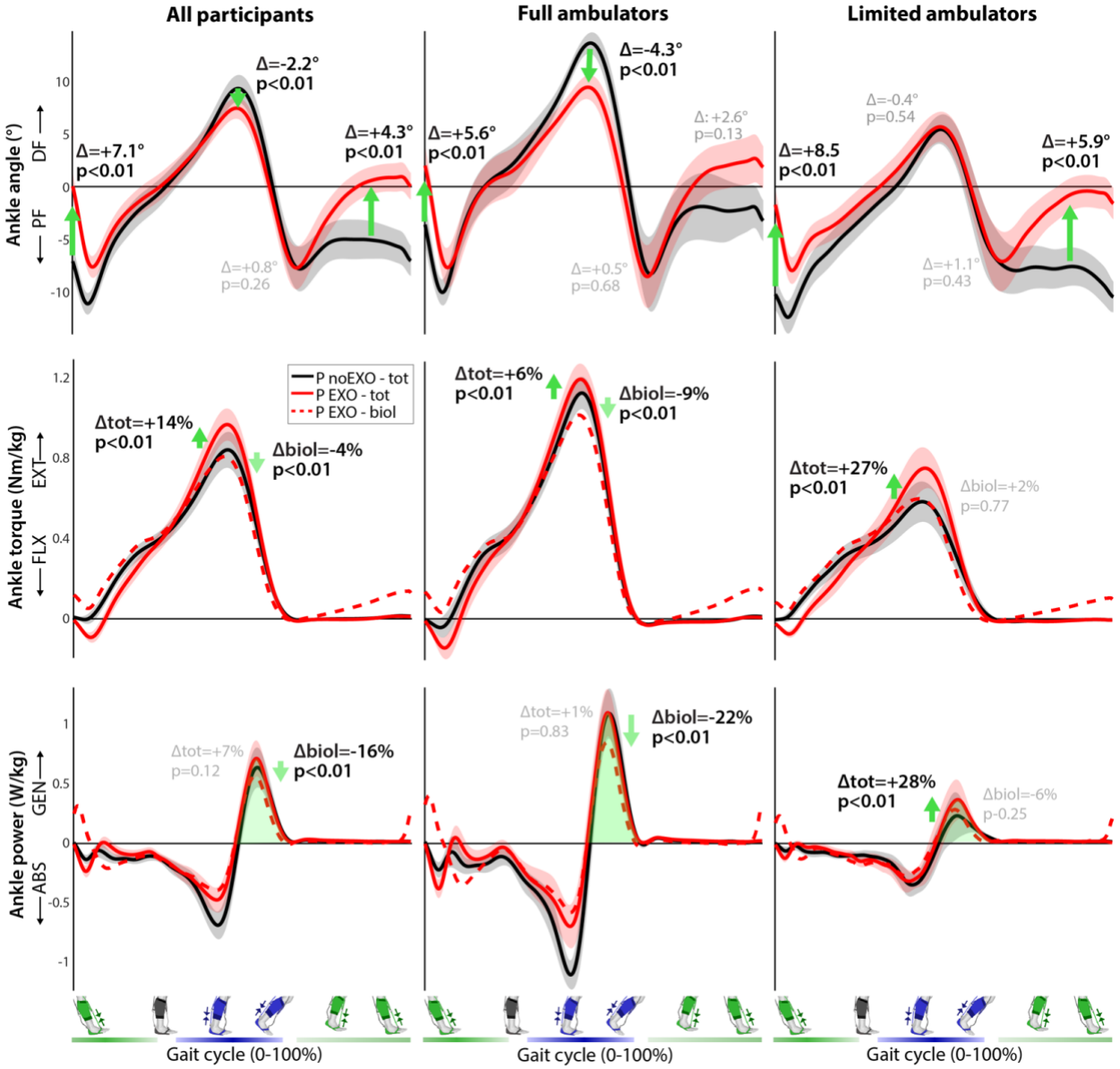

Figure 7.5. Effect of exosuit assistance on paretic limb sagittal plane ankle kinematics and kinetics in both limited and full community ambulatory groups. Time-normalized graphs are averaged over all stroke participants (n=19, left column), full ambulators (speed>0.93 m/s, n=9, middle column) and limited ambulators (speed<0.93 m/s, n=10, right column). Average and standard deviation are shown for walking without the exosuit (black) and with exosuit assistance (red), as well as the average biological contribution (dashed) for the latter. Note that biological data was unavailable one limited ambulator. Changes are indicated for ankle angle at initial contact, peak dorsiflexion and peak plantar flexion angle during push-off, ankle angle mid swing, peak plantarflexion torque and positive power impulse during push-off. From the repeated-measures ANOVA the within-in subject exosuit effect p-values are indicated in the left column and post-hoc t-test exosuit effect p-values per ambulatory group in the other two columns in black (p<0.05).

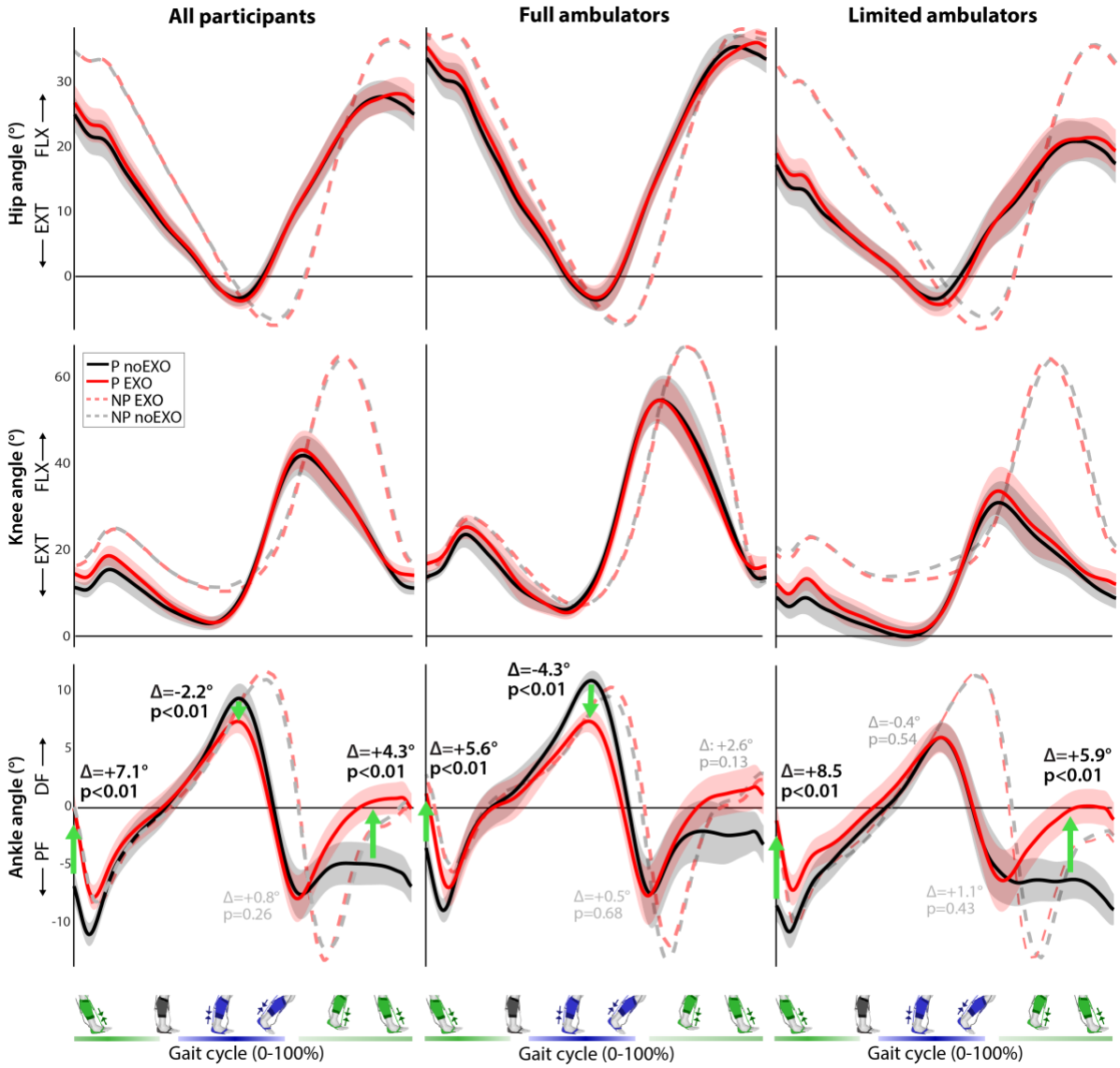

Figure 7.6. Effect of exosuit assistance on sagittal plane lower-limb kinematics in both limited and full community ambulatory groups. Ankle, knee and hip angles are shown for walking with (red) and without (black) exosuit assistance over all participants (n=19, left column), full ambulators (n=9, middle column) and limited ambulators (n=10, right column). Ankle and knee flexion angle increased at initial contact in both limited and full ambulator groups, with ankle angle flexion also increasing in limited ambulators during mid swing. The assistance did not change the ankle range of motion during push-off in the limited ambulators but decreased the maximum dorsiflexion angle before push-off in the full ambulators. Time plots are normalized to the paretic gait cycle (solid lines, average with standard deviation) as well as non-paretic gait cycle (dashed lines) for reference. Timing of dorsiflexion (green) and plantarflexion (blue) assistance is indicated at the bottom of the figure. Changes are indicated in blue for peak knee angle velocity during swing (none), ankle angle at initial contact, peak ankle PF and DF during stance and ankle DF angle during mid-swing. PF = plantarflexion, DF = dorsiflexion, biol = biological. From the repeated-measures ANOVA the within-in subject exosuit effect p-values are indicated in the left column and post-hoc t-test exosuit effect p-values per ambulatory group in the other two columns in black ($p<0.05$).

7.3.6. Preserved paretic propulsive muscle activity

We did not find any changes in paretic ankle plantarflexor activation across all participants (Gastrocnemius, GS: +7%, p=0.08; Soleus, SO: -1%, p=0.82; see **Figure 7.2** and **Figure 7.7**), nor in paretic ankle dorsiflexor activations (Tibialis anterior, TA: -2% p=0.77) or thigh muscle activations (Biceps femoris, BF, -7%, p=0.19; Rectus femoris, RF, 2%, p=0.60). Interaction effect was not found as well. Subsequent equivalence testing showed that GS (p=0.004) and RF (p=0.025) did not change when wearing the exosuit.

In contrast, during swing, paretic TA activation was reduced by 17% (p=0.002) across all participants, while plantarflexor muscle activations increased (GS: 34%, p<0.001; SO: 15%, p=0.05). We did not find any changes in other measured muscles nor interaction effects, except for non-paretic BF activation that increased in full ambulators compared to limited ambulators (16% vs. -4%, interaction: p=0.04). Equivalence testing showed that GS (p<0.001), SO (p=0.001), and BF (p=0.018) indeed did not change with exosuit-assisted walking.

During loading phase, plantarflexor activity increased (GS: +15%, p=0.06; SO: +11%, p=0.02), while we did not find changes between conditions for paretic TA activity (-2%, p=0.72) or the other measured muscles nor interaction effects across subgroups during this phase. Equivalence testing showed that GS (p<0.001), SO (p=0.001), and RF (p=0.001) did not change in walking with exosuit.

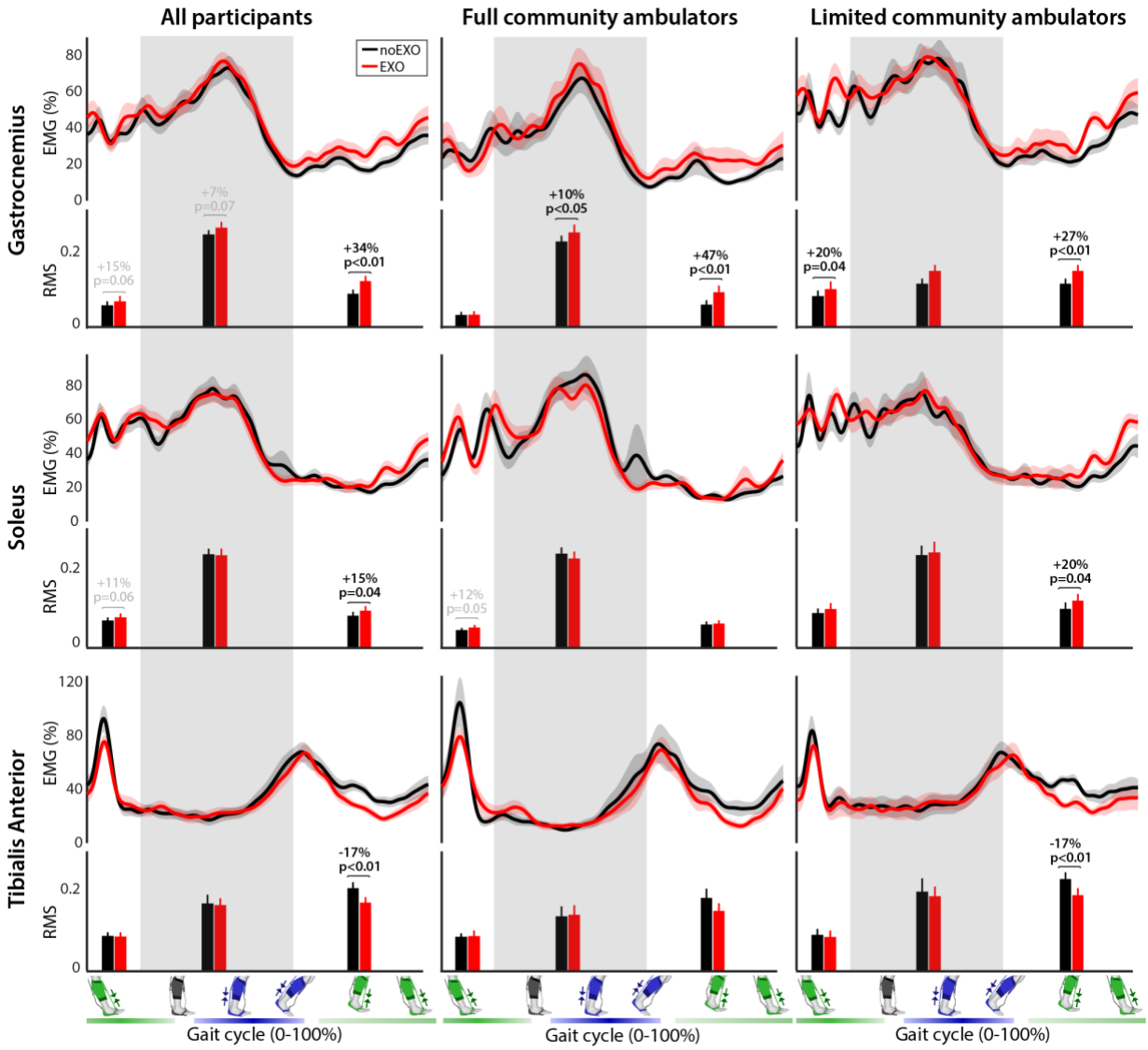

Figure 7.7. Effect of exosuit assistance on paretic limb ankle muscle activation. Across all participants (n=19), exosuit assistance did not reduce paretic gastrocnemius and soleus activity during push-off, while reducing tibialis activity on the paretic side during swing. There were no interaction effects, except for biceps femoris activity during swing. Muscle activity patterns are time normalized to the paretic gait cycle (solid line, average and standard deviation). Muscle activity is normalized to the average maximum of walking without exosuit condition per individual. Root-mean-square (RMS) activity are indicated for all muscles per phase, i.e. loading, push-off (gray box – phase where the plantar flexor muscles are activated to achieve propulsion, from non-paretic toe-off to paretic toe-off), and swing phase (average and standard error). Timing of dorsiflexion (green) and plantarflexion (blue) assistance are indicated at the bottom of the figure. EMG values are averaged over all participants (n=19) except for paretic soleus (n=18) because of an issue in data collection. From the repeated-measures ANOVA the within-in subject exosuit effect p-values are indicated in the left column and post-hoc t-test exosuit effect p-values per ambulatory group in the other two columns in black ($p<0.05$).

7.4. Discussion

This chapter presents the first comprehensive experimental study to evaluate the immediate impact of a portable soft exosuit on overground walking in post-stroke individuals, including both limited and full community ambulators. We thoroughly investigated a wide range of biomechanical metrics such as walking speed, metabolic cost of transport, body center-of-mass power, and voluntary muscle activation, which bear important relevance to patients' quality of life and effectiveness of gait rehabilitation [51], [213].

We found that the portable exosuit improved walking speed, especially in the limited community ambulators, while preserving metabolic cost of transport and stability of gait. As intended, dorsiflexion assistance improved control of foot landing during the loading phase and ground clearance during the swing phase, and plantarflexion assistance increased paretic propulsion without decreasing voluntary push-off muscle activation. While the dorsiflexion assistance had a similar effect in both ambulatory groups, the plantarflexion assistance increased paretic forward propulsion more in limited community compared with full ambulators.

Increased walking speed

Exosuit assistance significantly increased walking speed by 13% in post-stroke persons who exhibit slow walking speeds and are classified as limited community ambulators. This is an important finding, as it the first demonstration of ankle assisting robot's ability to increase walking speed in post-stroke patients, for which the ability to walk at an effective walking speed is critical for social participation [213]. Interestingly, this study suggests that exosuit could complement cane-assisted walking by further increasing walking speed: six out of seven participants who used canes in the study increased walking speed with exosuit by 0.10m/s (17%). The larger improvement in limited relative to full community ambulators could be explained by the smaller capacity to improve their limited walking speed on their own, and that they receive more push-off assistance relative to their baseline biological ankle moment (35% versus 7%).

Although the immediate exosuit-induced increase in walking speed of 0.04 m/s across participants is not substantial, the change is similar to the small minimal clinically important difference (MCID) of 0.04 m/s.

Even more, the change in walking speed found in the limited ambulators (0.08 m/s) is close to the substantial meaningful change of 0.10 m/s defined in [214]. The demonstrated effect of the exosuit on walking speed was on the higher end of the immediate effect found from walking with a passive ankle-foot orthosis (0.05-0.09 m/s) and functional electric stimulation (0.02-0.07 m/s) [215]. For reference, it was also in the same order or larger than the therapeutic effect reported in several post-stroke training studies, including training with exoskeletons, ankle-foot-orthosis, functional electrical stimulation, and treadmill walking with or without body support [75], [215]–[219].

It should be noted that this study examined the immediate, in-session gait improvements induced by exosuit assistance alone, as we did not give any cues related to gait patterns or utilization of exosuit, and the only cue given to all participants were to walk at comfortable walking speed. Indeed, it might be possible that the verbal instruction to walk in comfortable walking speed interfered with exosuit-induced changes, as some of participants mentioned that they tried to preserve their walking speed in both walking conditions because they thought that was what comfortable walking speed meant. We also posit full community ambulators might benefit more from the exosuit assistance in more challenging conditions such as at faster walking speed, non-level walking or over farther distances. Indeed, our previous pilot study with the portable exosuit protype presented in Section 3.5.2 demonstrated that post-stroke participants were able to leverage the exosuit assistance to increase their fast walking speed. Specifically, this study showed that while the five included full community ambulators did not increase their walking speed during the test when walking at preferred walking speed (+0.05±0.08 m/s, p=0.23), but they could increase when walking at fast walking speed (+0.10±0.07 m/s, p=0.03). Further study is therefore warranted to investigate the impact of different walking speeds on exosuit-induced changes. Additionally, most participants in this study had limited exosuit exposure prior to the experimental sessions, and may have required more familiarization periods to generate larger gait improvement. Learning curves for walking with robotic devices have not been investigated as much in post-stroke participants, only one study mentioned a required period of 20 minutes [119], which aligns with time periods of 15-30 minutes for healthy subjects [200], [201], [220]–

[223]. Furthermore, the exosuit-induced changes were evaluated at comfortable walking speed, while individuals might be able to leverage the exosuit assistance differently during different conditions such as faster walking speed or non-level walking. Understanding the optimal training regimen required for familiarization to exosuit assistance as well as the added effect of cueing remains an area of future exploration for our group.

Furthermore, our subgrouping analysis using a single cut-off threshold value on participants' comfortable walking speed may not be the optimal to understand the different impact of exosuit on different impairment level. Our rationale to use the walking speed threshold was that gait speed is the most widely accepted clinical measures that is the resultant effect of other components of the gait cycle, and it is a common prognostic and indicator of success of intervention or level of propulsion asymmetry [224]. Although the walking speed cut-off threshold used in this study (0.93 m/s) was selected from a meta-scale study with 441 post-stroke patients [204], we acknowledge that our findings could be affected by our threshold selection. Therefore, we repeated the analysis using another well-recognized cut-off threshold value of 0.80 m/s [134], [225]. Interestingly, we found the exact same result from the subgroup analysis based on this new cut-off threshold. Although the cut-off did not seem to effect results, we would like to emphasize that we analyze group means here that dichotomizing the data based on speed might have washed-out different effects. Further research is therefore necessary to characterize and find predictor variables for individual exosuit response.

Augmented propulsion and preserved muscle activity

Forward propulsion during push-off is a key determinant of walking function and therefore improving paretic propulsion is often the main goal of post-stroke gait training [121]. By delivering partial assistance of only 22% of peak biological ankle moment, the exosuit improved forward body COM propulsion power by 14% across all participants. These results align with our previous finding of increased propulsion force and propulsive COM power comparing walking with powered versus unpowered exosuit [90], [92]. Moreover, this study provides new evidence of successful translation of paretic ankle function improvement

to whole body mechanics improvements and functional gait performance: increases in ankle power were strongly correlated with increases in body COM power [92], which was correlated with increases in step length. Ultimately, increased step length was correlated to increased walking speed. This aligns with studies associating weaker propulsion with reduced gait speeds and reduced step length asymmetries in post-stroke walking [23], [112], [226].

This study also contributes to understanding that different strategies could be utilized to increase propulsion depending on functional ambulation level: limited ambulators leveraged the assistance by maintaining their biological paretic ankle moment and power; full ambulators leveraged it to compensate for decreased biological push-off. This aligns with our previous finding of the negative correlation between baseline walking speed and improvement in propulsion during treadmill walking [90]. As muscular effort did not reduce, kinematic changes could be underlying the biological reductions in the full ambulators, specifically reduced ankle dorsiflexion angle before push-off. The reduction in ankle dorsiflexion angle could result in (partial) replacement of Achilles tendon energy storage by the assistance, to less optimal trailing limb position, and inhibited tibial progression as has been suggested for other devices [119], [227]. Since our previous study demonstrated forward propulsion improvements to be affected by onset timing of plantarflexion assistance differently between individuals [90] and as this study only investigated one generic timing, individualizing the onset timing might further increase propulsion.

Even though patient participation is of vital importance for effective post-stroke gait training, the effect of active assistive devices on muscle activity has not often been considered in previous clinical studies of wearable robots. This first study evaluating the effect of exosuit assistance on muscle activity demonstrates preserved voluntary paretic plantarflexion muscle activity during push-off, with even a trend of increased GS activity. Dorsiflexion muscle activity did not change either, indicating that no increase in co-contraction was required to stabilize the ankle during push-off. The retained propulsive muscle activity is in contrast with literature, reporting reductions in both post-stroke [119] and able-bodied individuals [199], [200], [203], [221], [222] walking with active ankle devices. Increasing propulsion while retaining active muscle

activity indicates that exosuit assistance could be a beneficial tool for post-stroke gait rehabilitation, as it could encourage participants' active involvement in generating forward propulsion.

Restored ground clearance

Foot drop and the resulting difficulty in clearing the ground during swing are common post-stroke gait deficits related to instability and falls [14]–[17]. This study calculated toe clearance directly and showed it improved when walking with exosuit assistance. There are several strategies to achieve ground clearance, including dorsiflexing the ankle, flexing the knee or compensating at the hip. Dorsiflexion assistance directly targeted and increased ankle dorsiflexion by over 4° on average, which is almost five times larger than the 0.9° minimal detectable change [128] and comparable to improvements previously found during treadmill walking [90], [92]. Slightly larger dorsiflexion increases of around 10° have been reported using other active ankle devices; however, these studies included few subjects with pronounced ground clearance deficits [228]–[231]. Alternatively, the plantarflexion assistance could potentially target reduced knee flexion during swing, and although no such effect was found, further study should focus on stiff-knee gait patients. Finally, exosuit assistance tended to reduce the need for hip compensations. The reduction in hip hiking was less pronounced compared with previous results during treadmill walking (5% vs. 27%), but the reduction in hip circumduction was larger (13% vs. 2%) [182], possibly due to sample differences in baseline hip compensations and habitual strategies underlying overground speed changes.

As a result of the exosuit assistance during swing, paretic dorsiflexion TA activity reduced while paretic plantarflexion GS and SO muscle activity increased. Reduced TA activity has been reported for able-bodied subjects walking with dorsiflexion support [201], [230] as well as post-stroke participants walking with ankle-foot-orthoses [90], [93], [182], [232], [233]. Although reduced TA activity could be considered positive when exosuit serves as a gait assisting device, this may imply patients' insufficient exertion for effective training on DF function. Additionally. The increased plantarflexion activity could indicate a resistance to the pulling dorsiflexion force. Alternatively, it could be related to exaggerated responses by spastic muscles, although with max 30°/s the applied rotation of is far below any stretch velocity applied in

instrumented manual spasticity tests [234], [235], related to reduced negative feedback from the dorsiflexor muscle, although additional analysis did not show such a relation, or to altered proprioception in the foot sole by the applied force. Regardless of the cause, the assistance could potentially be further optimized by individual tuning, while reductions in TA activity might be avoided by new control strategies such as assist-as-needed strategy.

Restored heel landing

Control of foot landing is often impaired post-stroke, leading to flat foot landing and/or foot slapping and as such suggested to affect weight transfer to the paretic limb [33], [236]. While dorsiflexion assistance was designed to aid controlled foot landing by providing continued dorsiflexion assistance during the loading phase, the effect had yet to be evaluated. Indeed, ankle dorsiflexion angle at initial contact was increased by 7°, which is over four times the 1.6° minimal detectable change [128]. This resulted in improved heel landing as measured by the center of pressure and facilitated a controlled progression from heel strike to flat foot, regardless of ambulatory group. It should be noted that while several assistive devices were designed to improve foot landing or foot slap, few studies have evaluated their direct impact on these specific gait impairment metrics, therefore this study provides valuable information for future development of devices to address these impairments.

Muscle activity of the paretic TA, the primary muscle responsible for lifting the foot prior to and control of progression after heel strike, did not change when walking with the dorsiflexion exosuit assistance. This is in contrast with one study reporting increased TA values around heel strike in able-bodied individuals walking with a powered ankle device [237], but it might indicate that post-stroke individuals remain engaged during the loading responses. It should be noted that the magnitude provided during the loading phase was not separately tuned from the swing phase, and individual optimization might benefit from standardized metrics to tune to assist-as-needed and evaluation of assistance on weight transfer.

Preserved gait energetics and stability

Metabolic cost of transport as well as gait stability were not affected by exosuit assistance, in either ambulatory group. In contrast to the improvements in metabolic cost of transport previously found during tethered exosuit-assisted treadmill walking [90], [92], [182], we did not find a significant change during overground walking, similar to other studies applying assistive ankle devices to post-stroke gait [119], [227]. However, it should be noted that this new study with portable exosuit imposed additional weights on the participants with body-worn actuation and battery units which were not the part of tethered exosuit, indicating that the exosuit assistance compensated for the metabolic penalty caused by the additional weights. Interestingly, out of several metrics related to cost of transport, costly hip compensatory behavior was reduced; however, step width, step length variability and hip and ankle propulsion muscle activity were preserved, and walking speed increased. Allowing individuals more adaptation time [119] or applying higher levels of assistance [100] might contribute to reductions in metabolic cost; however, in the context of gait training, the retained metabolic cost of transport was considered a positive finding as it aligns with retained voluntary muscle activity and intensity of walking.

Further, to our best knowledge, the impact of the weight and applied assistance by wearable robots on gait stability has not yet been assessed in post-stroke gait, while stability and thus safety is a major concern for the more severe and unstable patients. As a previous study showed that young adults select a propulsive force generation that maximizes dynamic stability at their preferred walking speed [238], the impact of the exosuit assistance that is designed to increase propulsion on gait stability was evaluated. We did not find a change in the proxy measures of gait stability, possibly the freedom to select another walking speed resulted in a new "optimum" between propulsion, speed and stability. While our findings on the preserved stability metrics are encouraging, the metrics used in our study are mostly indirect measures and different from the aforementioned study that used dynamic stability measures such as maximum divergent (Lyapunov) exponent. Thus, further investigation with specific stability and balance metrics are therefore warranted.

Potential for post-stroke gait training

Although improvement of walking ability is one of the major goals of post-stroke rehabilitation, current gait training does not provide sufficient therapeutic gain, thus providing an opportunity for rehabilitation robotics [96]. One of the compelling aspects of the exosuit is its potential to provide assistance during both treadmill and overground gait training. The latter is favored during conventional gait training because visual and attentional demand, self-initiation of gait and taking turns are considered more effective for motor learning and representative of real-world ambulation [47], [239]. Indeed, this study showed translation of previously found gait improvements during controlled treadmill walking to overground walking. These immediate gait improvements found when walking with exosuit assistance can be utilized in post-stroke gait training to increase the therapeutic gain.

This study supports our hypothesis that exosuit assistance could indeed help achieve three fundamental aspects of post-stroke gait training: dose, specificity and intensity [51]. First, through increased paretic push-off and walking speed the exosuit could facilitate training at a higher dose. Second, it could facilitate specificity by reducing ankle impairments and hip compensatory strategies thus allowing patients to focus on specific aspects of their gait. Third, walking with exosuit assistance maintains patients' muscle and metabolic exertion or even increases it, thus enabling high-intensity gait training. As such, the exosuit seems to show promise for gait training, and may not have the limitations of conventional ankle foot orthoses, which have been shown to reduce propulsion by kinematically restraining the ankle [41], [42] and rigid exoskeletons which reduce muscle activation [197], [202]. Moreover, the portable exosuit provides a promising platform for further gait training innovation, as assistance can be tuned to individual's specific gait impairments and adapted within the session to facilitate training of a specific aspect of gait, increase carry-over effects and wane off specific part of the assistance in a controlled manner.

In conclusion, we demonstrate immediate restorative benefits of a portable exosuit system that is amenable to overground use, and as such complements the needs of conventional gait training to achieve rapid attainment of normal and independent walking in post-stroke patients.

Chapter 8.

Controller performance of portable exosuit in post-stroke overground walking

8.1. Introduction

In Chapter 7, we presented a biomechanics experimental study with 19 individuals in the chronic phase of post-stroke recovery to compare walking overground with and without the portable exosuit. This chapter presents a supplementary analysis to validate the controller performance of portable exosuit during the experiment. Specifically, exosuit system performance was evaluated to understand (1) how accurately exosuits estimated gait event timings, and (2) if exosuit delivered consistent mechanical assistance to the paretic ankle in biomechanically sensible timings. To this effort, we firstly synchronized sensor and control parameter data collected from exosuit with the biomechanics data collected from motion capture system and force plates, segmented the exosuit data into the paretic gait cycles, and analyzed the data in relation to biomechanical gait events. This study would provide an insight on current exosuit performance and guides our future development to improve exosuit controller and actuation strategies.

8.2. Control strategy of portable soft exosuit for paretic ankle assistance

This section gives an overview of the control strategy of portable exosuit used in this study (see **Figure 8.1**). More details about exosuit system can be found in Chapter 6 [93]. The exosuit delivers ankle PF assistance to improve paretic forward propulsion by generating tensile force on the Bowden cable anchored between the calf and the heel during paretic stance. It also delivers DF assistance to improve ground clearance and foot landing by generating tensile force through the other Bowden cable anchored between the shin and the toe during paretic swing and weight acceptance. To enable consistent DF and PF assistance at the biomechanically sensible timings, the exosuit implements (1) a real-time gait event estimation and segmentation and (2) force-based cable position command generation algorithms.

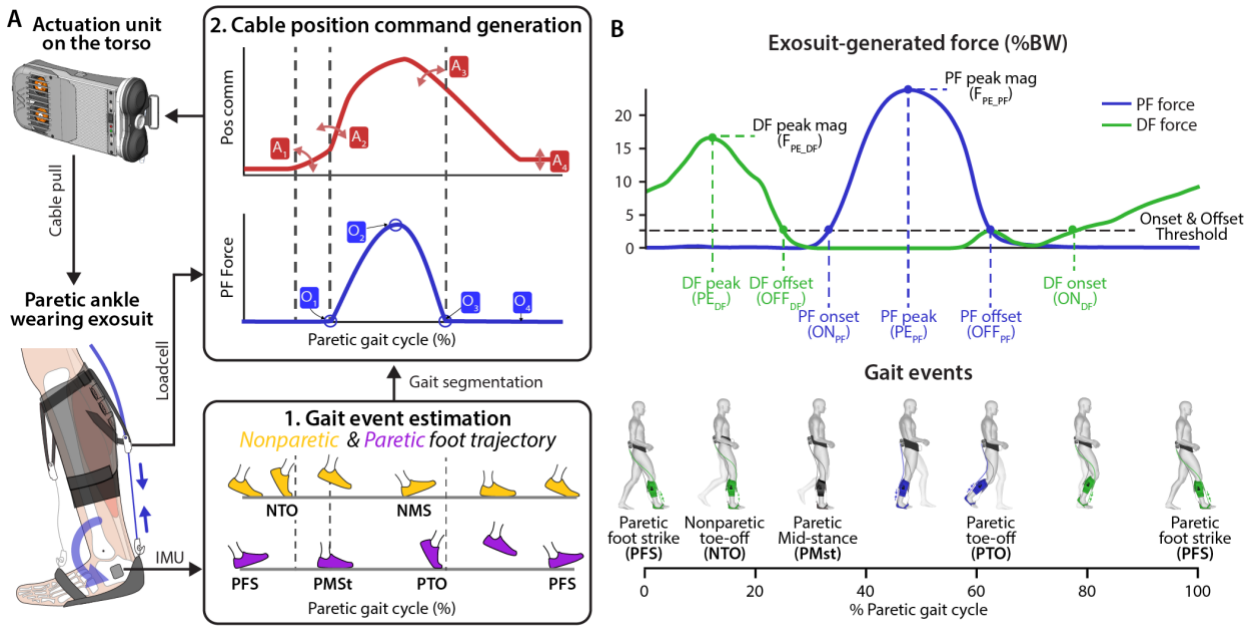

Figure 8.1. Illustration of exosuit controller and exosuit-generated force profile. (a) exosuit controller estimates gait events (e.g. PFS, NTO, NFS, PMSt, PTO, and PFS see **Table 8.1** for their definitions), segment the paretic gait cycle real-time during walking, and generate cable position command to deliver consistent force profile at the biomechanically-sensible timings. (b) Exosuit-generated force profiles for paretic PF and DF assistance and the definition of force timing and magnitude parameters (top row). The definitions of gait events are also presented (bottom row).

More specifically, gait event estimation algorithm monitors sagittal plane foot orientation and angular velocity using IMUs on the shoes to (1) detect peak signals that align well with biomechanical gait events and (2) segment the gait cycle into three phases. The gait events estimated by the algorithm are listed in

Table 8.1 with their definitions in a chronological order in the paretic gait cycle (see **Figure 8.1** (b)). The list also describes how the algorithm estimates the gait events (see **Figure 8.2** (a)):

Table 8.1. Gait events estimated by a portable exosuit and their definitions

Gait events	Definition	How exosuit estimates
Paretic foot-strike (PFS)	When the paretic foot makes initial contact with the ground	When paretic foot orientation signal creates positive peak
Nonparetic toe-off (NTO)	When the nonparetic foot lifts off from the ground	When nonparetic foot angular velocity signal creates negative peak followed by sign change
Paretic mid-stance (PMSt)	Midpoint of paretic single support (i.e. midpoint between nonparetic toe-off to nonparetic foot-strike)	When nonparetic foot orientation signal is at the half magnitude of negative peak signals during nonparetic swing
Nonparetic foot-strike (NFS)	When the nonparetic foot makes initial contact with the ground	When nonparetic foot orientation signal creates positive peak
Paretic toe-off (PTO)	When the paretic foot lifts off from the ground	When paretic foot angular velocity signal creates negative peak followed by sign change

Note that the gait events estimated by exosuit are denoted with subscripts 'exo'. For instance, a paretic foot-strike estimated by exosuit is denoted as PFS_{exo}.

Moreover, the algorithm executes a real-time gait cycle segmentation for a real-time adaptive control. The segmentation occurs at three segmentation points (SPs) listed in **Table 8.2**, therefore one gait cycle is segmented into three phases (P_1-P_3) (see **Figure 8.2**(a)):

Table 8.2. Exosuit gait segmentation points and their definitions

Segmentation points	Definition
1st segmentation point ($SP1_{exo}$)	The timing when the sign of nonparetic gyroscope signal changes from negative to positive after the negative peak signal at NTO_{exo}. This instance transitions gait phase from P_1 to P_2. Furthermore, the timings of PHS_{exo} and NTO_{exo} are updated and saved at this moment.
2nd segmentation point ($SP2_{exo}$)	The timing when $PMSt_{exo}$ is detected. This instance transitions gait phase from P_2 to P_3, and update and save the timing of $PMSt_{exo}$ simultaneously.
3rd segmentation point ($SP3_{exo}$)	The timing when the sign of paretic gyroscope signal changes from negative to positive following the negative peak signal at PTO_{exo}. This instance transitions gait phase from P_3 to P_1. The timings of NHS_{exo} and PTO_{exo} are updated and saved at this moment.

Note that $SP1_{exo}$ and $SP3_{exo}$ are detected based on the sign changes of gyroscope signals which follow after peak signals corresponding to NTO_{exo} and PTO_{exo}, therefore they occur slightly later than exosuit-estimated

toe-offs (NTO_{exo} and PTO_{exo} respectively). Consequently, there exist delays between the gait phase transitions from exosuit-estimated toe-off event.

Further, with the real-time cable position command generation algorithm, exosuit controller adapts cable position commands based on the gait segmentation and force measurements by loadcells in order to generate assistance force profile with consistent onset and offset timings and peak magnitude. Specifically, the algorithm adapts cable position commands to make it consistent for following parameters in **Table 8.3** (see **Figure 8.1** and **Figure 8.2**):

Table 8.3. Exosuit force parameters with which exosuit controller adapts assistance force profiles

Exosuit force parameters	Definition
Force onset timing (ON_{DF} and ON_{PF})	Timing at which DF or PF cable starts to generate tensile force. For validation, this timing is defined as when cable force rises to 10% of peak force magnitude.
PF peak force magnitude (F_{PE_PF})	PF force magnitude at which the peak force is reached. In this study, target peak magnitude for PF assistance was set to 25%BW for all participants with one exception. On the other hand, DF peak force was chosen based on PT's visual observation on patients' foot clearance improvement during swing, so the target level was different across patients.
Force offset timing (OFF_{DF} and OFF_{PF})	Timing at which DF or PF cable force is terminated. For validation, this timing is defined as when cable force decays to 10% of peak force magnitude.

To evaluate the gait event estimation and cable position command generation algorithms, the following evaluation metrics were calculated.

- Accuracy of exosuit-estimated gait event timings was evaluated based on the absolute difference of baseline gait event timings calculated based on ground reaction forces (ground truth measurement) and estimated timings by exosuit.
- The delays in segmentation points ($SP1_{exo}$ and $SP3_{exo}$) with respect to toe-offs (NTO and PTO) were calculated to understand how the segmentation delays affected exosuit-actuation timings. Specifically, $SP3_{exo}$ served as a trigger of DF assistance onset, and $SP1_{exo}$ began the ramp-down of DF cable position (see **Figure 8.2**(b)). Therefore, $SP1_{exo}$ and $SP3_{exo}$ were compared (1) with the baseline toe-offs and (2) with exosuit-estimated toe-offs.

- Consistency of DF and PF assistance profile across gait cycles was evaluated using root mean square error (RMS-E) to the average force across all measured strides (f_{avg}).
- Consistency in DF and PF peak force magnitude was evaluated using stride-to-stride standard deviations of peak force values.
- Consistency in force onset, peak, and offset timings was evaluated using their stride-to-stride standard deviations of peak force values.
- Finally, the force timings were compared to baseline gait event timings in order to evaluate if the force was delivered in a biomechanically sensible manner.

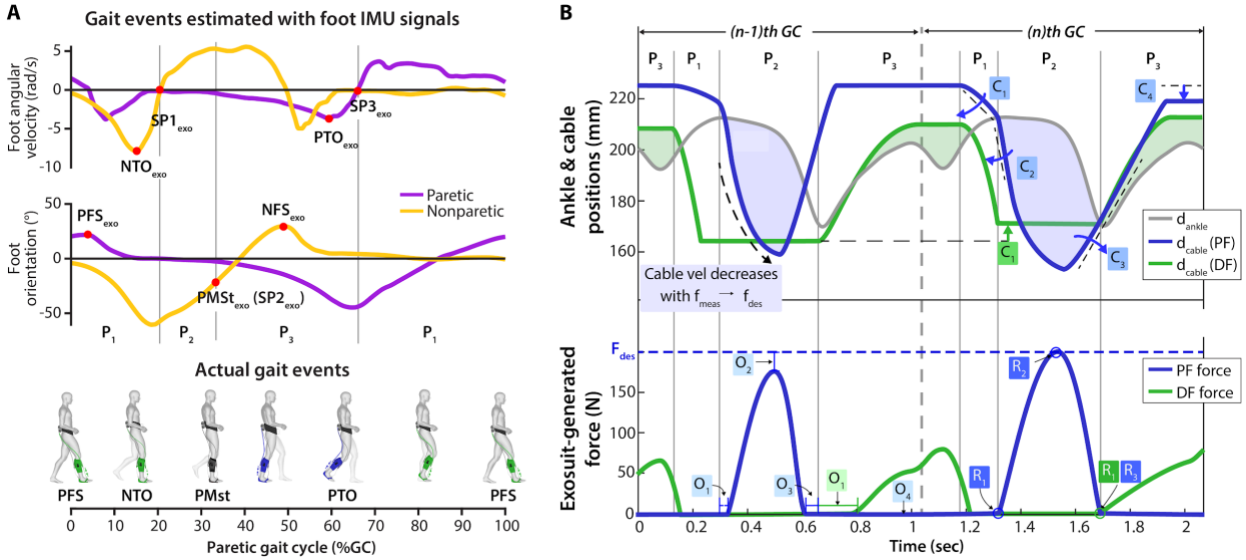

Figure 8.2. Illustrations of exosuit gait event estimation and cable position command generation algorithms. (a) Sagittal plane foot IMU measurements during the paretic gait cycle. Exosuit-estimated gait events ($Event_{exo}$) and segmentation points (SP_{exo}) are also presented in relation to actual gait events. The gait estimation algorithm estimates paretic/nonparetic foot-strikes (PFS_{exo} and NFS_{exo}) and paretic mid-stance ($PMSt_{exo}$) based on foot orientation measurements, and toe-offs (PTO_{exo} and NTO_{exo}) based on the foot angular velocity measurements by foot IMUs. Further, the algorithm segments the gait cycle into three phases (P1- P3) in real-time during walking for actuation control. b) Illustration of cable position and delivered force trajectories in two consecutive gait cycles. PF cable position trajectory generator adjusts cable velocity and baseline cable position parameters (C_1-C_4) for the next GC based on their previous values and force observations (O_1-O_4) from previous GC. Through the adjustments (C_1-C_4), the algorithm generates consistent and desired force outcomes at the right timing with target magnitude (R_1-R_4). Additionally, cable pull velocity is adapted each control loop (1000Hz) when PF force ramps up to reach the desired peak force (F_{des}).
* Abbreviations- PFS: Paretic foot strike; NTO: Nonparetic toe-off; PMSt: Paretic mid-stance; PFS: Nonparetic foot strike; PTO: paretic toe-off

8.3. Methods

8.3.1. Data collection

This study utilized the data collected for the biomechanics study presented in Chapter 7. In brief, 19 individuals in the chronic phase of post-stroke recovery participated in the biomechanics study to compare overground walking with and without portable exosuit. Each participant completed a single session experiment. In each session, a participant walked on a 36.9 m indoor walking track for five minutes with their paretic side inside the track at their comfortable walking speed in two different conditions: one not wearing the exosuit (baseline), and one wearing active exosuit (active). The order of walking conditions was randomized, and 10-minutes seated rest was provided between conditions to reduce the effect of fatigue. Participants were connected with an overhead safety harness during walking, and their vital signs were closely monitored (see **Figure 7.1** for experimental setup).

2 out of 19 participants (Participant #5 and 19 in **Table 7.1**) were excluded from this controller performance evaluation due to technical issues in exosuit data storage and synchronization. The remaining 17 participants were 7 females and 10 males; 53.0±11.2 years old; 7.22±2.4 years post-stroke (See **Table 7.1** for more details). Motion capture and GRF data were collected and synchronized with the sensor and controller variable data collected from exosuit and were used for controller performance analysis. Average number of strides collected from participants were 14.88±5.59 (min=6, max=28).

8.3.2. Data analysis

Baseline gait event timings and estimated gait event timings by exosuit

Baseline gait event timings ($Event_{base}$) were calculated using ground reaction force (GRF) data measured with floor-mounted force plates to be compared with gait event timings estimated by exosuit (see **Figure 8.3** for the comparison between baseline gait events and gait events estimated by exosuit). See **Table 8.4** for their calculation methods.

Table 8.4. Baseline gait events and their calculations

Baseline gait devent	How to calculate
Paretic/nonparetic foot-strike (PFSbase, NFSbase)	When paretic/nonparetic GRF rises to pre-defined threshold (15N)

Paretic/nonparetic toe-off (PTObase, NTObase)	When paretic/ nonparetic GRF decays to pre-defined threshold (15N)
Paretic mid-stance (PMStbase)	the midpoint between NTO_{base} to NFS_{base}

Gait event timings were normalized by paretic stride times and calculated in the paretic gait cycle percentage (%GC) defined between two successive PFSs (0%GC and 100%GC respectively). Synchronizing these baseline events with aforementioned gait events estimated with exosuit ($Event_{exo}$) allowed calculation of the error between IMU-detected events and actual gait events. Specifically, we compared the difference between baseline gait event timings ($Event_{base}$) and estimated gait event timings by exosuit ($Event_{exo}$). Note that the gait events include PFS, NFS, PTO, NTO, PMSt. Further, the gait segmentation points $SP1_{exo}$ and $SP3_{exo}$ following NTO_{exo} and PTO_{exo} were also compared to baseline toe-off and exosuit-estimated toe-off events to evaluate the segmentation delay.

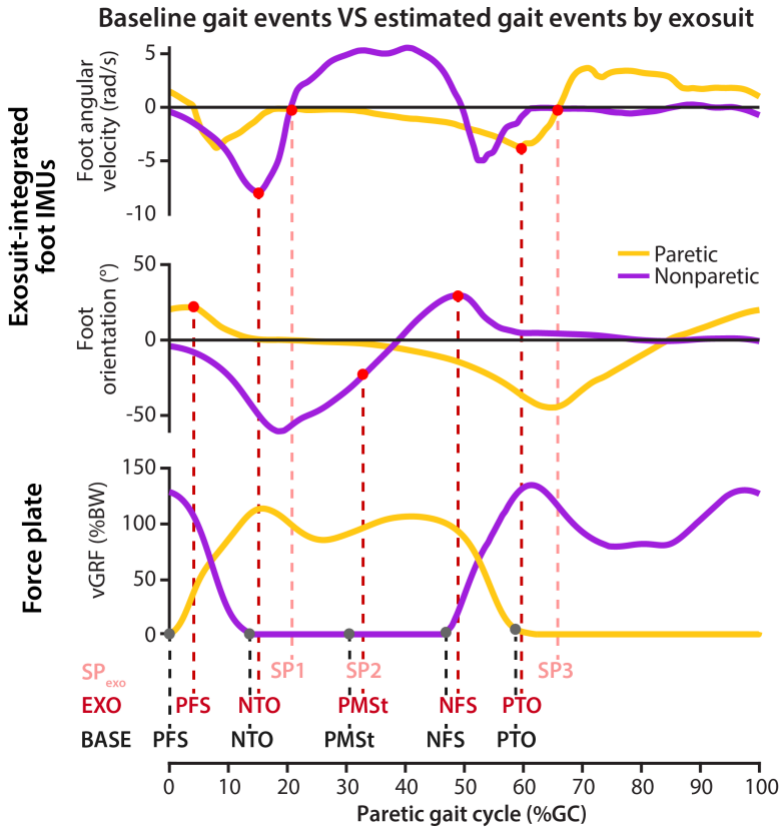

Figure 8.3. Illustration of baseline gait events ($Event_{base}$) calculated using GRF data, gait events estimated by exosuit, and gait segmentation points (SP_{exo}). One of the main goals in controller analysis is to compare $Event_{exo}$ and SP_{exo} to $Event_{base}$ and evaluate the accuracy of exosuit gait event estimation and segmentation.
* Note that $SP2_{exo}$ and $PMSt_{exo}$ occur simultaneously.

Exosuit assistance force

Exosuit-generated force was measured by loadcells connected to Bowden cables (see **Figure 8.1**), and the measurements were analyzed to evaluate for its consistency and timings in relation to baseline gait events. To be specific, force profile consistency was evaluated using root mean square error (RMS-E) to the average force across all measured strides (f_{avg}) using following equation (8.1)):

$$f_{RMSE} = \sqrt{\frac{\sum_{gc=0}^{100}\left(f_{meas}(gc) - f_{avg}(gc)\right)^2}{n_{gc}}} \tag{8.1}$$

Consistency in peak force magnitudes was also evaluated with stride-to-stride standard deviations of peak force values. Additionally, the onset, peak, and offset timings of force profile were calculated as described in section 8.2 (see **Figure 8.1**(b)), and their consistency was evaluated using stride-to-stride standard deviations.

The force profile timings were compared with baseline gait event timings to understand if the force was delivered in a biomechanically sensible manner: First, PF force onset timing (ON_{PF}) was compared to paretic mid-stance ($PMSt_{base}$) to understand if PF assistance was triggered early or late in the paretic single support. Our previous study on a tethered exosuit in treadmill walking [90] demonstrated that biomechanical response to exosuit assistance of post-stroke patients could be sensitive to PF onset timing relative to $PMSt_{base}$. More specifically, two onset timings were evaluated in this previous study, one earlier than PMST (early onset), and the other later than PMST (late onset). We found that three out of seven patients improved paretic forward propulsion more with early onset timing, while others improved more with late onset timing. The comparison between ON_{PF} and $PMSt_{base}$ can therefore provide a further understanding on how onset timing influences biomechanical outcomes in overground walking. Secondly, PF peak force timing (OFF_{PF}) was compared to $NPFS_{base}$ and PTO_{base} to see if the peak occurred during the paretic trailing double support (i.e. 2nd double support in the paretic gait cycle. See **Figure 8.4**). Since both biological ankle power and moment have peaks during the paretic trailing double support, this analysis

demonstrates if the PF assistance peak timing occurs at biologically appropriate timing. Third, PF force offset timing was compared to PTO to see if residual PF force exists in paretic swing phase. Since PF moment during swing could negatively impact ground clearance, PF force offset at or earlier than PTO was desired. Fourth, DF force onset timing was compared to PTO to see if DF assistance started at the beginning of swing and support ground clearance early in the swing phase. Finally, DF force offset timing was compared to PMSt to see if residual DF force existed throughout paretic mid-stance and had overlap with PF force.

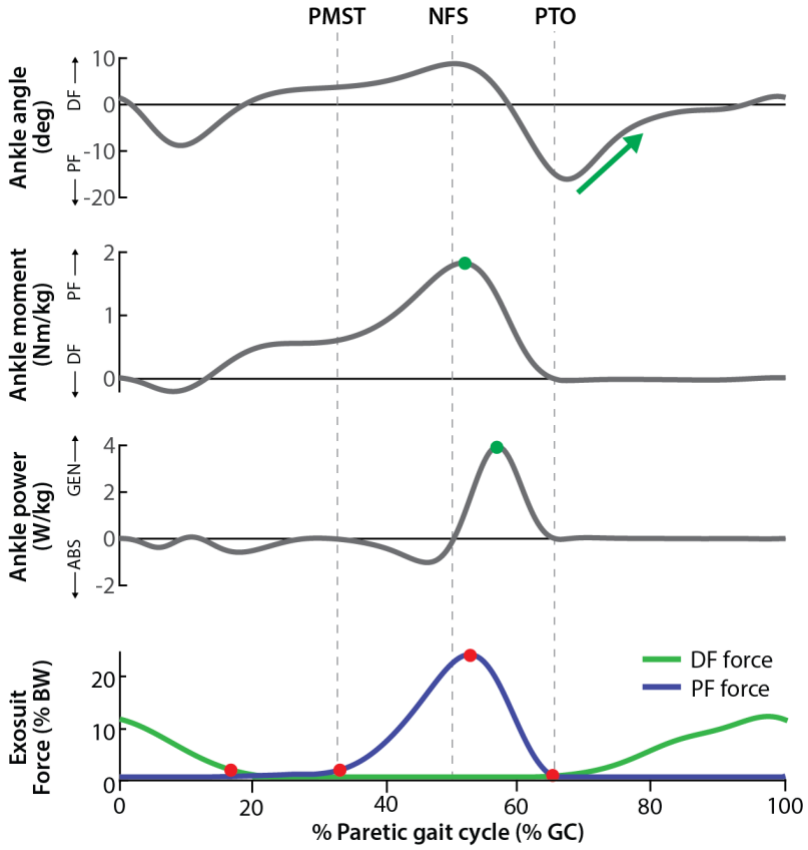

Figure 8.4. Healthy sagittal plane biological ankle angle, moment, and power and exosuit-generated forces. To understand if exosuit force timings are biomechanically appropriate (i.e. in line with biological ankle kinematics and kinetics), the onset, peak, and offset timings of PF force were compared to PMSt, NFS, and PTO respectively, and the onset and offset timings of DF force were compared to PTO and PMSt.

8.4. Results

The exosuit system performance was evaluated (1) the accuracy of gait event detection algorithm implemented in exosuit controller, (2) consistency of DF and PF assistance profile across gait cycles, and (3) biomechanical validity of DF and PF assistance timings with respect to gait events.

8.4.1. Baseline gait event timing

Before evaluating the gait event estimation accuracy, baseline gait event timings using GRF data (i.e. actual gait event timings) were presented to give an idea of patients' baseline gait characteristics and their inter/intra participant variability. Group averages and standard deviations are presented in **Table 8.5**, and individual participant data are presented in **Table 8.12**. The average timing data suggested that there was around 2% to 3.5% of inter-participant variability in gait event timings. Further, based on average standard deviation we found 1.0 to 1.6% intra-participant variability (i.e. stride-to-stride variability) in gait event timings.

Table 8.5. Group statistics on baseline gait event timings

	Nonparetic toe-off (NTO)	Paretic Mid-stance (PMSt)	Nonparetic Foot strike (NFS)	Paretic Toe-off (PTO)
Average mean (%GC)	15.44±3.15	29.33±2.40	43.22±2.56	61.57±3.43
Average STD (%GC)	1.16±0.42	1.07±0.36	1.45±0.55	1.60±0.44

8.4.2. Accuracy of gait event timings estimation by exosuit

Accuracy of exosuit-estimated gait event timings was evaluated based on the absolute difference of baseline gait event timings and estimated timings by exosuit (i.e. abs($Event_{exo}$-$Event_{base}$)). **Table 8.6** presents group statistics of the absolute estimation error in %GC and msec scales. Individual data can also be found in **Table 8.13**. On average, all the gait events were estimated with similar errors ranging from 1% GC to 2.5% GC (15-30ms). The average intra-participant variability in estimation error (i.e. stride-to-stride variability. See average STD in **Table 8.6**) were in the range from 1%GC to 2%GC.

Table 8.6. Group statistics of absolute error of different gait event timings estimated by exosuit

	Unit	PFS	NTO	PMSt	NFS	PTO
Average mean	%GC	1.98±1.91	1.24±0.93	2.17±1.37	1.89±1.19	2.44±1.81
	msec	25.43±23.76	15.69±11.60	28.65±19.51	23.83±14.13	29.29±20.95
Average STD	%GC	2.16±1.12	1.20±0.60	0.99±0.35	1.07±0.33	1.21±0.76
	msec	29.23±19.81	15.78±8.09	13.44±6.13	14.21±5.46	15.10±8.88

* Top row shows mean estimation errors in different gait events, and the bottom row shows intra-participant variability (i.e. stride-to-stride variability) in estimation errors.

8.4.3. Delay in segmentation points from exosuit-estimated toe-offs and baseline toe-offs

The delays in segmentation points ($SP1_{exo}$ and $SP3_{exo}$) from toe-off events (NTO and PTO) were calculated to understand how the impact of segmentation delays on exosuit-actuation timings (see **Table 8.7** for group statistics and **Table 8.14** for individual data): The difference of the segmentation points from (1) the baseline toe-offs and (2) from exosuit-estimated toe-offs were calculated. The segmentation delay from baseline gait event timings (i.e. SP_{exo}-$Event_{base}$=4.7 to 5.6%GC) was significantly larger than the aforementioned gait event estimation errors (i.e. $Event_{exo}$-$Event_{base}$=1 to 2.5%GC). Further, the segmentation delay from baseline gait events (i.e. SP_{exo}-$Event_{base}$=4.7 to 5.6%GC) were larger than those from exosuit-estimated event (SP_{exo}-$Event_{exo}$=3.6 to 4.6%GC). The delay on nonparetic side was less than on paretic side. Intra-participant variability in the delay was ~1%GC, similar to the variability in estimation error (i.e. $Event_{exo}$-$Event_{base}$).

Table 8.7. Group statistics of delays in gait phase segmentation from baselines toe-offs ($Event_{base}$) and toe-offs estimated by exosuit ($Event_{exo}$)

		SP_{ex} - $Event_{base}$ (%GC)		SP_{exo} - $Event_{exo}$ (%GC)	
	Unit	**NTO**	**PTO**	**NTO**	**PTO**
Average mean	%GC	4.74±1.32	5.58±2.41	3.65±1.14	4.61±2.09
	msec	60.10±12.22	71.05±28.03	46.66±12.73	60.70±29.58
Average STD	%GC	0.98±0.50	0.98±0.51	0.69±0.39	1.05±0.61
	msec	12.37±6.42	12.19±5.71	9.39±5.68	13.22±7.42

8.4.4. Consistency of exosuit-generated force

Consistency of PF assistance

Table 8.8 presents group statistics in magnitude and timing values of PF force profiles (see **Table 8.15** for individual participants' data). RMS-E of PF force profile was 1.35%BW on average (i.e. 5.4% of the target peak force at 25%BW). The average PF peak force across patients was 24.16±0.75%BW given peak target force at 25%BW, and intra-participant variability in the peak force was 1.08±0.32%BW. Note that one of the participants whose target force was set to 18%BW due to discomfort was excluded from group statistics. Intra-participant variability in PF assistance timings was similarly within 1 to 2%GC in onset, peak, and offset timings (see average STD in **Table 8.8**).

Table 8.8. Group statistics in PF assistance timing and magnitude variables.

	Magnitude variables (%BW)		Timing variables (%GC)		
	RMS-E$_1$	**Peak**	**Onset**	**Peak**	**Offset**
Average mean	1.35±0.39	24.16±0.75	32.56±2.75	48.58±2.38	61.05±2.41
Average STD	0.73±0.29	1.08±0.32	1.38±0.43	1.63±0.65	2.01±0.73

* See equation (1) in methods section for RMS-E calculation.

Consistency of DF assistance

Table 8.9 presents group statistics in magnitude and timing values of DF force profiles (see **Table 8.17** for individual participants' data). DF assistance force profile was slightly higher RMS-E (1.58±0.58%BW) than PF assistance force profile (1.35±0.39%BW), while the intra-participant variability in RMS-E was similar in DF and PF force profiles. Moreover, DF peak force magnitude has more inter-participant variability (25.72±12.15%BW) compared to PF peak force (24.16±0.75%BW), similarly for intra-participant variability (2.82±1.50%BW in DF VS 1.08±0.32 in PF). It should be noted that the DF peak force magnitude was chosen individually based on clinicians' visual observation on participants' improvement in ground clearance for different DF force levels, therefore higher inter-participant variability in DF peak force compared to PF peak force was anticipated.

Table 8.9. Group statistics in DF assistance timing and magnitude variables

	Magnitude variables (%BW)		Timing variables (%GC)		
	RMS-E	**Peak Mag**	**Onset**	**Peak**	**Offset**

Average mean	1.58±0.58	25.72±12.15	73.98±5.08	8.69±5.76	23.86±5.53
Average STD	0.66±0.29	2.82±1.50	2.57±1.00	1.96±1.59	1.74±1.30

* See equation (1) in methods section for RMS-E calculation.

8.4.5. Biomechanical validity of exosuit-generated force timings

PF assistance

Table 8.10 presents group data on where PF assistance timings were with respect to baseline gait event timings (see **Table 8.16** for individual participant data). PF Onset timing was slightly later than baseline paretic mid-stance ($PMSt_{base}$) for 15 out of 17 patients. PF peak force occurred during paretic trailing double support (i.e. between NFS_{base} and PTO_{base}) for all 17 participants, similarly to peak biological ankle power and moments. PF offset, which is preferable when occurred at PTO, occurred before PTO for 9 out of 17 participants, while it occurred after PTO for 8 out of 17 participants: The whole group average of difference between PF offset and PTO was -0.52±2.19%GC. When focusing on participants whose offset timing was earlier than PTO, the average was -2.08±1.76%GC, while the average in the other group was 1.24±0.91%GC.

Table 8.10. PF assistance timings in relation to gait event timings.

	ON_{PF}-$PMSt_{base}$ (%GC)	**OFF_{PF}-PTO_{base} (%GC)**	**PF onset is after PMSt**	**PF peak is in paretic trailing DS**	**PF Offset is before PTO**
Average	3.23±2.37	-0.52±2.19	15/17	17/17	9/17

* First column is the difference between PF onset timings and baseline paretic mid-stance ($PMSt_{base}$) to evaluate if PF onset occured early or late in the paretic single support. Second column is the difference between PF offset timings and PTO to evaluate if residual PF force existed during paretic swing. Third to fifth column present number of participants whose 1) PF onset timing is after $PMSt_{base}$ (3rd col), 2) PF peak timing is during paretic trailing double support (4th col), and 3) PF offset timing is before PTO (5th col).

DF assistance

Table 8.11 presents group data on where DF assistance timings were with respect to baseline gait event timings (see **Table 8.18** for individual participant data). DF onset timing was consistently later than paretic toe-off (PTO_{base}) for all 17 participants, which indicates insufficient assistance during early swing: the

average delay of DF onset timing from PTO_{base} was 12.41±4.48%GC. DF force offset timing was before paretic mid-stance ($PMSt_{base}$) for 16 out of 17 participant, while for other one participant, the offset happens 5.96±1.10%GC later than PMST.

Table 8.11. DF force timings in relation to baseline gait event timings

	ON_{DF}-PTO_{base}	OFF_{df}-$PMSt_{base}$	DF Onset is after PTO	DF Offset is before PMST
Average	14.98±2.91	-7.00±1.38	17/17	16/17

* Second column is the timing difference between DF assistance onset and PTO to evaluate if DF assistance onset at the initiation of paretic swing. Third column is the timing difference between DF offset and PMSt to evaluate if residual DF force existed at paretic mid stance.

8.5. Discussion

In this chapter, we present a controller performance validation using the data collected from an overground walking study with 17 post-stroke individuals. Specifically, we evaluated (1) the accuracy of gait event detection algorithm implemented in exosuit controller, (2) consistency of DF and PF assistance profile across gait cycles, and (3) biomechanical validity of DF and PF assistance timings with respect to baseline gait events.

8.5.1. Accuracy of gait event timings estimated by exosuit

Firstly, we evaluated gait event timings estimated by exosuit ($Event_{exo}$) through the comparison with baseline gait event timings based on GRF measurements ($Event_{base}$). The comparison demonstrated that the error range of exosuit-estimated gait events was 1 to 2.5%GC (15 to 30 msec). This error range is significantly less than previously reported errors in three different methods for temporal gait event estimation using wearable IMUs in post-stroke overground walking (4-5%GC) [240]. Although the group average in our gait event estimation error was lower than the state-of-the-art estimation methods, it should be noted that individual error magnitude widely varied across participants (see **Table 8.13**): For instance, paretic foot strike (PFS) estimation error for participant 5 was as low as -0.02±0.88 %GC while same variable for participant 8 was -7.17±2.26 %GC. Indeed, participant 8 walked with a compensatory gait

pattern during the paretic swing phase where he forcefully kicked his swing limb to compensate foot drop, causing excessive anterior advancement of the limb, and then brought the limb back for foot landing (i.e. kicking compensation). This compensatory gait pattern caused the peak of foot-to-floor angle signal appeared earlier than foot strike. This example signifies that individual foot rotation patterns could impact gait event estimation accuracy.

Although the estimated gait event timings had an accuracy with average errors ranging from 1% GC to 2.5% GC (15-30ms) the real-time gait segmentation points 1 and 3 ($SP1_{exo}$ and $SP3_{exo}$) following exosuit-estimated toe-offs were significantly delayed from baseline toe-off timings (3.5 to 5.6%GC delay). This delay might have caused negative impacts on assistance timings: Specifically, $SP3_{exo}$ serves as a trigger of DF assistance cable pull [93], and we found significant delay in DF force onset timing after PTO_{base} as well (14.9%GC. see **Table 8.11**). This delay in DF onset was mainly caused by the delays in $SP3_{exo}$ from PTO_{base}. Interestingly, the delay in $SP1_{exo}$ detected based on the nonparetic foot velocity signals was less than the delay in $SP3_{exo}$ detected based on the paretic velocity signals. This implies that faster foot rotations on nonparetic side caused faster zero-crossing in foot velocity after toe-off, reducing segmentation delays. Further, the segmentation delays from baseline gait event timings were larger than those from exosuit-estimated timings. This implies that the exosuit-estimated toe-offs were later than the baseline toe-offs, and the segmentation delays were partially attributed by the delay of exosuit-estimated toe-offs from baseline toe-offs. This could be addressed by accurately estimating percent gait cycle (%GC). To be specific, %GC estimation allows to understand where in the gait cycle the wearer is and therefore to provide assistance at the right timing without delays. Indeed, our tethered exosuit in Chapter 2 implemented %GC estimation based on stride times measured in previous strides. However, this estimation method assumes consistent stride times across multiple strides, which is not valid in overground walking with increased stride-stride variability. Therefore, new method to improve the estimation accuracy is warranted (see Chapter 12 for details).

8.5.2. Evaluation of PF assistance force

Secondly, the consistency and biomechanical validity of PF assistance were evaluated. RMS-E of PF force profile (1.35%BW; 5.4% of the target peak force at 25%BW) was slightly higher than previously reported RMS-E in hip assistance with exosuit during healthy walking on a treadmill (3.4% of the target peak force) [81]. Although the RMS-E value was higher in this study, it should be noted that our study was on post-stroke overground walking which is more variable and inconsistent than healthy treadmill walking, therefore more likely to cause inconsistent assistance force profile. As far as we understand, this is the first report of RMS-E value in assistance profile during post-stroke overground walking, therefore future reports on this topic could benefit from this report as a reference point.

The average peak PF force was lower than target force by 0.8%BW (24.16±0.75%BW where target peak force was 25%BW). Our previous study on post-stroke treadmill walking with a tethered exosuit [90] reported 25.02±2.43%BW average PF peak force, which was closer to the same target value. However, it should be noted that the inter-participant variability of peak force was lower in this study (0.75%BW in this study VS 2.43%BW in [90]), signifying more consistent peak force across participants. Intra-participant variability in peak force magnitude in this study (1.08±0.32%BW) was also lower than the previous study (1.15 ±0.31%BW). Still, the low average peak force is not desirable, therefore further improvement is warranted. Regarding PF force timings, we observed similar Intra-participant variability in onset, peak, and offset timings ranging from 1 to 2%GC. In the previous study [90], intra-participant variability in PF onset timing was reported as 1.51±1.01%GC, which was slightly higher than this study (1.38±0.43%BW). Variabilities in other timings were not reported in the previous study. Although limited, the data demonstrated that our new controller generated similar, or slightly improved, consistency in PF force timing compared to the previous study. Moreover, it should be noted that the previous study was on the treadmill which was less variable than overground walking.

To understand biomechanical validity of different PF force profiles, the previous study [90] investigated two different PF assistance onset timings defined as earlier than PMSt (early onset; 27.5±1.94%) and later than PMSt (Late onset; 36.9±0.76%GC), and found that four out of seven participants benefited more from

a late-onset timing of PF force delivery and two benefited more from an early-onset timing. One participant benefited equally from both onset timings. Further, the previous study also demonstrated all the participants could improve paretic forward propulsion with late PF onset timing while some participant reduced the paretic forward propulsion with early onset timing. Our new study utilized the new control strategy to generate the generic PF assistance force profile, the onset timing of which was slightly later than PMSt for 15 out of 17 participants and was very close to PMSt for other 2 participants. The new onset timings that were generally later than PMST are desirable given the finding from the previous study demonstrating that all the previous participants could benefit from late PF onset timings, but not from early PF onset timings. Moreover, PF peak force from the new control strategy occurred during the paretic trailing double support (i.e the peak PF force timing was always between NFS_{base} and PTO_{base}). Since both biological ankle power and moment have peaks during the paretic trailing double support, this result demonstrated that the PF assistance peaks occurred at biomechanically appropriate timings. Finally, PF offset occurred close to paretic toe-off (OFF_{pf} - PTO_{base}=-0.52±2.19%GC) on average. However, PF offset occurred before PTO_{base} for 9 out of 17 participants, while it occurred after PTO_{base} for other 8 participants. PF force offset after PTO indicates residual PF force in early swing, which might disturb ankle DF function. The late PF offset could have been caused by the delay in PTO confirmations (i.e. PTO_{exo_c}), therefore reduction in PTO confirmation timing could improve PF controller and reduce residual PF force in paretic swing phase. Still, the residual PF force was as low as 3%BW, therefore we believe the negative impact of the residual PF force was not significant. Still, future improvement to reduce the residual force is warranted.

8.5.3. Evaluation of DF assistance force

The consistency and biomechanical validity of DF assistance were also evaluated. DF force profile demonstrated slightly higher RMS-E than PF assistance. Similarly, DF peak force magnitude had higher inter-participant variability (25.72±12.15%BW) than PF peak force (24.16±0.75%BW). This was because DF assistance controller did not adapt cable position travel to generate consistent force profile as in PF assistance controller. Rather, DF cable position travel was fixed at the value selected based on clinicians'

visual observations on patients' ground clearance improvement for different assistance level (see [93]for further details). DF assistance timings were also less consistent than the previous study: intra-participant variabilities in onset, peak, and offset timings were 1.7 to 2.7%BW. In the previous study [90], intra-participant variabilities in DF onset and offset timings were reported as 2.71±0.62 %GC and 0.91±0.77 %GC respectively. The variabilities in this study were similar, or slightly higher than the previous study. This could be attributed to increased variability in overground walking than treadmill walking.

The main limitation in the DF controller was that DF onset timing was significantly later than paretic toe-off (PTO_{base}) for all 17 participants (14.9%GC). As discussed in the previous section, this delay in DF onset timing was largely attributed by the delays in the real-time segmentation point $SP3_{exo}$. Still, the delays in $SP3_{exo}$ was only 5.6%GC, therefore extra 9%GC delays in DF onset timings might have come from other sources: one of potential sources would be individuals' voluntary DF motion at the early swing which was faster than DF cable pull. If this happened, DF cable would not generate tensile force even when it was pulling at the correct timing. Regardless, since no DF assistance in early swing could increase the risk of trip hazard and some patients did give feedbacks that DF assistance triggered later than the timing they wanted, thus future development of DF controller that triggers assistance early in swing phase is warranted.

8.6. Conclusion and future work

In this chapter, we evaluated the accuracy of exosuit gait event detection algorithm, consistency of DF and PF assistance profile, and biomechanical validity of DF and PF assistance timings during post-stroke overground walking. First of all, the evaluation demonstrated that the gait event detection algorithm outperformed previous detection algorithms presented in [240]. Still, the accuracy varied depending on individual gait patterns, therefore future development of gait event detection algorithm that is robust to various gait patterns is warranted. Utilization of other sensor signals signals (i.e. gyroscope and foot-to-floor angle) could improve the robustness. Additionally, the estimation accuracy could be also improved

by increasing IMU sampling rates. The current sampling rate (100Hz) could cause up to 10-msec error in gait event timings, which account for 30 to 60% of current average error (15 to 30 msec). Possible areas of future research to address these challenges is discussed in Section 12.1.1 and 12.1.2.

Although the gait event timing estimation had a reasonable error range between 1% GC to 2.5% GC, the real-time segmentations (SP_{exo}) were significantly delayed from toe-off events, therefore they caused residual PF force during the paretic swing phase and significantly delayed onset of DF force in early swing. The delayed DF force onset timing signifies insufficient support on foot clearance in early-swing phase, which could increase trip hazard. Further investigation to reduce this segmentation delay is therefore warranted.

Second part of the evaluation demonstrated that exosuit consistently delivered DF and PF assistance during post-stroke overground walking. However, PF assistance controller did not reach the target peak force, and the actual peak force was lower than the target by 1%BW. We think this might have been caused by within stride cable velocity adaptation that reduced cable velocity command as measured force reached target force (see Chapter 6 [93] for further details). This could be improved by developing direct force controller and improving force tracking performance. Indeed, our previous study on hip assistance with exosuits in healthy individuals [81] demonstrated force controller with desirable force tracking performance using admittance control strategies, and this approach would be applicable to exosuit for paretic ankle assistance.

Finally, the timings of DF and PF assistance profiles used in this study were biomechanically sensible given our prior biomechanics knowledge. However, they might not be optimal to provide the best biomechanical benefits to each individual. Indeed, recent studies has shown the importance of force profile individualization to maximize biomechanical outcomes induced by mechanical assistance provided by exosuits or exoskeletons [85], [90], [241]. These studies also highlighted that the optimal force profile might not be the ones that replicated biological joint moments or power (i.e. biomechanically sensible profile). Future study therefore requires further investigation of different force profile and timings and using online

optimization strategy to individualize the profiles. Potential areas of future research related to this topic are discussed in Section 12.1.4.

8.7. Supplementary materials

Table 8.12. Individual baseline gait event timings represented in paretic gait cycle percentage (%GC).

Participant	Nonparetic toe-off (NTO)	Paretic Mid-stance (PMSt)	Nonparetic Foot strike (NFS)	Paretic Toe-off (PTO)
1	14.74±1.01	30.71±0.90	46.67±0.99	62.76±1.36
2	16.52±1.04	28.18±1.08	39.84±1.48	58.32±2.29
3	14.94±1.19	28.31±0.98	41.68±1.40	59.35±1.54
4	14.73±1.43	28.19±1.42	41.65±1.66	60.78±1.97
5	19.66±1.96	32.68±1.53	45.70±1.89	59.05±1.48
6	14.26±0.66	29.00±1.01	43.73±1.92	60.47±1.94
7	15.85±0.93	31.88±0.78	47.92±1.13	63.93±0.85
8	12.25±0.63	25.71±0.87	39.18±1.41	57.45±1.01
9	21.33±1.56	33.35±1.03	45.37±1.03	64.23±1.42
10	11.25±1.89	26.90±1.30	42.55±1.45	62.63±1.94
11	11.66±0.77	26.35±0.69	41.04±1.12	58.17±2.06
12	11.42±0.77	25.49±0.75	39.56±0.94	55.88±1.27
13	17.27±1.20	30.78±1.79	44.29±2.93	62.98±1.35
14	15.85±0.63	30.23±0.55	44.61±0.93	66.64±1.32
15	16.48±1.09	30.69±1.05	44.89±1.32	62.56±1.95
16	13.09±1.25	28.62±0.80	44.14±0.81	62.24±1.13
17	21.24±1.64	31.57±1.68	41.90±2.25	69.24±2.29
Average mean	15.44±3.15	29.33±2.40	43.22±2.56	61.57±3.43
Average STD	1.16±0.42	1.07±0.36	1.45±0.55	1.60±0.44

*Paretic foot strike timing (PFS) is not presented as it is always 0 %GC.

** Average number of strides (i.e. number of samples) were 14.86±4.76.

Table 8.13. Individual data of absolute error in different gait event timings estimated by exosuit

Participant	Paretic Footstrike (PFS)	Nonparetic toe-off (NTO)	Paretic Mid-stance (PMSt)	Nonparetic Foot strike (NFS)	Paretic Toe-off (PTO)
1	1.30±1.81	0.47±0.64	0.41±0.81	1.67±0.92	-2.96±1.61
2	-3.51±4.01	1.29±1.10	3.76±0.67	3.76±0.85	-0.53±1.36
3	-0.82±2.58	1.93±2.25	1.60±1.93	4.63±1.68	4.10±2.81
4	-4.66±3.23	1.35±0.83	3.40±0.84	2.40±0.75	3.46±1.13
5	-0.02±0.88	1.47±1.59	0.27±1.19	0.69±1.49	-0.24±1.80
6	-3.92±2.19	1.03±0.58	0.15±0.93	2.91±0.81	6.14±2.85
7	-0.53±1.20	0.96±1.65	-1.78±0.69	0.27±0.90	3.35±0.70
8	-7.17±2.26	2.24±0.89	1.99±0.74	3.04±1.18	3.08±1.08
9	-0.09±0.96	1.48±1.86	3.11±1.59	2.20±0.82	0.11±0.69
10	1.10±1.98	-0.19±1.99	2.13±1.05	1.54±0.81	3.24±1.28
11	1.64±1.52	1.43±0.56	2.69±1.00	2.03±1.26	-0.83±0.75
12	-0.67±2.16	4.00±0.94	1.38±0.97	2.25±1.17	3.84±1.31
13	0.66±0.80	0.46±2.20	0.63±0.95	-1.08±1.65	0.87±0.69
14	0.77±0.67	1.51±0.60	-4.66±0.82	-0.87±0.84	-4.86±1.50
15	-2.11±2.60	0.19±1.27	-3.82±0.51	-1.19±1.44	-0.69±0.44
16	-1.75±4.22	-0.51±0.87	-3.37±0.85	0.87±0.68	-2.37±0.35
17	-2.88±3.65	-0.49±0.66	-1.82±1.22	0.72±0.94	0.72±0.18
Average mean (abs val)	1.98±1.91	1.24±0.93	2.17±1.37	1.89±1.19	2.44±1.81
Average STD (abs val)	2.16±1.12	1.20±0.60	0.99±0.35	1.07±0.33	1.21±0.76

Table 8.14. Individual data of toe-off event confirmation delays compared to gait event timings estimated by exosuit (GC_{exo}) and baselines(GC_{base}).

	SP_{ex} – $Event_{exo}$ (%GC)		SP_{ex} - $Event_{base}$ (%GC)	
Participant	**NTO**	**PTO**	**NTO**	**PTO**
1	5.45±0.46	5.94±0.97	5.92±0.57	5.97±1.24
2	2.93±0.65	9.11±0.45	4.22±0.63	8.58±1.39
3	4.91±0.55	6.36±2.53	6.85±2.17	10.46±1.83
4	4.59±0.48	2.85±0.95	5.94±0.98	6.30±0.88
5	2.57±0.69	6.16±1.47	4.03±1.68	5.92±0.68
6	4.44±0.48	3.33±1.97	5.47±0.67	9.48±2.27
7	4.24±1.46	1.81±0.44	5.21±1.02	5.15±0.74
8	3.89±0.63	4.86±1.08	6.13±0.76	7.94±1.04
9	3.39±1.24	3.54±1.07	4.87±1.43	3.64±0.81
10	5.31±0.87	2.70±1.31	5.12±1.64	5.94±0.67
11	4.20±0.22	6.51±0.67	5.63±0.55	5.69±0.61
12	1.90±0.40	2.15±0.36	5.90±0.93	5.99±1.22
13	2.63±1.18	3.49±1.41	3.09±1.31	4.35±1.23
14	1.57±0.22	7.36±1.55	3.08±0.56	2.51±0.57
15	3.39±1.34	3.19±0.51	3.58±0.50	2.50±0.44
16	3.79±0.56	5.99±0.75	3.28±0.77	3.62±0.71
17	2.80±0.33	3.02±0.31	2.31±0.48	3.74±0.28
Average mean	3.65±1.14	4.61±2.09	4.74±1.32	5.58±2.41
Average STD	0.69±0.39	1.05±0.61	0.98±0.50	0.98±0.51

Note that all the delay values are positive, so averages of raw and absolute values are identical (This table only presents only the average of raw values).

Table 8.15. Individual data of PF assistance magnitude and timing variables

	Magnitude variables (%BW)		Timing variables (%GC)		
Participant	**RMS-E[1]**	**Peak Mag (F_{PE_PF})**	**Onset (ON_{PF})**	**Peak (PE_{PF})**	**Offset (OFF_{PF})**
1	1.33±1.44	24.16±0.85	33.32±1.18	46.89±1.50	61.76±2.69
2	0.84±0.65	18.24±0.37	34.99±1.20	47.71±1.34	57.76±1.74
3	1.40±0.73	23.76±1.03	32.78±1.61	49.66±1.79	62.00±1.93
4	1.36±0.84	24.16±0.79	34.12±1.55	49.60±1.80	62.60±2.09
5	1.74±1.17	25.12±1.10	34.91±2.22	50.79±1.56	59.42±2.33
6	1.21±0.48	24.30±0.99	32.41±0.79	49.06±1.58	62.56±1.88
7	0.92±0.42	23.59±1.14	33.66±1.10	53.24±1.01	64.87±1.33
8	0.72±0.35	23.40±0.64	31.43±1.06	46.91±1.02	58.91±0.64
9	1.66±0.64	23.78±0.90	39.22±2.15	50.54±1.66	63.37±1.56
10	1.21±0.50	26.26±1.78	31.04±0.95	45.06±1.46	62.16±1.28
11	1.35±0.54	24.71±0.98	32.16±1.11	47.53±1.25	58.49±1.87
12	1.05±0.71	23.99±0.89	28.07±1.09	43.34±1.07	56.13±1.98
13	1.93±0.73	23.89±0.88	33.60±1.74	48.46±2.99	61.77±3.33
14	1.50±1.11	24.49±1.56	29.18±1.61	49.16±1.64	63.52±2.35
15	1.30±0.53	23.04±1.32	30.71±1.06	48.47±1.38	60.08±1.95
16	1.12±0.62	24.07±1.58	28.14±1.09	47.82±1.22	59.08±1.55
17	2.25±0.87	23.80±0.90	33.78±1.89	51.60±3.45	63.42±3.66
Average mean	1.35±0.39	24.16±0.75	32.56±2.75	48.58±2.38	61.05±2.41
Average STD	0.73±0.29	1.08±0.32	1.38±0.43	1.63±0.65	2.01±0.73

* RMS-E was calculated using equation (1) in methods.

**Subject 2's target peak magnitude was reduced to 18%BW due to comfort complaints, while other participants' target was 25%BW. Therefore, the peak magnitude measurement from subject 2 was not taken into account when calculating group mean and STD.

Table 8.16. Individual data of PF force timings in relation to baseline gait event timings

Participant	ON_{PF}-$PMSt_{base}$ (%GC)	OFF_{PF}-PTO_{base} (%GC)	PF onset is after PMSt	PF peak is in paretic trailing DS	PF Offset is before PTO
1	2.61±0.74	-1.00±2.76	Y	Y	Y
2	6.81±0.90	-0.56±1.66	Y	Y	Y
3	4.47±1.70	2.65±1.92	Y	Y	N
4	5.94±0.90	1.82±0.93	Y	Y	N
5	2.23±1.71	0.37±1.73	Y	Y	N
6	3.41±0.78	2.09±2.20	Y	Y	N
7	1.77±1.06	0.93±0.68	Y	Y	N
8	5.72±0.99	1.47±1.02	Y	Y	N
9	5.87±1.99	-0.86±0.91	Y	Y	Y
10	4.15±1.09	-0.47±1.42	Y	Y	Y
11	5.81±0.85	0.32±1.17	Y	Y	N
12	2.58±0.98	0.25±1.81	Y	Y	N
13	2.82±1.17	-1.20±3.17	Y	Y	Y
14	-1.06±1.41	-3.12±2.48	N	Y	Y
15	0.02±1.54	-2.48±0.89	Y	Y	Y
16	-0.48±0.96	-3.16±0.97	N	Y	Y
17	2.21±1.05	-5.83±2.06	Y	Y	Y
Average	3.23±2.37	-0.52±2.19	15/17	17/17	9/17

Table 8.17. Individual data of DF assistance magnitude and timing variables

	Magnitude variables (%BW)		Timing variables (%GC)		
Participant	**RMS-E**	**Peak Mag (F_{PE_DF})**	**Onset (ON_{DF})**	**Peak (PE_{DF})**	**Offset (OFF_{DF})**
1	1.51±0.60	17.05±2.28	77.74±3.46	11.35±1.79	23.71±1.68
2	1.31±0.52	24.75±1.26	72.01±1.56	19.09±5.42	26.87±1.31
3	1.58±0.55	13.32±3.36	78.31±2.32	-0.32±2.96	16.75±6.29
4	2.54±1.18	36.01±3.72	71.19±4.38	8.22±2.17	24.96±1.44
5	1.83±0.67	33.12±2.32	70.37±1.25	20.27±2.04	31.55±1.55
6	0.65±0.40	7.64±1.21	84.78±3.55	3.31±2.77	9.23±2.08
7	1.82±1.15	27.32±3.62	74.46±2.58	9.82±0.71	24.41±0.84
8	1.73±0.75	21.30±3.62	74.38±2.54	17.51±5.50	31.68±0.86
9	1.15±0.35	28.92±1.40	73.46±1.22	6.24±0.58	30.35±1.42
10	2.27±0.87	38.54±5.29	72.58±4.08	8.18±0.90	26.73±2.38
11	1.48±0.61	32.85±3.64	69.34±2.38	8.46±0.64	22.64±0.89
12	1.61±0.57	32.28±2.38	63.14±2.77	6.91±1.06	21.10±0.90
13	2.61±1.09	24.29±4.90	70.64±2.89	4.30±3.35	23.36±1.43
14	0.91±0.29	18.18±1.36	78.05±1.15	8.34±0.87	23.01±0.75
15	0.63±0.17	10.63±1.42	77.10±3.45	6.45±0.54	18.49±2.73
16	2.03±0.80	56.41±5.39	69.67±1.58	8.58±0.75	25.14±1.15
17	1.23±0.69	14.57±0.83	80.42±2.50	1.08±1.30	25.70±1.87
Average mean	1.58±0.58	25.72±12.15	73.98±5.08	8.69±5.76	23.86±5.53
Average STD	0.66±0.29	2.82±1.50	2.57±1.00	1.96±1.59	1.74±1.30

Table 8.18. Individual data of DF force timings in relation to baseline gait event timings

Subject No	$Onset_{df}$-PTO	$Offset_{df}$-PMSt	DF Onset is after PTO	DF Offset is before PMST
1	14.98±2.91	-7.00±1.38	Y	Y
2	13.69±1.44	-1.31±0.83	Y	Y
3	18.96±2.15	-11.56±6.13	Y	Y
4	10.41±3.38	-3.23±0.72	Y	Y
5	11.32±1.04	-1.13±1.29	Y	Y
6	24.31±3.18	-19.76±2.67	Y	Y
7	10.53±2.16	-7.47±0.95	Y	Y
8	16.93±3.01	5.96±1.10	Y	N
9	9.23±1.23	-3.00±0.99	Y	Y
10	9.96±3.87	-0.17±2.76	Y	Y
11	11.17±2.33	-3.71±1.02	Y	Y
12	7.26±3.14	-4.39±0.88	Y	Y
13	7.67±2.64	-7.42±1.09	Y	Y
14	11.41±1.12	-7.22±0.57	Y	Y
15	14.54±3.19	-12.20±2.76	Y	Y
16	7.43±1.45	-3.48±0.87	Y	Y
17	11.17±0.71	-5.87±1.40	Y	Y
Average	14.98±2.91	-7.00±1.38	17/17	16/17

***** Second column is the timing difference between DF assistance onset and PTO to evaluate if DF assistance onset at the initiation of paretic swing. Third column is the timing difference between DF offset and PMSt to evaluate if residual DF force existed at paretic mid stance.

Chapter 9.

Real-time gait metric estimation with portable exosuit

9.1. Introduction

Portable soft exosuit to assist with paretic ankle function in overground walking post-stroke was presented (Chapter 6), and their immediate biomechanical benefit in overground walking was experimentally evaluated in 19 chronic post-stroke patients in (Chapter 7). In brief, we demonstrated that portable exosuits increased overground walking speeds of post-stroke individuals by 5%, with greater increase in limited community ambulator by 13%, and reduced compensatory gait patterns such as hip hiking by 5% and circumduction by 13%, while preserving metabolic cost of transport and muscle activities. These outcomes highlight the potential of utilizing exosuits for post-stroke gait training by promoting improved overground walking with increased speeds and more natural gait patterns, while still requiring patients' own effort and exertion.

Our vision is to utilize the exosuit for post-stroke gait training not only in clinics, but also outside the clinics after patients are discharged from clinic-based rehabilitation programs (See Section1.2 for further details). Real-time gait monitoring using exosuit-integrated wearable sensors could serve as a useful tool for clinicians to collect patients' gait performance data over time and understand rehabilitation progress. It could enable clinicians to adapt and individualize exosuit-assisted gait training programs in clinics. Even more, the rehabilitation progress through community-based gait training with exosuits could be monitored, allowing clinicians to give instructions or adjust exosuit assistance to provide individualized gait training programs (i.e. tele-rehabilitation). For instance, when gait metric data shows reduced paretic stance time compared to nonparetic stance time, a clinician could give an instruction to spend more time on the paretic limb. Ultimately, with centralized data collection using cloud storage connected with exosuits from different patients in multiple sessions, researchers could build a large-scale database that could be used to study gait pathology and rehabilitation at scale, ultimately enabling us to acquire a more fundamental understanding of post-stroke gait rehabilitation.

Wearable IMUs has been investigated to provide quantitative clinical assessment and monitor the rehabilitation progress by estimating spatiotemporal gait metrics [242]. Since the portable exosuit includes two IMUs mounted laterally on each shoe (**Figure 6.2**), spatiotemporal gait metric estimation could be implemented without additional hardware integration. This chapter therefore focuses on development of a real-time spatiotemporal gait metric estimation algorithm with existing exosuit hardware and its validation. The algorithm leverages the robust gait event detection algorithm implemented in exosuit controller to accurately estimate spatial gait metrics (Section 6.4.1). We hypothesize that the robust gait event detection could improve gait metric estimation accuracy over previous gait metric estimation algorithms [101], [102]. To validate the hypothesis, we evaluated the estimation performance through following three studies: (1) comparison of exosuit-estimated gait speeds to treadmill speeds in healthy subjects (N=3), (2) comparison of gait metric estimation to baseline gait metrics using motion capture system in post-stroke overground walking (N=2), (3) comparison of gait metrics calculated with our method to gait metrics computed with 3

other existing methods using identical IMU data collected in post-stroke treadmill and overground walking (N=1).

9.2. State-of-the-art spatiotemporal gait metric estimation strategies with foot IMUs

Spatiotemporal gait metrics provide clinically important information regarding gait impairment level and rehabilitation progress. For instance, gait speed is the most significant and reliable biomarker of gait deficit and functional mobility after stroke [239], and inter-limb ratio of stance time is a reliable indicator of gait asymmetry post-stroke [243]. In this section, we first define the spatiotemporal gait metrics of interest, and then review state-of-the-art strategies in gait metric estimation using foot-mounted IMUs.

9.2.1. Temporal gait metric estimation

Temporal gait metrics are defined as time durations between two (different) gait events within a full gait cycle. Therefore, temporal gait metric estimation can be implemented by (1) estimating time instances of gait events, and (2) calculating the time difference between two relevant gait events. Indeed, exosuit controller implements a real-time gait event detection algorithm to segment the gait cycle and deliver mechanical assistance at biomechanically-sensible timing (see Section 6.4.1). Specifically, Chapter 8 demonstrated that the gait event detection algorithm could accurately estimate timings of key gait events such as foot-strikes (FS) and toe-offs (TO) with 1-2%GC error on average. As temporal gait metrics are the difference between different gait event timings, the implementation of temporal gait metric estimation is completed by additionally subtracting the respective gait event timings in exosuit controller pipeline. With this simple addition, exosuit can calculate various temporal gait metrics in **Table 9.1**.

Table 9.1. Temporal gait metrics estimated with exosuit

Metrics	Description
Stride time	time elapsed between successive foot-strikes of the same foot
Stance time	time elapsed from foot-strike to toe-off on the same foot (i.e. time duration of stance phase)
Swing time	time elapsed from toe-off to foot-strike on the same foot (i.e. time duration of swing phase)
Step time	time elapsed from ipsilateral foot-strike to following contralateral foot-strike.

Since the gait event detection accuracy was validated in Chapter 8 and the accuracy of temporal gait metric estimation is directly based on the gait event detection accuracy, this chapter from this point focuses on describing a new spatial gait metric estimation algorithm implemented in exosuit and its validation.

9.2.2. Spatial gait metric estimation

Spatiotemporal metrics are defined based on the foot position trajectory. **Table 9.2** summarizes commonly used to evaluate post-stroke gait impairments, which are target metrics of our estimation algorithm.

Table 9.2. Spatial gait metrics estimated with exosuit

Metrics	Description
Stride length	the distance between two successive instances of the same gait event (usually ground contact) for the same foot
Stance speed	Stride length divided by stride time
Foot circumduction	maximum lateral deviation of swing foot position relative to stance foot (out of the sagittal plane)
Foot clearance	Maximum foot height during swing

Three different approaches for spatial gait metric estimation with IMUs can be found from the literature: Kinematic model-based method, statistical abstraction models using machine learning techniques, and direct integration methods.

Kinematic model-based methods

This approach estimates foot trajectories using the human lower extremities motion using a kinematic model in combination with sensor measurements such as the thigh or hip angles. The kinematic models found in previous literatures are single inverted pendulum models [244], inverted double pendulum models [245], [246], and wire frame models [247]. The main challenge of this approach is that if the kinematic model is too generic, the model may not be sufficient to represent individual anthropometry, ultimately decreasing estimation accuracy. Furthermore, fitting the kinematic model to individual anthropometry requires accurate measurements of individual segment lengths and inertial properties, increasing model tuning effort and complexity.

Statistical abstraction models using Machine Learning Techniques

This approach generates a statistical model and train the model using IMU measurement. Specifically, it creates statistical models mapping IMU data to specific gait metrics. The model is trained based on the labelled pair of raw IMU data and gait metrics (e.g. accelerations labelled with ground truth stride length). This approach includes deep learning methods (CNN, RNN) [248], [249] and linear regression models [250]. Although promising, this approach has two main limitations: first, statistical models have shown to work best when they are personalized based on subject specific training data [250]. This however may cause overfitting. Furthermore, training of statistical models requires big datasets, which are usually not available and also need to be labelled with ground truth on a stride by stride basis.

Double Integration Methods

Lastly, this approach estimates foot position trajectories by double-integrating accelerometer data and compensating integration error on a stride basis either deterministically using strapdown methods [251]–[257], or stochastically using Error-state Kalman filters [258]–[260]. The errors of double integration methods are mainly caused by the noise and bias in IMU measurement. IMU measurements include a quasi-

constant offset referred to as bias and zero mean white noise. The bias is often difficult to calibrate as it changes randomly when turning the IMU on and off (on-off variability) and during IMU operation (in-run instability). Furthermore, any orientation estimation error from the IMU could lead to velocity and position estimation errors [261], [262]. Direct integration of the acceleration signals, including these bias terms leads to linearly growing velocity errors and quadratically growing position errors, called IMU integration drift (see **Table 9.3**).

Table 9.3. IMU measurement errors and resulting integration drifts

IMU measurement errors		
Type	**Description**	**Integration drift caused by the measurement error**
Bias	Constant offset	Linearly growing error in velocity estimation and quadratically growing error in position estimation
Bias instability	Changes in bias over time	Third-order random walk in position
White noise	Random noise around zero	First order random-walk error in velocity and a second-order random-walk error in position

This table is based on [262] and modified.

In order to compensate the significant integration drift, direct integration often utilize error compensation strategy called Zero-Velocity Updates (ZUPTs). ZUPTs leverage foot flat phase of the single limb support in the gait cycle to periodically correct the velocity drift. More specifically, each gait cycle includes a foot flat phase where the foot is stationary on the ground, thus the foot velocity can be assumed to be zero. The velocity error at this point can be therefore calculated as the difference between the current estimated velocity and actual velocity (i.e. zero velocity).

Two different approaches for ZUPT, threshold-based methods and machine-learning based methods (i.e. error state Kalman filtering), can be found in literature. First, the threshold-based method detects foot flat phase when either IMU sensor signal or a predefined metric (acquisition function) based on combinations of these signals falls below a predefined threshold. It generates a binary function that is 1 if the test metric or a signal falls below the threshold (foot flat) and 0 if not. Given the obtained binary function, some of

previous studies perform a ZUPTs at every instance the binary function is equal to 1[101], [263], while others execute an additional step to define the ZUPT instance as the median of every stance phase identified by the binary function [255], [264], [265]. The latter approach is only available through post-processing, since finding the median requires information about the total foot flat window length, which cannot be acquired in real-time.

Although promising, these methods may fail to detect the foot flat phase because of the noise and inconsistency of IMU signals. Furthermore, different IMUs are likely to provide generate different bias and noise level, limiting the scalability of this approach. Consequently, this approach often requires the thresholds to be manually tuned and adapted for each subject and different IMUs. Even after tuning, there could still be a non-negligible number of false positives (e.g. foot flat is detected during swing) and false negatives (e.g. foot flat is not detected during stance) (see example in **Figure 9.1**). These detection errors greatly affect the robustness and accuracy of the algorithm.

Figure 9.1 gives an example of a ZUPT method based on the angular rate signal and manually tuned thresholds. The binary function (black solid line) is defined as 1 (i.e. foot flat is detected) when the angular rate falls in between the upper and lower bounds of threshold (red dashed line) and 0 otherwise. The figure also illustrates the aforementioned common challenges of threshold-based ZUPT detection: When the angular rate signal crosses the threshold window, there is a risk that this method falsely detects foot flat. If the angular rate temporarily leaves the threshold window during foot flat due to the sensor noise, the binary function gives false negative. Additional constraints are often introduced to address these issues. However, this requires additional tuning process, increasing further risk of false detection.

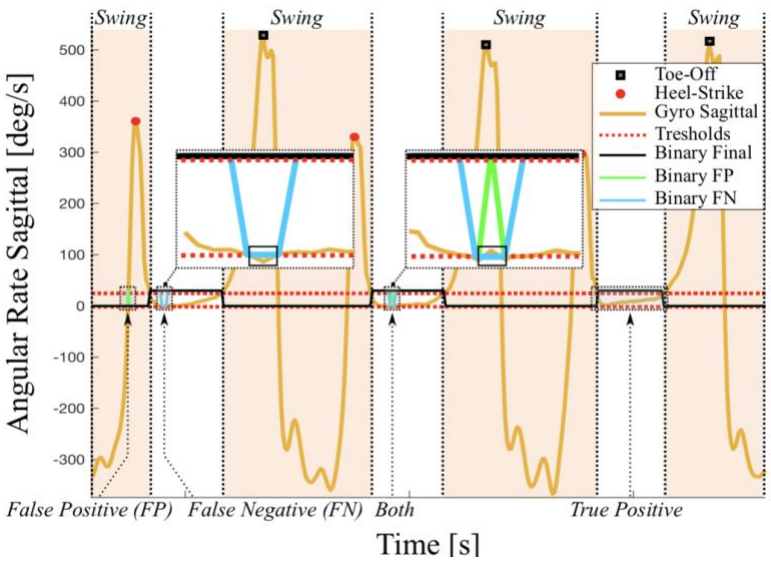

Figure 9.1. Example of a threshold based ZUPT detection method using sagittal plane gyroscope signals (yellow). Binary function indicating stance phases is shown in black. Common challenges are also illsutrated: short stance intervals/false positives (green) and short distances between stance intervals/false negatives (blue) in blue.

On the other hand, machine learning based ZUPT methods identifies recurring patterns within a person's gait cycle to perform temporal gait segmentation (i.e. detect individual strides) to detect foot flat phase. Based on labelled training data, the models learn which moments in the gait cycle are indicative of ZUPT instances. Common examples include pattern similarity approaches like dynamic time warping or hidden markov models [250], [256]. Similar to machine learning technique for directly mapping IMU signals to spatial gait metrics, this requires either individualization of training data or large training data set to increase scalability [250], [266].

9.3. Exosuit real-time spatial gait metric estimation algorithm

Based on the literature review in Section 9.2, we implemented real-time spatial gait metric estimation algorithm with exosuit based on a double integration method with strapdown ZUPT strategy. The main reason for choosing a double integration method was to minimize tuning process required for model-based estimation approaches (i.e. kinematic model and statistical abstraction model). Strapdown ZUPT methods were chosen over machine-learning based error compensation methods to further minimize the required tuning procedure [242]. Strapdown methods also require less computational power compared to machine learning methods, making them more favorable for implementation with limited computational resource of

portable system. Moreover, to address the aforementioned limitations of existing ZUPT methods in their accuracy, robustness, and real-time applicability, we developed a new ZUPT detection method leveraging the exosuit gait event detection algorithm described in Section 6.4.1, which allows to robustly detect ZUPT moment in real-time without using thresholds.

9.3.1. ZUPT detection method

Our real-time spatial gait metric estimation leverages the gait event detection algorithm presented in Section 6.4.1. In brief, the algorithm detects the nonparetic toe-off (NTO) and paretic toe-off (PTO) using the negative peaks in angular rate signal in the sagittal plane (see **Figure 9.2**). It searches for a negative peak in the angular rate signal in real-time and then confirm the detection of the negative peak at the subsequent zero-crossing. Interestingly the toe-off confirmation (i.e. realtime gait segmentation point) on the contralateral side indicates early single limb support on the ipsilateral side, the beginning of foot flat phase (**Figure 9.2**). Leveraging this biomechanical observation and the toe-off confirmation provided by the gait event detection algorithm, exosuit can reliably detect foot-flat phase to execute ZUPT based on the IMU signal of the contralateral foot. To the best of our knowledge, this is the first approach to utilize contralateral foot IMU information for the ipsilateral ZUPT.

The gait segmentation is delayed compared to the actual toe-off event approximately 4-6% of the gait cycle (Section 8.4.3), therefore ZUPT also occurs 4-6% after the beginning of single limb support. This latency could be desirable in our application. As shown in **Figure 9.2**, defining the ZUPT moment based on the zero-crossing of the gyro signal reduces the risk of residual motion of the IMU on the ipsilateral, single-support side during early stance (See higher standard deviation of the angular velocity signal around the actual NTO event). Moreover, some post-stroke individuals present vaulting motion to compensate for reduced paretic ground clearance by lifting their nonparetic foot up during late single-support [188]. By detecting ZUPTs slightly at early single limb support could minimize the negative effect of vaulting motion on the velocity update.

More importantly, our new ZUPT method does not rely on thresholds but only on the detection of a single gait event, therefore does not require any subject-dependent manual tuning, significantly reducing the risk of false positives and negatives. Since this gait event was validated to be reliably detected (Chapter 8), this new ZUPT can also perform with high accuracy and robustness across different subjects with highly heterogeneous gait patterns.

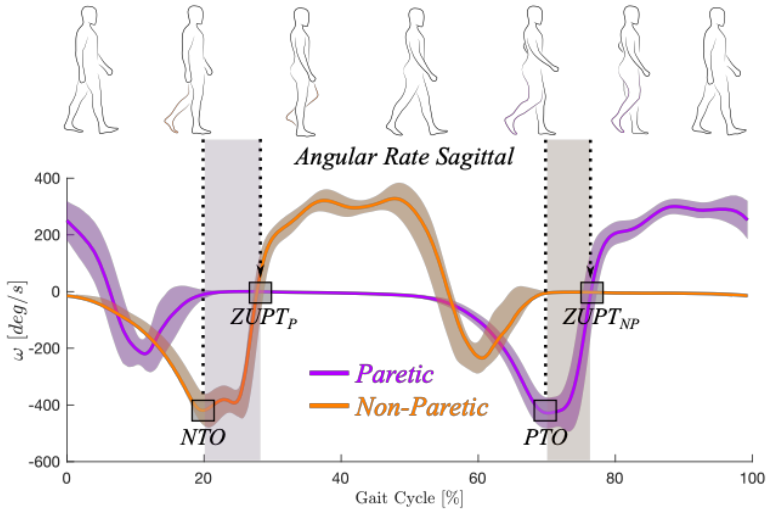

Figure 9.2. Zero-Velocity Update (ZUPT) algorithm based on exosuit gait event detection
In the gait event detection algorithm toe-off events are detected based on negative peaks in the sagittal plane angular rate signal (NTO, PTO). In the real-time implementation, the algorithm first saves the negative peaks as toe-off candidates, and then confirms toe-offs at the subsequent zero-crossings of the angular rate signal. These confirmation points are used as ZUPT moment for the contralateral side ($ZUPT_P$ for paretic side and $ZUPT_{NP}$ for nonparetic side)

9.3.2. Strap-down double integration with linear drift compensation

Using the aforementioned ZUPT method, we implemented a strapdown double integration method with linear drift compensation (see **Figure 9.3**). The algorithm utilizes three IMU measurements: (a) three-axis gravity-free, global frame acceleration a_W, (b) orientation θ in the sagittal plane and (c) angular velocity ω in the sagittal plane. The orientations and angular rates in the sagittal plane are used by the gait detection algorithm for ZUPT detection. The acceleration signal is integrated once over the duration of a full stride using trapezoidal integration to obtain a velocity estimate. A full stride is defined as between two consecutive ZUPT moments (T_{start} and T_{end}) of the same foot. Based on the velocity error at the second ZUPT moment (v_{End}), a linear drift function between the first and last (k)th sample point of the (i) th stride is defined by following equations..

$$d_v = \frac{v_{End}}{T_{End} - T_{Start}} k \tag{9.1}$$

$$k = n\,\Delta t\,(n \in N_0 \mid n \leq \frac{T_{Start} - T_{End}}{\Delta t}) \tag{9.2}$$

This drift function is subtracted from the estimated velocity at every sample within the current stride to obtain a drift compensated velocity estimate.

$$v_{corrected}(k) = v_n(k) - d_v(k) \tag{9.3}$$

The corrected velocity signal is then integrated using trapezoidal integration to obtain the position trajectory estimates, and finally the spatial gait metrics are computed based on the position trajectories.

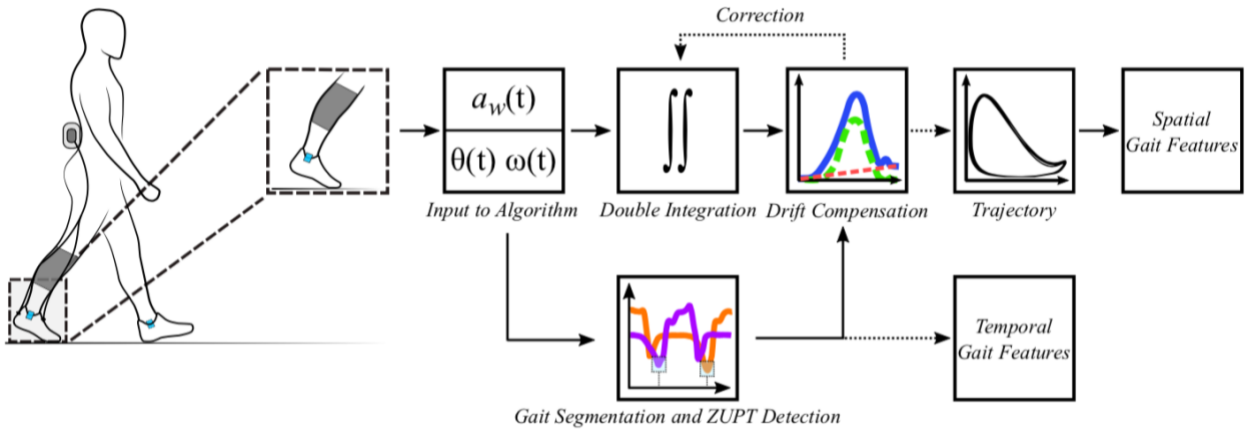

Figure 9.3. Implementation of exosuit ZUPT method and double-Integration with linear drift compensation

Figure 9.4 exemplifies the different steps of our algorithm for the vertical position trajectory and the effect of ZUPT based drift compensation. The raw gravity-free global acceleration signal (red) is integrated once between two subsequent ZUPT instances at (i)th stride (i.e. from $T_{Start}(i)$ and $T_{End}(i)$) to obtain the velocity estimate (blue solid). This offset is used to define a linear drift function (orange dotted) between $T_{Start}(i)$ and $T_{End}(i)$ with the slope of this drift function computed as

$$m_v = \frac{v_{End}(i)}{T_{End}(i) - T_{Start}(i)} \tag{9.4}$$

After subtracting the drift function from the original velocity estimate, the corrected velocity estimate (grey dashed) is obtained. The corrected velocity is then integrated again to obtain the desired position signal

(green solid). If we assume level-ground walking conditions, the same drift correction method could be applied for the vertical position trajectory as well: The drift function (orange dotted) based on the vertical position offset at the end of the stride is subtracted from the original position estimate (green solid) to yield the corrected trajectory (green dashed). This, however, can only be done for the vertical position trajectory in level-ground walking conditions as the end position is known to be the same as it was at the beginning of the stride (i.e. the difference in position should be zero).

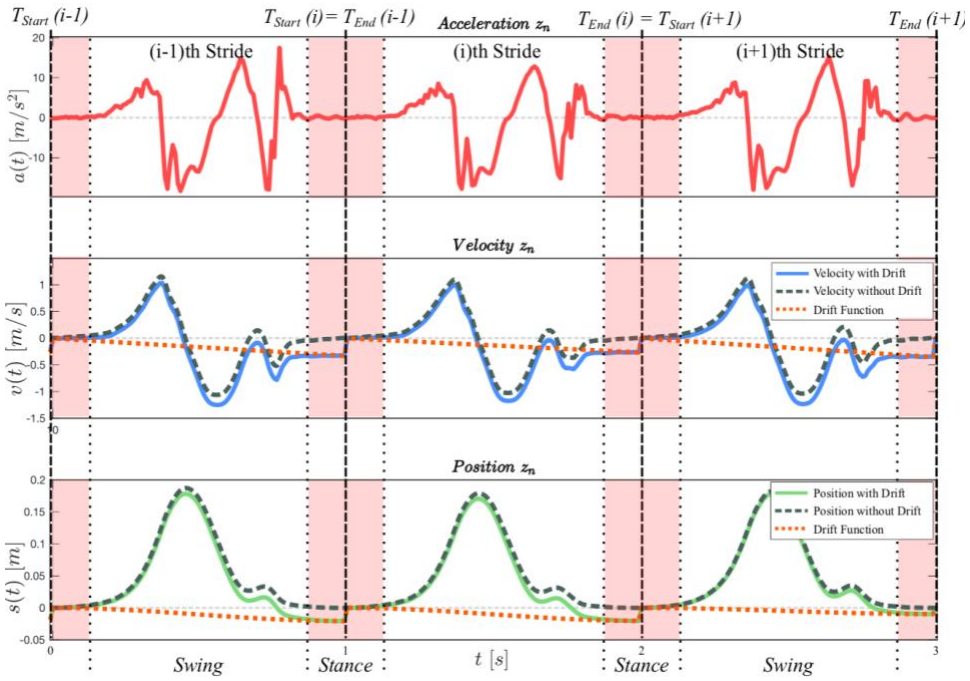

Figure 9.4. Example of strapdown double integration with linear drift compensation in vertical axis

9.3.3. Implementation of real-time drift compensation

Correcting the velocity estimate with drift function requires storing the velocity estimates throughout entire previous stride. However, the number of samples for an entire stride (~100 samples) could be challenging for limited data storage of portable embedded system. Therefore, instead of correcting the velocity estimate every sample and then integrating the corrected velocity to obtain the desired position trajectories, our real-time algorithm directly corrects position. It subtracts the position errors accumulated by integrating a linear velocity drift model. The amount of position error caused by integrating this velocity drift can be described as follows (red area underneath velocity plot in Figure 9.5):

$$s_{corrected}(T_{End}) = s_n(T_{End}) - \frac{1}{2}(T_{End} - T_{Start})\, v_{End} \tag{9.5}$$

It should be noted that drift is only corrected for the current sample in which the ZUPT is performed with this strategy (see green position trajectory in Figure 9.5). However, this is sufficient for our application since gait metrics, by definition, should be updated every stride (see the following Section 9.3.4).

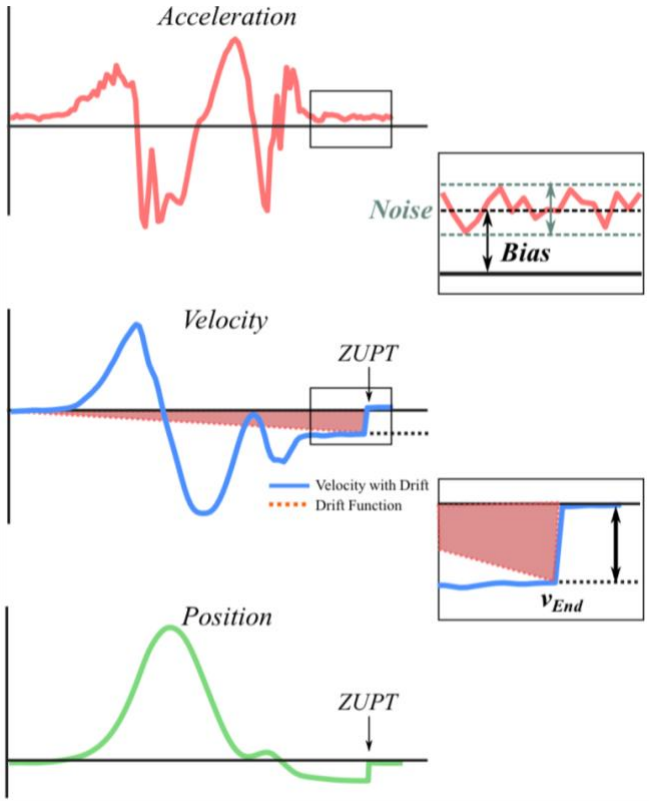

Figure 9.5. Adjusted drift correction in real time implementation

9.3.4. Gait Metric Computation

Stride Length and Stride Speed

Stride length can be computed the displacement in the transverse plane (**Figure 9.6**) between two consecutive stance phases can then be computed based on the reconstructed x and y position trajectories (s_x and s_y) as follows:

$$d_x(i) = s_x(T_{End}) - s_x(T_{Start}) \tag{9.6}$$

$$d_y(i) = s_y(T_{End}) - s_y(T_{Start}) \tag{9.7}$$

Based on the overall transverse plane displacements the current (i)th stride length can directly by computed as:

$$SL\ (i) = \sqrt{d_x^2(i) + d_y^2(i)} \tag{9.8}$$

Which allows to directly compute the average stride velocity as:

$$SV\ (i) = \frac{SL\ (i)}{T_{End}(i) - T_{Start}(i)} \tag{9.9}$$

Circumduction

Circumduction was measured with the shortest (perpendicular) distance between a point P (on the foot trajectory) at every sample k of the (i)th stride and a line with direction vector u in **Figure 9.6** can be computed as:

$$dist_i(k) = \frac{\left||AP(k) \times u|\right|}{\left||u|\right|} \tag{9.10}$$

With point A defining the start point of the current stride at time instance $T_{Start}(i)$. Based on this the maximum lateral displacement (MLD, i.e. circumduction) can be found as:

$$MLD(i) = max\{dist_i(k)\} \tag{9.11}$$

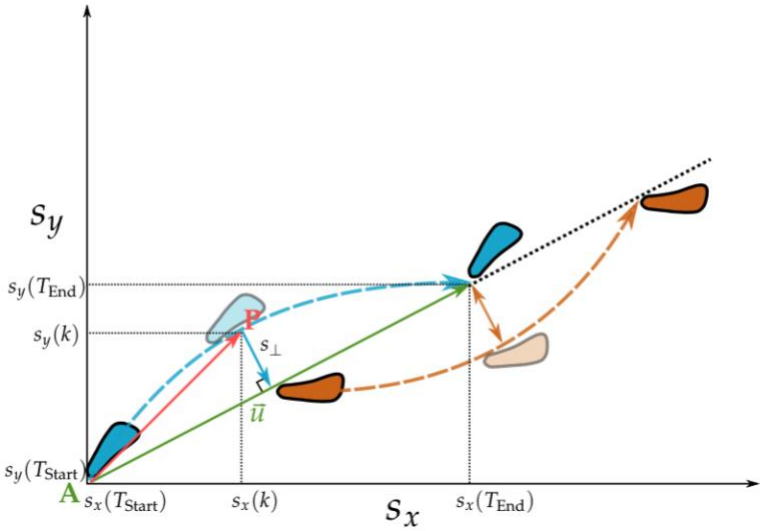

Figure 9.6. Illustration of stride length and circumduction defined by transverse plane foot trajectory

Ground Clearance

Ground clearance can be computed as the maximum vertical displacement (MVD) of foot from the vertical position trajectory s_z (see **Figure 9.7**). It should be noted that t exosuit IMU only allows to assess the trajectory of IMU position attached on the foot, and does not represent entire foot position.

$$MVD(i) = max\{s_z(k)\} \tag{9.12}$$

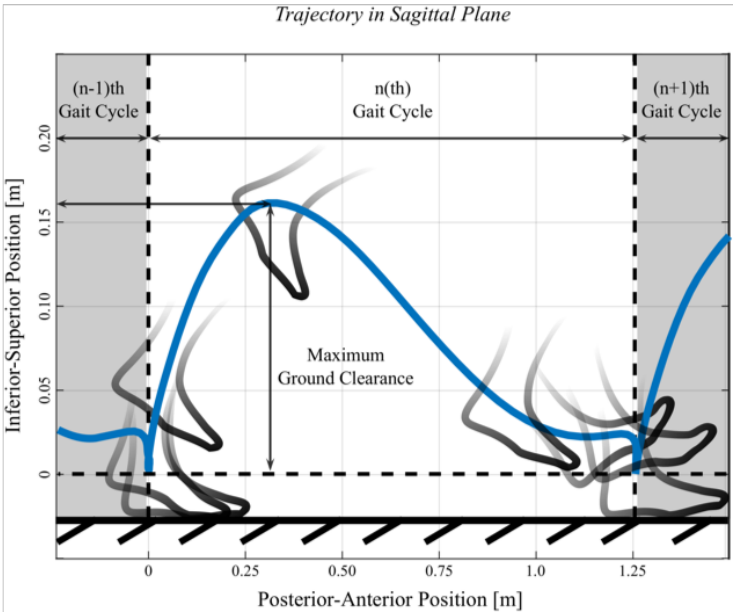

Figure 9.7. Illustration of ground clearance defined by sagittal plane foot trajectory

9.4. Validation

Three experiments were performed to validate the exosuit spatial gait metric estimation: For the initial feasibility test, the gait speed estimated with exosuit in real-time during treadmill walking was compared to the treadmill speed settings in three healthy individuals. Second, real-time stride length and stride speed estimation during overground walking in two post-stroke individuals was validated using motion capture system. Finally, we conducted a benchmark analysis to compare our methods to previously presented ZUPT methods [101], [102] by post-processing the collected from a post-stroke individual walking overground and on a treadmill.

9.4.1. Validation 1: Healthy treadmill Walking (N=3)

The goal of this experiment was to show the feasibility of our new gait metric estimation algorithm by comparing to treadmill speed setting. We used linear regression analysis to show correlation between actual (treadmill) and reconstructed walking speeds and computed RMSEs, coefficients of determination (r^2), and slopes of the obtained regression lines.

Error! Reference source not found. illustrates the experimental setup. Participants walked on a treadmill (Sole TT8, USA) wearing exosuit in 5 different speeds (0.49m/s, 0.68m/s, 0.89m/s, 1.12m/s, 1.35m/s) for 1 minute each in both exosuit active (A) and slack (S). Since the participants were healthy individuals, their virtual paretic side (i.e. where the suit was worn) was arbitrarily chosen to be their left side.

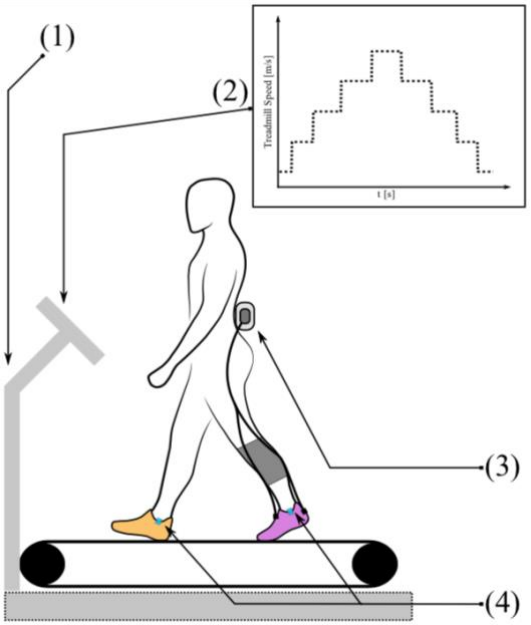

Figure 9.8. Experimental setup for treadmill walking in healthy individuals (validation 1)

Error! Reference source not found. and **Error! Reference source not found.** summarize results for all subjects. The RMSE was below 7% (0.06m/s) across all subjects and conditions. Strong linear correlation between estimated and reference speeds was found through regression analysis (r^2= 0.98) for all subjects and conditions. Furthermore, slopes of the linear regression lines were within 3% of the identity line. A slight overestimation was observed across subjects (except P1 on NP Side). Interestingly, we also observed a slightly higher overestimation on the paretic (left) side compared to nonparetic side. No trend was observed in speed-dependent errors.

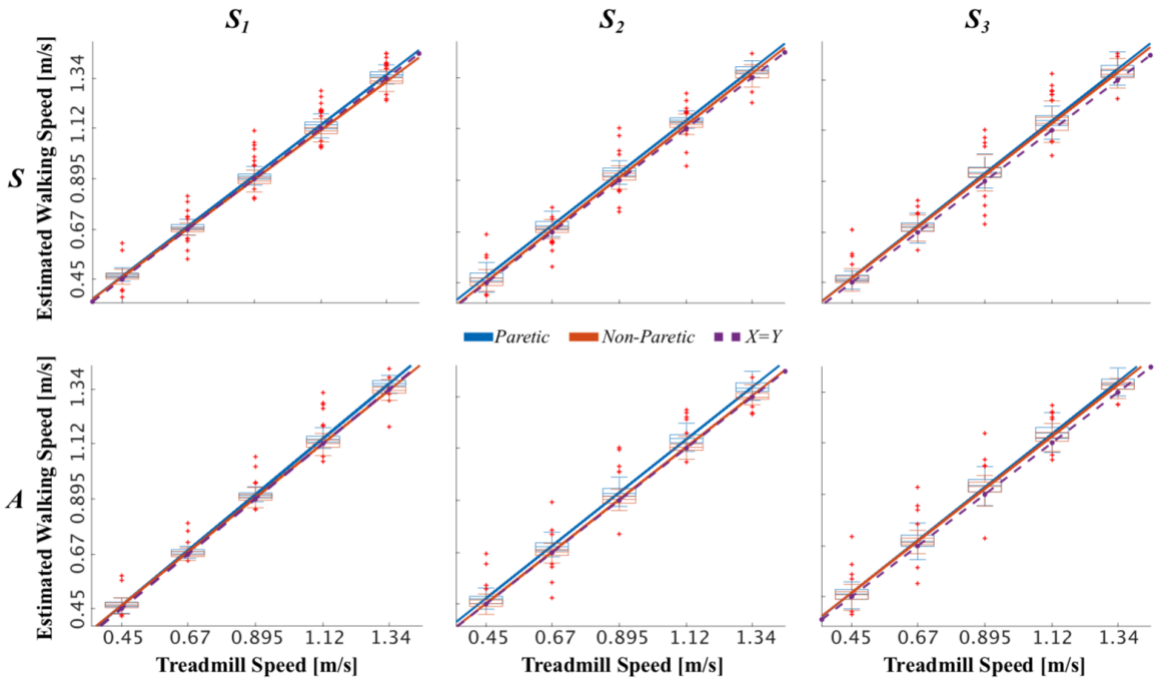

Figure 9.9. Linear regression outcomes between exosuit-estimated gait speed and treadmill speed

Table 9.4. Linear regression analysis outcomes from validation 1

			RMSE (cm/s)		RMSE (%)		R_2		Slope	
	Participant	**Paretic side**	**P**	**NP**	**P**	**NP**	**P**	**NP**	**P**	**NP**
Slack (S)	P1	L	3.22	2.97	398	3.87	0.99	0.99	1.00	0.97
	P2	L	4.64	3.14	6.19	3.95	0.99	0.99	1.01	1.01
	P3	L	5.23	4.86	6.05	5.82	0.98	0.98	1.03	1.02
Active (A)	P1	L	3.15	2.69	3.49	3.46	0.99	0.99	1.01	0.98
	P2	L	4.86	2.89	6.34	3.57	0.99	0.99	1.02	1.00
	P3	L	5.27	4.29	6.27	5.86	0.98	0.99	1.03	1.02

9.4.2. Validation 2: Post-stroke overground walking (N=2)

The second experiment was conducted to validate our algorithm under more challenging and irregular walking in post-stroke individuals and compare the outcomes to motion capture data (see **Error! Reference source not found.** for participants' characteristics). We performed regression analysis between stride length/speed estimated by exosuit and ones calculated using motion capture data. Since there was no significant difference in accuracy between the suit slack and active condition from Section **Error! Reference source not found.**, only the suit active condition was investigated for this experiment.

Table 9.5 Participant's stroke and gait characteristics

Participant	Paretic side	Sex	Age (y)	Chronicity (y)	Type of stroke	Weight (kg)	Height (m)	Walking speed (m/s)
P1	L	F	57	9.3	Ischemic	53	1.63	0.45
P2	L	M	44	9.0	Ischemic	99	1.81	0.70

Both participants walked on a straight line of an overground track equipped with a motion capture system (Qualisys AB, Sweden) (see **Error! Reference source not found.**). Baseline foot trajectories were calculated based on the motion capture marker position attached on the exosuit-integrated IMUs. The motion capture data was processed with Qualysis (Qualisys AB, Sweden) and Visual 3D (Acuity Brands Lighting, Inc).

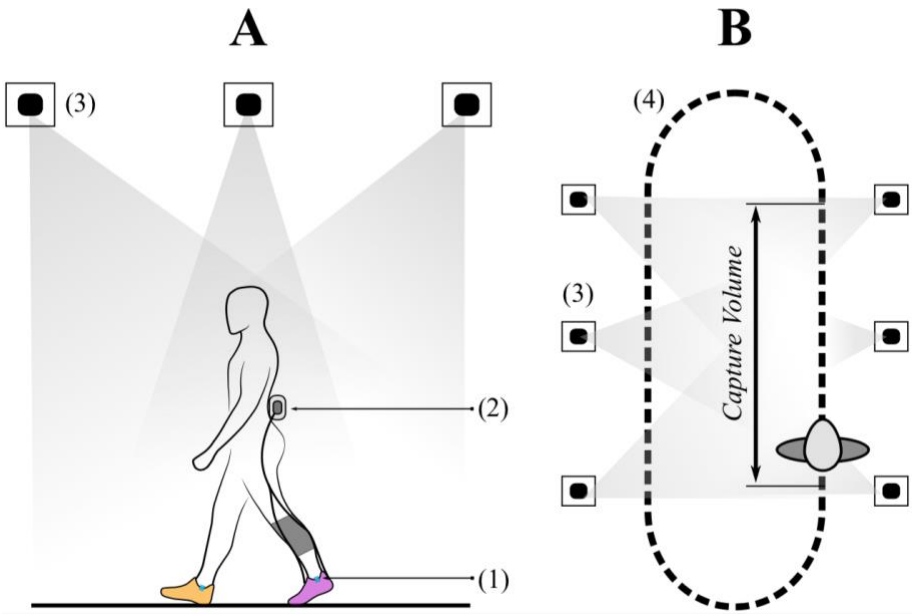

Figure 9.10. Experimental setup for post-stroke overground walking (Validation 2)

Error! Reference source not found. summarizes the results. The RMSE of both the stride length and stride speed metrics were below 4% (0.03m, 0.03m/s) for the paretic side and below 8% (0.07m, 0.07m/s) for the nonparetic side for both subjects. The regression analysis shows comparable results to the previous experiment with $r^2 > 0.91$ for all subjects and metrics, while the slopes of the regression lines are within 5% of the identity line. Unlike seen in the first experiment, there seemed to be a higher overestimation for the nonparetic (right) side.

Table 9.6. Linear regression analysis outcomes from validation 2

		RMSE		RMSE (%)		R_2		Slope	
	Participant	**P**	**NP**	**P**	**NP**	**P**	**NP**	**P**	**NP**
Stride length (cm)	P1	2.93	6.38	2.94	6.43	0.98	0.99	1.04	1.03
	P2	2.81	5.65	3.80	7.71	0.92	0.95	1.01	0.98
Stride speed (cm/s)	P1	2.94	6.03	2.93	6.39	0.98	0.99	1.02	1.04
	P2	2.54	5.13	3.72	7.72	0.93	0.96	1.05	0.97

9.4.3. Validation 3: Comparison of different ZUPT methods in post-stroke walking (N=1)

The final validation step was to directly compare our ZUPT method to other methods from literature by integrating them into our existing algorithm framework and then comparing gait metric reconstruction accuracy based on the same dataset. One post-stroke individual (paretic side: left, Age: 58y, years after stroke: 4.5y) participated in this two-day protocol. On the first day, the participant walked on a treadmill in both comfortable walking speed (CWS, 0.45m/s) and fast walking speed (FWS, 0.61m/s) wearing exosuit delivering paretic ankle assistance. On the second day, the participant walked on an overground walking track in both CWS (mean=0.43m/s) and FWS (mean=0.49m/s).

For the benchmark comparison analysis, we implemented 3 different threshold-based ZUPT methods, called SHOE, ARE, and MAG, presented in [101], [102]. For a "one-to-one" comparison of the computed gait metrics, we introduced a neutral foot-flat moment, and all the methods including ours were compared at the neutral moment through post-processing.

Neutral Stance Instance

Foot-flat moments are detected differently with different ZUPT methods, therefore the time window used for gait metric calculation for different methods could also be different. This makes it challenging to directly compare gait metrics across different methods. To address this, we first defined a neutral foot-flat moment based on Ground Reaction Force (GRF) data collected by instrumented treadmill or force plate to allow for a fair comparison between all methods. **Error! Reference source not found.** illustrates how the neutral stance instances (black dots) are defined based on the contralateral GRF data (red). It also shows their

occurrence within the motion capture based anterior-posterior position trajectory (blue). As can be seen, the location of the stance instances lies almost perfectly centered within phases of no displacement in the shown trajectory, confirming their validity as neutral ZUPT comparison points.

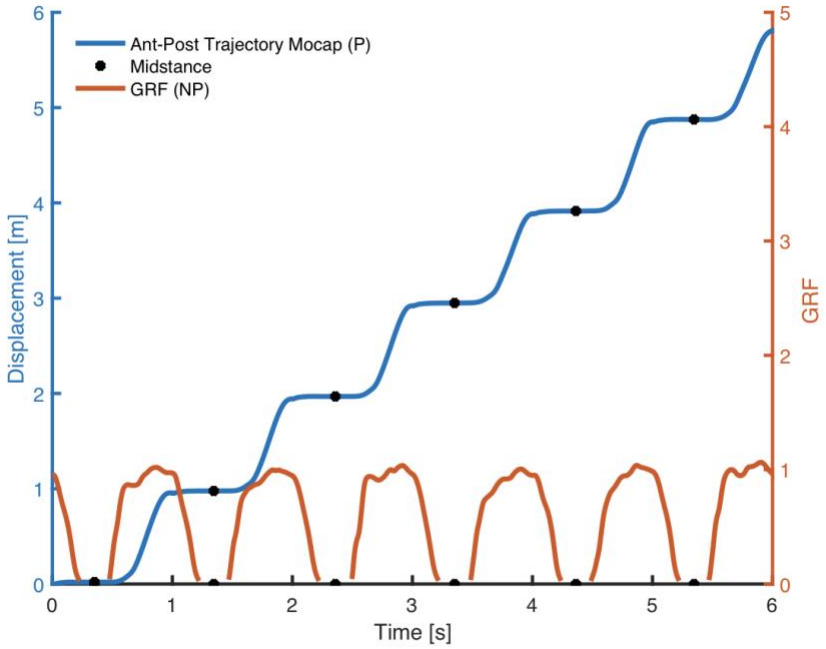

Figure 9.11. Definition of neutral ZUPT/foot-flat moments. ZUPT moments (black dots) are shown with respect to the contralateral GRF data (red) based on which they are defined, as well as on the ipsilateral foot trajectory in anterior-posterior position (based on mocap) to validate their location within phases of no movement (stance)

Analysis

We computed foot trajectories from different ZUPT methods (i.e. SHOE, ARE, MAG, and exosuit methods) based on the algorithm framework shown in **Error! Reference source not found.**. Tuning parameters for threshold-based ZUPT methods (i.e. SHOE, ARE, MAG) were chosen as reported in the previous studies [101], [102].

Validation in treadmill walking

Mean absolute estimation errors for the gait metrics calculated from different ZUPT methods were calculated. The estimation errors were not normally distributed, therefore we performed Kruskal-Wallis non-parametric analysis of variance to test statistically significance difference (see **Error! Reference**

source not found.). On the paretic side metrics, our method performed significantly better than other methods in most of the cases except for paretic ground clearance (MVD) in FWS. On the nonparetic side, our method performed significantly better for ground clearance, while it was worse for stride length and maximum lateral distance. It should be noted that no other method consistently showed superior performance to all other methods on these two metrics: While MAG performed best for nonparetic stride length, ARE or SHOE performed better for circumduction (MLD) across speed conditions.

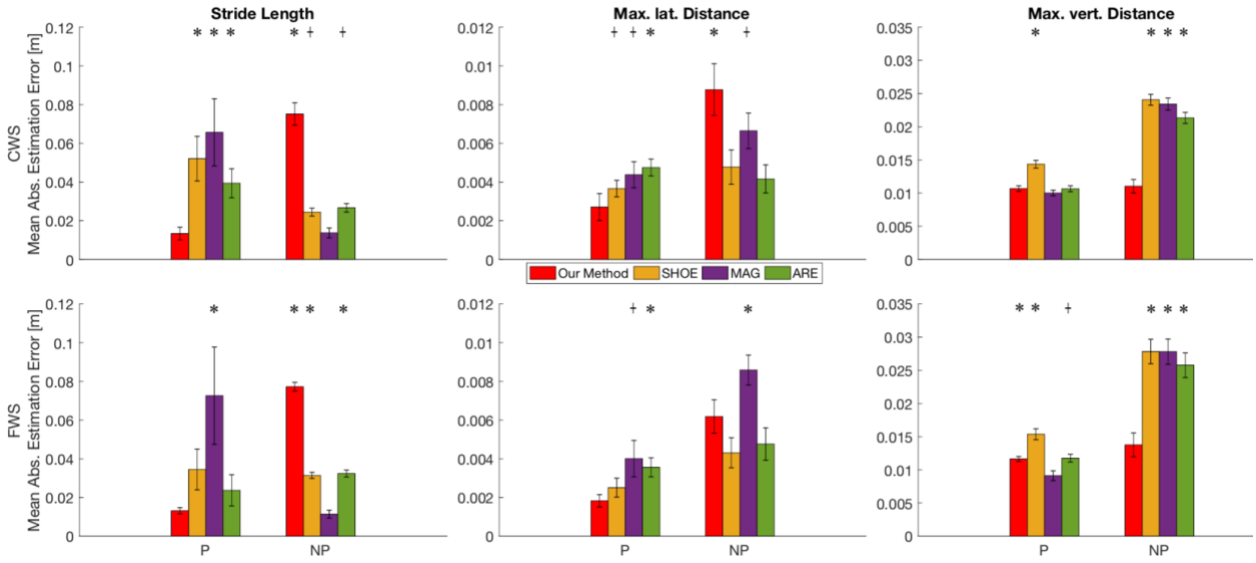

Figure 9.12. Comparison of different ZUP methods in post-stroke treadmill walking. We computed mean absolute estimation errors, as well as their standard errors which are shown as black error bars. Errors are shown based on comfortable walking speed (CWS) and fast walking speed (FWS) for each metric evaluated.
Note: Max. lat. Distance: Maximum lateral distance (i.e. circumduction), Max. ver. Distance: Maximum vertical distance (i.e. ground clearance).
*: $p < 0.001$; +: $p < 0.05$

Validation in overground walking

Same as the treadmill validation, mean absolute estimation errors for the gait metrics calculated from different ZUPT methods were calculated (see **Error! Reference source not found.**). First, all methods generally performed better for the paretic side compared to the nonparetic side. Also, our method performed better for stride length estimation and ground clearance, while showing worse accuracies for circumduction for both sides and across different speeds. The other methods in general showed significantly increased accuracies for the paretic side across all metrics and speeds compared to the previous experiment. For the nonparetic side a slight decrease of accuracy was observed for stride-length as well as a noticeable decrease

for circumduction. Lastly, for ground clearance our method performed significantly better for the "CWS, NP" condition, while performing in comparable ranges to the other methods for the remaining conditions.

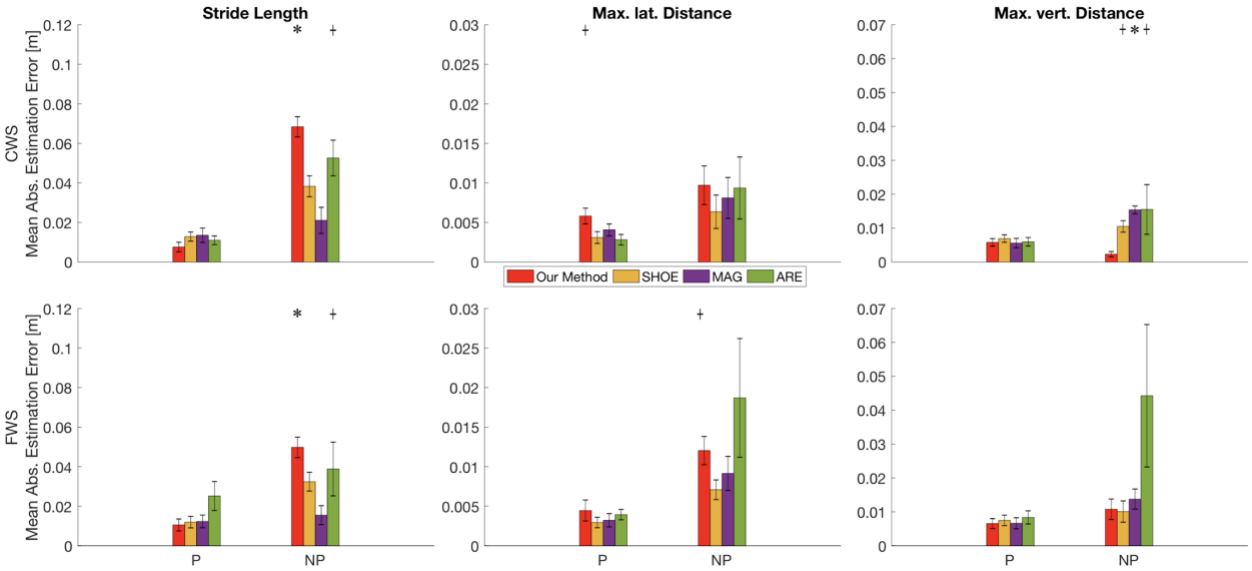

Figure 9.13. Comparison of different ZUP methods in post-stroke overground walking. We computed mean absolute estimation errors, as well as their standard errors which are shown as black error bars. Errors are shown based on comfortable walking speed (CWS) and fast walking speed (FWS) for each metric evaluated.
Note: Max. lat. Distance: Maximum lateral distance (i.e. circumduction), Max. ver. Distance: Maximum vertical distance (i.e. ground clearance).
*: $p < 0.001$; +: $p < 0.05$

Main sources of estimation errors

Error! Reference source not found. gives an example of ZUPT detection for different methods in one stride. Based on the raw IMU signals, the ZUPT acquisition function "T" are constructed (blue line) and a binary function (black) is set to 1 once the detection signal falls below a pre-defined threshold (black dashed). Baseline foot flat phat phase based on the contralateral GRF data is also shown. This figure demonstrates that three other ZUPT methods experienced following major challenges:

- ZUPT moments are not detected within foot flat phase. This issue is characterized by very short distances between subsequent stance phases illustrated by the occurrence of multiple ZUPT periods within foot flat phase. This issue occurs when the test metric (acquisition function) momentarily leaves the threshold within the true stance interval, which for SHOE and ARE coincides quite precisely with

a spike in the angular rate signals round 25%GC in **Error! Reference source not found.**. This issue is referred to as false negatives.

- ZUPTs are falsely detected outside of the true single support window. This issue is characterized by ZUPTs being detected outside of the true stance phase. Examples are observed from **Error! Reference source not found.** during late sing phase (>80% GC) in SHOE, MAG, and ARE. This issue is referred to as false positive.

- ZUPTs are detected too early or late compared to the true single support window. Based on **Error! Reference source not found.**, all three other methods perform ZUPT before (~9%GC) and after (~5-10%GC) the true foot flat phase. ZUPT detections that occur too early or too late can introduce wrong constraints into the integration procedure, as actual foot motion might still be happening when the updates are performed.

- The last issue, although not as common as the aforementioned issues, happens when ZUPT detection does not happen entirely during foot flat phase, which allows drift to accumulate unbounded until the next ZUPT update

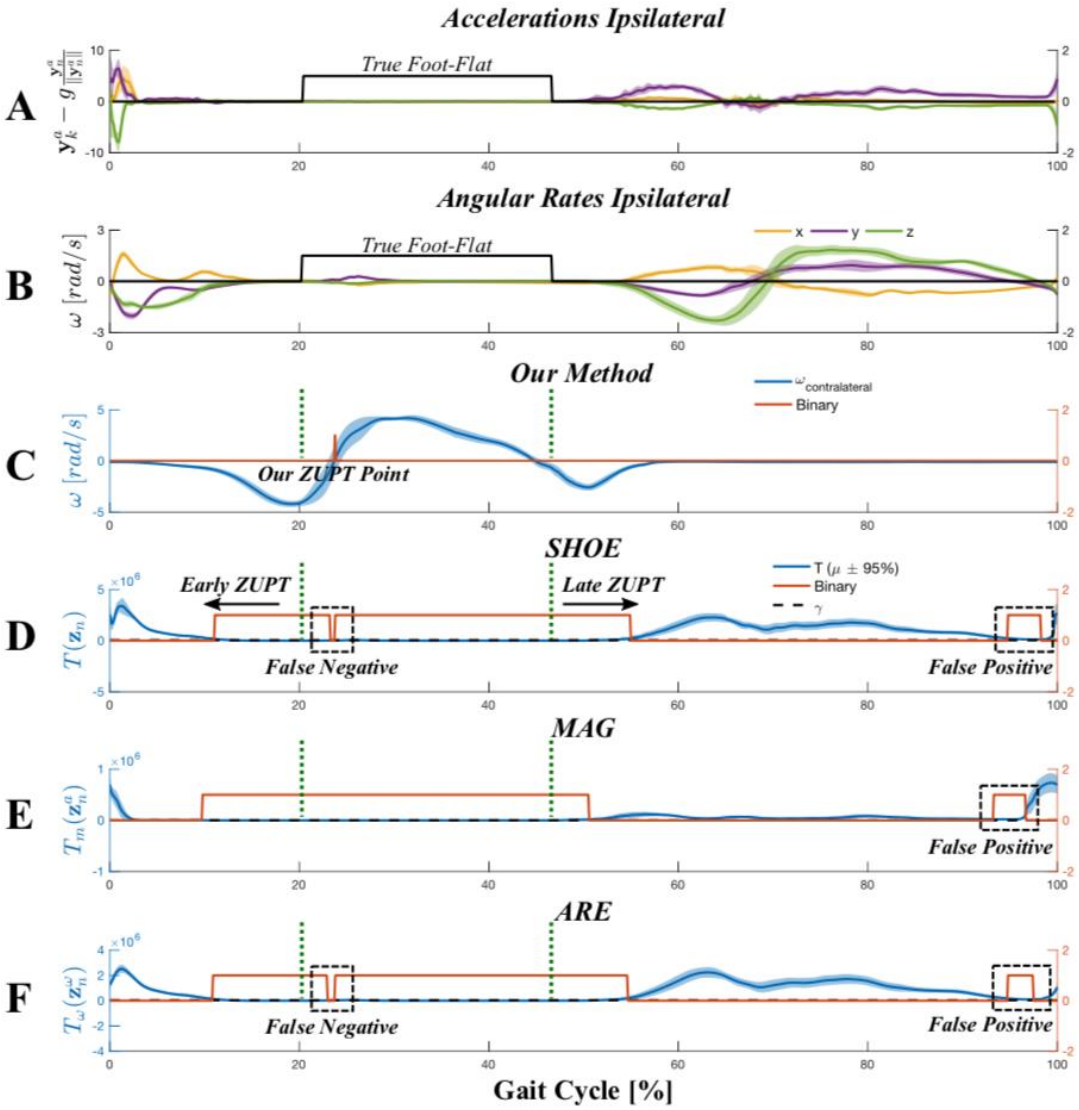

Figure 9.14. Detailed comparison showing how different ZUPT methods work and their challenges
. The graphs A and B show the raw signals based on which the respective test statistics (blue) are computed. If the test statistic T falls below its respective threshold y (black dashed, because of dimensions hard to see) a ZUPT is detected and the binary function (red) is set to 1. As can be seen, in our case in graph C the ZUPT is only performed once throughout the gait cycle (instantaneous) while other methods define a ZUPT phase based on their respective binary function. The green dotted lines in graphs C-F mark the true single support window.

Error! Reference source not found. and **Error! Reference source not found.** provide a more detailed overview with regard to the occurrence of the aforementioned errors from three other methods (SHOE, MAG, ARE).

Table 9.7. Number of error occurrence for different ZUPT methods during post-stroke treadmill walking

	Method	Baseline Stride #	Early ZUPT	Late ZUPT	FP	FN	No ZUPT
Paretic	SHOE	118	118	118	9	84	0
	MAG	118	116	24	11	94	0

	ARE	118	118	114	4	32	0
Nonparetic	SHOE	116	115	116	20	49	0
	MAG	116	116	22	4	92	0
	ARE	116	113	113	5	73	0

FN = False Negative, FP = False Positive.

Table 9.8. Number of error occurrence for different ZUPT methods during post-stroke treadmill walking

	Method	Baseline Stride #	Early ZUPT	Late ZUPT	FP	FN	No ZUPT
Paretic	SHOE	56	39	17	9	98	0
	MAG	56	41	0	1	72	0
	ARE	56	40	4	0	99	0
Nonparetic	SHOE	54	29	0	3	137	0
	MAG	54	37	0	2	101	0
	ARE	54	19	0	6	109	7

FN = False Negative, FP = False Positive.

During treadmill walking (**Error! Reference source not found.**), a high occurrence rate of early ZUPTs were observed across all three methods. ARE and SHOE also demonstrated late ZUPT occurrences, while the MAG presented frequent false positive within the true foot flat window resulting in less occurrence of late ZUPTs. False positive rates were fairly low across different methods. As the false positives for the SHOE and ARE were very close to the true foot flat window, their negative impacts on estimation accuracy were smaller compared to the false positives for the MAG method. For MAG, the false positives occurred more often outside of the true foot flat window, which explains the generally worse accuracies of the MAG compared to others. False negatives also occurred fairly often across different methods. However their impact on accuracy was negligible. Lastly, there were no cases of missing ZUPTs for any of the evaluated methods. During overground walking (**Error! Reference source not found.**), we observed fairly high occurrence rates of early ZUPTs however relatively lower than the treadmill walking. Interestingly the occurrence of late ZUPTs decreased noticeably for both sides, as well as the false positive rate. The False negative rate on the other hand was quite high, indicating multiple false negatives per stride. Lastly the ARE method in seven cases failed to detect a ZUPT entirely for the nonparetic side.

More interestingly, in both treadmill and overground walking, we observed decreased estimation accuracies in most of the metrics on the nonparetic side compared to the paretic side. Even more, our method's

estimation accuracy seems to be relatively more affected by the side than the other methods. This could be mainly caused by acceleration bias/noise differences between the two IMUs on the paretic and nonparetic sides and how the different methods mitigated these. We found that the IMU signals from nonparetic side showed higher bias (instability) levels than the paretic side. **Error! Reference source not found.** illustrates the effect of these bias differences on the foot velocity estimation for SHOE and our methods. The figure demonstrates that the paretic side velocity estimate is almost identical for both methods. In contrast, on the nonparetic side, we observed noticeable differences in the velocity signals, with our method clearly showing higher velocity estimates between 25% and 65% GC compared to SHOE. The estimation difference is shown in blue, and directly illustrates the higher position estimation resulting from integrating this velocity signal. Higher estimation errors on the velocity as shown here would directly affect higher estimation errors in gait metrics. Based on this observation, more noticeable error on the nonparetic side compared to the paretic side in our method might be explained by higher acceleration bias instabilities due to faster foot motion on the nonparetic side. While our ZUPT performed at a single sample per a stride, all other methods implemented ZUPTs over certain time window. Because of integration during foot flat phase in our method, bias instabilities could have more impact on our estimation accuracies.

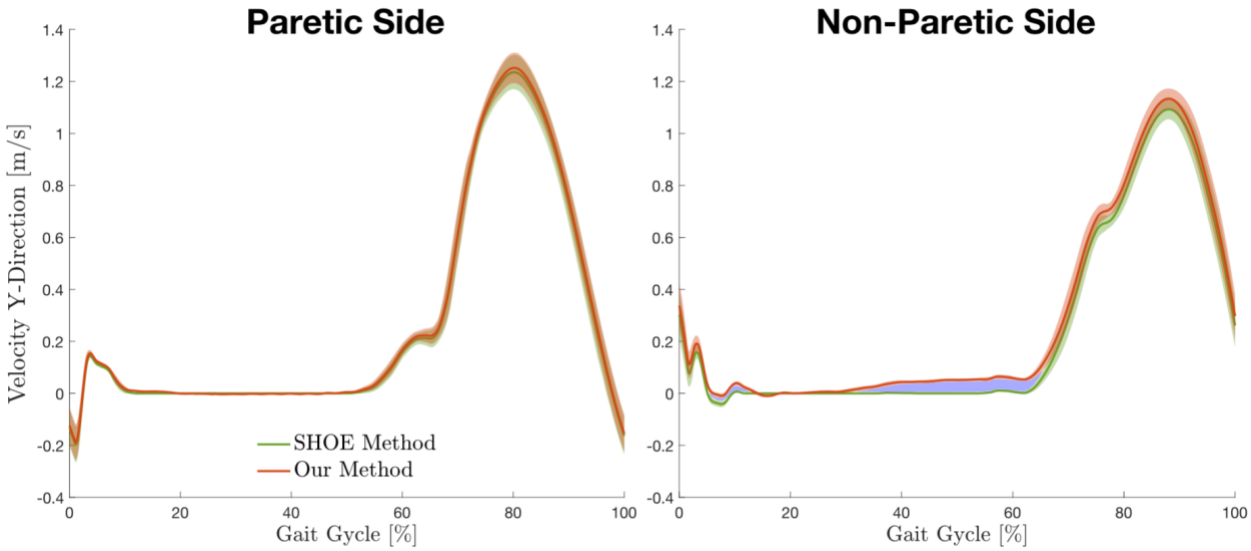

Figure 9.15. Comparison of estimated foot velocity averaged over 15 strides based on treadmill walking study for our method and one of other methods (SHOE). The plot shows estimation differences for the paretic and nonparetic side. The blue area on the nonparetic side indicates the position estimation difference that results from integrating our velocity estimate compared to the other methods velocity estimate.

9.5. Discussion

In this chapter, we demonstrated a real-time algorithm to estimate spatiotemporal gait metrics using two IMUs mounted on the shoes. We combined a strap-down double integration algorithm with a newly developed zero velocity update (ZUPT) algorithm to robustly estimate gait metric estimates based on the foot position trajectory reconstructed on a stride-by-stride basis. Our ZUPT algorithm is different from previously presented algorithm since it utilizes IMU data from the contralateral foot (i.e. toe off event) for ZUPT and does not utilize thresholds. Because our algorithm leverages the robust gait event detection algorithm validated in post-stroke overground walking (Chapter 8), it robustly executes ZUPT every stride in highly variable post-stroke overground walking. Moreover, it does not require any parameter tuning specific to different individuals or walking conditions.

To quantify the performance of our algorithm we conducted a three-stage validation analysis in healthy and stroke individuals. The analysis demonstrated that the maximum RMSE for walking speed estimation in healthy treadmill walking (<7%) is comparable to what is reported in literature [256], [264]. Additionally, the regression analyses demonstrated strong linear correlations between estimated and treadmill walking speeds (r^2>0.98) with slopes of the regression lines being close to the identity line (i.e. perfect estimation). Interestingly, under more irregular post-stroke overground walking conditions, the estimation of stride length and stride speed showed maximum RMSEs up to 8%, showing significant differences between paretic (Max RMSE=4%) and nonparetic side (Max RMSE=8%). However, similar to the regression analysis from healthy treadmill walking, strong linear correlation between estimated and actual metrics were found in post-stroke overground walking.

The strong linear correlations between estimation and actual metrics as well as regression line slopes close to the identity line indicate that the algorithm accurately captured relative changes in the respective metrics. This is particularly critical for clinical assessment since changes in gait metrics are of the main interest from clinical perspective. Further, [267] reported Minimal Detectable Changes (MDCs) in step length for

individuals after incomplete spinal cord injury with 36% for the more impaired limb and 24% for the less impaired limb. These MDCs suggest that the observed errors of our method were significantly below the required resolution. Further, regarding the validation of walking speed in stroke, our gait metric estimation algorithm demonstrated errors significantly lower than the Minimal Clinically Important Difference for speed (MCID) which is reported at 0.16m/s [268].

Regarding the benchmark analysis with three other methods, our method demonstrated better performance for some metrics in certain conditions, while demonstrated worse performance in other cases. For instance, our method performed significantly better or equally good compared to other methods on the paretic side (except max. vert. distance FWS), while it performed significantly worse on the nonparetic side for stride length and circumduction during post-stroke treadmill walking. Interestingly, all the compared methods demonstrated worse performance for the nonparetic side, indicating that there could have been a difference in the IMU provided raw signals as the same estimation algorithm was implemented for both sides. The performance discrepancy between sides could be also caused by the different gait speeds. However, the actual cause is still unknown, therefore further research is warranted (see Section 12.1.2 for further details). For overground walking our method performed in very similar accuracy ranges as seen in the treadmill experiment, while the other methods showed significant improvements on both sides compared to their performance in the treadmill experiment. The reason that the general estimation accuracy declines for the nonparetic side can be explained by bias differences for the two IMUs. As observed in **Figure 9.15**, the nonparetic side demonstrated higher bias instabilities in acceleration measurements leading to nonlinear drift errors in velocity estimation. This might be caused by that our approximation of drift as a linear function was not be sufficient to compensate the nonlinear drift errors. Indeed, we compared polynomial functions with different orders for drift compensation in terms of estimation errors through post-processing, and observed significant reduction in estimation error with higher-order drift function on the non-paretic side (see **Figure 9.16**). The example shown in **Figure 9.4** also corroborates this hypothesis: The example demonstrates the estimated position trajectory in vertical direction for level walking, which allows to not

only observe the velocity error but also the position error. Specifically, the vertical displacement between two foot-flat instances should be zero for level walking but the example shows non-negligible vertical displacement even after compensating linear drift function. As the sample size for the benchmark analysis was small (N=1) for both treadmill and overground experiment, this observation needs to be further investigated with a larger group of post-stroke individuals. In particular it needs to be investigated if this error difference occurs systematically on the non-paretic side and if the non-linearities show a certain degree of repeatability. The reason why other methods performed better than our method for the nonparetic side can be explained by that they executed ZUPT during certain time window rather than doing it instantaneously as in our method. Our follow-up analysis demonstrated the drift error during foot-flat phase generated overestimation errors, and by forcing the velocity to be zero during the designated ZUPT window, these methods reduce the risk of residual drift error when using linear drift compensation.

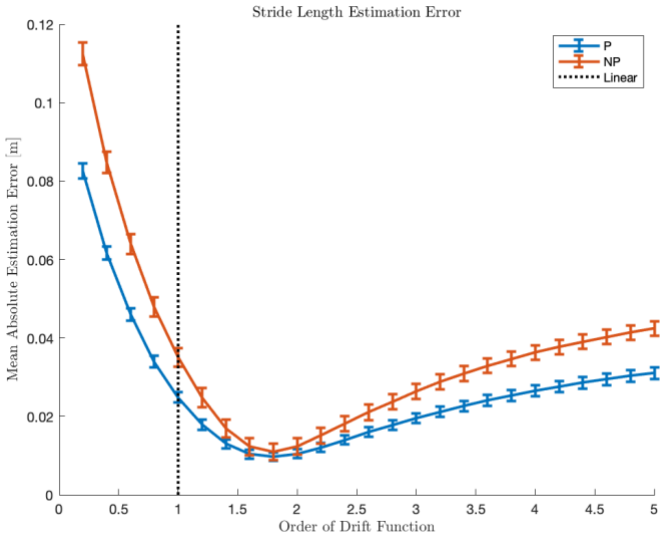

Figure 9.16. Sensitivity analysis on the impact of the order of drift function on stride length estimation error

The other methods that were compared to our method demonstrated a number of ZUPT detection errors that may cause inaccuracies and make their real-time application not feasible. Specifically, detecting ZUPT phase too early or too late could introduce false constraints by setting the velocity to zero. Detecting ZUPT outside of the true foot flat window (false positive) could also impact the accuracy of the algorithm as a ZUPT with false velocity constraints. False negative detection could also impact the accuracy, while it is

not as significant as other error sources. This is because the acceleration measurement was close to zero during foot flat phase, therefore false velocity integration caused by false negative did not significantly affect the accuracy. Lastly, in few cases a ZUPT was missed entirely which allows drift to accumulate uncorrected for this stride and greatly impacts the reconstruction accuracy. This particularly caused high estimation errors for the ARE method on the nonparetic side in overground walking. Based on this comparison analysis, we hypothesize that using a window-based ZUPT might show accuracy improvements for our algorithm.

9.6. Conclusion and future work

In this chapter, we presented a real-time gait metric estimation algorithm that enables online clinical assessment in exosuit assisted post stroke gait training. The algorithm utilizes a robust zero-velocity update method, designed based on exosuit gait detection algorithm. By using contralateral foot information and not relying on ZUPT detection thresholds, the proposed method does not require any subject specific tuning. This also makes it very robust in heterogeneous walking conditions as expected in chronic post-stroke walking conditions, while other methods are highly sensitive to the method specific threshold and parameter configurations [101]. Achieved accuracies were below the reported MDCs and MCIDs, while showing significant differences between paretic and nonparetic side. These differences can be explained by bias stability differences of the IMUs. A potential solution is the use of ZUPT windows instead of instances. In benchmarking our method against other ZUPT methods we saw higher robustness for our method, due to not falsely detecting or missing ZUPT instances. In cases of high bias instabilities our method was less accurate compared to other methods, which can also be attributed to the fact that our method executes ZUPT once per each stride. Furthermore, no other method consistently showed superior performance across metrics and conditions. This study therefore demonstrated that our proposed method has shown to be feasible for the envisioned training scenarios with soft exosuits.

In the future, the significant accuracy difference observed between paretic and non-paretic side needs to be further investigated with a larger group of post-stroke individuals. It is important to understand if the higher estimation errors on the non-paretic side were caused by hardware difference or other sources such as different gait speeds between paretic and non-paretic side. Additionally, higher order drift functions instead of a linear function could improve the estimation accuracy. Even more a predictive method to adaptively estimate the drift function could further improve the estimation accuracy. Lastly, we observed generally improved accuracy with window-based ZUPT executed by the three other methods presented in this chapter compared to our method. Since our method currently execute ZUPT at a single time point each stride, we may be able to improve our method by detecting zero-velocity window instead of moment and compensate errors based on the windows. Potential solutions could be using the contralateral mid-swing event (or modifications of that), or the second zero-crossing of the contralateral sagittal plane angular rate signal. Further discussion on future research area related to this topic can be found in Section 12.1.2.

Chapter 10.

Impact of exosuit intermittent assistance on assisted and unassisted gait patterns in post-stroke overground walking

10.1. Introduction

In the previous chapters, we validated a portable soft exosuit for (1) its immediate biomechanical benefits during post-stroke overground walking (Chapter 7) and (2) the accuracy of real-time spatiotemporal gait metric estimation using onboard sensors (Chapter 9). These promising outcomes demonstrated the potential for exosuit technology to improve post-stroke overground gait training. Another useful aspect of the exosuit for gait training is its capability to deliver intermittent assistance. Unlike most existing rigid exoskeletons, exosuits do not utilize mechanical hinges around human body joints, and therefore are capable of completely eliminating interaction torques by disengaging Bowden cable tension. Moreover, exosuits can instantaneously disengage cable tension by slacking the cable during walking, therefore enabling true intermittent assistance (see **Figure 10.1** for the illustration). We hypothesize that intermittent assistance

could play an important role in facilitating gait training with an exosuit. To be specific, our results show that when individuals post-stroke walk with the exosuit delivering gait assistance (i.e. exosuit in active mode), they may have improved walking (e.g. higher speeds, reduced compensations, less asymmetry). Furthermore, previous studies that investigated the carryover effect of novel environments on post-stroke gait have suggested that gait patterns adapted to a new environment such as a split-belt treadmill, could transfer to natural walking such as overground walking [269], [270]. This suggests a potential for gait patterns improved during exosuit-assisted walking to transfer to post-assistance periods. Moreover, a pilot study using intermittent assistance from Functional Electrical Stimulation (FES) in post-stroke gait training suggested that intermittent assistance using FES could promote motor learning for gait rehabilitation to improve paretic propulsion [271]. Thus, one possible approach to leverage the intermittent assistance is to encourage a wearer to maintain their assisted walking patterns when the exosuit turns inactive (slack) after a period when assistance is delivered, to promote motor learning of gait function without assistance.

Given the aforementioned considerations, our vision is to develop an automatically individualized gait training program using exosuit intermittent assistance and real-time gait metric estimation. Specifically, since motor learning studies have shown that changing motor training schedule can affect training outcomes [272], [273], we envision a new exosuit software paradigm that automatically adapts intermittent assistance scheduling based on real-time gait metric estimation, such as comfortable gait speeds without exosuit assistance, and their changes in response to exosuit assistance. One hypothetical example of intermittent assistance scheduling strategy to train for gait speed increases is as follows: exosuit-assisted gait training begins with the exosuit in inactive mode (i.e. unassisted walking). The exosuit measures gait speeds, and after steady-state is reached, the exosuit turns active to deliver gait assistance while measuring positive changes in gait speeds. Once the speed has stayed in steady-state for certain duration, the suit turns back to inactive mode and monitors if the change in speed is maintained. If the speed diminishes, the suit returns to active mode and repeats the previous steps. As such, this strategy could promote gait training both in exosuit assisted and unassisted walking to improve gait speed. It should be noted that this strategy is not

limited to train for gait speeds but could be also used to promote improvement in other gait variables (Further discussion on this topic can be found in Section 12.1.5).

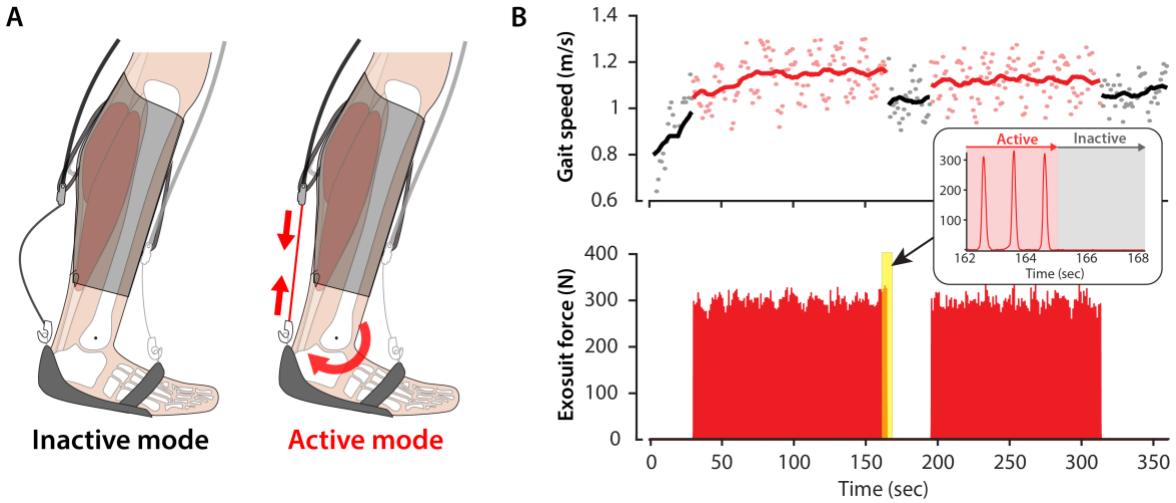

Figure 10.1. Illustration of intermittent assistance and sample exosuit data collected from overground walking with exosuit intermittent assistance. (a) exosuit can deliver intermittent assistance by changing between active and inactive modes. (b) Sample data of gait speed and exosuit PF force collected during walking with intermittent assistance.

As a first step towards this goal, this chapter evaluates the impact of exosuit intermittent assistance on post-stroke overground walking using online exosuit gait metric estimation. Specifically, we conducted a series of case studies with three post-stroke individuals to demonstrate a proof-of-concept overground walking session using intermittent assistance and gait metric estimation. The studies were conducted to answer the following questions:

- If exosuit assistance can generate an immediate benefit to post-stroke walking that can be detected during a bout of intermittent assistance through online exosuit gait metric estimation.
- Given that the immediate benefit exists, if the intermittent assistance approach can enable short-term carryover of exosuit-induced gait improvement in post-assistance period, and the carryover can be detected through online exosuit gait metric estimation.
- If varying intermittent assistance scheduling alters the carryover effect.

To answer these questions, we collected gait speed, paretic circumduction, and temporal symmetry as estimated by the exosuit during the case studies. This study will be an important step toward developing a new post-stroke gait training strategy using a soft exosuit.

10.2. Methods

10.2.1. Intermittent assistance implementation

To systematically investigate intermittent assistance, we developed custom software to (1) establish real-time communication with the exosuit over Bluetooth, (2) command active and inactive modes to the exosuit automatically using pre-programmed timings during continuous walking, and (3) run a graphical user interface (GUI) to facilitate data collection and online data labeling during the experiments. Specifically, the software exports the exosuit-generated data such as the gait metric estimates (see Chapter 9 for further details) and sensor measurements over Bluetooth in 100Hz. It also executes a timer to automatically change the system modes using pre-programmed timings: When the software commands active mode, the exosuit delivers ankle assistance using the controller algorithm presented in Chapter 6. When it commands inactive mode, the Bowden cables become completely slack and no ankle torque is generated from the exosuit. The transitions from inactive to active are made smoothly by the gradual increase in the target force level across the first three strides following the transition.

10.2.2. Experimental design

Three post-stroke survivors in the chronic phase of recovery were recruited for this pilot study (see **Table 10.1** for participant characteristics). Two pilot participants (P1 and P2) were recruited to investigate the impact of exosuit intermittent assistance on post-stroke gait speed. These participants were selected from different groups of community ambulatory levels based on the post-stroke activity classification method described in [204], to represent the range of post-stroke gait impairments. Specifically, P1 was selected from the limited community ambulatory group (i.e. comfortable walking speed between 0.49m/s and 0.93m/s), and P2 was from the household ambulatory group (i.e. comfortable walking speed lower than

0.49m/s). The third participant (P3) was recruited to investigate the impact of intermittent assistance on compensatory gait patterns and gait asymmetry. This participant was a limited community ambulator and presented significant paretic circumduction and gait asymmetry in our previous study discussed in Chapter 7.

Table 10.1. Participant stroke and gait characteristics

	Paretic side	Sex	Age (y)	Chronicity (y)	Type of stroke	Weight (kg)	Height (m)	Daily AD	MAS	CWS (m/s)	Ambulatory level
P1	L	M	44	9.0	Ischemic	99	1.81	Cane, hAFO	1	0.70	Limited community
P2	R	F	55	9.0	Hemorrhagic	114	1.65	Cane, AFO	2	0.43	Household
P3	R	M	54	2.4	Hemorrhagic	81	1.76	None	0	0.53	Household

MAS: Modified Ashworth scale describing muscle tone in plantar flexor muscles on the paretic side (score range= 0-4); CWS is comfortable walking speed; AD is assistive device; hAFO is hinged AFO.

Each participant completed a single-day experimental session. At the beginning of each session, the participant walked on an indoor track illustrated in **Figure 7.1** for 2 minutes without wearing the exosuit and another 2 minutes during which the exosuit alternated between active and inactive modes every 30 seconds to get warmed up and familiarized with the testing environment. Next, the participant completed three 8-minute overground walking bouts with different exosuit assistance conditions in the following chronological order (see **Figure 10.2**).

- Slack (SLK): walking with inactive (slack) exosuit
- Intermittent assistance 1 (INT1): walking with the exosuit delivering two cycles of intermittent assistance of 2-minute active assistance followed by 1.5-minutes in inactive mode.
- Intermittent assistance 2 (INT2): walking with the active exosuit delivering two cycles of intermittent assistance of 1-minute active assistance followed by 2.5-minutes in inactive mode.

Note that both INT1 and INT2 conditions started with inactive mode for 1 minute. Before each condition, the experimenter gave verbal instructions to walk as fast as possible, safely, to promote high-intensity gait training. For safety, a licensed physical therapist (PT) walked with the patient and an overhead harness was

connected to the patient for the entire walking bout. Moreover, the PT gave a verbal warning three seconds before the transition of assistance mode (i.e. from suit inactive to active or vice versa). A 10-minute seated break was given to participants before each bout to minimize the effect of fatigue.

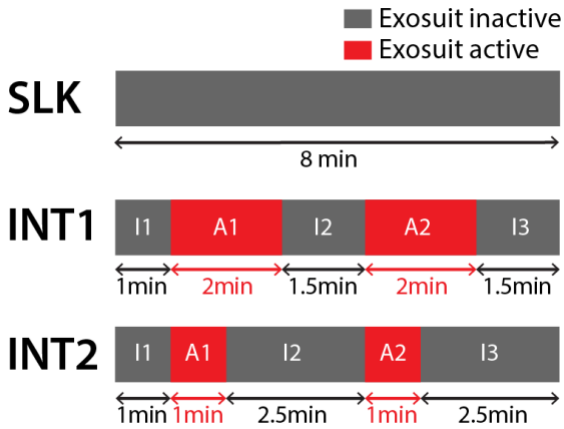

Figure 10.2. Illustration of experimental conditions. 8-minute overground walking bouts in three different conditions were tested and compared with three post-stroke individuals. The first condition was walking with exosuit in inactive (i.e. cable slack) mode (SLK), and the second and third conditions (INT1 and INT2) were walking with exosuit delivering intermittent assistance. Note that INT1 and INT2 have different time durations for intermittent active assistance (A1 and A2) and the following durations of inactive mode (I2 and I3).

10.2.3. Data collection

A real-time gait metric estimation algorithm using two IMUs, one mounted on each shoe, was implemented in the exosuit used in this study. Our previous study validated that the estimation algorithm accurately calculates changes in gait metrics to within 5% error during post-stroke walking (see Chapter 9 for more details). Using the gait metric estimation algorithm, gait speed, paretic limb circumduction, paretic foot clearance, and step-time symmetry were collected during the experiment (see **Table 10.2** for definitions).

Table 10.2. Gait metrics for the validation of intermittent assistance

Gait metric	Unit	Definition
Gait speed (V)	m/s	Displacement of the foot between two successive ipsilateral foot strikes divided by stride time.
Paretic limb circumduction (PC)	m	The largest lateral displacement of the paretic foot during swing from the ipsilateral foot position during stance.
Paretic limb foot clearance (PFC)	m	The highest vertical position of the exosuit-integrated IMU attached on the paretic foot during the swing phase.

Step-time symmetry index (SI_{step})	%	Step time is the time elapsed from ipsilateral foot-strike to the following contralateral foot-strike. The inter-limb symmetry of step time was calculated using the symmetry index expression in (10.1).

Symmetry index for step-time symmetry measurement is defined as

$$SI = \left| \frac{(T_{np} - T_p)}{0.5 \cdot (T_{np} + T_p)} \right| \cdot 100\ (\%) \tag{10.1}$$

where T_{np} and T_p are the nonparetic and paretic step times (unit: %; Note that 0% SI signifies perfect symmetry). To differentiate data from straight and curved walkways on the track (see **Figure 7.1** for the design of the track), an experimenter manually indicated when participants walked on the straightaways during the experiments using the GUI.

10.2.4. Data analysis

The gait metric data only from the straight portion of the track were used for data analysis to minimize the effect of environmental changes (i.e. walking on a curve). To understand the impact of the intermittent assistance on individual gait patterns, we ran multiple statistical comparison analyses on the gait metric data from each individual separately. Specifically, the following analyses were conducted on individual participants' data: First, to investigate if exosuit in active mode influenced participants' gait during intermittent assistance conditions (immediate assistive effect), data collected from the active suit (d_{act}) were compared to data from the inactive suit (d_{inact}) within the same intermittent assistance condition (i.e. INT1 or INT2) through paired t-tests. Second, to investigate if the immediate assistive effect of exosuit changed from INT1 to INT2, d_{act} of INT1 and INT2 were compared through paired t-tests. Changes in the immediate effect within INT1 or INT2 were also investigated through the comparison of d_{act} from two different time segments of the same bout (A1 and A2 in **Figure 10.2**). Third, to investigate if intermittent assistance affected participants' unassisted gait (i.e. walking in inactive mode) (carryover effect), d_{inact} in different conditions (SLK, INT1, and INT2) were compared through one-way ANOVA. When null hypotheses were rejected from ANOVA, Tukey's HSD tests for post-hoc multiple comparison were subsequently conducted.

Finally, to investigate if unassisted gait patterns changed within INT1 or INT2 bouts (within-bout changes), d_{inact} of three time segments in inactive mode (I1, I2, and I3 in **Figure 10.2**) within the same condition were compared through one-way ANOVA. Similar to the previous analysis, Tukey tests for post-hoc pairwise comparison were conducted when null hypotheses were rejected from ANOVA. For all statistical analysis, the significance level was set to p=0.05.

10.3. Results and discussion

10.3.1. Changes in gait speed

Changes in gait speed were evaluated with two participants: One participant was a limited community ambulator (P1), and the other participant was a household ambulator (P2).

Changes from limited community ambulator (P1)

Immediate assistive effect on the gait speed was observed: average gait speed in active mode (V_{act}) was higher than the speed in inactive mode (V_{inact}) for both INT1 (+0.04m/s; p<0.0001) and INT2 (+0.04m/s; p=0.0103) (see **Error! Reference source not found.**). Further, changes in the immediate effect were observed within and across bouts: V_{act} was higher in INT2 than INT1 (+0.02m/s, p=0.018). V_{act} also increased from A1 and A2 within INT1 (i.e. A1<A2, p<0.0001).

Regarding carryover effect, changes in unassisted gait speed V_{inact} in INT1 and INT2 were observed: V_{inact} increased in INT1 and INT2 compared to SLK (INT1: +0.06m/s; INT2: +0.09m/s; p<0.0001 for both). More interestingly, systematic increases of carryover effect following more exposure to the intermittent assistance bouts were observed: We found gradual within-bout increase in V_{inact} during INT1 (i.e. I1<I2<I3; p<0.0001) and increase from I1 to I2 (p<0.0001) in INT2.

These results suggest that immediate improvements could be generated even when exosuit assistance was delivered intermittently, and there could exist a short-term carryover of exosuit-induced gait improvement in post-assistance period (see Section 10.4 for further discussion).

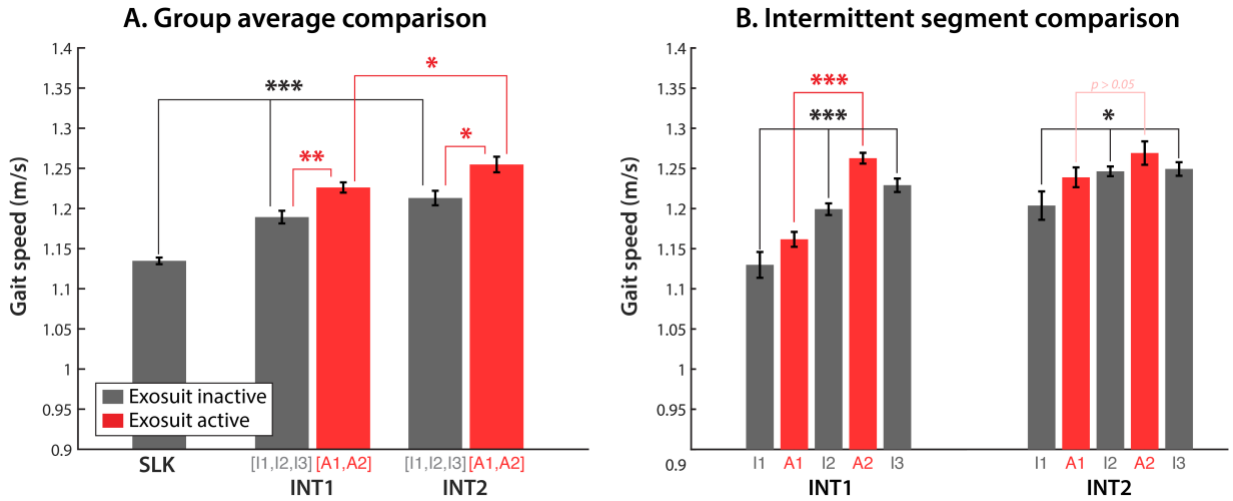

Figure 10.3. Gait speed changes induced by exosuit intermittent assistance in a limited community ambulator. (a) Average gait speeds in active (Vact) and inactive modes (Vinact) from different conditions and their standard errors of the mean (SEM) are presented. Moreover, analytical results from (1) One-way ANOVA of the data from inactive mode in different conditions, (2) t-tests of the data from inactive and active modes in the same condition, and (3) t-test of the data from active mode in different conditions are also presented. (b) Average data in different time segments from INT1 and INT2 and their SEM are presented. Moreover, the analytical results from One-way ANOVA of the data from time segments with inactive mode (I1-I3), and t-test of the data from time segments with active mode (A1-A2) are presented. Post-hoc pairwise comparisons were followed after ANOVA, but the results are not presented in these plots for simplicity (See main text for the post-hoc analysis).
*: p<0.05; **: p<0.001, ***: p<0.0001

Changes from household ambulator (P2)

Similar to P1, an immediate assistive effect of intermittent assistance on gait speed was observed: V_{act} was higher than V_{inact} in both INT1 (+0.05m/s, p<0.0001) and INT2 (+0.03m/s, p=0.0103) (see **Figure 10.4**). However, within- and across-bout changes of the immediate effect were not as significant as in P1: V_{act} did not change from INT1 to INT2, and it also did not change within INT2. The only significant change in the immediate effect was a decrease in V_{act} within INT1, from A1 to A2 (-0.03m/s, p=0.0004).

Changes in walking speed in inactive suit were found, but not in the same manner as P1 who showed a carryover effect: V_{inact} decreased in INT1 compared to SLK (-0.03m/s, p=0.0001), while SLK and INT2 were not statistically different. The within-bout changes in the walking speed were also different from P1: In INT1, V_{inact} decreased in I2 and I3 from in I1 (p=0.0092), with no difference between I2 and I3. In INT2, contrarily, V_{inact} increased in I2 compared to I1 and I3 (p<0.0001), with no difference between I1 and I3.

These results, in combination with the results from P1, may imply that the immediate assistive effect and could be generated across post-stroke individuals with different gait impairment levels. In contrast, the data suggest short-term carryover of exosuit-induced improvement may not be always generated, and the generation of carryover might be dependent on individual gait impairment level. (see Section 10.4 for further discussion).

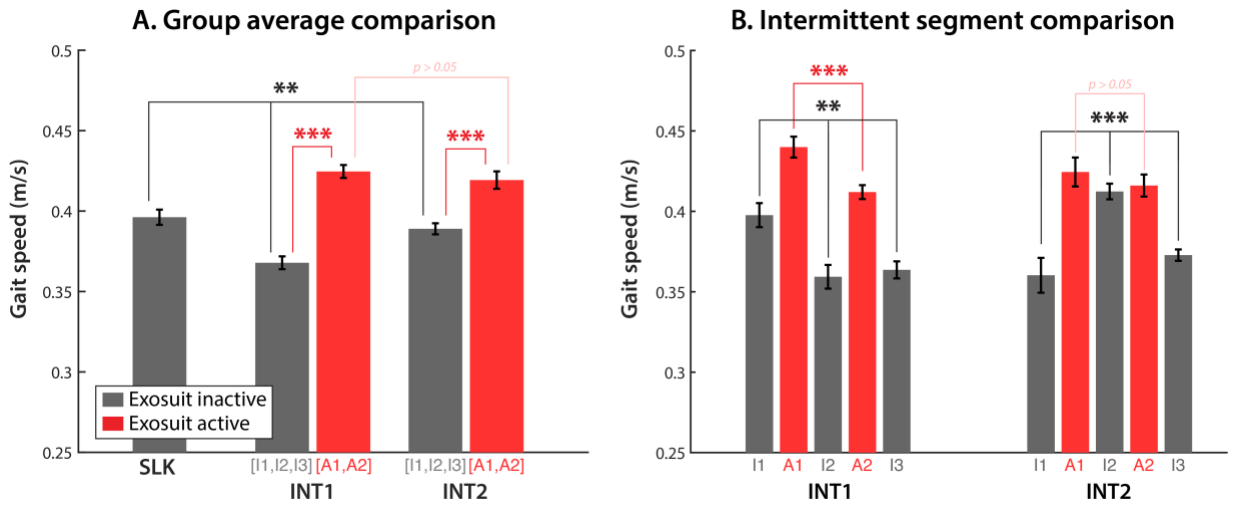

Figure 10.4. Gait speed changes induced by exosuit intermittent assistance in a household ambulator. (a) Average gait speeds in active (Vact) and inactive modes (Vinact) from different conditions and their SEM are presented. Statistical analysis results are also presented as in fig. 3a. (b) Average data in active (A1, A2) and inactive (I1-I3) time segments from INT1 and INT2 and their SEM are presented. Statistical analysis results are also presented similarly as **Figure 10.3**.
*: p<0.05; **: p<0.001, ***: p<0.0001

10.3.2. Changes in paretic limb circumduction and temporal symmetry (P3)

Data from P3 were analyzed to investigate the changes in paretic circumduction (PC), paretic foot clearance (PFC), and step time symmetry index (SI) (see **Figure 10.5** and **Figure 10.6**).

Paretic limb circumduction and foot clearance

Immediate effect of exosuit assistance on paretic circumduction (PC) was observed: PC reduced in active mode (PC_{act}) compared to inactive mode (PC_{inact}) in both INT1 and INT2 (-2cm, p<0.0001 for both). Interestingly, we also observed complementary increases of paretic foot clearance when the suit was active (PFC_{act}) in both conditions (INT1: +2cm, p<0.0001; INT2: +2cm, p<0.0001) (see **Figure 10.5**). The

immediate reductions in circumduction increased within intermittent assistance bouts, while no changes in foot clearance increases were observed: PC_{act} in A2 was lower than in A1 both in INT1 (-1cm, p=0.0015) and INT2 (-2cm, p=0.0039). No changes in the immediate effects were observed between INT1 and INT2 in PFC_{act} and PC_{act}.

Carryover effects of paretic circumduction in inactive exosuit were found: PC_{inact} in INT2 reduced from SLK and INT1 (-1cm, p=0.0009). Also, PC_{inact} in I1 was higher than in I3 in both INT1 (-2cm, p=0.026) and INT2 (-1cm, p=0.022). However, carryover effect was not found in foot clearance except a within-bout increase from I1 to I2 in INT1 (+1cm, p=0.036).

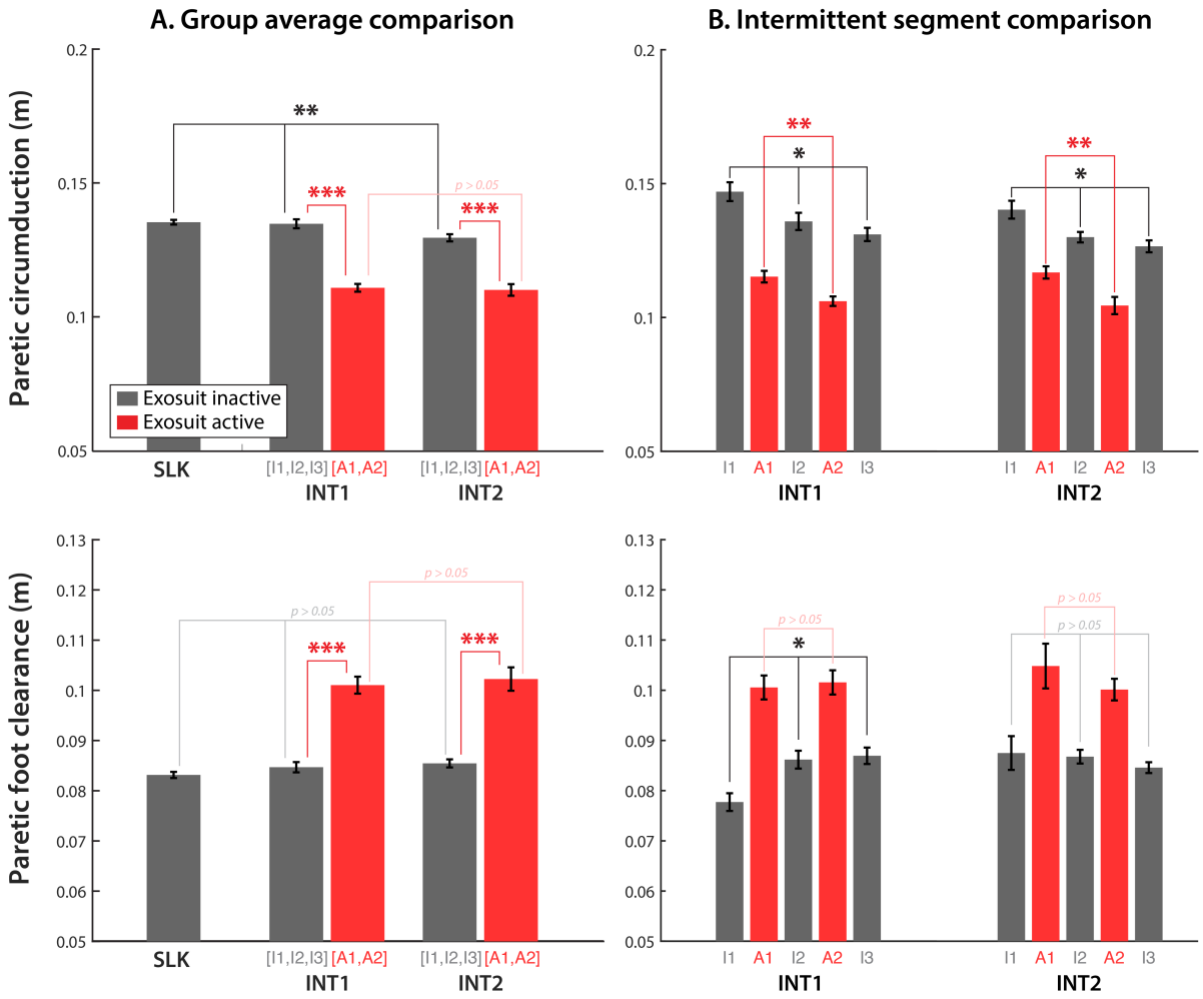

Figure 10.5. Changes in paretic circumduction and foot clearance induced by intermittent assistance. The top row presents paretic circumduction (PC) and the bottom row presents paretic foot clearance (PFC). Similar statistical analysis results as in **Figure 10.3** are also presented.

*: p<0.05; **: p<0.001, ***: p<0.0001

Temporal gait symmetry

Significant immediate impact of active exosuit on step-time asymmetry was observed in INT1 and INT2: step-time symmetry index in active mode (SI_{act}) significantly reduced from inactive mode (SI_{inact}) both in INT1 (-39.3%, p<0.0001), and INT2 (-42.0%, p<0.0001) (see **Figure 10.6**). However, the step-time asymmetry in active suit increased in INT1 and INT2 compared to SLK (INT1: 7%, INT2:12%, p=0.0006). Further, no within-bout change in SI_{act} was observed from the asymmetry during active suit modes, neither in INT1 nor in INT2.

Across-bout negative changes in the step-time asymmetry were found when the suit was inactive during INT2: SI_{inact} increased in INT2 compared to SLK and INT1 (p=0.0001). No within-bout changes in SI_{inact} were found in INT1 and INT2.

These results provide evidence that the immediate assistance effect and carryover effect during intermittent assistance could exist in not only walking speeds, but also other gait variables. Moreover, the data suggest that different gait variables could be affected by exosuit intermittent assistance differently, (e.g. one variable shows positive changes while the other shows negative changes), therefore intermittent assistance should be carefully implemented in clinical practice . (see Section 10.4 for further discussion).

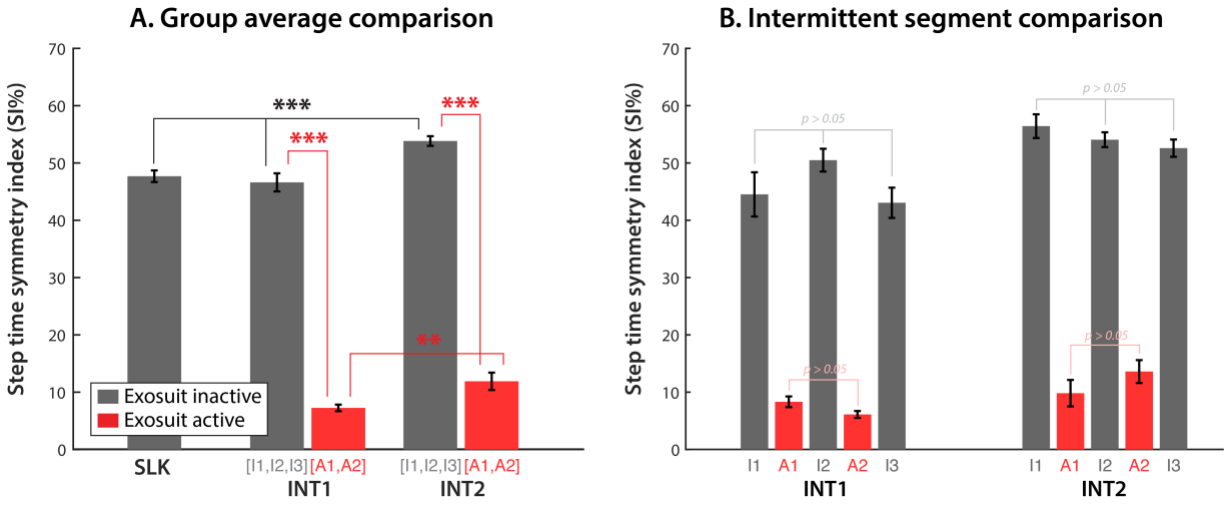

Figure 10.6. Changes in step time symmetry index induced by intermittent assistance. (a) Step time symmetry index in active (SI_{act}) and inactive modes (SI_{inact}) from different conditions and their SEM are presented. Statistical analysis results are also presented similarly to fig. 3a. (b) Average data in active (A1, A2) and inactive (I1-I3) time segments from INT1 and INT2 and their SEM. Statistical analysis results similar to fig. 3b are also presented.
*: $p<0.05$; **: $p<0.001$, ***: $p<0.0001$

10.4. Discussion

This chapter presents a case-series study to investigate the impact of intermittent ankle assistance provided by the exosuit on post-stroke overground walking. The study first demonstrated an immediate assistive effect of exosuit intermittent assistance on post-stroke walking. It also demonstrated that the immediate effect could vary within and across walking bouts. Even more, we found that in some cases, the gait changes induced by the active exosuit could be carried over through post-assistance periods to allow post-stroke individuals to walk in gait patterns similar to exosuit-assisted walking with their own effort. Interestingly, the study outcomes suggest that intermittent assistance scheduling could affect carryover effects, but further study is required.

Immediate assistive effect

Our previous study in Chapter 7 demonstrated that continuous exosuit assistance applied in post-stroke overground walking could improve gait speed and reduce gait circumduction, as measured through lab-based biomechanics measurement equipment. This study extended the previous study by demonstrating that these immediate improvements could be preserved when assistance was applied intermittently using online gait metric estimation. Specifically, immediate increases in gait speeds with intermittent assistance were observed in both a limited community ambulator (P1) and a household ambulator (P2). Additionally, we found that a post-stroke individual with pronounced paretic limb circumduction (P3) reduced the circumduction while increasing paretic limb foot clearance with intermittent assistance. This individual also demonstrated significant reduction in step-time asymmetry with intermittent assistance.

More interestingly, this study suggests that the immediate benefit of active exosuit could change by providing assistance intermittently. We observed changes in gait speed or paretic circumduction with the active suit across and within walking bouts. Specifically, gait speeds in the active exosuit for P1 increased

from INT1 to INT2, and within INT2 from A1 to A2. Similarly, the reduction in paretic circumduction for P3 improved within bout in INT1. These observations suggest that post-stroke individuals could leverage exosuit assistance to improve their assisted gait more by training with intermittent assistance. However, the changes in the exosuit's immediate effects could be influenced by many other factors such as the subject's familiarization to exosuit assistance and experimental environments. Therefore, further study with a larger sample size and randomized conditions is warranted to generate better understanding on this topic.

Carryover effect

We also found that some post-stroke participants could additionally change their unassisted walking (i.e. walking in inactive exosuit) with intermittent assistance: P1 increased gait speed during the inactive exosuit mode when walking with intermittent assistance from walking without assistance (i.e. SLK < INT1 & INT2, see **Figure 10.3**(a)). The participant also increased gait speed across inactive segments within one bout of intermittent assistance (i.e. I1 < I2 < I3 in INT1) (**Figure 10.3**(b)). A positive carryover effect was also found in paretic circumduction. P3 reduced paretic circumduction during the inactive exosuit modes when walking with intermittent assistance (INT1 and INT2) compared to walking without assistance (SLK). Further this participant also gradually reduced circumduction in inactive suit from I1 to I3 within INT2 (**Figure 10.5**).

However, we also found that there could be negative changes in unassisted walking after intermittent assistance was delivered in some of participants. P2 reduced unassisted gait speed in one of the conditions with intermittent assistance (INT1) (**Figure 10.4**). In this condition, the participant started with the gait speed similar to SLK condition, and significantly reduced gait speed after first and second intermittent assistance. More interestingly, P3 who demonstrated positive carryover effect in paretic circumduction demonstrated negative changes in temporal gait symmetry with inactive suit: the participant increased temporal gait asymmetry during the inactive segments in INT2 compared to SLK.

The aforementioned outcomes highlight the importance of targeting the right individuals and outcomes to generate positive carryover effects from intermittent assistance. First, given the difference in carryover effects between P1 and P2 (increase in gait speed for P1 and decrease for P2), we hypothesize that carryover effect could vary depending on individual neurological impairment levels. Indeed, P1 was a limited community ambulator whose comfortable walking speed was 0.7m/s but whose fast walking speed was as high as 1.1m/s. This may indicate that P1 preserved the physical ability to walk faster, but his gait patterns and strategies, or even fear of falling down, limited his gait speed to under full community ambulation level. By training with intermittent assistance and learning to walk similar to exosuit-assisted walking, we hypothesize P1 could improve his gait speed more than conventional gait training. In contrast, P2 was a household ambulator whose comfortable and fast walking speeds were similarly around 0.4m/s. This participant did increase gait speed when assisted by active exosuit, but reduced the speed in post-assistance period. The reduced speed in post-assistance period could be caused by fatigue, but it might be also because this participant did not preserve physical capacity to replicate the speed change when exosuit assistance was turned off, but rather experienced motor de-adaptation similar to changes in gait symmetry found in a previous study on motor learning with split-belt treadmills [274]: This study demonstrated that healthy individuals initially walked asymmetrically on a split belt treadmill (i.e. step length was not symmetric between different sides of limbs) but recovered symmetry soon after as they adapted to the new environment (adaptation effect). Interestingly, when they walked again on a tied-belt treadmill after the adaptation, their walking was initially asymmetric, and slowly became symmetric again (de-adaptation effect). Our observation of increase of gait speed in exosuit-assisted walking and reduction in post-assistance period is similar to the previous observation in split-belt treadmill study, and therefore might be related to motor adaptation/de-adaptation. Additionally, there might be a cognitive factor that contributed to the reduced speed. Our preliminary study to validate the safety of intermittent assistance before conducting the presented case-series study showed that if the transition of assistance between active and inactive was abrupt without any cues, the exosuit wearer might limit their walking speed for the entire walking bout because of the destabilization that the transition might cause. To address this, we implemented three-second

warnings before the transition in this case study series (see Section 10.2.1 for the details), but there still might be possibility that participants reduced their walking speed with the warning. Another contributing factor to this result may be the lack of experience with intermittent assistance, and with more training with intermittent assistance, P2 may be able to increase unassisted gait speed. Indeed, P2 recovered unassisted gait speed similar to the speed in SLK during INT2. This participant started INT2 with reduced gait speed similar to the last unassisted walking speed from INT1 (i.e. I3 in INT1 was similar to I1 in INT2), but increased speed in I2. This may suggest that the participant could create positive carryover effect in gait speed with more experience in walking with intermittent assistance.

The other interesting finding was that for a given individual, intermittent assistance could generate both positive and negative carryover effects across different gait characteristics. For instance, P3 demonstrated reduced paretic foot circumduction and increased foot clearance through the post-assistance period, a potentially desirable carryover effect towards more normal gait patterns. However, the participant simultaneously demonstrated increased temporal asymmetry, a negative effect that makes walking less symmetric and more inefficient. This may suggest that the participant introduced a new temporal compensatory pattern to increase time spent on nonparetic limb to enable reduced paretic circumduction. These outcomes highlight the importance of targeting the right outcomes to train improved gait patterns that result in desirable carryover effects induced by intermittent assistance. Still, it is unclear what allows post-stroke individuals to benefit from a positive carryover effect, and in which gait metrics. Further biomechanics studies on intermittent assistance is therefore warranted to better understand the carryover effect and its use in post-stroke training.

Additionally, although walking bouts with different intermittent scheduling (INT1 and INT2) generated different carryover effects in some of the trials (e.g. P1 and P2 on gait speed), these outcomes varied across participants and gait metrics, limiting our understanding of the impact of scheduling on the carryover effect. Thus, further study of intermittent assistance scheduling with a larger group of post-stroke participants is also needed.

Sensitivity of gait metric estimation in detecting biomechanical impact of intermittent assistance

Finally, this study demonstrated that the spatiotemporal gait metric estimation implemented in exosuit was sensitive enough to detect the impact of intermittent assistance. Our previous study in Chapter 9 validated the accuracy of the gait metric estimation in post-stroke overground walking (within 5% error). However, it was not validated if this accuracy was enough to detect biomechanical changes induced by exosuit intermittent assistance. This study demonstrated the gait metric estimation could be used to investigate the immediate gait improvement induced by the active exosuit, and carryover of the gait improvement through the post-assistance period. These outcomes highlight an exciting opportunity to utilize exosuit intermittent assistance in gait training outside a constrained lab environment, and still provide quantitative data to monitor training progress. This study is thus an important first step towards home-based rehabilitation with exosuit intermittent assistance and gait metric estimation.

10.5. Conclusion and future work

In conclusion, this case-series study explored the impact of intermittent assistance on post-stroke individuals' gait patterns when the exosuit was active and when the exosuit was inactive. It suggests that the intermittent assistance could promote unassisted walking in gait patterns and speeds similar to exosuit-assisted walking within a single session, which has not yet been shown with other exoskeletons. We believe that this has a great implication for post-stroke gait training that facilitates training faster gait speeds with improved gait patterns using exosuit intermittent assistance. Further, this study suggests that gait training with intermittent assistance should be carefully used with the right gait characteristics and target outcomes to be most effective. Finally, it demonstrated potential for the exosuit to be a stand-alone device that enables enhanced gait training with intermittent assistance and monitors gait training progress with online gait metric estimation.

Although interesting, the outcomes related to the carryover effect from this study varied across individuals and gait metrics, thereby limiting our understanding on how to generate a positive carryover effect for

different individuals and gait aspects. Moreover, it is not clear if the observed changes in gait metrics during post-assistance periods were purely caused by carryover effects or contributed by other factors such as warm-up effects or fatigue [273]. Moreover, this study was a single-session study which did not investigate long-term retention of the changes in unassisted gait induced by intermittent assistance, an ultimate goal of post-stroke gait training. Further study with a larger sample and full randomization of conditions is therefore required to fully understand how to improve the positive carryover effect by controlling the intermittent assistance schedule and targeting the right outcomes. Longitudinal studies on post-stroke gait training with intermittent assistance are also warranted to investigate long-term retention. Still, our findings from this case-series study suggest the potential of exosuit intermittent assistance in post-stroke training and the importance of individualizing exosuit-assisted gait training programs with different intermittent assistance schedules and target outcomes, and is therefore an important first step toward effective exosuit-assisted gait training.

Chapter 11.

Proof-of-concept pilot study on gait training with portable exosuit

11.1. Introduction

Thus far, we validated the immediate biomechanical and physiological benefits of continuous assistance (Chapter 7) and intermittent assistance (Chapter 10) delivered by exosuits during post-stroke overground walking. Although these previous studies provide indirect evidences that exosuit could be utilized to improve post-stroke overground gait training, they did not evaluate the therapeutic effect of exosuit-assisted gait training (i.e. changes in walking without exosuit assistance from pre-training to post-training), the ultimate goal of post-stroke gait rehabilitation.

Improving gait speed is often the main focus of post-stroke gait training, because gait speed has the ability to determine prognosis of level of mobility function following stroke [275]; however, gait speed alone does not always signify the recovery of the paretic limb, as gait compensations may drive increased gait speeds [276]. This is manifested through increased dependence on non-paretic leg or assistive devices, or through

compensatory movement patterns such as paretic hip hiking and circumduction [12], [158]. In the repair of impaired central nervous system, there is increased recognition of the importance of interventions that are designed to harness neuromotor restitution over compensation [277], [278].

In designing interventions that seek to facilitate restitution, it is important to target specific mechanisms that mediate gait speed dysfunction. Reduced paretic propulsion has been shown to be an important determinant of reduced gait speeds [112], [128], [276]. Further, decreased paretic propulsion has been shown to be related to severity of stroke, gait asymmetry, and walking speed [23]. Current literature suggests that targeted interventions that seek to restore specific deficits such as propulsion may render more meaningful outcomes in stroke rehabilitation [113], [276].

Gait training through physical therapy is one of the mainstays of post-stroke management. This is largely achieved through overground and treadmill gait training, where a physical therapist assesses, cues, or assists the person while walking. While well-integrated in current stroke care, gait training has its challenges. There is limited evidence at best with small benefits in support of overground walking on gait speed and the 6-Minute walking distance [279]. To overcome these challenges, the modern locomotor rehabilitation framework based on motor-learning theories (see Chapter 1 for further details) suggest that these modest responses to traditional gait rehabilitation may be enhanced by interventions that focus more on training intensity [278], targeting specific deficits of paretic ankle [276], and through overground gait training among other strategies.

The use of rehabilitation robotics, when engineered and utilized based on a current understanding of motor learning and brain plasticity, carry great potential in enabling motor recovery post-stroke. While promising, the evidence from clinical trials using robotics over the past two decades [62] is uncompelling, resulting in an unfavorable recommendation from current physical therapy guidelines to not use robotics for gait training in chronic stroke [62]. Notably, the guidelines were generated based on clinical trials that largely

utilized treadmill-based exoskeletons described in Section 1.1.3 that provided substantial assistance to patients who are able to ambulate even without device.

We hypothesize that a portable exosuit could enhance motor restitution during post-stroke gait training through the aforementioned positive impact of exosuit continuous and intermittent assistance on post-stroke overground walking. Therefore, to investigate the potential of exosuit-assisted gait training, this chapter presents a pilot study on gait training with a portable exosuit. The primary aim of this study was to examine the rehabilitative effects of exosuit-augmented locomotor training on clinical and biomechanical outcomes of gait in chronic stroke. Additionally, we examined whether exosuit-augmented locomotor training has added value relative to conventional training. Finally, as exploratory aim, we examined if the rehabilitative effects from each intervention persist 7 weeks after the completion of the intervention (long-term retention effects).

11.2. Methods

11.2.1. Participant recruitment

One participant in the chronic phase of stroke recovery was recruited from the greater Boston area. The participant was a 58-year old male with chronic (54-month) left-sided hemiparesis, having a Lower-extremity subsection score of 25 out of 34 from the Fugl-Meyer test. Eligibility to participate in study was based on the following inclusion criteria: (1) have chronic stroke of > 6 months; (2) able to follow instructions; (3) able to walk 20 meters with or without assistive devices; and (3) have functional range of motion on key joints of lower extremity. (4), have comfortable walking speed lower than 0.93 m/s, a threshold for full community ambulation as defined in [204]. Participant was excluded if they had severe aphasia or cognitive deficits that limit safe participation, and presence of other neurological, orthopedic, or medical condition that may impact mobility. To establish participant eligibility, a series of pre-evaluation procedures were performed before study participation. For the pre-evaluation, a graded exercise test (GXT) [280] was performed to identify safe physiologic parameters (i.e. cardiac parameters for training that

corresponds to 85% of GXT-assessed heart rate maximum). A clinical screening test was also performed which included the Fugl-Meyer Assessment, the 10-Meter Walk Test (10MWT), 6-Minute Walk Test (6MWT), and the participation subsection of the Stroke Impact Scale to assess quality of life. This study was approved by the Institutional Review Board of Harvard University, and informed consents were obtained prior to participation in study.

11.2.2. Study design

To compare exosuit-assisted gait training with conventional gait training, a crossover comparison study with AB design was conducted as illustrated in **Error! Reference source not found.**. The participant received both an experimental (exosuit-assisted training) and a control arm (conventional training) of intervention with a 7-week washout period in between. The exosuit-assisted gait training utilized a portable exosuit described in Chapter 6 for all walking conditions. Evaluation time points included pre-training, post-training, and retention following 7 weeks of washout. The sequence of interventions was randomly chosen to start with exosuit-assisted training and then provide conventional training. It should be noted that the follow-up study to test with larger number of patients will continue to use the randomly chosen sequence for each patient.

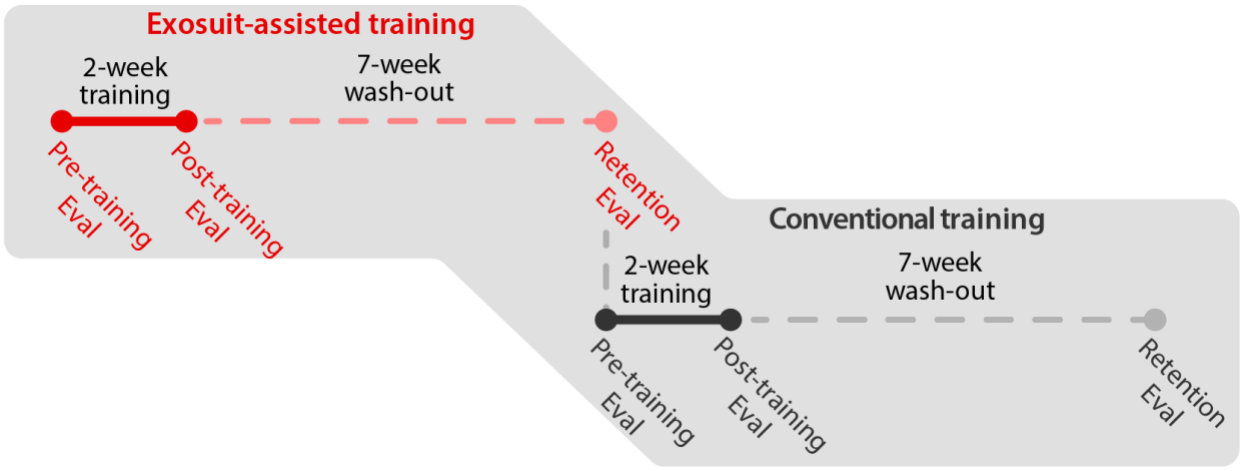

Figure 11.1. Schematic diagram of training study design. A participant was given both exosuit-assisted training and conventional training with 7-week washout period in between. Note that Retention evaluation for exosuit-assisted training and pre-training evaluation of conventional training happened at the same day.

11.2.3. Gait training interventions

For both exosuit-assisted and conventional interventions, a physical therapist administered progressive, task-specific [275], [281], and high-intensity[276], [281] gait training directed at a fast walking speed. Each intervention included six 2-hour training sessions for 2 weeks, with a 7-weak washout period separating each intervention. Each training session comprised of five 6-minute walking bouts of fast walking, equivalent to at least 115% of comfortable walking speed measured at the beginning of the session. Training progression was based on a clinical algorithm that manipulated environmental complexity and practice variability [12], [281] (**Error! Reference source not found.**). Specifically, the participant started with training on a treadmill, and progressively moved to overground closed (e.g. a laboratory setting) and open (e.g. university sports track) walking environments. Also, practice variability in exosuit-assisted training increased through the progression from continuous to intermittent assistance delivered by exosuit (see **Error! Reference source not found.** for the further details about exosuit intermittent assistance). Conventional gait training shared the same training progression strategy as exosuit-assisted gait training, with the only exception of the use of exosuit.

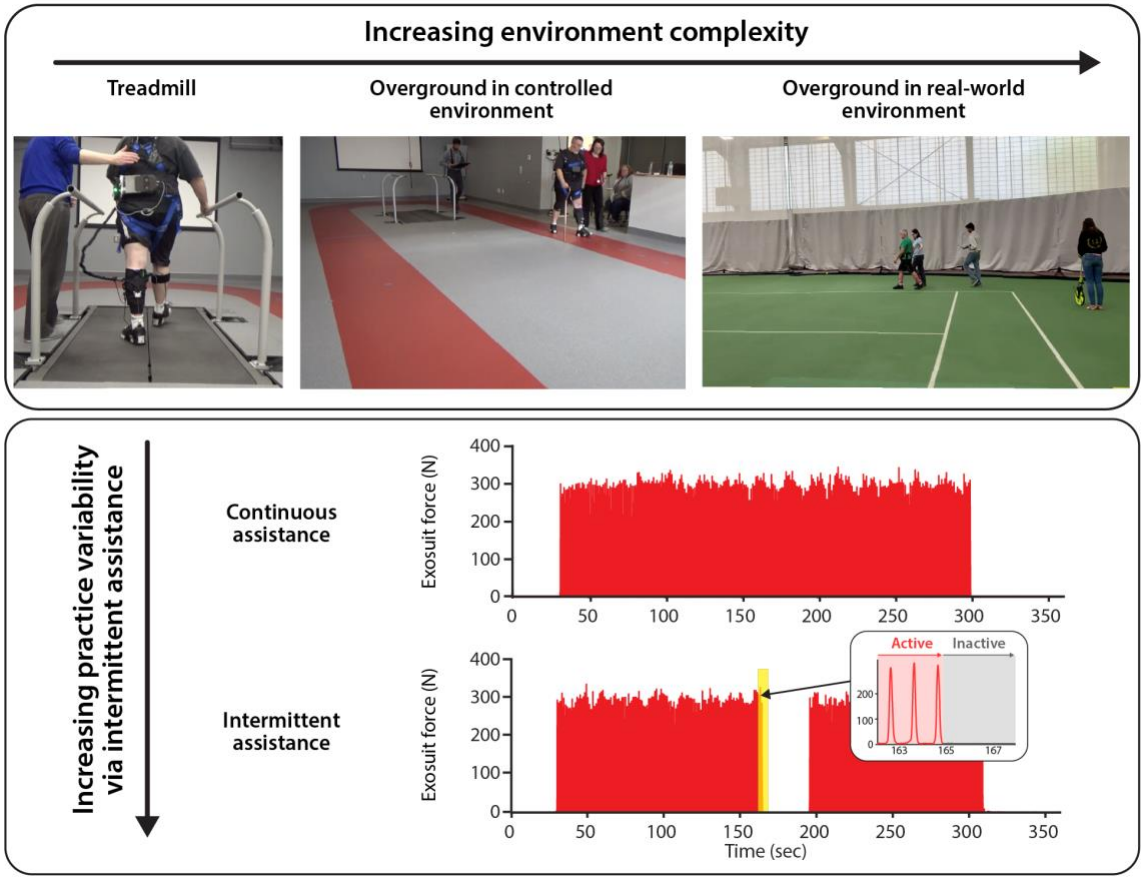

Figure 11.2. Clinical training progression strategy in exosuit-assisted gait training. Throughout the training intervention, training session progresses to increase environmental complexity from treadmill to open overground walking environment and practice variability using intermittent assistance delivered by exosuit.

11.2.4. Evaluation sessions

Evaluation of the training effect was performed by having the participant walk on an instrumented treadmill for 4 minutes per condition at three different time points (pre-training, post-training, and retention). The treadmill speed was set at patient's fast walking speed (115% of comfortable walking speed on the treadmill). The speed was then matched across three evaluation time points (i.e. pre-training, post-training, and retention) specific to each intervention condition. Walking conditions during each evaluation session comprised of baseline walking without exosuit (No Suit), and four exosuit-assisted walking with different PF assistance profiles: The force profiles were (1) with 150N peak and early onset timing (Early 150N), (2) with 150N peak and late onset timing (Late 150N), (3) with 300N peak and early onset timing (Early 300N), and finally (4) with 300N peak and late onset timing (Late 300N) (**Error! Reference source not found.**).

Different force profiles were tested to select PF assistance profile that maximizes paretic limb forward propulsion for the exosuit-assisted gait training. Specifically, we determined the PF assistance profile used in the gait training based on which profile generated the largest peak forward propulsion that exceeds the within-session minimum detectable change (MDC) of 0.80% body weight (BW) [128] during the pre-training evaluation session. If MDC was not reached, we selected the profile with 300N peak and late onset timing, as we posit that higher forces delivered later in stance phase would promote the most biomechanically appropriate ankle mechanics based on our current understanding on the role of ankle during push-off [161].

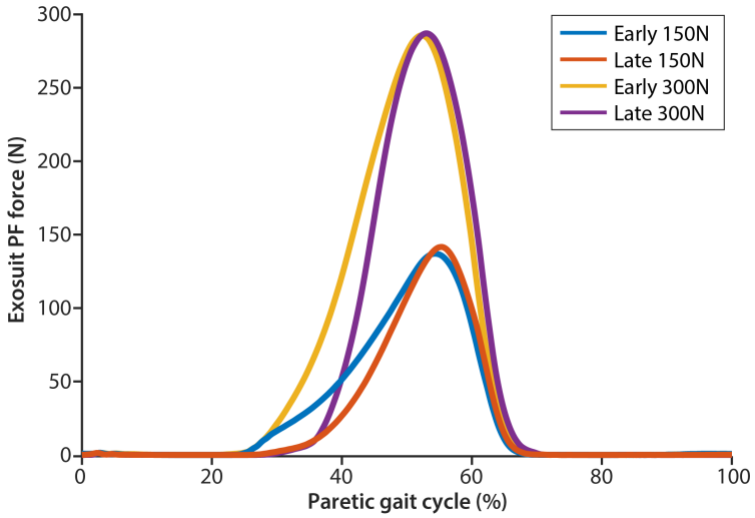

Figure 11.3. PF assistance profiles tested during pre-training evaluation

11.2.5. Motion analysis for evaluation sessions

To collect biomechanical data during evaluation sessions (i.e. pre- and post-training, and retention sessions), we used an 8-camera motion capture system (Qualisys, Göteburg, Sweden) while having the participant walk on an instrumented treadmill (Bertec, Columbus, Ohio, USA) that collected three-dimensional ground reaction forces (GRF). Kinematic data from motion capture was sampled at 100 Hz, and kinetic data from GRF were sampled at 2000 Hz. Single, retroreflective markers were placed bilaterally on pelvis (iliac crest, waist, anterior superior iliac spine), greater trochanter of hip, medial and lateral malleoli of knees and ankles, and areas corresponding to heel, toe, 1st and 5th metatarsophalangeal joints,

and rear foot directly distal to ankle malleoli. Clusters of four markers were placed on bilateral thigh and shank. All kinematic and kinetic data were filtered and processed through V3D software (C-Motion, Inc., Germantown, MD, USA), that implemented a zero-lag 4th order Butterworth filter with cutoff frequency at 20 Hz. Inverse kinematics was then used to calculate biomechanical measures. Further analysis was performed using Matlab (Mathworks, Natick, MA, USA).

11.2.6. Gait metric estimation during training days

To monitor the changes during the gait trainings, gait metric estimation presented in **Error! Reference source not found.** was implemented in both exosuit-assisted and conventional training. For the exosuit-assisted training, spatiotemporal gait metrics were estimated directly from the portable exosuit. For the conventional training, we developed a simple and lightweight sensor harness (total 0.56kg) for the gait metric estimation without an exosuit hardware, which included two foot IMUs (MTi-3, XSens, Netherlands) and a custom-made electronics board using an Atmel processor (SAME70N21, Atmel Co, USA), all of which were same as the components included in exosuit. Through the gait metric estimation, we calculated the total number of walking steps covered in each training day to evaluate the amount of gait training provided in different training conditions. We also calculated the average overground gait speeds in both conditions to evaluate the intensity of gait training.

11.2.7. Outcomes

Clinical gait function was evaluated using 10-meter walking test (10MWT) and 6-minute walking test (6MWT). Further, to understand biomechanical mechanisms underlying the changes in gait function, peak paretic propulsion (%body weight, %BW), peak paretic ankle moment (Nm/kg) at push off, maximum paretic trailing limb angle (TLA, m), stride length (m), and cadence were measured based on motion capture and GRF data. Due to the time constraints, the clinical walk tests were collected only in pre- and post-training evaluation sessions, while the biomechanical outcomes were collected in all three evaluation sessions (i.e. pre- and post-training, and retention).

11.2.8. Statistical analyses

To examine effects of intervention on biomechanical outcomes, we analyzed the last 30 seconds of treadmill walking when participant was not wearing the exosuit in three evaluation time points. Normality of distribution of data was confirmed using Shapiro-Wilk test. To examine differences in gait performance at different time points, we used a One-way ANOVA with multiple comparisons. The significance level was set at $p < 0.05$ after Bonferonni corrections to account for post-hoc multiple comparisons. SPSS Version 25 (IBM, Armonk, NY, USA) was used for statistical analyses. Analyses were done per individual participant, and not at group level.

11.3. Results

11.3.1. Exosuit intervention

Forward propulsion data from four different assistance profiles illustrated in **Figure 11.3** were collected to select the profile used for exosuit-assisted gait training (**Table 11.1**). None of exosuit assistance profile created changes from No Suit condition that exceeded MDC of 0.8%BW, therefore the PF force profile with late onset and 300N peak was implemented for the exosuit-assisted training as suggested in Section 11.2.4.

Table 11.1. Peak paretic forward propulsions for different walking conditions in pre-training evaluation session

	No Suit	Early 150N	Late 150N	Early 300N	Late 300N
Paretic peak forward propulsion (%BW)	9.25±0.23	9.61±0.24	9.53±0. 25	9.24±0. 27	8.60±0.25

11.3.2. Clinical outcomes from pre- and post-training evaluations

Figure 4 summarizes the changes in 10-meter walking speed and 6-meter walking distance between pre- and post- training evaluation sessions for both exosuit-assisted and conventional gait training. After exosuit-assisted gait training, clinically meaningful increases [268] were noted for gait speed (+0.12 m/s) and distance (+86 m). In contrast, conventional gait training resulted in modest increases in gait speed (+0.04 m/s) and distance (+37 m).

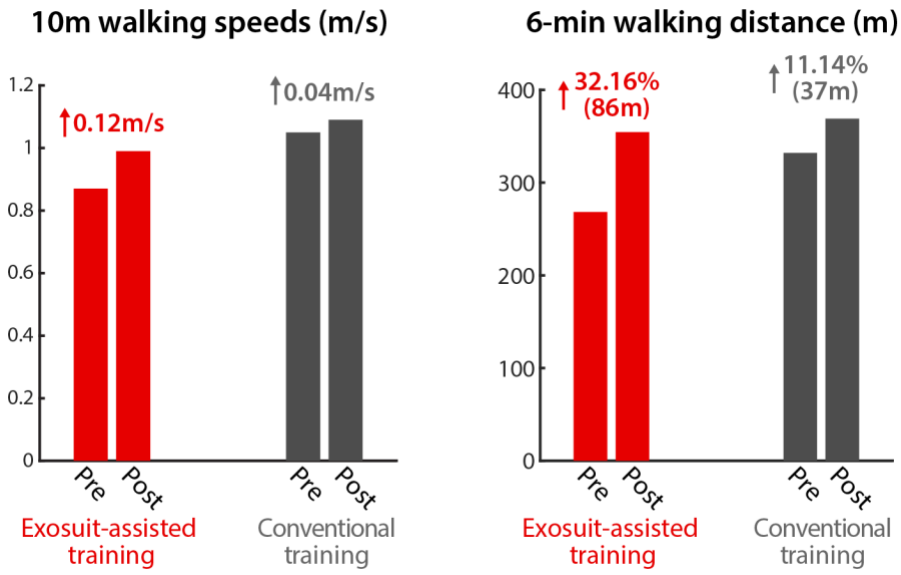

Figure 11.4. Gait speeds and distance based on 10-meter walk test and 6-minute walk test at pre- and post- training evaluations for both exosuit-assisted and conventional training

11.3.3. Biomechanical outcomes at pre- and post-training and retention evaluations

Table 11.2 and **Table 11.3** summarize biomechanical outcomes from exosuit-assisted gait training and conventional gait training respectively, and **Figure 11.5** presents the percent changes of data collected in post-training and retention from pre-training data.

First, exosuit-assisted gait training resulted in significant increases at post-training based on peak forward propulsion by +10.5%, ankle moment at push off by +8.3%, stride length by +6.7%, and TLA by +6.7% relative to pre-training ($ps<0.05$). Cadence decreased from pre- to post-training by -6.1%. In contrast, conventional gait training resulted in a significant decrease in peak forward propulsion by -9.2% at post-training relative to pre-training ($p<0.05$), while no significant differences were noted for ankle moment, stride length, and TLA at post-training relative to pre-training ($ps>0.05$). Cadence was largely maintained from pre- to post-training ($p > 0.05$).

Second, retention of biomechanical changes after gait training was assessed after 7 weeks of washout for each intervention. Following exosuit-assisted training, stride length was maintained from post-training to retention evaluations with statistically negligible change (-0.73%, $p=1.00$). Complementary to this, there were trends suggesting retention in other measures as demonstrated by insignificant changes with peak

propulsion (-0.28%; p=1.00), and TLA (-1.925, p=0.916) relative to post-training. Ankle moment, however, was not maintained after washout, dropping by -9.12% relative to post-training (p=0.02). On the other hand, 7 weeks after conventional training resulted in further increased TLA by +3.31% relative to post-training (p=0.001), and no change in stride length (-1.50%) relative to post-training (p=0.232). However, the washout following conventional training also resulted in reduction of ankle moment by -10.36% relative to post-training (p<0.001), and a trend of diminished peak propulsion by -8.77% relative to post-training (p=0.059).

Table 11.2. Biomechanical changes in paretic leg at pre, post, and retention from exosuit-assisted gait training

Metrics	Pre	Post	Ret	P-val		
				Across Conds	Pre VS Post	Post VS Ret
Peak propulsion (% body weight)	9.255 [8.756, 9.754]	10.230 [9.784, 10.677]	10.201 [9.036, 11.367]	0.01	0.012	1.00
ankle moment (Nm kg^-1)	0.840 [0.804, 0.875]	0.910 [0.885, 0.936]	0.827 [0.783, 0.872]	0.01	0.003	0.02
Stride length (m)	0.895 [0.877, 0.913]	0.955 [0.943, 0.966]	0.948 [0.913, 0.982]	<0.001	<0.001	1.00
TLA (deg)	21.543 [20.992, 22.094]	22.980 [22.632, 23.328]	22.539 [21.942, 23.137]	<0.001	<0.001	0.916

* Treadmill speed used for this evaluation was 0.49m/s.
** The data for Pre-training, post-training, and retention columns present mean values and 95%CIs in brackets.
*** Abbreviations: Pre: Pre-training session; Post: Post-training; Ret: Retention: Conds: Conditions;

Table 11.3. Biomechanical changes in paretic leg at pre, post, and retention from conventional gait training

Metrics	Pre	Post	Ret	P-val		
				Across Conds	Pre VS Post	Post VS Ret
Peak propulsion (% body weight)	9.776 [9.452, 10.100]	8.879 [8.354, 9.404]	8.100 [7.540, 8.660]	<0.001	0.018	0.059
ankle moment (Nm kg^-1)	1.006 [0.971, 1.040]	1.032 [1.000, 1.064]	0.925 [0.890, 0.960]	<0.001	0.710	<0.001

Stride length (m)	1.040 [1.026, 1.053]	1.057 [1.045, 1.069]	1.041 [1.027, 1.055]	0.089	0.146	0.232
TLA (deg)	23.848 [23.577, 24.119]	23.797 [23.495, 24.098]	24.584 [24.294, 24.873]	<0.001	1.00	0.001

* Treadmill speed used for this evaluation was 0.61m/s.

** The data for Pre-training, post-training, and retention columns present mean values and 95%CIs in brackets.

*** Abbreviations: Pre: Pre-training session; Post: Post-training; Ret: Retention; Conds: Conditions

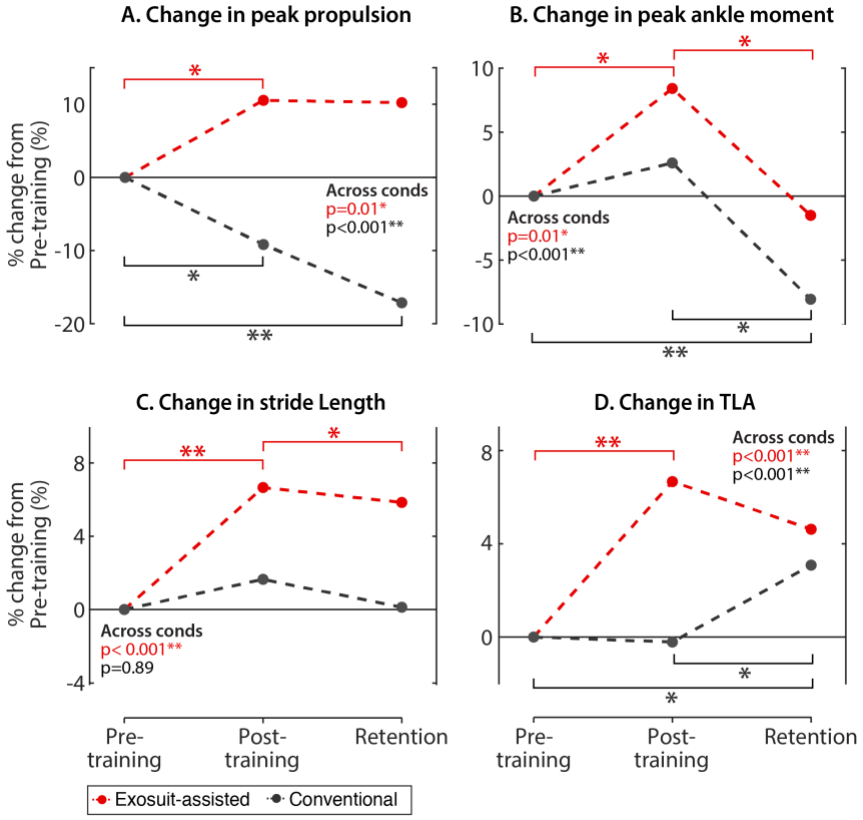

Figure 11.5. Percent change in biomechanical measures at post-training and retention compared to pre-training. (a) peak forward propulsion, (b) peak paretic ankle moment, (c) stride length, and (d) and paretic trailing limb angle (TLA).

11.3.4. Gait changes across training sessions

The changes across gait training sessions were evaluated for total number of walking steps covered and average overground gait speed in each training session (**Figure 11.6**). Total number of steps gradually increased in exosuit-assisted gait training from the first (D1) to the last session (D6) by +17.34% (+75 steps), while it slightly decreased in conventional training by -2.8% (-14 steps). We also observed larger

increases in average overground gait speed from D1 to D6 in exosuit-assisted gait training (14.61%; +0.13m/s) compared to conventional gait training (7.52%; +0.07m/s).

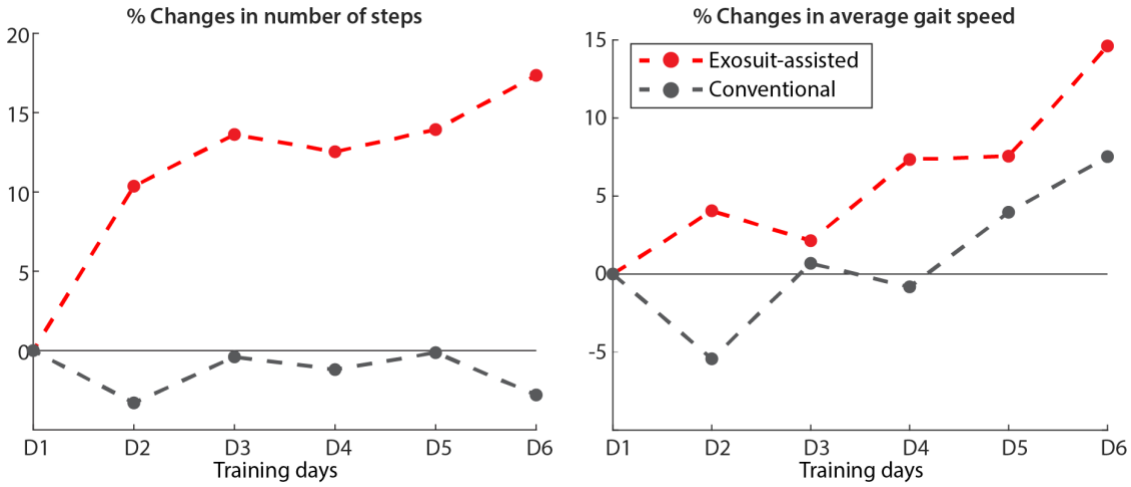

Figure 11.6. Percent changes in number of steps and average gait speed across training sessions from first training day for both exosuit-assisted and conventional gait training. The changes were estimated using spatiotemporal gait metric estimation algorithm presented in Chapter 9.

11.4. Discussion

This pilot study serves as the first investigation of the training-related effects of a soft robotic device in stroke. The focus of this study was on rehabilitative effects, which refer to changes in participant's baseline, unassisted gait performance that is independent of the exosuit. Thus, our study tackled a pragmatic and clinically relevant question of what training effects persist beyond the use of robotic device. Our results provide a proof of concept demonstration that exosuits, when used in gait training, are capable of delivering rehabilitative benefits on walking function, and moreover is accompanied by restoration of impairments of the paretic ankle.

Exosuit training has meaningful impact on clinical gait function

Following each exosuit-assisted or conventional gait training, we observed increases in short-distance fast walking speed and long-distance walking function, with improvements in favor of exosuit-assisted gait training over conventional gait training. Specifically, gait training with exosuit resulted in clinically meaningful improvements [275] in both 10MWT and 6MWT, while conventional training resulted in rather

modest increases in these measures. Our interventions aimed at training at fast speeds, to ultimately impact long distance walking function, which is an important determinant for community walking participation [138], [282]. Short-distance fast walking speed, measured with 10MWT as used in our testing, has been shown to be an important determinant of long-distance walking function [283]. Indeed, our results show concordance with these findings, as both fast 10MWT speed and 6MWT distance were improved in exosuit-assisted training. Because both interventions implemented training at fast speeds, and meaningful effects emerge only with exosuit-training, this suggests an added value to training with exosuits over conventional training. One thing to note is that our pilot included an intervention period of 2 weeks, which is rather short relative to other clinical studies and standard-of-care physical therapy programs. Thus, our findings may be taken as a snapshot of a training epoch, and that this amount may not be sufficient for conventional training to provide meaningful sustained benefit. In the same vein, this also highlights the efficiency of training with exosuits in delivering meaningful benefits even when implemented in short, condensed periods.

Exosuit-assisted training restores paretic ankle biomechanics

While clinical outcomes are important, these measures alone offer an incomplete picture of the recovery process, a limitation faced by several studies in the literature [127], [284]. Further, the clinical measures cannot differentiate between restored gait speed caused by restitution versus compensation [127]. To overcome the limitation, we examined biomechanical changes, particularly on variables that are actively being targeted by the exosuit. Specifically, the exosuit is designed to provide targeted benefits to the paretic ankle. Therefore, to directly assess the effects of training, we examined peak propulsion, ankle moment at push off, TLA, and stride length. These measures were selected to gain insight on underlying mechanisms related to paretic ankle that could compromise gait speed. Propulsion, along with TLA are important determinants of gait speed, and are shown to increase in response to faster walking speeds [159]. Ankle moment, in turn is an important contributor to the generation of propulsive forces [132], and is correlated with walking speed [285].

In favor of exosuit-assisted gait training, we indeed find improvements in paretic ankle and leg function as demonstrated by significant increases in peak paretic propulsion, increased ankle moment, and enhanced TLA. These likely in turn assist in generating longer stride lengths that are complementary to gains in clinical gait speed function. On the other hand, conventional gait training had negligible impact on ankle moment, TLA, and stride length (ps > 0.05), and a significant reduction in peak paretic propulsion. The seemingly divergent trajectories in the change in propulsion between interventions shown in **Figure 11.5**(a) suggest that training with exosuits enhance propulsion, and training without exosuits may lack the specificity in recovering a propulsion-based strategy despite improvements in speed in both conditions. Since reduced paretic limb propulsion has been shown to be one of the major determinants of reduced gait speed post-stroke [112], [128], [276], the unfavorable reduction in variables related to paretic propulsion support previous studies showing that speed can be improved with compensatory strategies, and may be the "default" recovery strategy for patients with impaired propulsive abilities. Indeed, our secondary analysis also revealed that the patient increased hip hiking more during conventional gait training compared to exosuit gait training by 36.8% (2.3cm). It is worth highlighting that both interventions included therapist-led cues that were structured mainly on generating propulsion to drive speed. Our results suggest that training without exosuits even with therapist cues to promote propulsion based on a 2-week intervention may not be sufficient to target propulsion deficits after stroke.

Exosuit-assisted training effectively increases the dose and intensity of training sessions

Although the aforementioned clinical and biomechanical outcomes comparing pre- and post-training demonstrated the improved efficacy of exosuit-assisted gait training over conventional training, it is still unclear how exosuit improved the clinical and biomechanical gains. Spatiotemporal gait metrics collected during training sessions suggested that exosuit-assisted gait training effectively increased the dose (i.e. number of steps) and the intensity (i.e. walking speed) along the progression of gait training, while conventional gait training did not increase the dose with modest increase the intensity throughout the progression. This might explain the improved gains from exosuit training based on the motor-learning based

rehabilitation theory highlighting the importance of the dose, intensity, and specificity [51]. Since both exosuit-assisted and conventional training administered the same environmental progression from treadmill walking to overground walking in open environment, we believe specificities of both gait training scenarios were similar. The different outcomes generated from different training scenarios might be therefore caused by other variables such as progressive increases in dose and intensity throughout exosuit-assisted gait training. Still, it should be noted that the initial walking speed at D1 in conventional training was higher than in exosuit-assisted gait training, therefore the overall intensity (i.e. average gait speed throughout entire training days) might be also higher in conventional training. This data therefore highlights the importance of progression of intensity and dose for effective gait training. Importantly, the higher gait speed observed during exosuit-assisted gait training could be induced by exosuit assistance and not by the restoration of gait function, therefore may not be directly related to training intensity. Future study with intensity measurements such as heart rate and metabolic cost during training sessions would further elucidate the improved intensity during exosuit-assisted gait training. Since published studies on across-day gait adaptation or motor learning with wearable robots are limited in validation with healthy individuals and most of the measurements in the studies were focused on metabolic cost of transport [221], [286] or electromyography data [223], [287], future study with post-stroke participant with intensity measurements similar to [288] would serve an important step toward exosuit-assisted high-intensity gait training paradigm.

Retention

One of the important hallmarks of motor learning is the persistence of performance improvements over the passage of time [271], [289]. As an exploratory aim in this study, we examined how these changes fared after 7 weeks post-training. Following exosuit-assisted gait training, evidence of retention relative to post-training performance was observed such that stride length (p=1.00) and TLA were maintained (p=0.916) after a 7-week period. Likewise, paretic propulsion had comparable values to the benefits manifested at post-training (p=1.00), suggesting maintenance of gait improvements. Interestingly, ankle moment significantly decreased at retention compared to post-training (p<0.05), returning to pre-training levels

(p=1.00). This reflects the delicate nature of recovery of the paretic ankle function, and also demonstrates the difference in susceptibility to time and forgetting [289] among these seemingly related biomechanical measures.

Conventional training led to significant reductions in ankle moment ($p < 0.001$), and a tendency for reduced propulsion ($p = 0.059$) at retention relative to post-training. Furthermore, propulsion at retention was significantly reduced even further relative to pre-training levels ($p < 0.001$). In other words, there is progressive degradation in propulsion at post-training and further with passing of time. This suggests that conventional training, although capable of maintaining gait speeds, fails to promote a propulsion-based strategy. It is also worth noting that the participant exhibited an unusual propulsion pattern with which he generated more propulsion from paretic side (propulsion: 9.776%BW) than nonparetic side (9.483%BW), with significant nonparetic braking (-11.218%BW) during the pre-training evaluation. The reduction in paretic propulsion during retention could therefore be compensated by changes in non-paretic propulsion or braking. Indeed, we found significant reduction in nonparetic braking (-9.219%BW, $p < 0.005$) during the retention, which could be the cause of reduced paretic propulsion. Still, both nonparetic and paretic propulsion magnitudes were significantly lower than healthy propulsion level, therefore the paretic propulsion reduction in retention was not desirable.

An increase in TLA was noted at retention relative to post-training with conventional training. While this may seem positive, it is also important to consider concomitant biomechanical factors. Indeed, previous research [121] suggests that an increase in TLA was beneficial only if it resulted in increases in propulsion. Our findings that increase in TLA was accompanied by degraded propulsion during conventional training therefore may not be desirable outcomes. Further, albeit statistically significant, the magnitude of increase in TLA was minimal at 0.79 deg, which was significantly lower than minimal detectable change reported in [128]. As such, the increase at TLA may not be sufficient to impact gait speeds, and that targeted treatment directed to paretic ankle may be needed. In summary, notwithstanding ankle moment, training with exosuits may have potential to retain gait restorative benefits that is maintained after several weeks

after training. Stronger effects on the maintenance of exosuit-related benefits may be observed when examined at shorter retention intervals.

Conclusion and future work

This pilot study demonstrates the potential of exosuits in facilitating stroke recovery from both activity and impairment levels. In particular, the targeted exosuit assistance that seems to promote forward propulsion may be an important factor in facilitating neuromotor restitution of paretic ankle function for walking.

Although promising, the presented study was limited as a proof-of-concept with only a single pilot participant, therefore further study with a diverse cohort of stroke survivors is warranted. Moreover, in examining the value of the exosuit relative to customary care, we implemented a crossover design. While it bears the strength of having the participant be their own control and minimize inter-subject variability, a complete washout was not observed or anticipated as demonstrated by the retention effects. This is an inherent limitation of this design especially when implemented in behavioral studies as ours. Our results however, which show generally divergent responses to exosuit training versus conventional training, demonstrate intervention-specific responses. Third, the order of intervention may have an effect on responses. However, the seemingly distinct responses to each intervention, especially for the main outcome of propulsion suggest that effects are moderated primarily by the intervention and less so with order. Larger samples with balanced administration of sequences of intervention would strengthen this finding. Finally, the training duration in the pilot study was relatively short compared to real-world clinical gait training (two weeks), therefore validation on long-term exosuit-assisted training is warranted.

Chapter 12.

Conclusion

This dissertation contributes to the field of rehabilitation and wearable robotics through the first demonstration of soft exosuits to assist post-stroke locomotion and gait training. Through multidisciplinary research across robotics, biomechanics, and rehabilitation science, it successfully generated fundamental understanding on the biomechanical and physiological impact of exosuit assistance on post-stroke walking and demonstrated great potential of exosuit technology to improve post-stroke gait training. Specifically, Chapter 2 presented a tethered exosuit prototype designed for treadmill-based study, and Chapter 3 to Chapter 5 experimentally validated biomechanical and physiological benefits of the tethered exosuit on treadmill walking post-stroke and their underlying mechanisms. Based on the knowledge generated from the studies with the tethered exosuit, Chapter 6 presented a lightweight and efficient portable exosuit with a controller strategy robust to post-stroke overground walking, and Chapter 7 and **Error! Reference source not found.** validated the biomechanical and physiological benefit of portable exosuit in post-stroke overground walking and its controller performance. Furthermore, to enable continuum of rehabilitation care with exosuit from clinics-based to community-based gait training, **Error! Reference source not found.** presented a real-time spatiotemporal gait metric estimation with portable exosuit, and **Error! Reference**

source not found. evaluated the impact of intermittent assistance on overground gait speed and patterns post-stroke. Finally, **Error! Reference source not found.** demonstrated the feasibility of exosuit-assisted gait training through a pilot study that compared exosuit-assisted gait training to conventional gait training.

12.1. Limitations and future work

While the outcomes from the research in this dissertation provide preliminary evidence on the efficacy of soft exosuits in post-stroke gait training, there are a number of avenues to be explored for more rigorous validation and improvements in the exosuit systems and their utilization strategy. We consider the limitation and potential improvements in the remainder of this chapter.

12.1.1. Gait event detection and segmentation

Although the latest gait event detection algorithm presented in Chapter 6 and **Error! Reference source not found.** outperformed previously published algorithms [240] on average, the data suggest that for certain individual gait patterns, significant inaccuracy compared to actual gait events recorded with lab equipment could be present. It is possible that this inaccuracy could be addressed by using other sensors rather than foot IMUs used in our current algorithm or using multiple sensors with the foot IMUs. For instance, thigh motions during walking have a larger range of motion with relatively simpler movement patterns than foot motions, therefore using IMU attached on the thigh could improve the robustness. Additionally, the estimation accuracy could be improved by increasing IMU sampling rates. The current sampling rate of exosuit IMUs (100Hz) could cause up to 10-msec error in gait event timing estimation, which account for 30 to 60% of current average error. Furthermore, the gait phase segmentation points for realtime actuation control described in Section 8.2 (e.g. $SP1_{exo}$ and $SP3_{exo}$) are detected based on the sign changes of gyroscope signals which follow after peak signals corresponding to exosuit-estimated toe-offs (NTO_{exo} and PTO_{exo} respectively), therefore they had extra delays from estimated gait event timings which caused significant delay in onset of DF force during early swing, therefore reducing the segmentation delay could improve assistance timing (see Section 8.2 for further details).

Better real-time estimation of percent gait cycle (%GC) could also enable an exosuit to adapt the force profile to deliver optimal benefits for different individuals (See Section 12.1.4 for further details). The current control strategy for portable exosuit changes the cable position command generation policy at each segment of the gait cycle (see Section 8.2 for further details). Since it executes the same policy within each segment, the controller does not allow adaptation of the entire force profile and is limited to adapt only onset and offset timings and peak magnitude. Calculating %GC and generating force profile defined in %GC could therefore improve exosuits' adaptability. Indeed, our tethered exosuit in Chapter 2 implemented %GC estimation based on stride times measured in previous strides. However, this estimation method assumes consistent stride times across multiple strides, which is not valid in overground walking with increased stride-stride variability. Previous research [290] proposed different methods to calculate %GC such as using adaptive oscillator [291] or Hidden Markov Model [292]. Still, these works are limited in validation with healthy individuals or with clinical population on treadmills, therefore developing new %GC estimation method and validation in post-stroke overground walking are warranted.

12.1.2. Spatial gait metric estimation

Our work on spatial gait metric estimation with portable exosuit in Chapter 9 demonstrated improved robustness in compensating velocity drift over published methods, but its maximum estimation errors were up to 8% of baseline values during post-stroke overground walking, and therefore further improvements to accurately estimate gait metrics is required. Specifically, higher estimation errors from non-paretic side than paretic side were observed, that needs to be further investigated. Additionally, our preliminary study in Section 9.5 suggests that using higher order drift compensation function instead of a linear function was shown to improve the estimation accuracy, and therefore further investigation to determine the choice of drift function. Moreover, we observed improved accuracy from the published methods [101], [102] that used window-based ZUPT. Since our current method executes ZUPT at a single time point each stride, we may be able to improve our method by detecting zero-velocity window instead of a single moment and

compensate errors based on the windows. A potential approach could be using the time window between contralateral mid-swing event and contralateral heel-strike.

Another limitation of our gait metric estimation algorithm is that it estimates foot clearance based on the height of the foot IMU which does not represent the entire foot. This could be improved by incorporating foot model and IMU orientation measurements. Additionally, the algorithm is not able to estimate step length since it requires the relative position between two feet. Given the importance of step length in determining post-stroke compensatory gait patterns [293], enabling estimation of relative position between two feet would therefore improve the gait metric estimation. Previous research suggests to use non-inertial based sensors such as ultrasound sensors on the shoes [294], therefore incorporating wearable sensors such as proximity sensors or ultrasound sensors in combination with IMUs on the shoes may enable us to estimate relative position of two feet. Pedestrian position tracking would be also useful to monitor patient's activity level outside the clinics. Finally, our current gait metric estimation algorithm may not be sufficient to fully understand post-stroke compensatory gait patterns. Although it estimates gait variables related to compensatory patterns such as circumduction and foot clearance, there are other compensatory mechanisms that cannot be captured by those variables. For instance, some of post-stroke individuals increase foot clearance through hip hiking or knee flexion. Therefore, 3D kinematics estimation for hip, knee, and ankle joints using additional wearable IMUs would enable to provide a thorough dataset to understand post-stroke gait compensatory patterns.

12.1.3. Force tracking performance

Our portable exosuit implemented the control algorithm that adapts the Bowden cable position commands based on selected force measurements such as force magnitude at onset, peak, and offset (see Section 8.2 for more details). The controller performance was validated that it could consistently deliver assistance force with less than 1.6%BW average RMS-E for both DF and PF assistance. However, this approach only allows to adjust onset and offset timings and peak magnitude, limiting us from prescribing an entire force

profile throughout a gait cycle. Further, the peak force of PF assistance did not reach the target peak force by 0.8%BW, which may have been caused by with-in stride cable velocity adaptation that reduced cable velocity as the measured force reached the target force.

These limitations could be addressed by implementing a force controller that enables us to command entire force trajectory. Our lab's previous work has developed a force controller for a tethered exosuit for hip extension assistance in healthy individuals that was based on admittance control framework and two feedforward compensators [81]. In this work, two feedforward control blocks were used to compensate for the changes in Bowden cable length induced by joint motions (joint motion compensator) and human-exosuit stiffness (i.e. the relationship between exosuit deformation and force generation). Residual force errors were then compensated through a feedback admittance control block that generated desired cable velocity based on force error measurement. Motivated by the previous work, we conducted a preliminary study to develop direct force controller for the portable exosuit for paretic ankle assistance (See **Figure 12.1**). In this work, the changes in Bowden cable length induced by ankle motion was compensated based on ankle kinematics estimation using IMUs attached on the paretic shank and foot, and human-exosuit stiffness was modeled based on empirical data of the relationship between Bowden cable length and the tensile force (**Figure 12.1**(b)). Preliminary validation of this controller in treadmill walking with one healthy individual demonstrated that it could enable to change the onset and peak timings with RMS-E less than 6N (**Figure 12.1**(c)), which is similar to the error range reported in [81]. Still, more validation in overground walking with post-stroke individuals is warranted.

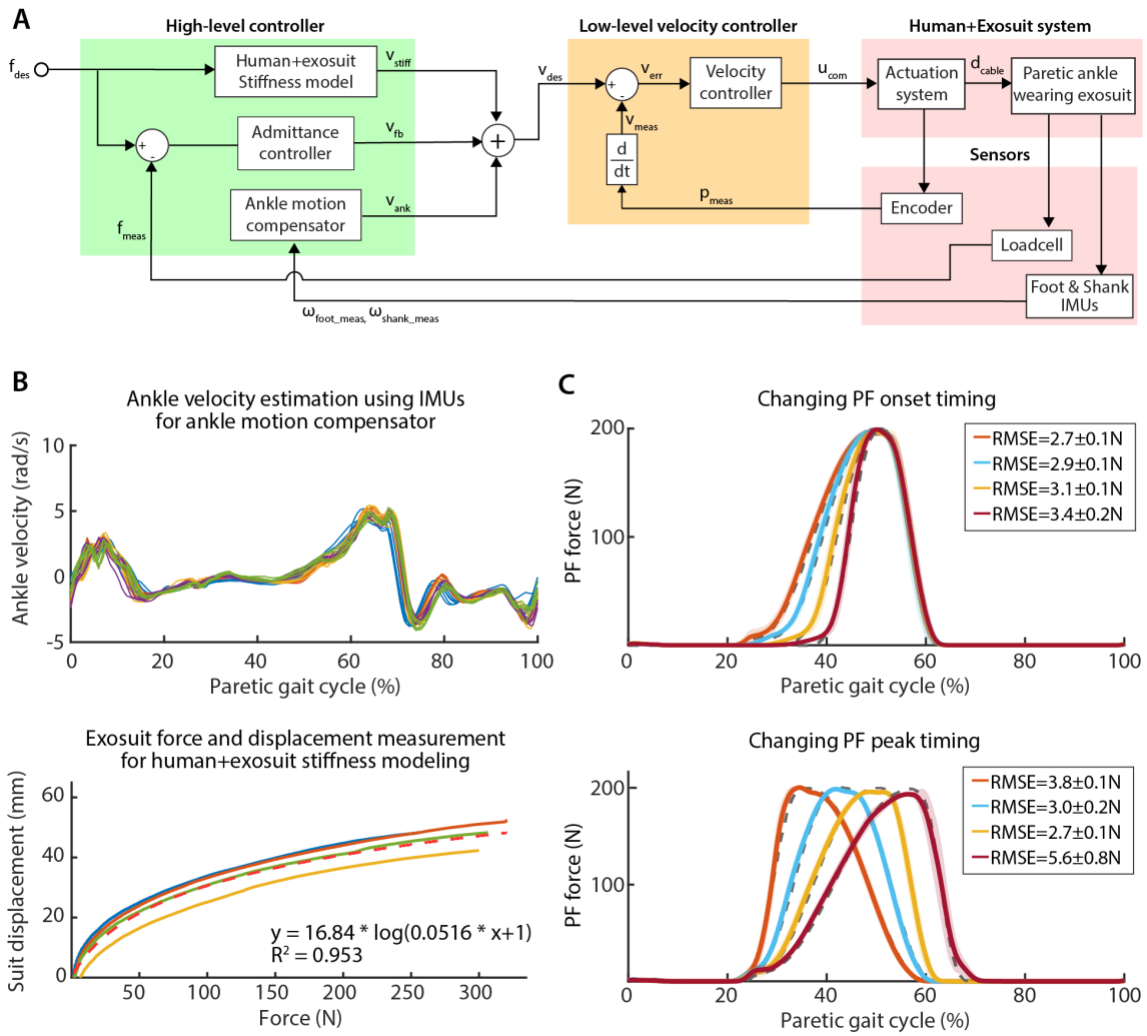

Figure 12.1. Force controller implementation for PF assistance with portable exosuit
. (a) Controller block diagram, (b) Ankle velocity measurement and exosuit force and displacement measurements for feedforward compensator models, (c) Preliminary results in PF assistance force consistency during healthy treadmill walking (N=1)

12.1.4. Improving immediate assistive effect through assistance profile individualization

The immediate biomechanical and physiological benefits of wearing exosuits for paretic ankle assistance was validated in both treadmill (Chapter 3) and overground walking post-stroke (Chapter 7). However, it is still unclear if exosuits delivered the optimal assistance that maximized the immediate benefits. Indeed, our treadmill-based study in Chapter 3 demonstrated different PF assistance profiles could generate different biomechanical outcomes related to forward propulsion. Even more, different post-stroke individuals preferred different assistance profiles to generate more forward propulsion. These observations

suggest further increase of biomechanical benefits could be enabled by individualizing exosuit assistance profiles. On the other hand, current exosuit DF assistance is largely based on manual tuning of assistance magnitude and may not provide optimal benefits to post-stroke gaits. The overground walking study in Chapter 7 demonstrated increased PF muscle activity during swing when walking with portable exosuit which might indicate resistive PF muscle exertion against DF force. Further, we also observed reduction in DF muscle activity during swing which might indicate reduced exertion that inhibits training gain on DF function. These undesirable changes in muscle activity could be diminished by automatic tuning based on EMG or ankle kinematics measurements.

Recent studies on a hip-assisting soft exosuit [85] and ankle-assisting exoskeleton [241] demonstrated that individualization of gait assistance provided by wearable robots through 'Human-in-the-loop' control optimization (HIL) could reduce metabolic cost of transport more than generic assistance profile in healthy walking. In these works, The HIL controller measured objective metrics such as metabolic cost of transport to adapt assistance profile online and maximize the objective outcomes. We think the HIL control strategy could improve the immediate biomechanical and physiological benefits of exosuits in post-stroke walking. Moreover, because post-stroke gait deficits are highly heterogeneous, we hypothesize different post-stroke individuals may require different objective metrics to restore gait functions. Given the aforementioned considerations, future studies on multi-objective HIL control development could improve the immediate assistive effect of exosuit to achieve patient-specific goals (see **Figure 12.2** for the illustration). In this proposed control framework, multiple objective metrics are measured using onboard or offboard sensors, and exosuit assistance profiles are adapted based on the objective measurements in order to maximize patient specific objective outcomes. Toward this goal, future researches are required to understand (1) if control optimization could improve the immediate benefits of exosuit in post-stroke individuals, (2) if exosuit could generate individual-specific objective functions based on sensor data collected with wearable sensors , and finally (3) if multi-objective online optimization could enable exosuit to assist with individual-specific goals .

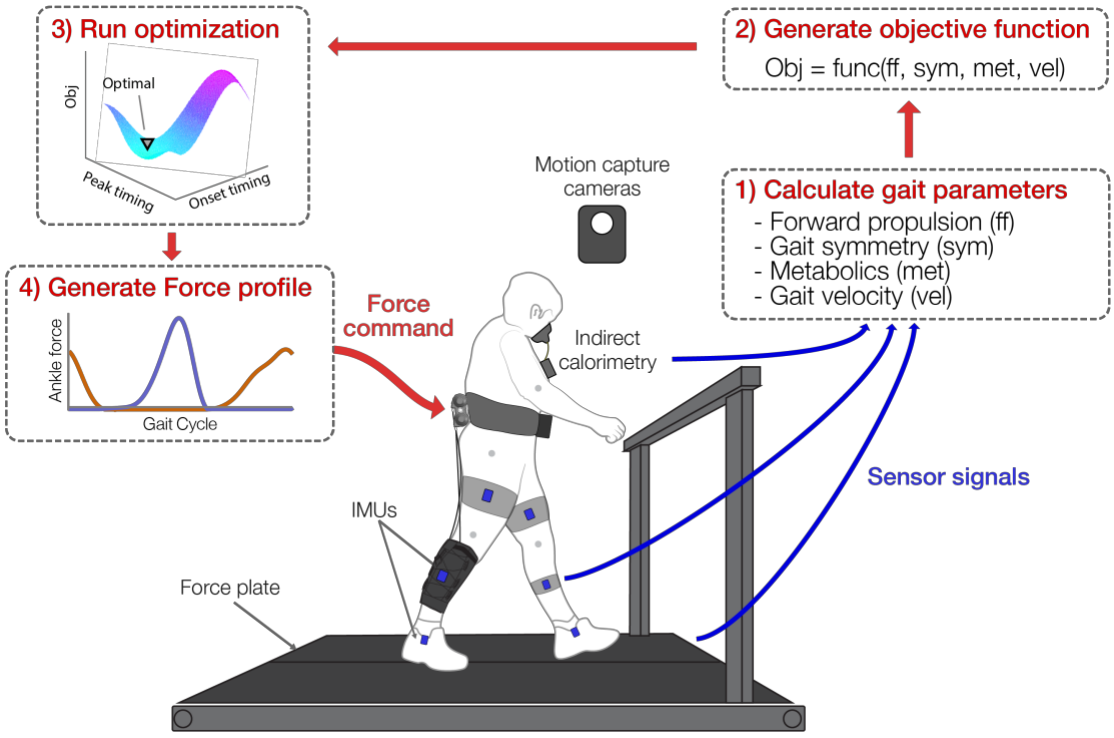

Figure 12.2. Proposed multi-objective Human-in-the-loop (HIL) optimization to improve immediate benefit of wearing exosuits in post-stroke walking

12.1.5. Intermittent/variable exosuit assistance to promote motor learning

Our case-series study on intermittent assistance delivered from the portable exosuit in Chapter 10 suggested that intermittent assistance could promote the carryover of exosuit-induced improvement in gait patterns through a post-assistance period within a continuous walking session. Although interesting, the carryover effect observed in this study varied across individuals and target gait metrics, thereby limiting our understanding on how to generate a positive carryover effect on target gait metrics across different individuals. Moreover, it is not clear if the observed changes in gait metrics during post-assistance periods were purely caused by carryover effects or caused by other factors such as warm-up effects or fatigue [273]. Even more, this study was a single-session study which did not investigate long-term retention of the changes in unassisted gait induced by intermittent assistance, an ultimate goal of post-stroke gait training. Further study with a larger sample and full randomization of conditions is therefore required to fully understand how to improve the positive carryover effect on target gait outcomes. After gaining fundamental understanding on the impact of intermittent assistance in post-stroke walking, we may be able to develop

an automatically individualized gait training program using exosuit intermittent assistance and real-time gait metric estimation. Specifically, since motor learning studies have shown that changing motor training schedule can affect training outcomes [272], [273], it may be possible to develop a new exosuit software paradigm that automatically adapts intermittent assistance scheduling based on real-time gait metric estimation (see Section 10.1 for further details).

Even more, systematically varying exosuit assistance may facilitate motor learning to restore gait function in post-stroke gait training even more than intermittent assistance. Our research works have focused on delivering consistent assistance profile when suit was active, and intermittent assistance added variability by changing exosuit between active and inactive mode to promote motor learning. This approach was motivated by recent studies suggesting that motor variability may be a feature of how sensorimotor systems operate and learn [295]. This view, rooted in reinforcement learning theory, equates motor variability with purposeful exploration of motor space that can drive motor learning. Given this motor learning framework, delivering systematic variability with exosuit assistance during gait training session may facilitate restoration of gait functions more than delivering intermittent assistance. Designing variable assistance strategy to promote motor learning and validation of the approach with multiple post-stroke individuals are therefore warranted.

12.1.6. Participant-centric approach for experimental study design

Experimental studies with post-stroke individuals have played the key role in our works and need to continue for the future research. Based on our experience with the previous experiments, not only to design experiments in scientifically rigorous manner, we think it is also critical to design experiments with participant-centric approach such that study participants are not treated as experimental subjects, rather they play an active role throughout experimental iterations and their feedback is valued and reflected on those. We found this approach helps participants to continue to participate in follow-up study sessions (e.g. longitudinal studies), and also helps to get valuable insights. Further, it seems important to let participants

understand that the ultimate goal of the study is to improve participants' life quality, and therefore participating in the study and giving feedback would eventually benefit their life. This seems to make patients more engaged in the study and impact research outcomes. Although researchers may not share all the information about the study, sharing the high-level goal and brief overview of our technology seems to facilitate experiments.

A welcoming atmosphere and personal interactions seem to impact research outcomes as well. For instance, a patient may not complete entire walking bouts if one gets tired of being a subject without much interaction with researchers. Licensed physical therapists in the study are usually well-trained for the interaction with clinical individuals, and engineering researchers may support the interaction by explaining exosuit technology or biomechanics knowledge in layman's language.

12.1.7. Longitudinal study on exosuit-assisted gait training

Our pilot study on exosuit-assisted gait training in Chapter 11 demonstrated the potential of exosuits in facilitating stroke recovery from both activity and impairment levels. In particular, the targeted exosuit assistance that seems to promote forward propulsion may be an important factor in facilitating neuromotor restitution of the paretic ankle. Although promising, the study was limited as a proof-of-concept with only a single pilot participant, therefore further study with a diverse cohort of stroke survivors is warranted. Moreover, in examining the value of the exosuit relative to customary care, we implemented a crossover design with 7-week washout between interventions. However, a complete washout was not observed or anticipated as demonstrated by the retention effects. This is an inherent limitation of this experimental design especially when implemented in behavioral studies as ours. Larger samples (i.e. more participants) with balanced administration of sequences of intervention would strengthen this finding. Finally, the training duration in the pilot study was relatively short compared to real-world clinical gait training which is usually 6-8 weeks long, therefore validation on long-term exosuit-assisted training is warranted.

Reference

[1] P. S. Rodman and H. M. McHenry, “Bioenergetics and the origin of hominid bipedalism.,” *Am. J. Phys. Anthropol.*, vol. 52, no. 1, pp. 103–6, Jan. 1980.

[2] A. H. A. S. C. and S. S. Subcommittee, “Heart Disease and Stroke Statistics-2017 Update: A Report From the American Heart Association.,” *Circulation*, vol. 131, no. 4, pp. e29-322, 2017.

[3] D. J. Farris, A. Hampton, M. D. Lewek, and G. S. Sawicki, “Revisiting the mechanics and energetics of walking in individuals with chronic hemiparesis following stroke: from individual limbs to lower limb joints,” *J Neuroeng Rehabil*, vol. 12, p. 24, 2015.

[4] S. Olney and C. Richards, “Hemiparetic gait following stroke. Part I: Characteristics,” *Gait Posture*, vol. 4, pp. 136–148, 1996.

[5] C. L. Richards, F. Malouin, and C. Dean, “Gait in stroke: assessment and rehabilitation.,” *Clin. Geriatr. Med.*, vol. 15, no. 4, pp. 833–855, Nov. 1999.

[6] T. Kitago and J. W. Krakauer, “Motor learning principles for neurorehabilitation,” *Handb Clin Neurol*, vol. 110, pp. 93–103, 2013.

[7] C. K. Balasubramanian, R. R. Neptune, and S. A. Kautz, “Variability in spatiotemporal step characteristics and its relationship to walking performance post-stroke,” *Gait Posture*, vol. 29, no. 3, pp. 408–14, Apr. 2009.

[8] J. A. Schrack, E. M. Simonsick, P. H. M. Chaves, and L. Ferrucci, “The role of energetic cost in the age-related slowing of gait speed.,” *J. Am. Geriatr. Soc.*, vol. 60, no. 10, pp. 1811–6, Oct. 2012.

[9] S. A. Combs, M. Van Puymbroeck, P. A. Altenburger, K. K. Miller, T. A. Dierks, and A. A. Schmid, “Is walking faster or walking farther more important to persons with chronic stroke?,” *Disabil. Rehabil.*, vol. 35, no. 10, pp. 860–7, May 2013.

[10] N. E. Mayo *et al.*, “Disablement following stroke,” *Disabil Rehabil*, vol. 21, no. 5–6, pp. 258–268, 1999.

[11] P. W. Duncan *et al.*, “Body-Weight–Supported Treadmill Rehabilitation after Stroke,” *N. Engl. J. Med.*, vol. 364, no. 21, pp. 2026–2036, May 2011.

[12] T. H. Cruz, M. D. Lewek, and Y. Y. Dhaher, “Biomechanical impairments and gait adaptations post-stroke: Multi-factorial associations,” *J. Biomech.*, vol. 42, no. 11, pp. 1673–1677, Aug. 2009.

[13] C. Moriello, L. Finch, and N. E. Mayo, "Relationship between muscle strength and functional walking capacity among people with stroke.," *J. Rehabil. Res. Dev.*, vol. 48, no. 3, pp. 267–275, 2011.

[14] G. Chen, C. Patten, D. H. Kothari, and F. E. Zajac, "Gait differences between individuals with post-stroke hemiparesis and non-disabled controls at matched speeds.," *Gait Posture*, vol. 22, no. 1, pp. 51–56, Aug. 2005.

[15] T. H. Cruz and Y. Y. Dhaher, "Impact of ankle-foot-orthosis on frontal plane behaviors post-stroke," *Gait Posture*, 2009.

[16] D. C. Kerrigan, E. P. Frates, S. Rogan, and P. O. Riley, "Hip Hiking and Circumduction: Quantitative Definitions," *Am. J. Phys. Med. Rehabil.*, vol. 79, no. 3, 2000.

[17] S. Schmid, K. Schweizer, J. Romkes, S. Lorenzetti, and R. Brunner, "Secondary gait deviations in patients with and without neurological involvement: A systematic review," *Gait and Posture*. 2013.

[18] T. Susko, K. Swaminathan, and H. I. Krebs, "MIT-Skywalker: A Novel Gait Neurorehabilitation Robot for Stroke and Cerebral Palsy," *IEEE Trans. Neural Syst. Rehabil. Eng.*, 2016.

[19] S. A. Combs, E. L. Dugan, E. N. Ozimek, and A. B. Curtis, "Effects of body-weight supported treadmill training on kinetic symmetry in persons with chronic stroke," *Clin Biomech (Bristol, Avon)*, vol. 27, no. 9, pp. 887–892, 2012.

[20] A. L. Hall, M. G. Bowden, S. A. Kautz, and R. R. Neptune, "Biomechanical variables related to walking performance 6-months following post-stroke rehabilitation," *Clin Biomech (Bristol, Avon)*, vol. 27, no. 10, pp. 1017–1022, 2012.

[21] M. G. Bowden, A. L. Behrman, R. R. Neptune, C. M. Gregory, and S. A. Kautz, "Locomotor rehabilitation of individuals with chronic stroke: difference between responders and nonresponders.," *Arch. Phys. Med. Rehabil.*, vol. 94, no. 5, pp. 856–62, May 2013.

[22] D. S. Reisman, K. S. Rudolph, and W. B. Farquhar, "Influence of speed on walking economy poststroke.," *Neurorehabil. Neural Repair*, vol. 23, no. 6, pp. 529–34, 2009.

[23] C. K. Balasubramanian, M. G. Bowden, R. R. Neptune, and S. A. Kautz, "Relationship Between Step Length Asymmetry and Walking Performance in Subjects With Chronic Hemiparesis," *Arch. Phys. Med. Rehabil.*, vol. 88, no. 1, pp. 43–49, 2007.

[24] C. English, P. J. Manns, C. Tucak, and J. Bernhardt, "Physical activity and sedentary behaviors in people with stroke living in the community: a systematic review.," *Phys. Ther.*, vol. 94, no. 2, pp. 185–96, Feb. 2014.

[25] K. M. Michael, J. K. Allen, and R. F. Macko, "Reduced ambulatory activity after stroke: the role of balance, gait, and cardiovascular fitness," *Arch. Phys. Med. Rehabil.*, vol. 86, no. 8, pp. 1552–1556, Aug. 2005.

[26] P. H. Lee, H. Nan, Y.-Y. Yu, I. McDowell, G. M. Leung, and T. H. Lam, "For non-exercising people, the number of steps walked is more strongly associated with health than time spent walking.," *J. Sci. Med. Sport*, vol. 16, no. 3, pp. 227–30, May 2013.

[27] D. Rand, J. J. Eng, P.-F. Tang, C. Hung, and J.-S. Jeng, "Daily physical activity and its contribution to the health-related quality of life of ambulatory individuals with chronic stroke.,"

Health Qual. Life Outcomes, vol. 8, p. 80, 2010.

[28] J. Jutai *et al.*, "Mobility assistive device utilization in a prospective study of patients with first-ever stroke.," *Arch. Phys. Med. Rehabil.*, vol. 88, no. 10, pp. 1268–75, Oct. 2007.

[29] L. E. Skolarus, J. F. Burke, and V. A. Freedman, "The role of accommodations in poststroke disability management.," *J. Gerontol. B. Psychol. Sci. Soc. Sci.*, vol. 69 Suppl 1, no. Suppl_1, pp. S26-34, Nov. 2014.

[30] P. M. Kluding *et al.*, "Foot drop stimulation versus ankle foot orthosis after stroke: 30-week outcomes.," *Stroke.*, vol. 44, no. 6, pp. 1660–9, Jun. 2013.

[31] C. Marini, T. Russo, and G. Felzani, "Incidence of stroke in young adults: a review.," *Stroke Res. Treat.*, vol. 2011, p. 535672, Jan. 2010.

[32] D. Griffiths and J. Sturm, "Epidemiology and etiology of young stroke.," *Stroke Res. Treat.*, vol. 2011, p. 209370, Jan. 2011.

[33] J. Perry, *Gait Analysis: Normal and Pathological Function*, vol. 12. 2010.

[34] C. L. Peterson, A. L. Hall, S. A. Kautz, and R. R. Neptune, "Pre-swing deficits in forward propulsion, swing initiation and power generation by individual muscles during hemiparetic walking.," *J. Biomech.*, vol. 43, no. 12, pp. 2348–2355, Aug. 2010.

[35] S. Nadeau, D. Gravel, A. B. Arsenault, and D. Bourbonnais, "Plantarflexor weakness as a limiting factor of gait speed in stroke subjects and the compensating role of hip flexors.," *Clin. Biomech. (Bristol, Avon)*, vol. 14, no. 2, pp. 125–135, Feb. 1999.

[36] A. L. Hall, C. L. Peterson, S. A. Kautz, and R. R. Neptune, "Relationships between muscle contributions to walking subtasks and functional walking status in persons with post-stroke hemiparesis.," *Clin. Biomech. (Bristol, Avon)*, vol. 26, no. 5, pp. 509–515, Jun. 2011.

[37] P.-Y. Lin, Y.-R. Yang, S.-J. Cheng, and R.-Y. Wang, "The Relation Between Ankle Impairments and Gait Velocity and Symmetry in People With Stroke," *Arch. Phys. Med. Rehabil.*, vol. 87, no. 4, pp. 562–568, Apr. 2006.

[38] V. Weerdesteyn, M. de Niet, H. J. R. van Duijnhoven, and A. C. H. Geurts, "Falls in individuals with stroke.," *J. Rehabil. Res. Dev.*, vol. 45, no. 8, pp. 1195–213, 2008.

[39] H. Hsiao, L. N. Awad, J. A. Palmer, J. S. Higginson, and S. A. Binder-Macleod, "Contribution of paretic and non-paretic limb peak propulsive forces to changes in walking speed in individuals poststroke," *Neurorehabil. Neural Repair*, vol. 30, no. 8, pp. 743–752, Sep. 2016.

[40] G. Stoquart, C. Detrembleur, and T. M. Lejeune, "The reasons why stroke patients expend so much energy to walk slowly," *Gait Posture*, vol. 36, no. 3, pp. 409–413, 2012.

[41] A. Vistamehr, S. A. Kautz, and R. R. Neptune, "The influence of solid ankle-foot-orthoses on forward propulsion and dynamic balance in healthy adults during walking," *Clin. Biomech.*, vol. 29, no. 5, pp. 583–589, May 2014.

[42] R. van Swigchem, M. Roerdink, V. Weerdesteyn, A. C. Geurts, and A. Daffertshofer, "The Capacity to Restore Steady Gait After a Step Modification Is Reduced in People With Poststroke Foot Drop Using an Ankle-Foot Orthosis," *Phys. Ther.*, vol. 94, no. 5, pp. 654–663, May 2014.

[43] A. I. R. Kottink, L. J. M. Oostendorp, J. H. Buurke, A. V. Nene, H. J. Hermens, and M. J. IJzerman, *The orthotic effect of functional electrical stimulation on the improvement of walking in stroke patients with a dropped foot: A systematic review*, vol. 28, no. 6. Blackwell Science Inc, 2004, pp. 577–586.

[44] A. P. McGinn *et al.*, "Walking speed and risk of incident ischemic stroke among postmenopausal women," *Stroke*, vol. 39, no. 4, pp. 1233–1239, 2008.

[45] T. M. Kesar *et al.*, "Functional electrical stimulation of ankle plantarflexor and dorsiflexor muscles: Effects on poststroke gait," *Stroke*, 2009.

[46] M. R. Popovic, A. Curt, T. Keller, and V. Dietz, "Functional electrical stimulation for grasping and walking: Indications and limitations," *Spinal Cord*. 2001.

[47] J.-M. Belda-Lois *et al.*, "Rehabilitation of gait after stroke: a review towards a top-down approach.," *J. Neuroeng. Rehabil.*, vol. 8, no. 1, p. 66, Jan. 2011.

[48] A. Pollock *et al.*, "Physical rehabilitation approaches for the recovery of function and mobility following stroke.," *Cochrane database Syst. Rev.*, no. 4, p. CD001920, Apr. 2014.

[49] S. Lennon, "The Bobath concept: a critical review of the theoretical assumptions that guide physiotherapy practice in stroke rehabilitation," *Phys. Ther. Rev.*, vol. 1, no. 1, pp. 35–45, Sep. 1996.

[50] J. H. Carr and R. B. Shepherd, "A Motor Learning Model for Stroke Rehabilitation," *Physiother. (United Kingdom)*, vol. 75, no. 7, pp. 372–380, 1989.

[51] T. George Hornby *et al.*, "Importance of Specificity, Amount, and Intensity of Locomotor Training to Improve Ambulatory Function in Patients Poststroke," *Top. Stroke Rehabil.*, vol. 18, no. 4, pp. 293–307, 2011.

[52] P. Langhorne, J. Bernhardt, and G. Kwakkel, "Stroke rehabilitation.," *Lancet (London, England)*, vol. 377, no. 9778, pp. 1693–1702, May 2011.

[53] J. H. Carr, *Neurological rehabilitation : optimizing motor performance / Janet H. Carr, Roberta B. Shepherd*. Edinburgh ; New York: Churchill Livingstone, 2010.

[54] R. P. S. Van Peppen, G. Kwakkel, S. Wood-Dauphinee, H. J. M. Hendriks, P. J. Van der Wees, and J. Dekker, "The impact of physical therapy on functional outcomes after stroke: what's the evidence?," *Clin. Rehabil.*, vol. 18, no. 8, pp. 833–862, Dec. 2004.

[55] N. M. Salbach, N. E. Mayo, S. Wood-Dauphinee, J. A. Hanley, C. L. Richards, and R. Cote, "A task-orientated intervention enhances walking distance and speed in the first year post stroke: a randomized controlled trial.," *Clin. Rehabil.*, vol. 18, no. 5, pp. 509–519, Aug. 2004.

[56] L. Legg, A. Pollock, P. Langhorne, and C. Sellars, "A multidisciplinary research agenda for stroke rehabilitation," *Br. J. Ther. Rehabil.*, vol. 7, no. 7, pp. 319–324, 2000.

[57] B. French *et al.*, "Repetitive task training for improving functional ability after stroke," *Cochrane database Syst. Rev.*, vol. 11, p. CD006073, Nov. 2016.

[58] G. Kwakkel *et al.*, "Effects of augmented exercise therapy time after stroke: a meta-analysis.," *Stroke*, vol. 35, no. 11, pp. 2529–2539, Nov. 2004.

[59] M. Pohl, J. Mehrholz, C. Ritschel, and S. Ruckriem, “Speed-dependent treadmill training in ambulatory hemiparetic stroke patients: a randomized controlled trial.,” *Stroke*, vol. 33, no. 2, pp. 553–558, Feb. 2002.

[60] K. J. Sullivan, B. J. Knowlton, and B. H. Dobkin, “Step training with body weight support: effect of treadmill speed and practice paradigms on poststroke locomotor recovery.,” *Arch. Phys. Med. Rehabil.*, vol. 83, no. 5, pp. 683–691, May 2002.

[61] M. M. Ardestani, C. R. Kinnaird, C. E. Henderson, and T. G. Hornby, “Compensation or Recovery? Altered Kinetics and Neuromuscular Synergies Following High-Intensity Stepping Training Poststroke,” *Neurorehabil. Neural Repair*, vol. 33, no. 1, pp. 47–58, 2018.

[62] T. George Hornby *et al.*, “Clinical practice guideline to improve locomotor function following chronic stroke, incomplete spinal cord injury and brain injury.”

[63] R. A. States, Y. Salem, and E. Pappas, “Overground gait training for individuals with chronic stroke: a Cochrane systematic review.,” *J. Neurol. Phys. Ther.*, vol. 33, no. 4, pp. 179–186, Dec. 2009.

[64] J. Mehrholz, M. Pohl, and B. Elsner, “Treadmill training and body weight support for walking after stroke.,” *Cochrane database Syst. Rev.*, no. 1, p. CD002840, Jan. 2014.

[65] D. H. Saunders *et al.*, “Physical fitness training for stroke patients.,” *Cochrane database Syst. Rev.*, vol. 3, p. CD003316, Mar. 2016.

[66] I. Díaz, J. J. Gil, and E. Sánchez, “Lower-Limb Robotic Rehabilitation: Literature Review and Challenges,” *J. Robot.*, vol. 2011, no. i, pp. 1–11, 2011.

[67] A. Pennycott, D. Wyss, H. Vallery, V. Klamroth-Marganska, and R. Riener, “Towards more effective robotic gait training for stroke rehabilitation: a review,” *J. Neuroeng. Rehabil.*, vol. 9, p. 65, Jan. 2012.

[68] A. M. Dollar and H. Herr, “Lower extremity exoskeletons and active orthoses: challenges and state-of-the-art,” *Robot. IEEE Trans.*, vol. 24, no. 1, pp. 144–158, 2008.

[69] R. Gassert and V. Dietz, “Rehabilitation robots for the treatment of sensorimotor deficits: A neurophysiological perspective,” *J. Neuroeng. Rehabil.*, vol. 15, no. 1, pp. 1–15, 2018.

[70] S. Jezernik, G. Colombo, T. Keller, H. Frueh, and M. Morari, “Robotic orthosis lokomat: a rehabilitation and research tool.,” *Neuromodulation*, vol. 6, no. 2, pp. 108–15, Apr. 2003.

[71] A. Duschau-Wicke, J. Von Zitzewitz, A. Caprez, L. Lünenburger, and R. Riener, “Path control: A method for patient-cooperative robot-aided gait rehabilitation,” *IEEE Trans. Neural Syst. Rehabil. Eng.*, 2010.

[72] J. F. Veneman *et al.*, “Design and Evaluation of the LOPES Exoskeleton Robot for Interactive Gait Rehabilitation,” *IEEE Trans. Neural Syst. Rehabil. Eng.*, vol. 15, no. 3, pp. 379–386, Sep. 2007.

[73] S. Hesse and D. Uhlenbrock, “A mechanized gait trainer for restoration of gait.,” *J. Rehabil. Res. Dev.*, vol. 37, no. 6, pp. 701–708, 2000.

[74] J. Kang, V. Vashista, and S. K. Agrawal, “On the Adaptation of Pelvic Motion by Applying 3-dimensional Guidance Forces Using TPAD.,” *IEEE Trans. Neural Syst. Rehabil. Eng.*, vol. 25, no.

9, pp. 1558–1567, Sep. 2017.

[75] R. Dickstein, “Rehabilitation of gait speed after stroke: a critical review of intervention approaches.,” *Neurorehabil. Neural Repair*, vol. 22, no. 6, pp. 649–660, 2008.

[76] J. E. Sullivan, L. E. Espe, A. M. Kelly, L. E. Veilbig, and M. J. Kwasny, “Feasibility and outcomes of a community-based, pedometer-monitored walking program in chronic stroke: a pilot study.,” *Top. Stroke Rehabil.*, vol. 21, no. 2, pp. 101–110, 2014.

[77] V. Klamroth-Marganska *et al.*, “Three-dimensional, task-specific robot therapy of the arm after stroke: a multicentre, parallel-group randomised trial.,” *Lancet. Neurol.*, 2014.

[78] C. Tefertiller, B. Pharo, N. Evans, and P. Winchester, “Efficacy of rehabilitation robotics for walking training in neurological disorders: A review,” *J. Rehabil. Res. Dev.*, 2011.

[79] A. T. Asbeck, R. J. Dyer, A. F. Larusson, and C. J. Walsh, “Biologically-inspired soft exosuit,” in *IEEE International Conference on Rehabilitation Robotics*, 2013.

[80] A. T. Asbeck, S. M. M. M. De Rossi, I. Galiana, Y. Ding, and C. J. Walsh, “Stronger, smarter, softer: Next-generation wearable robots,” *IEEE Robot. Autom. Mag.*, vol. 21, no. 4, pp. 22–33, 2014.

[81] G. Lee *et al.*, “Improved assistive profile tracking of soft exosuits for walking and jogging with off-board actuation,” in *2017 IEEE/RSJ International Conference on Intelligent Robots and Systems (IROS)*, 2017, pp. 1699–1706.

[82] P. Malcolm *et al.*, “Varying negative work assistance at the ankle with a soft exosuit during loaded walking,” *J. Neuroeng. Rehabil.*, vol. 14, no. 1, p. 62, 2017.

[83] P. Malcolm *et al.*, “Continuous sweep versus discrete step protocols for studying effects of wearable robot assistance magnitude,” *J. Neuroeng. Rehabil.*, vol. 14, no. 1, pp. 1–13, 2017.

[84] G. Lee *et al.*, “Reducing the metabolic cost of running with a tethered soft exosuit,” *Sci. Robot.*, vol. 2, 2017.

[85] Y. Ding, M. Kim, S. Kuindersma, and C. J. Walsh, “Human-in-the-loop optimization of hip assistance with a soft exosuit during walking,” *Sci. Robot.*, vol. 3, no. 15, p. eaar5438, 2018.

[86] J. Kim *et al.*, “Autonomous and Portable Soft Exosuit for Hip Extension Assistance with Online Walking and Running Detection Algorithm,” in *2018 IEEE International Conference on Robotics and Automation (ICRA)*, 2018, pp. 1–8.

[87] F. A. Panizzolo *et al.*, “A biologically-inspired multi-joint soft exosuit that can reduce the energy cost of loaded walking,” *J. Neuroeng. Rehabil.*, vol. 13, no. 1, p. 43, Dec. 2016.

[88] S. Lee *et al.*, “Autonomous multi-joint soft exosuit with augmentation-power-based control parameter tuning reduces energy cost of loaded walking,” *J. Neuroeng. Rehabil.*, vol. 15, no. 1, p. 66, 2018.

[89] S. Lee *et al.*, “Autonomous Multi-Joint Soft Exosuit for Assistance with Walking Overground,” in *2018 IEEE International Conference on Robotics and Automation (ICRA)*, 2018, pp. 2812–2819.

[90] L. N. Awad *et al.*, “A soft robotic exosuit improves walking after stroke,” *Sci. Transl. Med.*, vol. 9, no. July, 2017.

[91] A. T. Asbeck, S. M. M. M. De Rossi, K. G. Holt, and C. J. Walsh, “A biologically inspired soft exosuit for walking assistance,” *Int. J. Rob. Res.*, vol. 34, no. 6, pp. 744–762, 2015.

[92] J. Bae *et al.*, “Biomechanical mechanisms underlying exosuit-induced improvements in walking economy after stroke,” *J. Exp. Biol.*, p. jeb.168815, 2018.

[93] J. Bae *et al.*, “A lightweight and efficient portable soft exosuit for paretic ankle assistance in walking after stroke,” in *Robotics and Automation (ICRA), 2018 IEEE International Conference on*, 2018, pp. 2820–2827.

[94] A. T. Asbeck, K. Schmidt, I. Galiana, and C. J. Walsh, “Multi-joint Soft Exosuit for Gait Assistance,” in *Robotics and Automation (ICRA), 2015 IEEE International Conference on*, 2015.

[95] Y. Ding, I. Galiana, A. Asbeck, B. Quinlivan, S. M. M. De Rossi, and C. Walsh, “Multi-joint actuation platform for lower extremity soft exosuits,” in *Robotics and Automation (ICRA), 2014 IEEE International Conference on*, 2014, pp. 1327–1334.

[96] S. Lee, S. Crea, P. Malcolm, I. Galiana, A. Asbeck, and C. Walsh, “Controlling negative and positive power at the ankle with a soft exosuit,” in *Proceedings - IEEE International Conference on Robotics and Automation*, 2016, vol. 2016-June, pp. 3509–3515.

[97] Y. Ding *et al.*, “Effect of timing of hip extension assistance during loaded walking with a soft exosuit,” *J. Neuroeng. Rehabil.*, vol. 13, no. 1, p. 87, 2016.

[98] Y. Ding, I. Galiana, C. Siviy, F. A. Panizzolo, and C. Walsh, “IMU-based iterative control for hip extension assistance with a soft exosuit,” in *Proceedings - IEEE International Conference on Robotics and Automation*, 2016, vol. 2016-June, pp. 3501–3508.

[99] Y. Ding *et al.*, “Biomechanical and physiological evaluation of multi-joint assistance with soft exosuits,” *IEEE Trans. Neural Syst. Rehabil. Eng.*, vol. 25, no. 2, pp. 119–130, 2017.

[100] B. T. Quinlivan *et al.*, “Assistance magnitude versus metabolic cost reductions for a tethered multiarticular soft exosuit,” *Sci. Robot.*, vol. 2, no. 2, p. eaah4416, 2017.

[101] I. Skog, P. Händel, J. O. Nilsson, and J. Rantakokko, “Zero-velocity detection-An algorithm evaluation,” *IEEE Trans. Biomed. Eng.*, vol. 57, no. 11, pp. 2657–2666, 2010.

[102] A. R. Jiménez, F. Seco, C. Prieto, and J. Guevara, “A comparison of pedestrian dead-reckoning algorithms using a low-cost MEMS IMU,” *WISP 2009 - 6th IEEE Int. Symp. Intell. Signal Process. - Proc.*, no. May 2014, pp. 37–42, 2009.

[103] M. Wehner *et al.*, “A lightweight soft exosuit for gait assistance,” *Proc. - IEEE Int. Conf. Robot. Autom.*, pp. 3362–3369, 2013.

[104] P. Polygerinos, Z. Wang, K. C. Galloway, R. J. Wood, and C. J. Walsh, “Soft robotic glove for combined assistance and at-home rehabilitation,” *Rob. Auton. Syst.*, Sep. 2014.

[105] P. Polygerinos, K. C. Galloway, E. Savage, M. Herman, K. O’Donnell, and C. J. Walsh, “Soft Robotic Glove for Hand Rehabilitation and Task Specific Training,” in *Robotics and Automation (ICRA), 2015 IEEE International Confernce on*, 2015.

[106] M. R. Tucker *et al.*, “Control strategies for active lower extremity prosthetics and orthotics: a review.,” *J. Neuroeng. Rehabil.*, vol. 12, no. 1, p. 1, 2015.

[107] J. Rueterbories, E. G. Spaich, B. Larsen, and O. K. Andersen, "Methods for gait event detection and analysis in ambulatory systems.," *Med. Eng. Phys.*, vol. 32, no. 6, pp. 545–52, Jul. 2010.

[108] H. Lau and K. Tong, "The reliability of using accelerometer and gyroscope for gait event identification on persons with dropped foot," *Gait Posture*, vol. 27, no. 2, pp. 248–257, 2008.

[109] B. R. Greene *et al.*, "An adaptive gyroscope-based algorithm for temporal gait analysis," *Med. Biol. Eng. Comput.*, vol. 48, no. 12, pp. 1251–1260, Dec. 2010.

[110] K. K. Patterson *et al.*, "Gait asymmetry in community-ambulating stroke survivors.," *Arch. Phys. Med. Rehabil.*, vol. 89, no. 2, pp. 304–310, Feb. 2008.

[111] S. Lauzière, M. Betschart, R. Aissaoui, and S. Nadeau, "Understanding Spatial and Temporal Gait Asymmetries in Individuals Post Stroke," *Int. J. Phys. Med. Rehabil.*, vol. 02, no. 03, 2014.

[112] M. M. G. M. Bowden, C. C. K. C. Balasubramanian, R. R. Neptune, and S. a. Kautz, "Anterior-posterior ground reaction forces as a measure of paretic leg contribution in hemiparetic walking," *Stroke*, vol. 37, no. 3, pp. 872–6, Mar. 2006.

[113] L. L. N. Awad, D. D. S. Reisman, T. M. Kesar, and S. A. Binder-Macleod, "Targeting Paretic Propulsion to Improve Poststroke Walking Function: A Preliminary Study," *Arch. Phys. Med. Rehabil.*, vol. 95, no. 5, pp. 840–8, May 2014.

[114] M. Goldfarb, B. E. Lawson, and A. H. Shultz, "Realizing the promise of robotic leg prostheses.," *Sci. Transl. Med.*, vol. 5, no. 210, p. 210ps15, Nov. 2013.

[115] D. R. Louie, J. J. Eng, and T. Lam, "Gait speed using powered robotic exoskeletons after spinal cord injury: a systematic review and correlational study.," *J. Neuroeng. Rehabil.*, vol. 12, p. 82, Jan. 2015.

[116] A. J. Veale and S. Q. Xie, "Towards compliant and wearable robotic orthoses: A review of current and emerging actuator technologies.," *Med. Eng. Phys.*, Feb. 2016.

[117] F. Panizzolo *et al.*, "Evaluation of a multi-joint soft exosuit for gait assistance," in *7th International Symposium on Adaptive Motion of Animals and Machines (AMAM)*, 2015.

[118] L. N. Awad, D. S. Reisman, R. T. Pohlig, and S. A. Binder-Macleod, "Reducing The Cost of Transport and Increasing Walking Distance After Stroke," *Neurorehabil. Neural Repair*, vol. 30, no. 7, pp. 661–670, Aug. 2016.

[119] K. Z. Takahashi, M. D. Lewek, and G. S. Sawicki, "A neuromechanics-based powered ankle exoskeleton to assist walking post-stroke: a feasibility study," *J. Neuroeng. Rehabil.*, vol. 12, no. 1, p. 23, 2015.

[120] A. Middleton, S. L. Fritz, and M. Lusardi, "Walking speed: the functional vital sign.," *J. Aging Phys. Act.*, vol. 23, no. 2, pp. 314–22, Apr. 2015.

[121] L. N. Awad, S. A. Binder-Macleod, R. T. Pohlig, and D. S. Reisman, "Paretic Propulsion and Trailing Limb Angle Are Key Determinants of Long-Distance Walking Function after Stroke," *Neurorehabil. Neural Repair*, vol. 29, no. 6, pp. 499–508, Nov. 2015.

[122] H. Hsiao, B. A. Knarr, J. S. Higginson, and S. A. Binder-Macleod, "Mechanisms to increase propulsive force for individuals poststroke.," *J. Neuroeng. Rehabil.*, vol. 12, p. 40, 2015.

[123] H. Hsiao, B. A. Knarr, J. S. Higginson, and S. A. Binder-Macleod, "The relative contribution of ankle moment and trailing limb angle to propulsive force during gait.," *Hum. Mov. Sci.*, vol. 39, pp. 212–21, Feb. 2015.

[124] H. Hsiao, J. S. Higginson, and S. A. Binder-Macleod, "Baseline predictors of treatment gains in peak propulsive force in individuals poststroke.," *J. Neuroeng. Rehabil.*, vol. 13, no. 1, p. 2, Jan. 2016.

[125] D. A. D. a. D. a. Winter, *Biomechanics and Motor Control of Human Movement*, vol. 2nd, no. Book, Whole. 2009.

[126] R. L. Waters and S. Mulroy, "The energy expenditure of normal and pathologic gait," *Gait Posture*, vol. 9, no. 3, pp. 207–231, 1999.

[127] M. G. Bowden, A. L. Behrman, M. Woodbury, C. M. Gregory, C. A. Velozo, and S. A. Kautz, "Advancing measurement of locomotor rehabilitation outcomes to optimize interventions and differentiate between recovery versus compensation," *Journal of Neurologic Physical Therapy*, vol. 36, no. 1. pp. 38–44, 2012.

[128] T. M. Kesar, S. A. Binder-Macleod, G. E. Hicks, and D. S. Reisman, "Minimal detectable change for gait variables collected during treadmill walking in individuals post-stroke," *Gait Posture*, vol. 33, no. 2, pp. 314–7, Feb. 2011.

[129] H. Hsiao, B. A. Knarr, R. T. Pohlig, J. S. Higginson, and S. A. Binder-Macleod, "Mechanisms used to increase peak propulsive force following 12-weeks of gait training in individuals poststroke," *J. Biomech.*, vol. 49, no. 3, pp. 388–395, 2016.

[130] J. Skidmore and P. Artemiadis, "On the effect of walking surface stiffness on inter-limb coordination in human walking: toward bilaterally informed robotic gait rehabilitation.," *J. Neuroeng. Rehabil.*, vol. 13, no. 1, p. 32, Jan. 2016.

[131] S. J. Mulroy, T. Klassen, J. K. Gronley, V. J. Eberly, D. A. Brown, and K. J. Sullivan, "Gait parameters associated with responsiveness to treadmill training with body-weight support after stroke: an exploratory study.," *Phys. Ther.*, vol. 90, no. 2, pp. 209–223, Feb. 2010.

[132] C. L. Peterson, J. Cheng, S. A. Kautz, and R. R. Neptune, "Leg extension is an important predictor of paretic leg propulsion in hemiparetic walking.," *Gait Posture*, vol. 32, no. 4, pp. 451–456, Oct. 2010.

[133] R. R. Neptune, S. A. Kautz, and F. E. Zajac, "Contributions of the individual ankle plantar flexors to support, forward progression and swing initiation during walking.," *J. Biomech.*, vol. 34, no. 11, pp. 1387–1398, Nov. 2001.

[134] M. G. Bowden, C. K. Balasubramanian, A. L. Behrman, and S. A. Kautz, "Validation of a speed-based classification system using quantitative measures of walking performance poststroke.," *Neurorehabil. Neural Repair*, vol. 22, no. 6, pp. 672–5.

[135] C. J. Wutzke, G. S. Sawicki, and M. D. Lewek, "The influence of a unilateral fixed ankle on metabolic and mechanical demands during walking in unimpaired young adults.," *J. Biomech.*, vol. 45, no. 14, pp. 2405–10, Sep. 2012.

[136] D. M. Wert, J. S. Brach, S. Perera, and J. VanSwearingen, "The association between energy cost of walking and physical function in older adults.," *Arch. Gerontol. Geriatr.*, vol. 57, no. 2, pp.

198–203, Jan. 2013.

[137] R. Lapointe, Y. Lajoie, O. Serresse, and H. Barbeau, “Functional community ambulation requirements in incomplete spinal cord injured subjects.,” *Spinal Cord*, vol. 39, no. 6, pp. 327–35, Jun. 2001.

[138] M. Franceschini, A. Rampello, M. Agosti, M. Massucci, F. Bovolenta, and P. Sale, “Walking performance: correlation between energy cost of walking and walking participation. new statistical approach concerning outcome measurement.,” *PLoS One*, vol. 8, no. 2, p. e56669, Jan. 2013.

[139] J. L. Moore, E. J. Roth, C. Killian, and T. G. Hornby, “Locomotor training improves daily stepping activity and gait efficiency in individuals poststroke who have reached a ‘plateau’ in recovery.,” *Stroke.*, vol. 41, no. 1, pp. 129–35, Jan. 2010.

[140] J. A. Schrack, V. Zipunnikov, E. M. Simonsick, S. Studenski, and L. Ferrucci, “Rising Energetic Cost of Walking Predicts Gait Speed Decline With Aging.,” *J. Gerontol. A. Biol. Sci. Med. Sci.*, p. glw002, Feb. 2016.

[141] S. Studenski *et al.*, “Gait speed and survival in older adults.,” *JAMA*, vol. 305, no. 1, pp. 50–8, Jan. 2011.

[142] B. A. Franklin, J. Brinks, R. Sacks, J. Trivax, and H. Friedman, “Reduced walking speed and distance as harbingers of the approaching grim reaper.,” *Am. J. Cardiol.*, vol. 116, no. 2, pp. 313–7, Jul. 2015.

[143] M. W. Brault, “Americans With Disabilities: 2010, Current Population Reports P70-131,” Washington, DC, 2012.

[144] D. Borton, S. Micera, J. del R. Millán, and G. Courtine, “Personalized neuroprosthetics.,” *Sci. Transl. Med.*, vol. 5, no. 210, p. 210rv2, Nov. 2013.

[145] T. M. Kesar, D. S. Reisman, J. S. Higginson, L. N. Awad, and S. A. Binder-Macleod, “Changes in Post-Stroke Gait Biomechanics Induced by One Session of Gait Training,” *Phys. Med. Rehabil. - Int.*, vol. 2, no. 10, p. 1072, 2015.

[146] C. P. Phadke, “Immediate effects of a single inclined treadmill walking session on level ground walking in individuals after stroke.,” *Am. J. Phys. Med. Rehabil.*, vol. 91, no. 4, pp. 337–45, Apr. 2012.

[147] R. L. Routson, D. J. Clark, M. G. Bowden, S. A. Kautz, and R. R. Neptune, “The influence of locomotor rehabilitation on module quality and post-stroke hemiparetic walking performance.,” *Gait Posture*, vol. 38, no. 3, pp. 511–7, Jul. 2013.

[148] K. R. Lohse, C. E. Lang, and L. A. Boyd, “Is more better? Using metadata to explore dose-response relationships in stroke rehabilitation.,” *Stroke.*, vol. 45, no. 7, pp. 2053–8, Jul. 2014.

[149] A. A. Schmid *et al.*, “Balance and balance self-efficacy are associated with activity and participation after stroke: a cross-sectional study in people with chronic stroke,” *Arch. Phys. Med. Rehabil.*, vol. 93, no. 6, pp. 1101–1107, Jun. 2012.

[150] A. Norlander *et al.*, “Long-Term Predictors of Social and Leisure Activity 10 Years after Stroke,” *PLoS One*, vol. 11, no. 2, p. e0149395, 2016.

[151] J. A. Kleim and T. A. Jones, “Principles of experience-dependent neural plasticity: implications

for rehabilitation after brain damage.," *J. Speech. Lang. Hear. Res.*, vol. 51, no. 1, pp. S225-39, Feb. 2008.

[152] L. R. Sheffler and J. Chae, "Technological advances in interventions to enhance poststroke gait.," *Phys. Med. Rehabil. Clin. N. Am.*, vol. 24, no. 2, pp. 305–23, May 2013.

[153] L. W. Forrester, A. Roy, C. Hafer-Macko, H. I. Krebs, and R. F. Macko, "Task-specific ankle robotics gait training after stroke: a randomized pilot study.," *J. Neuroeng. Rehabil.*, vol. 13, no. 1, p. 51, 2016.

[154] R. C. Browning, J. R. Modica, R. Kram, and A. Goswami, "The effects of adding mass to the legs on the energetics and biomechanics of walking," *Med. Sci. Sports Exerc.*, vol. 39, no. 3, pp. 515–525, 2007.

[155] K. Kempski, L. N. Awad, T. S. Buchanan, J. S. Higginson, and B. A. Knarr, "Dynamic Structure of Lower Limb Joint Angles during Walking Post-Stroke," *J. Biomech.*, 2017.

[156] K. A. Shorter, A. Wu, and A. D. Kuo, "The high cost of swing leg circumduction during human walking," *Gait Posture*, 2017.

[157] A. Morbi *et al.*, "Design, Control, and Implementation of a Robotic Gait Rehabilitation System for Overground Gait Training," Elsevier B.V., New York, New York, USA, United States, 2014.

[158] V. A. Stanhope, B. A. Knarr, D. S. Reisman, and J. S. Higginson, "Frontal plane compensatory strategies associated with self-selected walking speed in individuals post-stroke," *Clin. Biomech.*, 2014.

[159] C. M. Tyrell, M. A. Roos, K. S. Rudolph, and D. S. Reisman, "Influence of Systematic Increases in Treadmill Walking Speed on Gait Kinematics After Stroke," *Phys. Ther.*, 2011.

[160] B. A. Knarr, T. M. Kesar, D. S. Reisman, S. A. Binder-Macleod, and J. S. Higginson, "Changes in the activation and function of the ankle plantar flexor muscles due to gait retraining in chronic stroke survivors.," *J. Neuroeng. Rehabil.*, 2013.

[161] K. E. Zelik and P. G. Adamczyk, "A unified perspective on ankle push-off in human walking," *J. Exp. Biol.*, vol. 219, no. 23, pp. 3676–3683, 2016.

[162] G. B. Mahtani *et al.*, "Altered Sagittal- and Frontal-Plane Kinematics Following High-Intensity Stepping Training Versus Conventional Interventions in Subacute Stroke," *Phys. Ther.*, 2016.

[163] P. G. Adamczyk and A. D. Kuo, "Redirection of center-of-mass velocity during the step-to-step transition of human walking," *J. Exp. Biol.*, vol. 212, no. Pt 16, pp. 2668–2678, Aug. 2009.

[164] J. M. Donelan, R. Kram, and A. D. Kuo, "Mechanical work for step-to-step transitions is a major determinant of the metabolic cost of human walking," *J. Exp. Biol.*, vol. 205, no. 23, pp. 3717–3727, 2002.

[165] A. D. Kuo, J. M. Donelan, and A. Ruina, "Energetic consequences of walking like an inverted pendulum: step-to-step transitions.," *Exerc. Sport Sci. Rev.*, vol. 33, no. 2, pp. 88–97, 2005.

[166] H. Geyer, A. Seyfarth, and R. Blickhan, "Compliant leg behaviour explains basic dynamics of walking and running.," *Proc. Biol. Sci.*, vol. 273, no. 1603, pp. 2861–2867, 2006.

[167] C. H. Soo and J. M. Donelan, "Coordination of push-off and collision determine the mechanical

work of step-to-step transitions when isolated from human walking," *Gait Posture*, vol. 35, no. 2, pp. 292–297, 2012.

[168] R. G. Ellis, K. C. Howard, and R. Kram, "The metabolic and mechanical costs of step time asymmetry in walking.," *Proc. Biol. Sci.*, vol. 280, no. 1756, p. 20122784, 2013.

[169] X. Bonnet, C. Villa, P. Fode, F. Lavaste, and H. Pillet, "Mechanical work performed by individual limbs of transfemoral amputees during step-to-step transitions: Effect of walking velocity," *Proc. Inst. Mech. Eng. H.*, vol. 228, no. 1, pp. 60–66, 2014.

[170] H. C. Doets, D. Vergouw, H. E. J. (Dirkjan) Veeger, and H. Houdijk, "Metabolic cost and mechanical work for the step-to-step transition in walking after successful total ankle arthroplasty," *Hum. Mov. Sci.*, vol. 28, no. 6, pp. 786–797, 2009.

[171] J. Feng, R. Pierce, K. P. Do, and M. Aiona, "Motion of the center of mass in children with spastic hemiplegia: Balance, energy transfer, and work performed by the affected leg vs. the unaffected leg," *Gait Posture*, vol. 39, no. 1, pp. 570–576, 2014.

[172] H. Houdijk, E. Pollmann, M. Groenewold, H. Wiggerts, and W. Polomski, "The energy cost for the step-to-step transition in amputee walking," *Gait Posture*, vol. 30, no. 1, pp. 35–40, Jul. 2009.

[173] A. Lamontagne, J. L. Stephenson, and J. Fung, "Physiological evaluation of gait disturbances post stroke," *Clin. Neurophysiol.*, vol. 118, no. 4, pp. 717–729, Apr. 2007.

[174] L. J. Turns, R. R. Neptune, S. A. Kautz, J. Duysens, D. McAllister, and G. S. Beaupre, "Relationships Between Muscle Activity and Anteroposterior Ground Reaction Forces in Hemiparetic Walking," *Arch. Phys. Med. Rehabil.*, vol. 88, no. 9, pp. 1127–1135, Sep. 2007.

[175] L. N. Awad, J. A. Palmer, R. T. Pohlig, S. A. Binder-Macleod, and D. S. Reisman, "Walking speed and step length asymmetry modify the energy cost of walking after stroke," *Neurorehabil. Neural Repair*, vol. 29, no. 5, pp. 416–423, Oct. 2015.

[176] J. M. Finley and A. J. Bastian, "Associations between Foot Placement Asymmetries and Metabolic Cost of Transport in Hemiparetic Gait," *Neurorehabil. Neural Repair*, vol. 31, no. 2, pp. 168–177, 2017.

[177] K. E. Zelik and A. D. Kuo, "Human walking isn't all hard work: evidence of soft tissue contributions to energy dissipation and return," *J. Exp. Biol.*, vol. 213, no. 24, pp. 4257–4264, 2010.

[178] K. E. Zelik, K. Z. Takahashi, and G. S. Sawicki, "Six degree-of-freedom analysis of hip, knee, ankle and foot provides updated understanding of biomechanical work during human walking.," *J. Exp. Biol.*, vol. 218, no. Pt 6, pp. 876–886, 2015.

[179] J. M. Brockway, "Derivation of formulae used to calculate energy expenditure in man.," *Hum. Nutr. Clin. Nutr.*, 1987.

[180] C. E. Mahon, D. J. Farris, G. S. Sawicki, and M. D. Lewek, "Individual limb mechanical analysis of gait following stroke," *J. Biomech.*, vol. 48, no. 6, pp. 984–989, 2015.

[181] S. H. Collins, M. Bruce Wiggin, and G. S. Sawicki, "Reducing the energy cost of human walking using an unpowered exoskeleton," *Nature*, vol. 522, no. 7555, pp. 212–215, 2015.

[182] L. N. Awad *et al.*, "Reducing Circumduction and Hip Hiking During Hemiparetic Walking

Through Targeted Assistance of the Paretic Limb Using a Soft Robotic Exosuit.," *Am. J. Phys. Med. Rehabil.*, vol. 96, no. 10, pp. 157–164, 2017.

[183] K. Z. Takahashi, T. M. Kepple, and S. J. Stanhope, "A unified deformable (UD) segment model for quantifying total power of anatomical and prosthetic below-knee structures during stance in gait," *J. Biomech.*, vol. 45, no. 15, pp. 2662–2667, 2012.

[184] P. Malcolm, W. Derave, S. Galle, and D. De Clercq, "A Simple Exoskeleton That Assists Plantarflexion Can Reduce the Metabolic Cost of Human Walking," *PLoS One*, vol. 8, no. 2, Feb. 2013.

[185] L. M. Mooney, E. J. Rouse, and H. M. Herr, "Autonomous exoskeleton reduces metabolic cost of human walking," vol. 11, no. 1, pp. 1–5, 2014.

[186] C. Duclos, S. Nadeau, N. Bourgeois, L. Bouyer, and C. L. Richards, "Effects of walking with loads above the ankle on gait parameters of persons with hemiparesis after stroke," *Clin. Biomech.*, vol. 29, no. 3, pp. 265–271, Mar. 2014.

[187] J. Bae *et al.*, "A soft exosuit for patients with stroke: Feasibility study with a mobile off-board actuation unit," in *Rehabilitation Robotics (ICORR), 2015 IEEE International Conference on*, 2015, pp. 131–138.

[188] D. C. Kerrigan, H. M. Abdulhadi, T. A. Ribaudo, and U. Della Croce, "Biomechanic effects of a contralateral shoe-lift on walking with an immobilized knee," *Arch. Phys. Med. Rehabil.*, vol. 78, no. 10, pp. 1085–1091, 1997.

[189] B. Quinlivan, A. Asbeck, D. Wagner, T. Ranzani, S. Russo, and C. J. Walsh, "Force Transfer Characterization of a Soft Exosuit for Gait Assistance," *Vol. 5A 39th Mech. Robot. Conf.*, p. V05AT08A049, 2015.

[190] P. O. Riley, G. Paolini, U. Della Croce, K. W. Paylo, and D. C. Kerrigan, "A kinematic and kinetic comparison of overground and treadmill walking in healthy subjects," *Gait Posture*, vol. 26, no. 1, pp. 17–24, 2007.

[191] S. J. Lee and J. Hidler, "Biomechanics of overground vs. treadmill walking in healthy individuals," *J. Appl. Physiol.*, vol. 104, no. 3, pp. 747–755, 2008.

[192] K. Parvataneni, L. Ploeg, S. J. Olney, and B. Brouwer, "Kinematic, kinetic and metabolic parameters of treadmill versus overground walking in healthy older adults," *Clin. Biomech.*, 2009.

[193] J. R. Watt, J. R. Franz, K. Jackson, J. Dicharry, P. O. Riley, and D. C. Kerrigan, "A three-dimensional kinematic and kinetic comparison of overground and treadmill walking in healthy elderly subjects," *Clin. Biomech.*, 2010.

[194] M. L. Harris-Love, L. W. Forrester, R. F. Macko, K. H. C. Silver, and G. V. Smith, "Hemiparetic Gait Parameters in Overground Versus Treadmill Walking," *Neurorehabil. Neural Repair*, vol. 15, no. 2, pp. 105–112, 2001.

[195] R. Bayat, H. Barbeau, and A. Lamontagne, "Speed and temporal-distance adaptations during treadmill and overground walking following stroke," *Neurorehabil. Neural Repair*, 2005.

[196] B. Brouwer, K. Parvataneni, and S. J. Olney, "A comparison of gait biomechanics and metabolic requirements of overground and treadmill walking in people with stroke," *Clin. Biomech.*, 2009.

[197] D. J. Reinkensmeyer, O. M. Akoner, D. P. Ferris, and K. E. Gordon, "Slacking by the human motor system: Computational models and implic implications for robotic orthoses," in *Proceedings of the 31st Annual International Conference of the IEEE Engineering in Medicine and Biology Society: Engineering the Future of Biomedicine, EMBC 2009*, 2009.

[198] S. Galle, P. Malcolm, S. H. Collins, and D. De Clercq, "Reducing the metabolic cost of walking with an ankle exoskeleton: interaction between actuation timing and power," *J. Neuroeng. Rehabil.*, 2017.

[199] J. R. Koller, C. D. Remy, and D. P. Ferris, "Biomechanics and energetics of walking in powered ankle exoskeletons using myoelectric control versus mechanically intrinsic control," *J. Neuroeng. Rehabil.*, 2018.

[200] K. E. Gordon and D. P. Ferris, "Learning to walk with a robotic ankle exoskeleton," *J. Biomech.*, vol. 40, no. 12, pp. 2636–2644, 2007.

[201] D. P. Ferris, J. M. Czerniecki, and B. Hannaford, "An ankle-foot orthosis powered by artificial pneumatic muscles.," *J. Appl. Biomech.*, 2005.

[202] J. M. Hidler and A. E. Wall, "Alterations in muscle activation patterns during robotic-assisted walking," *Clin. Biomech.*, 2005.

[203] C. R. Kinnaird and D. P. Ferris, "Medial gastrocnemius myoelectric control of a robotic ankle exoskeleton," in *IEEE Transactions on Neural Systems and Rehabilitation Engineering*, 2009.

[204] G. D. Fulk, Y. He, P. Boyne, and K. Dunning, "Predicting Home and Community Walking Activity Poststroke," *Stroke*, vol. 48, no. 2, pp. 406–411, 2017.

[205] S. M. Bruijn, O. G. Meijer, P. J. Beek, J. H. van Dieën, and J. H. van Dieen, "Assessing the stability of human locomotion: a review of current measures," *J. R. Soc. Interface*, vol. 10, no. 83, Jun. 2013.

[206] S. A. Gard, S. C. Miff, and A. D. Kuo, "Comparison of kinematic and kinetic methods for computing the vertical motion of the body center of mass during walking," *Hum. Mov. Sci.*, 2004.

[207] J. L. Emken, R. Benitez, and D. J. Reinkensmeyer, "Human-robot cooperative movement training: Learning a novel sensory motor transformation during walking with robotic assistance-as-needed," *J. Neuroeng. Rehabil.*, 2007.

[208] S. E. Matsuda F, Mukaino M, Ohtsuka K, Tanikawa H, Tsuchiyama K, Teranishi T, Kanada Y, Kagaya H *et al.*, "Analysis of strategies used by hemiplegic stroke patients to achieve toe clearance," *Jpn J Compr Rehabil Sci ©Kaifukuki Rehabil. Ward Assoc.*, 2016.

[209] V. L. Little, T. E. McGuirk, and C. Patten, "Impaired limb shortening following stroke: What's in a name?," *PLoS One*, vol. 9, no. 10, 2014.

[210] E. M. Rose, T. Mathew, D. A. Coss, B. Lohr, and K. E. Omland, "A new statistical method to test equivalence: an application in male and female eastern bluebird song," *Anim. Behav.*, 2018.

[211] J. L. Rogers, K. I. Howard, and J. T. Vessey, "Using significance tests to evaluate equivalence between two experimental groups," *Psychol. Bull.*, 1993.

[212] D. Lakens, "Equivalence Tests: A Practical Primer for t Tests, Correlations, and Meta-Analyses," *Soc. Psychol. Personal. Sci.*, 2017.

[213] M. Warren, K. J. Ganley, and P. S. Pohl, "The association between social participation and lower extremity muscle strength, balance, and gait speed in US adults," *Prev. Med. Reports*, 2016.

[214] S. Perera, S. H. Mody, R. C. Woodman, and S. A. Studenski, "Meaningful change and responsiveness in common physical performance measures in older adults," *J. Am. Geriatr. Soc.*, 2006.

[215] K. Dunning, M. W. O'Dell, P. Kluding, and K. McBride, "Peroneal Stimulation for Foot Drop after Stroke," *American Journal of Physical Medicine and Rehabilitation*. 2015.

[216] O. A. Howlett, N. A. Lannin, L. Ada, and C. Mckinstry, "Functional electrical stimulation improves activity after stroke: A systematic review with meta-analysis," in *Archives of Physical Medicine and Rehabilitation*, 2015.

[217] T. G. Hornby, D. D. Campbell, J. H. Kahn, T. Demott, J. L. Moore, and H. R. Roth, "Enhanced gait-related improvements after therapist- versus robotic-assisted locomotor training in subjects with chronic stroke: a randomized controlled study.," *Stroke*, vol. 39, no. 6, pp. 1786–92, Jun. 2008.

[218] F. Molteni *et al.*, "Wearable robotic exoskeleton for overground gait training in sub-acute and chronic hemiparetic stroke patients: preliminary results.," *Eur. J. Phys. Rehabil. Med.*, 2017.

[219] R. S. Calabrò *et al.*, "Shaping neuroplasticity by using powered exoskeletons in patients with stroke: a randomized clinical trial," *J. Neuroeng. Rehabil.*, 2018.

[220] S. M. Cain, K. E. Gordon, and D. P. Ferris, "Locomotor adaptation to a powered ankle-foot orthosis depends on control method," vol. 13, pp. 1–13, 2007.

[221] S. Galle, P. Malcolm, W. Derave, and D. De Clercq, "Adaptation to walking with an exoskeleton that assists ankle extension," *Gait Posture*, 2013.

[222] P. C. Kao, C. L. Lewis, and D. P. Ferris, "Invariant ankle moment patterns when walking with and without a robotic ankle exoskeleton," *J. Biomech.*, vol. 43, no. 2, pp. 203–209, 2010.

[223] J. R. Koller, D. A. Jacobs, D. P. Ferris, and C. D. Remy, "Learning to walk with an adaptive gain proportional myoelectric controller for a robotic ankle exoskeleton," *J. Neuroeng. Rehabil.*, 2015.

[224] B. H. K. Dobkin *et al.*, "Prediction of responders for outcome measures of Locomotor experience applied post stroke trial," *J. Rehabil. Res. Dev.*, 2014.

[225] J. Perry, M. Garrett, J. K. Gronley, and S. J. Mulroy, "Classification of walking handicap in the stroke population.," *Stroke.*, vol. 26, pp. 982–989, 1995.

[226] T. M. Kesar *et al.*, "Combined effects of fast treadmill walking and functional electrical stimulation on post-stroke gait," *Gait Posture*, 2011.

[227] E. M. McCain *et al.*, "Mechanics and energetics of post-stroke walking aided by a powered ankle exoskeleton with speed-adaptive myoelectric control," *J. Neuroeng. Rehabil.*, vol. 16, no. 1, p. 57, May 2019.

[228] L. F. Yeung *et al.*, "Design of an exoskeleton ankle robot for robot-assisted gait training of stroke patients," *IEEE Int. Conf. Rehabil. Robot.*, pp. 211–215, 2017.

[229] J. a Blaya and H. Herr, "Adaptive control of a variable-impedance ankle-foot orthosis to assist

drop-foot gait.," *IEEE Trans. Neural Syst. Rehabil. Eng.*, vol. 12, no. 1, pp. 24–31, Mar. 2004.

[230] K. A. Shorter, G. F. G. F. Kogler, E. Loth, W. K. Durfee, and E. T. Hsiao-wecksler, "A portable powered ankle-foot orthosis for rehabilitation," *J. Rehabil. Res. Dev.*, vol. 48, no. 4, p. 459, 2011.

[231] J. Kim, S. Hwang, R. Sohn, Y. Lee, and Y. Kim, "Development of an active ankle foot orthosis to prevent foot drop and toe drag in hemiplegic patients: A preliminary study," *Appl. Bionics Biomech.*, 2011.

[232] J. Leung and A. M. Moseley, "Impact of ankle-foot orthoses on gait and leg muscle activity in adults with hemiplegia," *Physiotherapy*. 2003.

[233] C. Nikamp, J. Buurke, L. Schaake, J. Van Der Palen, J. Rietman, and H. Hermens, "Effect of long-term use of ankle-foot orthoses on tibialis anterior muscle electromyography in patients with sub-acute stroke: A randomized controlled trial," *J. Rehabil. Med.*, 2019.

[234] L. Bar-On, K. Desloovere, G. Molenaers, J. Harlaar, T. Kindt, and E. Aertbeliën, "Identification of the neural component of torque during manually-applied spasticity assessments in children with cerebral palsy," *Gait Posture*, 2014.

[235] L. Bar-On, E. Aertbeliën, G. Molenaers, B. Dan, and K. Desloovere, "Manually controlled instrumented spasticity assessments: A systematic review of psychometric properties," *Developmental Medicine and Child Neurology*. 2014.

[236] K. J. Nolan and M. Yarossi, "Preservation of the first rocker is related to increases in gait speed in individuals with hemiplegia and AFO," *Clin. Biomech.*, 2011.

[237] P.-C. Kao and D. P. Ferris, "Motor adaptation during dorsiflexion-assisted walking with a powered orthosis.," *Gait Posture*, vol. 29, no. 2, pp. 230–6, Feb. 2009.

[238] M. G. Browne and J. R. Franz, "Does dynamic stability govern propulsive force generation in human walking?," *R. Soc. Open Sci.*, vol. 4, no. 11, p. 171673, 2017.

[239] J. J. Eng, P. F. Tang, P. Fang Tang, P. F. Tang, and P. Fang Tang, "Gait training strategies to optimize walking ability in people with stroke: A synthesis of the evidence," *Expert Rev. Neurother.*, vol. 7, no. 10, pp. 1417–1436, 2007.

[240] D. Trojaniello, A. Ravaschio, J. M. Hausdorff, and A. Cereatti, "Comparative assessment of different methods for the estimation of gait temporal parameters using a single inertial sensor: Application to elderly, post-stroke, Parkinson's disease and Huntington's disease subjects," *Gait Posture*, vol. 42, no. 3, pp. 310–316, 2015.

[241] J. Zhang *et al.*, "Human-in-the-loop optimization of exoskeleton assistance during walking," *Science (80-.).*, vol. 356, no. 6344, pp. 1280–1283, 2017.

[242] S. Chen, J. Lach, B. Lo, and G. Z. Yang, "Toward Pervasive Gait Analysis With Wearable Sensors: A Systematic Review," *IEEE J. Biomed. Heal. Informatics*, vol. 20, no. 6, pp. 1521–1537, 2016.

[243] K. K. Patterson, W. H. Gage, D. Brooks, S. E. Black, and W. E. McIlroy, "Evaluation of gait symmetry after stroke: A comparison of current methods and recommendations for standardization," *Gait Posture*, vol. 31, no. 2, pp. 241–246, 2010.

[244] S. Miyazaki, "Long-term unrestrained measurement of stride length and walking velocity utilizing

a piezoelectric gyroscope," *IEEE Transactions on Biomedical Engineering*. 1997.

[245] Q. Li, M. Young, V. Naing, and J. M. Donelan, "Walking speed estimation using a shank-mounted inertial measurement unit," *J. Biomech.*, vol. 43, no. 8, pp. 1640–1643, 2010.

[246] K. Aminian, B. Najafi, C. Büla, P.-F. F. Leyvraz, and P. Robert, "Spatio-temporal parameters of gait measured by an ambulatory system using miniature gyroscopes," *J. Biomech.*, vol. 35, no. 5, pp. 689–699, May 2002.

[247] S. Tadano, R. Takeda, and H. Miyagawa, "Three dimensional gait analysis using wearable acceleration and gyro sensors based on quaternion calculations.," *Sensors*, vol. 13, no. Cc, pp. 9321–9343, 2013.

[248] K. Aminian, P. Robert, E. Jéquier, and Y. Schutz, "Estimation of speed and incline of walking using neural network," in *Conference Proceedings - 10th Anniv., IMTC 1994: Advanced Technologies in I and M. 1994 IEEE Instrumentation and Measurement Technology Conference*, 1994.

[249] J. Hannink *et al.*, "Stride Length Estimation with Deep Learning," pp. 1–9, 2016.

[250] A. Mannini, V. Genovese, and A. M. Sabatini, "Online decoding of hidden markov models for gait event detection using foot-mounted gyroscopes," *IEEE J. Biomed. Heal. Informatics*, vol. 18, no. 4, pp. 1122–1130, 2014.

[251] A. M. Sabatini, "Quaternion-based strap-down integration method for applications of inertial sensing to gait analysis," *Med. Biol. Eng. Comput.*, vol. 43, no. 1, pp. 94–101, 2005.

[252] H. M. Schepers, H. F. J. M. Koopman, and P. H. Veltink, "Ambulatory assessment of ankle and foot dynamics," *IEEE Trans. Biomed. Eng.*, vol. 54, no. 5, pp. 895–902, 2007.

[253] L. Ojeda and J. Borenstein, "Non-GPS navigation for security personnel and first responders," *J. Navig.*, vol. 60, no. 3, pp. 391–407, 2007.

[254] B. Mariani, S. Rochat, C. J. Büla, and K. Aminian, "Heel and toe clearance estimation for gait analysis using wireless inertial sensors," *IEEE Trans. Biomed. Eng.*, vol. 59, no. 12 PART2, pp. 3162–3168, 2012.

[255] J. R. Rebula, L. V. Ojeda, P. G. Adamczyk, and A. D. Kuo, "Measurement of foot placement and its variability with inertial sensors," *Gait Posture*, vol. 38, no. 4, pp. 974–980, 2013.

[256] A. Rampp, J. Barth, S. Schülein, K. G. Gaßmann, J. Klucken, and B. M. Eskofier, "Inertial Sensor-Based Stride Parameter Calculation From Gait Sequences in Geriatric Patients," *IEEE Trans. Biomed. Eng.*, 2015.

[257] J. Hannink, M. Ollenschläger, F. Kluge, N. Roth, J. Klucken, and B. M. Eskofier, "Benchmarking Foot Trajectory Estimation Methods for Mobile Gait Analysis," *Sensors*, vol. 17, no. 9, p. 1940, 2017.

[258] E. Foxlin, "Pedestrian tracking with shoe-mounted inertial sensors," *IEEE Comput. Graph. Appl.*, vol. 25, no. 6, pp. 38–46, 2005.

[259] R. Jiménez-Fabián and O. Verlinden, "Review of control algorithms for robotic ankle systems in lower-limb orthoses, prostheses, and exoskeletons," *Med. Eng. Phys.*, vol. 34, no. 4, pp. 397–408, 2012.

[260] R. Schwesig, S. Leuchte, D. Fischer, R. Ullmann, and A. Kluttig, “Inertial sensor based reference gait data for healthy subjects,” *Gait Posture*, 2011.

[261] M. Kok, J. D. Hol, and T. B. Schön, “Using Inertial Sensors for Position and Orientation Estimation,” 2017.

[262] W. H. Baird, “An introduction to inertial navigation,” *Am. J. Phys.*, vol. 77, no. 9, pp. 844–847, 2009.

[263] A. M. Sabatini, C. Martelloni, S. Scapellato, and F. Cavallo, “Assessment of walking features from foot inertial sensing,” *IEEE Trans. Biomed. Eng.*, vol. 52, no. 3, pp. 486–494, 2005.

[264] B. Mariani, C. Hoskovec, S. Rochat, C. Büla, J. Penders, and K. Aminian, “3D gait assessment in young and elderly subjects using foot-worn inertial sensors,” *J. Biomech.*, 2010.

[265] L. Ojeda, J. R. Rebula, P. G. Adamczyk, and A. D. Kuo, “Mobile platform for motion capture of locomotion over long distances,” *J. Biomech.*, vol. 46, no. 13, pp. 2316–2319, 2013.

[266] O. Perrin, P. Terrier, Q. Ladetto, B. Merminod, and Y. Schutz, “Improvement of walking speed prediction by accelerometry and altimetry, validated by satellite positioning,” *Med. Biol. Eng. Comput.*, 2000.

[267] P. Mohandas Nair, T. George Hornby, and A. Louis Behrman, “Minimal Detectable Change for Spatial and Temporal Measurements of Gait After Incomplete Spinal Cord Injury,” *Top. Spinal Cord Inj. Rehabil.*, vol. 18, no. 3, pp. 273–281, Jul. 2012.

[268] J. K. Tilson *et al.*, “Meaningful Gait Speed Improvement During the First 60 Days Poststroke: Minimal Clinically Important Difference,” *Phys. Ther.*, 2010.

[269] D. S. Reisman, R. Wityk, K. Silver, and A. J. Bastian, “Locomotor adaptation on a split-belt treadmill can improve walking symmetry post-stroke,” *Brain*, vol. 130, no. 7, pp. 1861–1872, 2007.

[270] D. S. Reisman, H. McLean, and A. J. Bastian, “Split-belt treadmill training poststroke: A case study,” *J. Neurol. Phys. Ther.*, vol. 34, no. 4, pp. 202–207, 2010.

[271] T. M. Kesar, M. J. Sauer, S. A. Binder-Macleod, and D. S. Reisman, “Motor learning during poststroke gait rehabilitation: A case study,” *J. Neurol. Phys. Ther.*, vol. 38, no. 3, pp. 183–189, 2014.

[272] K. M. Newell, G. Mayer-Kress, S. L. Hong, and Y. T. Liu, “Adaptation and learning: Characteristic time scales of performance dynamics,” *Hum. Mov. Sci.*, vol. 28, no. 6, pp. 655–687, 2009.

[273] F. M. Verhoeven and K. M. Newell, “Unifying practice schedules in the timescales of motor learning and performance,” *Hum. Mov. Sci.*, vol. 59, no. September 2017, pp. 153–169, 2018.

[274] D. S. Reisman, H. J. Block, and A. J. Bastian, “Interlimb coordination during locomotion: what can be adapted and stored?,” *J. Neurophysiol.*, 2005.

[275] A. Schmid *et al.*, “Improvements in speed-based gait classifications are meaningful,” *Stroke*, 2007.

[276] S. A. Roelker, M. G. Bowden, S. A. Kautz, and R. R. Neptune, “Paretic propulsion as a measure of walking performance and functional motor recovery post-stroke: A review,” *Gait and Posture*.

2019.

[277] D. J. Reinkensmeyer *et al.*, "Computational neurorehabilitation: Modeling plasticity and learning to predict recovery," *Journal of NeuroEngineering and Rehabilitation*. 2016.

[278] J. W. Krakauer, S. T. Carmichael, D. Corbett, and G. F. Wittenberg, "Getting neurorehabilitation right: What can be learned from animal models?," *Neurorehabilitation and Neural Repair*. 2012.

[279] R. A. States, E. Pappas, and Y. Salem, "Overground physical therapy gait training for chronic stroke patients with mobility deficits," *Stroke*, 2009.

[280] S. a. Billinger *et al.*, "Physical activity and exercise recommendations for stroke survivors: A statement for healthcare professionals from the American Heart Association/American Stroke Association," *Stroke*, vol. 45, pp. 2532–2553, 2014.

[281] P. W. Duncan *et al.*, "Protocol for the Locomotor Experience Applied Post-stroke (LEAPS) trial: a randomized controlled trial.," *BMC Neurol.*, vol. 7, no. c, p. 39, Jan. 2007.

[282] D. S. Reisman, S. Binder-MacLeod, and W. B. Farquhar, "Changes in Metabolic Cost of Transport Following Locomotor Training Poststroke," *Top. Stroke Rehabil.*, 2013.

[283] L. N. Awad, D. S. Reisman, T. R. Wright, M. A. Roos, and S. A. Binder-Macleod, "Maximum Walking Speed Is a Key Determinant of Long Distance Walking Function After Stroke," *Top. Stroke Rehabil.*, vol. 21, no. 6, pp. 502–509, 2014.

[284] C. Krishnan, D. Kotsapouikis, Y. Y. Dhaher, and W. Z. Rymer, "Reducing robotic guidance during robot-assisted gait training improves gait function: A case report on a stroke survivor," *Arch. Phys. Med. Rehabil.*, 2013.

[285] S. J. Olney, M. P. Griffin, and I. D. McBride, "Temporal, kinematic, and kinetic variables related to gait speed in subjects with hemiplegia: A regression approach," *Phys. Ther.*, 1994.

[286] F. A. Panizzolo *et al.*, "Metabolic cost adaptations during training with a soft exosuit assisting the hip joint," *Sci. Rep.*, vol. 9, no. 1, p. 9779, 2019.

[287] D. A. Jacobs, J. R. Koller, K. M. Steele, and D. P. Ferris, "Motor modules during adaptation to walking in a powered ankle exoskeleton," *J. Neuroeng. Rehabil.*, vol. 15, no. 1, p. 2, 2018.

[288] C. Buesing *et al.*, "Effects of a wearable exoskeleton stride management assist system (SMA(R)) on spatiotemporal gait characteristics in individuals after stroke: a randomized controlled trial.," *J. Neuroeng. Rehabil.*, vol. 12, p. 69, Aug. 2015.

[289] J. W. Krakauer and R. Shadmehr, "Consolidation of motor memory," *Trends in Neurosciences*. 2006.

[290] J. Taborri, E. Palermo, S. Rossi, and P. Cappa, "Gait partitioning methods: A systematic review," *Sensors (Switzerland)*, vol. 16, no. 1, pp. 40–42, 2016.

[291] E. Zheng, S. Manca, T. Yan, A. Parri, N. Vitiello, and Q. Wang, "Gait Phase Estimation Based on Noncontact Capacitive Sensing and Adaptive Oscillators," *IEEE Trans. Biomed. Eng.*, vol. 64, no. 10, pp. 2419–2430, 2017.

[292] J. Bae and M. Tomizuka, "Gait phase analysis based on a Hidden Markov Model," *Mechatronics*, 2011.

[293] J. L. Allen, S. A. Kautz, and R. R. Neptune, “Step length asymmetry is representative of compensatory mechanisms used in post-stroke hemiparetic walking,” *Gait Posture*, 2011.

[294] G. Zizzo and L. Ren, “Position tracking during human walking using an integrated wearable sensing system,” *Sensors (Switzerland)*, vol. 17, no. 12, 2017.

[295] A. K. Dhawale, M. A. Smith, and B. P. Ölveczky, “The Role of Variability in Motor Learning,” *Annu. Rev. Neurosci.*, vol. 40, no. 1, pp. 479–498, Jul. 2017.